

MCIC Report/April 1977

MCIC-77-30

AD A 0 40690

# DISPERSION STRENGTHENING OF METALS

AD No. 1  
DDC FILE COPY



Metals and Ceramics Information Center

Battelle  
Columbus Laboratories  
505 King Avenue  
Columbus, Ohio 43201

DDC  
RECEIVED  
JUN 17 1977  
REGISTERED

Unclassified

SECURITY CLASSIFICATION OF THIS PAGE (When Data Entered)

REPORT DOCUMENTATION PAGE		READ INSTRUCTIONS BEFORE COMPLETING FORM												
1. REPORT NUMBER (14) MCIC-77-30 ✓	2. GOVT ACCESSION NO.	3. RECIPIENT'S CATALOG NUMBER												
4. TITLE (and Subtitle) (6) DISPERSION STRENGTHENING OF METALS.		5. TYPE OF REPORT & PERIOD COVERED												
		6. PERFORMING ORG. REPORT NUMBER MCIC-77-30												
7. AUTHOR(s) (10) F. R. Morral	(15)	8. CONTRACT OR GRANT NUMBER(s) DSA900-76-C-2471 ✓												
9. PERFORMING ORGANIZATION NAME AND ADDRESS Metals and Ceramics Information Center ✓ Battelle-Columbus Laboratories, Columbus, Ohio		10. PROGRAM ELEMENT, PROJECT, TASK AREA & WORK UNIT NUMBERS (12) 170P.												
11. CONTROLLING OFFICE NAME AND ADDRESS (11)		12. REPORT DATE April 1977												
		13. NUMBER OF PAGES 169												
14. MONITORING AGENCY NAME & ADDRESS (if different from Controlling Office) Army Materials & Mechanics Research Center Watertown MA 02172		15. SECURITY CLASS. (of this report)  Unclassified												
		15a. DECLASSIFICATION/DOWNGRADING SCHEDULE												
16. DISTRIBUTION STATEMENT (of this Report)  Approved for public release; distribution unlimited														
17. DISTRIBUTION STATEMENT (of the abstract entered in Block 20, if different from Report)														
18. SUPPLEMENTARY NOTES														
19. KEY WORDS (Continue on reverse side if necessary and identify by block number)  <table border="0"> <tr> <td>Dispersion hardening</td> <td>Chromium</td> <td>Tungsten</td> </tr> <tr> <td>Aluminum</td> <td>Iron</td> <td>Oxides</td> </tr> <tr> <td>Cobalt</td> <td>Steel</td> <td></td> </tr> <tr> <td>Copper</td> <td>Nickel</td> <td></td> </tr> </table>			Dispersion hardening	Chromium	Tungsten	Aluminum	Iron	Oxides	Cobalt	Steel		Copper	Nickel	
Dispersion hardening	Chromium	Tungsten												
Aluminum	Iron	Oxides												
Cobalt	Steel													
Copper	Nickel													
20. ABSTRACT (Continue on reverse side if necessary and identify by block number) <p>This review consists of a brief assessment of the developments in dispersion strengthening of 21 metals and their alloys on both a commercial and experimental level with a special emphasis on the last 10 years. For purposes of this report, dispersion strengthening is defined as the process of strengthening a metal or alloy by incorporating a fine insoluble phase dispersed uniformly throughout the matrix of the parent metal. Precipitation hardening is not covered in this report</p> <p style="text-align: right;">(Continued) ✓</p>														



## 20. (Continued)

although it is a form of dispersion strengthening in which the precipitated particles usually redissolve in the matrix at high temperatures. Because this has been a very active field of research and development, properties obtained recently (primarily within the past 10 years), or from difficult-to-obtain sources, have been given preference along with work not covered in previous reviews. This report also identifies the most recent reviews which have been prepared for each of these metals. Each section has its own reference list to assist the reader interested only in particular metals. For copper and nickel (which are two of the largest chapters), a bibliography of added references, not cited in the overview, has been provided as an additional information source.

MCIC Report/April 77

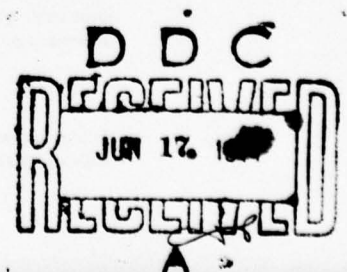
**DISPERSION STRENGTHENING OF METALS**

F. R. Morral, Consultant  
Battelle's Columbus Laboratories  
Columbus, Ohio

MCIC-77-30

**METALS AND CERAMICS INFORMATION CENTER**  
*A Department of Defense Information Analysis Center*  
Columbus, Ohio

Approved for public release; distribution unlimited



## ACKNOWLEDGEMENT

This document was prepared by the Metals and Ceramics Information Center (MCIC), Battelle's Columbus Laboratories, 505 King Avenue, Columbus, Ohio 43201. MCIC's objective is to provide a comprehensive current resource of technical information on the development and utilization of advanced metal- or ceramic-base materials.

The Center is operated by Battelle-Columbus under Contract Number DSA900-76-C-2471 for the U. S. Defense Supply Agency; technical aspects of MCIC operations are monitored by the Army Materials and Mechanics Research Center. The support of these sponsor organizations is gratefully acknowledged.

The author also gratefully acknowledges the technical assistance of Vincent Barth, Roger Runck, and Dan Maykuth who are all Battelle-Columbus staff members or retired staff members. The editorial and typing assistance of Mrs. Jeanne Pigeon are also gratefully acknowledged.

ACCESSION for	
NTIS	White Section <input checked="" type="checkbox"/>
DDO	Self Section <input type="checkbox"/>
UNANNOUNCED	<input type="checkbox"/>
JUSTIFICATION.....	
BY.....	
DISTRIBUTION/AVAILABILITY CODES	
Dist. AVAIL. and/or SPECIAL	
A	21

This document was prepared under the sponsorship of the Department of Defense. Neither the United States Government nor any person acting on behalf of the United States Government assumes any liability resulting from the use or publication of the information contained in this document or warrants that such use or publication will be free from privately owned rights.

Approved for public release; distribution unlimited

All rights reserved. This document, or parts thereof, may not be reproduced in any form without written permission of the Metals and Ceramics Information Center.



## TABLE OF CONTENTS

	Page
SUMMARY .....	v
INTRODUCTION .....	1
BACKGROUND INFORMATION .....	2
SILVER .....	5
ALUMINUM .....	9
Commercial Aluminum .....	9
Experimental Aluminum .....	18
GOLD .....	24
BERYLLIUM .....	26
COLUMBIUM .....	29
COBALT .....	31
DS Co Alloys .....	31
DS Co-M Alloys .....	33
DS Co-Cr-Base Alloys .....	37
CHROMIUM .....	46
Cr-MgO Alloys .....	46
Cr-ThO <sub>2</sub> Alloys .....	48
Other Chromium Alloys .....	49
COPPER .....	52
IRON AND STEEL .....	66
DS Fe Alloys .....	66
DS Fe-Cr Alloys .....	71
MAGNESIUM .....	80
MOLYBDENUM .....	84
NICKEL .....	90
Ni-ThO <sub>2</sub> Alloys .....	91
Ni-Al <sub>2</sub> O <sub>3</sub> Alloys .....	94
Ni-HfO <sub>2</sub> Alloys .....	96
Other Dispersoids in Unalloyed Nickel .....	98
DS Ni-M Alloys .....	99
Ni-Cr Alloys .....	101
Experimental Ni-Cr-ThO <sub>2</sub> Alloys .....	101
Commercial Ni-20Cr-2ThO <sub>2</sub> Alloys .....	102
Other Ni-Cr Alloys .....	105
Ni-Cr-Al Alloys .....	106
DS Superalloys .....	110
Oxidation and Hot-Corrosion Resistance .....	113
LEAD .....	121
PLATINUM .....	129

TABLE OF CONTENTS  
(Continued)

TIN.....	135
TANTALUM.....	138
TITANIUM.....	139
URANIUM.....	145
TUNGSTEN.....	147
W-ThO <sub>2</sub> Alloys.....	147
Other Dispersoids in Unalloyed Tungsten.....	151
W-Re Alloys.....	155
ZINC.....	160
ZIRCONIUM.....	162

## SUMMARY

Nearly 70 years ago, the first dispersion-strengthened alloy was marketed commercially. This material, thoriated tungsten, has been of considerable industrial importance since then and new uses for the alloy are still being found. Much later, in the early 1950's, the marketing of sintered aluminum products (SAP) was started with great expectations that never materialized. This development, however, encouraged research and development in applying dispersion hardening to many metals and alloys, a number of which have been offered to industry. The main reason for interest is that these materials have markedly improved creep resistance over the original base metal and that this strength advantage can be maintained at very high temperatures, e.g., frequently up to 90 percent of the base metals' homologous melting temperature ( $0.9 T_m$ ).

Unfortunately, most of the dispersion-strengthened materials that have been marketed could not compete pricewise with other materials available. Joining problems have also inhibited their wider use. However, as the pressure for increasing service temperatures becomes greater, particularly in thermal shields and aircraft gas-turbine engines, the prospects of using dispersion-strengthened alloys to meet these needs becomes brighter. This would not be true without several important processing developments that have occurred within the past 10 years. These include mechanical alloying, directional recrystallization, and new concepts in thermomechanical processing. The net result should be a promising future for the most advanced of the dispersion-strengthened (DS) alloys. It is also probable that new uses will continue to be found for the important established, though less glamorous, DS alloys of tungsten, silver, and copper.

This review consists of a brief assessment of the developments in dispersion strengthening of 21 metals and their alloys, with a special emphasis on the last 10 years.



## INTRODUCTION

For the purpose of this report, dispersion strengthening is defined as the process of strengthening a metal or an alloy by incorporating a fine insoluble phase dispersed uniformly throughout the matrix of the parent metal or dispersant. The dispersoid is usually present in small amounts, e.g., less than 10 volume percent, and is stable (i.e., inert) at temperatures approaching the melting point of the matrix. The dispersoids are not coherent with the matrix and are so small that electron-microscopy techniques may be required to identify them. This report does not cover precipitation hardening, which is a form of dispersion strengthening in which the precipitated particles usually redissolve in the matrix at high temperatures. The precipitated particles may or may not be coherent with the matrix.

The dispersion strengthening of metals has been an active field of research and development for the last two or three decades. Much work has been done with many materials. For example, a cursory check of the literature reveals that dispersion strengthening has been explored on over 20 of the most widely used industrial metals. Moreover, for some metals like aluminum, copper, and nickel, several hundred reports and publications are available. Obviously, an in-depth analysis covering all of the work done on all of these metals would be a formidable task.

As a compromise, this report presents an overview of the major developments which include the dispersion hardening of 21 metals on both commercial and experimental levels. Properties obtained recently (primarily within the past 10 years), or from difficult-to-obtain sources, have been given preference along with work not covered in previous reviews. This report also identifies the most recent reviews which have been prepared for each of these metals. Each section has its own reference list to assist the reader interested only in particular metals. Finally, for copper and nickel, a bibliography of added references, not cited in the overview, has been provided as an additional information source.

The units of measurement in the report are those used by the original authors. However, in order to derive some consistency, where English units were used in the original, SI units have been added in parentheses in the text of this report. This has also been done in the captions of figures and tables. In tables, where columns of stress data appear in English units or in  $\text{kg/mm}^2$ , a column showing megapascals (MPa or  $\text{MN/m}^2$ ) has been added. Factors for these conversions are:  $1 \text{ kg/mm}^2$  (or  $\text{kp/mm}^2$ )  $\times 9.8067 = 1 \text{ MPa}$  and  $1 \text{ ksi} \times 6.89 = 1 \text{ MPa}$ . Units on figures have been left as they appeared in the original.

## BACKGROUND INFORMATION

What we now designate as "dispersion-strengthened metals" probably originated with the development of "ductile tungsten".<sup>(1)</sup> Ductile tungsten lamp filaments were developed more than 65 years ago at the General Electric Laboratories by C. G. Fink and W. D. Coolidge.<sup>(2)</sup> The 1913 patent<sup>(3)</sup> on the process mentioned a product "containing additional material which will prevent coarse crystallization of the tungsten at high temperatures". Shortly thereafter Fink<sup>(4)</sup> indicated that "large quantities of drawn wire, flexible and strong, are being daily produced and used as filaments in incandescent lamps". He also suggested further applications.

The effect of ThO<sub>2</sub> additions to tungsten was studied by Zay Jeffries.<sup>(5)</sup> He observed that these additions retarded grain growth at high temperatures and consequently resulted in longer lives for the filaments. At that time, thoriated tungsten wires containing about 0.7 percent ThO<sub>2</sub> were mainly used for incandescent lamps. Wires for cathodes usually contained 1.5 percent ThO<sub>2</sub>. Additions of ThO<sub>2</sub> were limited to a maximum of about 2 percent since it was difficult to work tungsten with higher ThO<sub>2</sub> contents. These alloys were produced from a mixture of WO<sub>3</sub> and an aqueous solution of Th(NO<sub>3</sub>)<sub>4</sub> which was dried, pulverized and sifted. The WO<sub>3</sub> was reduced to tungsten by sintering the mixture in hydrogen. The ThO<sub>2</sub> remained stable through the sintering process. However, Fink found<sup>(6)</sup> that if rods of ductile tungsten were heated high enough in an oxygen-free atmosphere, the tungsten and thorium alloyed.

In 1930, Smith<sup>(7)</sup> proposed internal oxidation of powders as a means of dispersion strengthening. The process was later applied by Rhines<sup>(8)</sup> and Meijering<sup>(9)</sup> using copper and silver alloys and by De Jong<sup>(10)</sup> on beryllium and copper alloys.

The use of an inert oxide as a dispersoid was not realized until later, as reported in a historical review by Goetzel.<sup>(11)</sup> He discusses what may have been forerunners of dispersion-strengthened aluminum going back to 1940 and possibly even to a report by Masing in 1909. In 1942, a patent was issued on dispersion-strengthened (DS) Pt-ThO<sub>2</sub><sup>(12)</sup>, as a logical extrapolation of techniques used on DS-W-ThO<sub>2</sub> for the lamp industry.

Around 1946, Irman<sup>(13)</sup> developed an Al<sub>2</sub>O<sub>3</sub>-strengthened aluminum named SAP, an acronym for either "sintered aluminum powder" or "sintered aluminum product". SAP is a registered trade name of Aluminum Industrie A.G. of Neuhausen a. Rheinf., Switzerland. The manufacturing process for SAP consists primarily of preparing the aluminum powder by a grinding process in a special atmosphere to produce an oxide film about 100 Angstroms (0.01 micron) thick on the surface of the powder particles. Further dry grinding breaks up the oxide-coated particles to produce a powder consisting of isometric particles that are not only oxidized on the surface, but also contain fine oxide particles in the interior. After compacting, sintering, and hot working, the resultant material contains a fine dispersion of very small particles of Al<sub>2</sub>O<sub>3</sub>. This SAP process was the first of the mechanical, or nonchemical, processes used successfully to provide a uniform dispersion of very small particles of oxide in a metal. Many investigators then decided to try adding other refractory oxides, to obtain a similar effect. The process, of course, is confined to those metals or alloys that form stable oxides that will serve as dispersoids. The dispersion of Al<sub>2</sub>O<sub>3</sub> conferred strength to the SAP system up to the melting point of the aluminum matrix. SAP was the first dispersion-strengthened material designed as a structural load-bearing system. Considerable research has been done by companies in the U.S. and elsewhere to further improve this material since it first appeared on the market. SAP alloys, however, have not found widespread usage.

---

\* References are listed at the end of this section and each section in the report.

Nevertheless, in view of the promising properties achieved in these materials, Jaffee and his associates at Battelle Memorial Institute<sup>(14)</sup> and Grant and his students at M I T<sup>(15)</sup> undertook a continuing series of studies of oxide dispersion strengthening of metals, including copper, cobalt, nickel, molybdenum, and tungsten. In the late 1950's, several Russian investigators, including Antsiferov and Paisov, were involved with similar studies.

One important breakthrough which occurred in the late 1950's was the development by Du Pont of a chemical codeposition process for making powders of Ni-ThO<sub>2</sub>.<sup>(16)</sup> This process allowed the production of much finer powders than did mechanical mixing. In the final wrought products, the stable ThO<sub>2</sub> particles were very fine (from about 50-1000 Angstroms) and their distribution was quite uniform. This discovery spurred interest in applying these materials to the high-temperature regime in competition with conventionally prepared superalloys.

It was soon recognized that the oxidation resistance of the simple Ni-ThO<sub>2</sub> alloy was inadequate. Research efforts were then applied to alloying to improve the hot-corrosion resistance of the base material. This research led to the development of DS-Ni-Cr, Ni-Cr-Al, Ni-Cr-Al-Y, and Co-Cr-Al-Y alloys plus several others which display a high degree of oxidation resistance.

Concurrently, Benjamin and his coworkers at the International Nickel Company developed mechanical alloying. This process made it possible for the first time to combine the strengthening effects of stable oxide particles with those from coherent intermetallics such as gamma prime. Inconel MA 754, which consists nominally of Ni-20Cr-0.3Al-0.5Ti-0.6Y<sub>2</sub>O<sub>3</sub>, is the newest and most commonly advanced alloy to be made by this process. This material is presently accumulating an impressive performance record in General Electric's F-101 aircraft gas-turbine engines.

Much effort has been given to a study of dispersion-strengthening mechanisms. Orowan was among the first to offer an explanation based on the particles acting as barriers to dislocation movement during deformation. His dislocation bowing concept<sup>(17, 18)</sup> has since been amplified by others<sup>(19, 20)</sup>, yet this is only one of several mechanisms describing "direct dispersion strengthening". "Direct strengthening" is one of two classifications devised by Ansell<sup>(21)</sup> to describe the ways in which dispersed particles can influence mechanical behavior as well as total microstructure. The other is "indirect strengthening".

Direct strengthening is achieved by particles acting as barriers to dislocation motion during deformation. Here, strengthening can be described by the various mechanisms whereby dislocations bypass particles. Indirect strengthening by second-phase particles arises because the particles influence the total microstructure as alloys are fabricated by thermomechanical processing, and the total microstructure affects the mechanical properties. Here, the influence of particles on grain size and shape is of substantial importance.

As pointed out by Wilcox and Clauer<sup>(22)</sup>, in reality, both direct and indirect strengthening occur simultaneously in dispersion-strengthened alloys. Hence, the mechanisms are quite complex. Aside from these general observations, it is not possible to delve more deeply into the theoretical bases of dispersion strengthening in this overview. Rather, the reader is referred to several excellent summaries including those by Wilcox and Clauer<sup>(22)</sup>, Ansell<sup>(21)</sup>, Kelly and Nicholson<sup>(19)</sup>, and Ashby<sup>(23)</sup>.

Similarly, numerous reviews have been published and many technical sessions have been held on various aspects of dispersion strengthening. For purposes of record, three of the more comprehensive and most recent of these are identified as follows:

- "Non-Metallic Dispersions in Powder Metallurgy", Powder Metallurgy,<sup>(10)</sup> (December 1962)



- "Strengthening Mechanisms - Metals and Ceramics", 1965 Sagamore Conference, Syracuse University (1966)
- "Oxide Dispersion Strengthening", Proceedings of Metallurgical Society Conferences, 47, Gordon and Breach Science Publications (June 1966).

Finally, Hansen's comprehensive bibliography on dispersion-hardened metals warrants recognition.<sup>(24)</sup> This effort was initiated in 1963 with a collection of over 400 references and later was expanded, in two supplements, into a bibliography of over 2000 references.

#### REFERENCES AND BACKGROUND INFORMATION

1. Fink, C. G., "Ductile Tungsten and Molybdenum", Trans. Am. Electrochem. Soc., 17, 229-234 (1910).
2. Coolidge, W. D., "Ductile Tungsten", Trans. Am. Inst. Electr. Eng., 29, 961-965 (1910).
3. U.S. Patent 1,082,933 (1913).
4. Fink, C. G., "Applications of Ductile Tungsten", Trans. Am. Electrochem. Soc., 22, 499 (1912).
5. Jeffries, Z., "Grain Growth in Metals", Bull. Am. Inst. Mining Engrs., 119, 2065 (1916); J. Inst. of Metals, 20 (2), 109-140 (1918).
6. Fink, C. G., Discussion, Trans. Am. Electrochem. Soc., 50, 399 (1926).
7. Smith, C. S., "Mining and Metallurgie", 11, 213 (1930).
8. Rhines, F. N., "Metallographic Study of Internal Oxidation in  $\alpha$ -Solid Solutions of Copper", Trans. AIME, 137, 249-290 (1940).
9. Meijering, J. L., and Druyveteyn, M. J., "Hardening of Metals by Internal Oxidation", Part 2, Phillips Res. Rep., 2, 260-280 (1947).
10. DeJong, J. J., Ingenieur, 64, 0.92 (1952).
11. Goetzel, C. G., "Dispersion Strengthened Alloys: The Possibilities for Light Metals", J. of Metals, 189-194 (1959).
12. British Patent 578,956 (1942).
13. Irman, R., "SAP: Ein Neuer Werkstoff der Pulvermetallurgie aus Al", Technische Rundschau (Bern), (36), 19-26 (1949).
14. Bruckart, W. L., Craighead, C. M., and Jaffee, R. I., "Investigation of Molybdenum and Molybdenum-Base Alloys Made by Powder Metallurgy Techniques", Battelle Memorial Institute, U.S. Office of Technical Services, PB 127913, 172 (January 1955).
15. Grant, N. J., and Preston, O., "Dispersed Hard Particle Strengthening of Metals", Trans. AIME, 209, 349-357 (1957).
16. Anders, F. J., Alexander, B. B., and Wartel, W. S., "Metal-Oxide Composition", U.S. Patent 2,972,529 (May 12, 1958).
17. Orowan, E., Trans. Inst. Eng. Shipbuilders in Scotland, 89, 165 (1946).
18. Orowan, E., Dislocations in Metals, M. Cohen, Editor, AIME, New York (1954), p 131.
19. Kelly, A., and Nicholson, R. B., Prog. in Mat. Sci., 10, 151 (1963).
20. Ashby, M. F., Physics of Strength and Plasticity, A. Argon, Editor, the MIT Press, Cambridge, Massachusetts (1969), p 113.
21. Ansell, G., Oxide Dispersion Strengthening, G. Ansell, et al., Editors, Gordon and Breach, New York (1968), p 61.
22. Wilcox, B. A., and Clauer, A. H., The Superalloys, C. T. Sims and W. C. Hagel, Editors, John Wiley and Sons, New York (1972), p 197.
23. Ashby, M. F., Second Int. Conf. Strength Met. Alloys, American Soc. For Metals, Metals Park, Ohio (1970), p 507.
24. Hansen, N., Lilholt, H., and Hahnkamm, M., "Bibliography on Dispersion-Strengthened Metals", Riso Report, (48), (1962), plus supplements (1963, 1964, and 1967). (AD 453 028 and AD 476 152)

## SILVER

Silver, with its excellent electrical and thermal properties, is an important material for electrical, electronics, and chemical industry equipment. Because the pure metal is extremely soft, most applications require silver alloys. In electrical applications particularly, dispersion-strengthened silver alloys have great merit since the dispersions accomplish strengthening without the severe degradation of electrical conductivity that always accompanies solid-solution strengthening.

The maximum solubility of oxygen in silver is about 0.01 percent (by mass) at 939 C, but this decreases to approximately 0.0002 percent at room temperature. Silver oxide, however, is unstable. Thus, other oxides are preferred as the dispersoid. Internal oxidation of alloys and of powders and their mixtures are all useful ways for fabricating DS silver alloys.

As reported by Harmsen, et al.<sup>(1)</sup>, the first Ag-CdO contact alloys were produced in the 1940's by pressing, sintering, and high-pressure compacting mixtures of silver and CdO powders. These compacts were porous and brittle because of a coarse dispersion of the oxide. The density of the materials was also undesirably low. Some improvements in properties were achieved by using internal oxidation techniques on Ag-Cd alloys, but these materials were also characterized by coarse CdO crystals. The next processing advance was to reduce mixtures of  $\text{Cd}(\text{OH})_2$  and  $\text{AgNO}_3$  and process the resulting powders.<sup>(1)</sup> Fine particles of CdO (10 to 15 weight percent) in the silver prevent the growth of the silver crystals even after critical deformation and recrystallization annealing for several hours at 800 C.

DS Ag-CdO, Ag-ZnO, and Ag-SnO<sub>2</sub> alloys were tested by Harmsen, et al., for arc erosion using different currents as shown in Figure 1. The Ag-ZnO and the Ag-SnO<sub>2</sub> alloys both had a higher erosion rate than the Ag-CdO alloy. The welding, or sticking, tendency of these alloys was also determined using the ASTM recommended weld test fixture.

Vinaricky and Harmsen<sup>(2)</sup> investigated possible silver contact materials by the addition of up to 25 percent each of CdO, CuO, ZnO, SnO<sub>2</sub>, PbO, NiO, MgO, Al<sub>2</sub>O<sub>3</sub>, and ZrO<sub>2</sub>, all having a particle size between 4 and 8 microns. The mixtures were compacted to bars and sintered at 900 C except for the Ag-PbO, which was sintered at 600 C. The bars were then hot worked into 12-mm diameter wires. At the 25-percent oxide level, all the materials were very brittle. The hardness and electrical conductivity of these materials are shown in Table 1. Figure 2 shows the relation between oxide content and the reignition voltage. In contact materials, the ability to stop arcing on ac currents depends on the thermal stability of the metal oxide present. The presence of metal oxides such as CdO, CuO, ZnO, SnO<sub>2</sub>, PbO, and NiO, whose decomposition temperatures are below the boiling point of silver, increases the arc extension or reignition voltage, as shown in Figure 2. On the other hand, ZrO<sub>2</sub>, MgO, and Al<sub>2</sub>O<sub>3</sub> decreases the reignition voltage.

Kornienko, et al.<sup>(3)</sup>, points out that fine, structural contacts made from "chemical mixtures" have substantially improved wear resistance over those made from mechanical mixtures. These authors investigated the possibilities of developing a technique to prepare a DS 70Ag-15Ni-15Cd alloy. They started with a mixture of Ag<sub>2</sub>CO<sub>3</sub> or silver oxalate plus nickel oxalate and CdCO<sub>3</sub>, which was thermally decomposed at 450 C under carefully controlled conditions. The mixture of powders was sintered for 1 hour at 850 C in a CO<sub>2</sub> atmosphere followed by extrusion and annealing at 700 C. The porosity

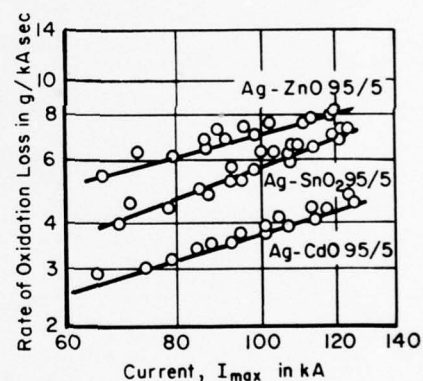


Figure 1. Oxidation of Various Silver-Oxide Composite Materials

Table 1. Density, Hardness, and Electrical Properties of Silver-Metal Oxide Composite Materials<sup>(2)</sup>

Material	Oxide Content		Density, g/cm <sup>3</sup>	Vickers Hardness		Electrical Conductivity m/Ohm mm <sup>2</sup>
	v/o	w/o		kg/mm <sup>2</sup>	MPa	
AgCdO	6.4	5	10.25	82	804.1	54
	12.5	10	10.02	85	833.6	49
	18.5	15	9.75	88	863.0	45
	24.4	20	9.60	83	814.0	39
	30.4	25	9.48	90	882.6	31
AgCuO	7.9	5	10.13	78	764.9	53
	15.2	10	9.82	82	804.1	42
	22.2	15	9.51	85	833.6	38
	29.4	20.5	9.25	87	853.2	29
AgSnO <sub>2</sub>	7.4	5	10.11	82	804.1	52
	14.4	10	9.85	84	823.8	45
	21.0	15	9.48	88	863.0	38
	27.2	20	9.26	88	863.0	32
AgZnO	7.2	4	10.20	84	823.8	52
	19.4	11.2	9.58	85	833.6	45
	25.0	15	9.12	83	814.0	38
	32.0	20	8.69	82	804.1	37
AgPbO	5.5	5	10.41	38	372.7	57
	10.9	10	10.32	49	480.5	51
AgNiO	8.0	5	10.12	60	588.4	52
	15.5	10	9.75	67	657.0	45
AgAl <sub>2</sub> O <sub>3</sub>	7.1	2.5	9.66	45	441.3	57
	13.7	5	9.18	60	588.4	48
AgMgO	7.1	2.5	9.95	74	725.7	52
	13.7	5	9.35	88	863.0	44
AgZrO <sub>2</sub>	7.6	5	10.08	65	637.4	52

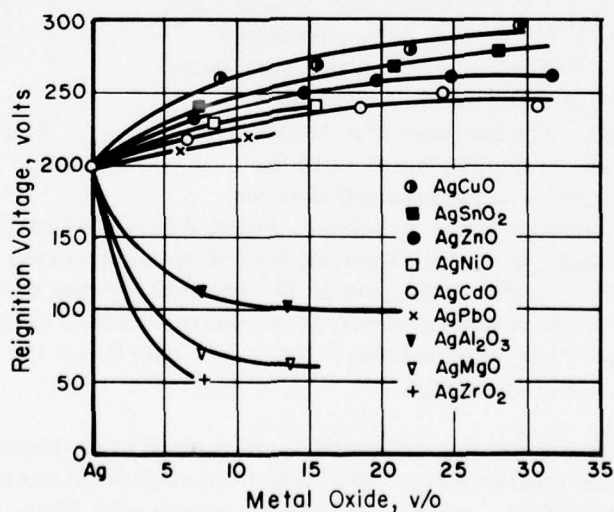


Figure 2. Dependence of Reignition Voltage of Various Silver-Metal Oxide Materials on the Metal-Oxide Volume Content <sup>(2)</sup>



was found to be only 2.8 percent and the Brinell hardness was 63 kg/mm<sup>2</sup> (617.8 MPa), a value close to the hardness obtained on fine structural contacts of Ag-CdO. The wear resistance of these electrical contacts was approximately 40 percent higher than that of the Soviets' standard SN 30 (Ag-30Ni) contacts. With an addition of 1 percent of graphite, the DS Ag-Ni-CdO alloy could be used both in moving and stationary contacts and the risk of contact sticking was practically eliminated.

Recently, Severin, et al.<sup>(4)</sup>, described the production of a whole series of DS Ag-CdO contact materials and contacts at the Albert Funk plant in Freiberg, East Germany. These carry the designations AgCdO-6, AgCdO-10, AgCdO-6K, and AgCdO-10K.

CONSIL 900<sup>(5)</sup> is a U.S. commercial Ag-CdO electrical contact alloy with long life. Reportedly, it often replaces fine silver and conventional silver alloys if requirements call for higher current-carrying capacity, greater resistance to sticking or welding, and/or lower temperature rise. The electrical conductivity, depending on the temper of the material, is between 81 and 87 percent IACS at 21 C. At contact temper it is 86 percent IACS. The alloy is available as strip, rod, or wire. Suggested applications include heavy-duty devices such as starting motors and contacts where high current, high inrush capacity, and resistance to arc erosion are needed. Poniatowski and Clasing<sup>(6)</sup> have produced silver and cadmium powders of 200- to 1000-microns diameter by internal oxidation. Ag-Al<sub>2</sub>O<sub>3</sub> powders with a particle size of less than 500 microns were also produced by atomizing the alloys. On further processing, several DS Ag-Al<sub>2</sub>O<sub>3</sub> alloys were made with the properties shown in Table 2.

Table 2. Mechanical and Electrical Properties of DS Ag-Al<sub>2</sub>O<sub>3</sub> Alloys at Room Temperature<sup>(6)</sup>

Al <sub>2</sub> O <sub>3</sub> %	Ultimate Strength		Yield Strength		Hardness		Elongation, %	Electrical Conductivity, m/ohm mm <sup>2</sup>
	kg/mm <sup>2</sup>	MPa	kg/mm <sup>2</sup>	MPa	kg/mm <sup>2</sup>	MPa		
1.0	35.0	343.2	30.0	294.2	105	1029.7	8	49.5-52.5
2.0	36.5	357.9	32	313.8	110	1078.7	16	42.0-44.0
0	14.0	137.3	2.5	24.5	26	255.0	40-50	62

Note that the yield strength was increased by a factor of 12 by the addition of 1 percent Al<sub>2</sub>O<sub>3</sub>. The rupture strength, determined on the Ag-Al<sub>2</sub>O<sub>3</sub> alloy at various temperatures, is given in Figure 3. The particle size in this alloy was ~130 Å. The electrical conductivity is about 80 percent that of pure silver while the chemical corrosion resistance is comparable. The authors recommend brazing techniques for joining. The high-temperature tensile and yield strengths of the DS Ag-Al<sub>2</sub>O<sub>3</sub> alloy are compared with those of pure silver in Figure 4.

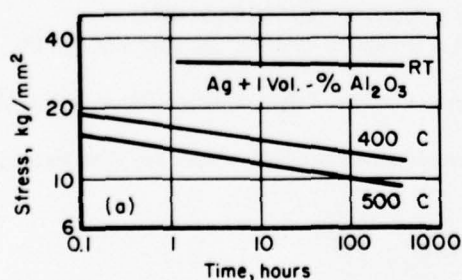


Figure 3. Stress-Rupture Strength of 2-mm-Diameter Ag-Al<sub>2</sub>O<sub>3</sub> Alloy Wire<sup>(6)</sup>

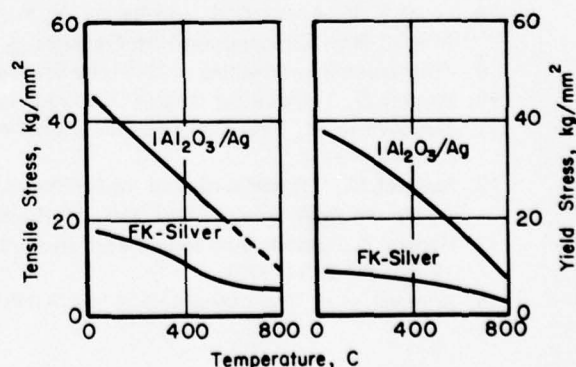


Figure 4. Elevated Temperature Tensile and Yield Strength of 2-mm-Diameter Ag-Al<sub>2</sub>O<sub>3</sub> Wire<sup>(6)</sup>

Sauer<sup>(7)</sup> covered  $\gamma$ -Al<sub>2</sub>O<sub>3</sub> particles having a size between 0.005-0.030 microns with 4-6 volume percent of silver in an electroplating bath. Control of pH in the HNO<sub>3</sub>-AgNO<sub>3</sub> electrolyte was very critical because of the effect on the microstructure and physical properties of the finished material. The powders were compacted, sintered, and extruded. The high-temperature rupture strength Ag-Al<sub>2</sub>O<sub>3</sub> (1.38 weight percent) 2-mm-diameter wire was 31.5 kg/mm<sup>2</sup> (308.9 MPa) at 200 C, 27 kg/mm<sup>2</sup> (264.8 MPa) at 400 C, 21 kg/mm<sup>2</sup> (205.9 MPa) at 600 C, and 16 kg/mm<sup>2</sup> (156.9 MPa) at 800 C. Stress-rupture strength at 800 C after 100 hours reached values of 8-9 kg/mm<sup>2</sup> (78.5-88.2 MPa).

Lenel<sup>(8)</sup> investigated DS Ag-GaO alloys by two techniques. One consisted in the freeze drying and subsequent reduction of AgNO<sub>3</sub> and Ga(NO<sub>3</sub>)<sub>2</sub> to silver and GaO, followed by pressing and sintering of the powder mixture. The other technique involved internal oxidation of a Ag-1 atomic percent Ga solid solution under conditions that yielded a uniform dispersion of oxides through the specimen cross section. No significant difference was noted between the average particle size and the particle spacing of the second phase in either alloy. However, the grain size of the internally oxidized type was 40 times that of the consolidated - powder type alloy. The temperature and stress dependence of the steady-state creep rate differed widely for the two alloys. This was attributed to the difference in grain size. More recently, other investigators have produced dispersion-strengthened silver by electrophoresis.<sup>(9)</sup>

Stoeckel<sup>(10)</sup>, Miskovicova<sup>(11)</sup>, and Besterici<sup>(12)</sup> have investigated the parameters of internal oxidation of Ag-Al and Ag-Mg alloys and how they relate to the theories of dispersion hardening.

Hansen<sup>(13)</sup> summarized the work of Brimhall, et al.<sup>(14)</sup> on the accelerated and delayed recrystallization of DS Ag alloys.

#### REFERENCES

1. Harmsen, U., Merl, W., Mery, C. L., and Vinaricky, E., "Untersuchungen an Silber-Metalloxid-Verbundwerkstoffe für elektrische Kontakte", *Z. Metallkunde*, **58** (11), 752-757 (1967).
2. Vinaricky, E., and Harmsen, U., "Einfluss des Silber-Metalloxid-Kontaktwerkstoffe auf die Löschung kurzer Wechselstromlichtbögen", *Metall.*, **25** (7), 749-754 (1971).
3. Kornienko, V. P., Namitkov, K. K., Semenov, M. W., and Yudin, B. A., "Ternary Compositions for Fine-Structural Electrical Contacts", *Poroshkovaya Metallurgiya*, **55** (7), 68-73 (July 1967).
4. Severin, G., Hesse, E., and Haussler, G., "Production of Dispersion-Strengthened Contact Materials and Contacts Containing Silver and Cobalt at the Albert Funk Establishments", *Freiberg, Neue Hütte*, **20** (2), 111-113, 116-117 (1975).
5. Alloy Digest, Filing Code Ag-8 (June 1975).
6. Poniatowski, M., and Clasing, M., "Dispersionsgehärtete Werkstoffe auf Silber- und Kupferbasis", *Z. Metallkunde*, **59** (3), 165-170 (1968).
7. Sauer, L., "Herstellung Dispersionsgehärteter Silberwerkstoffe", *VDI-Z*, **114** (16), 1189-1192 (1972).
8. Lenel, F. V., Ansell, G. S., and Nazmy, M. Y., "The Creep Properties of Dispersion Strengthened Silver-Gallium Alloys", *High Temperatures-High Pressures*, **3**, 439-444 (1971).
9. "Dispersion Strengthening of Metals by Electrophoresis", *Pokroky Praskove Met.*, **4**, 29-34 (1973).
10. Stockel, D., "Kinetik der inneren Oxydation von Ag-Al Legierungen", *Metall*, **25** (7), 755-760 (1971).
11. Miskovicova, M., "Verification of the Dispersion Hardening Theories in the Ag-Mg Systems", *Kovove Mat.*, **12** (4), 531-542 (1974).
12. Besterici, M., "Determination of the Parameters of Internal Oxidation in the Case of the Dispersion Strengthening of Ag-Mg and Ag-Al Alloys", *Prot. Met.*, **10** (6), 666-668 (1974).
13. Hansen, N., "Accelerated and Delayed Recrystallization in Dispersion-Hardened Materials", *Mem. Sci. Rev. Metall.*, **72** (3), 189-203 (1975).
14. Brimhall, et al., *Trans Metallurgical Soc. AIME*, **233**, 1076 (1965).

## ALUMINUM

### Commercial Alloys

The original development of SAP (sintered aluminum product) alloys in the 1940's spawned an intensive series of international alloy development programs for these materials. This is evident from Table 3, which lists the designations of some of the commercial SAP alloys that were subsequently developed in seven of the world's major manufacturing countries. Unfortunately, for reasons which are not completely clear, several of the earlier leading producers have at least temporarily discontinued production of these materials. This includes Alusuisse in Switzerland and Alcoa in the U.S. The suspected reasons for this disinterest include:

1. Comparatively high production costs relative to melted and wrought alloys
2. Lack of customer confidence due to insufficient accumulated service experiences
3. Difficulties with joining
4. Reports of embrittlement on long-time stressing.<sup>(1)</sup>

On the other hand, much work has been and continues to be done with these materials and these interests alone are deemed sufficient cause to document the characteristics of these famous SAP alloys in this review.

Some physical properties for alloys containing 6-14 percent  $\text{Al}_2\text{O}_3$  are given in Table 4. Room- and elevated-temperature tensile properties for some of these same materials in the as-received condition are given in Table 5.

Hammad<sup>(4)</sup> has investigated the effect of testing temperature, strain rate, and annealing treatments on the tensile properties of alloys containing from 1-7 percent alumina. Some of his results for the ISML 960-4 percent  $\text{Al}_2\text{O}_3$  alloy are shown in Figures 5-7. As shown in Figure 5, the ultimate tensile strength decreases rapidly with temperature to 400-450 C and slowly in the temperature interval 450-670 C. The effect of temperature on ductility is strongly dependent on extension rate, particularly at high temperatures. From room temperature to 300 C the ductility increases slightly and does not seem to be influenced by strain rate. At temperatures from 300-650 C, increasing strain rates markedly increase tensile ductility, particularly for material in the as-received condition. As expected, annealing the 4-percent  $\text{Al}_2\text{O}_3$  alloy for 4 hours at 600 C decreases its ultimate strength and increases tensile ductility, with these effects being most notable at temperatures below 350 C.

The tensile properties of SAP alloys as a function of alumina content at 400 C were determined by Gualandi and Jehenson<sup>(5)</sup> as shown in Figure 8. Figure 9 from this same study shows the stress to produce rupture in 1000 hours at 400 C on these same materials.

Solomir<sup>(6)</sup> has determined the effect of 2-year annealing treatments at temperatures up to 500 C on the tensile properties of a SAP alloy and compared these with the same treatments on conventional commercial alloys. In general, the SAP alloy showed inferior strengths at test temperatures below about 150 C, but considerably greater strengths above 150 C. The tensile ductility of the SAP alloy, however, was the lowest for all of the materials tested and decreased, with increasing exposure and test temperatures, to nearly zero after holding 2 years at 500 C and testing at 500 C.

Porembka<sup>(7)</sup> has reported extensively on the creep and stress-rupture properties of the alloys produced by Alcoa and Alusuisse. Some of his stress-rupture data for the SAP 895 alloy at 371 C (700 F), 427 C (800 F), and 482 C (900 F) are given in Figure 10.



Table 3. Nomenclature and Alumina Content of International Commercial DS Aluminum Alloys

Alumina Content, wt. %	Country and Alloy Designations					
	France(a)	Italy(b)	UK(c)	USA(d)		Switzerland(e)
				Pre 1962	Post 1962	
4	—	ISML 960	—	—	—	—
5	Frit 120-20-B	—	—	—	—	—
6	Frit 50-10-B	—	—	AMP-M257	XAP001(f) XAP005(g)	—
7	—	ISML 930	—	AMP-M583	—	SAP 930
8	Frit 50-15-B	—	—	AMP-M658	XAP002	SAP 920
10-11	Frit 20-07-D	ISML 895	Hiduminium 100	AMP-M470	XAP003	SAP 895
13-14	—	ISML 865	—	AMP-M430	XAP004	SAP 865

(a) Produced by Societ  des Trefileries et Laminoirs du Havre.

(b) Produced by Istituto Sperimentali Metalli Leggeri.

(c) Produced by Rolls Royce.

(d) Produced by Aluminum Company of America (Alcoa).

(e) Produced by Alusuisse.

(f) Made from flake.

(g) High-purity, low-iron-content nuclear grade.

Table 4. Physical Properties of Aluminum-Aluminum Oxide Alloys<sup>(2)</sup>

Property		XAP001, XAP005	XAP002, SAP 920	XAP003, SAP 895	XAP004, SAP 865
Specific gravity		2.74	2.74	2.75	2.77
Density, lb per cu in		0.099	0.099	0.099	0.100
Electrical conductivity at 25 C (77 F), %IACS		47	44	39	34
Thermal conductivity, cgs units (calculated on basis of electrical conductivity)	75 F	0.43	0.40	0.36	0.32
	400 F	0.44	0.43	0.39	0.36
	500 F	0.45	0.43	0.40	0.37
	600 F	0.45	0.43	0.41	0.38
	700 F	0.45	0.44	0.41	0.38
	800 F	0.45	0.44	0.42	0.39
	900 F	0.45	0.44	0.42	0.40
	1000 F	0.45	0.44	0.42	0.40
Average coefficient of thermal expansion, per F x 10 <sup>-6</sup>	68-212 F	12.0	11.8	11.5	11.1
	68-392 F	12.6	12.4	12.0	11.7
	68-572 F	13.1	12.9	12.5	12.1
	68-752 F	13.6	13.3	12.8	12.3
	68-842 F	13.9	13.8	13.0	12.5
Melting range of aluminum phase, F		Solidus for all alloys = 1180-1200 F			
		Liquidus for all alloys = 1215 F			
		Oxide phase melts at 3700 F (approx)			
Specific heat, cal per g (calculated)	68 F	0.213	0.212	0.211	0.210
	212 F	0.225	0.224	0.223	0.223
Damping		1.5 to 2.5 times as much damping capacity as other bare wrought alloys			

Table 5. Tensile Properties of Selected SAP Alloys<sup>(3)</sup>

Materials	Temp., C	Yield Strength (0.2% Offset) kg/mm <sup>2</sup>	Ultimate Ten- sile Strength, kg/mm <sup>2</sup>	Elongation, %
SAP 930	R.T.	11.8-14.7	22.6-24.6	18-26*
	400	6.8- 8.4	6.8- 8.8	6-11*
SAP 895	R.T.	17.8-22.5	28.6-36.4	8-12*
	400	8.8-10.8	9.8-11.8	3- 7*
SAP 865	R.T.	20.6-23.7	33.4-36.4	6.9*
	400	10.8-11.6	11.6-14.0	2.5-6*
SAP-ISML 930	R.T.	16.4-17.9	24.2-25.8	15.0* 18.1**
	400	7.5- 8.8	8.2- 9.2	6.3* 3.4**
SAP-ISML 895	R.T.	21.2-22.7	29.5-30.9	12.0* 11.8**
	400	8.9-12.6	10.7-13.1	3.5* 1.9**
SAP-ISML 865	R.T.	25.7-28.0	36.0-38.2	7.5* 7.9**
	400	11.9-14.5	13.5-14.5	2.0* 1.7**

\* Elongation in 5 diam.

\*\* Elongation in 10 diam.

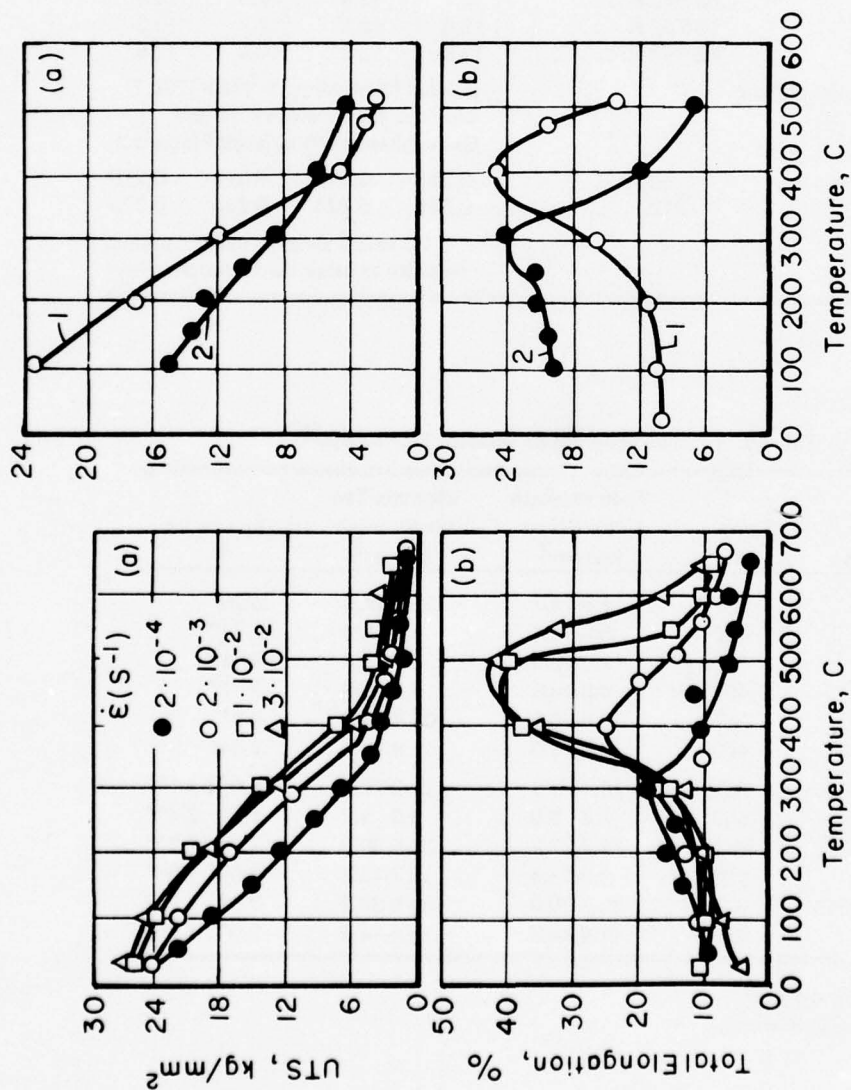


Figure 5. Effect of Temperature and Extension Rate on Tensile Properties of As-Received ISML 960 (4% Al<sub>2</sub>O<sub>3</sub>)<sup>(4)</sup>

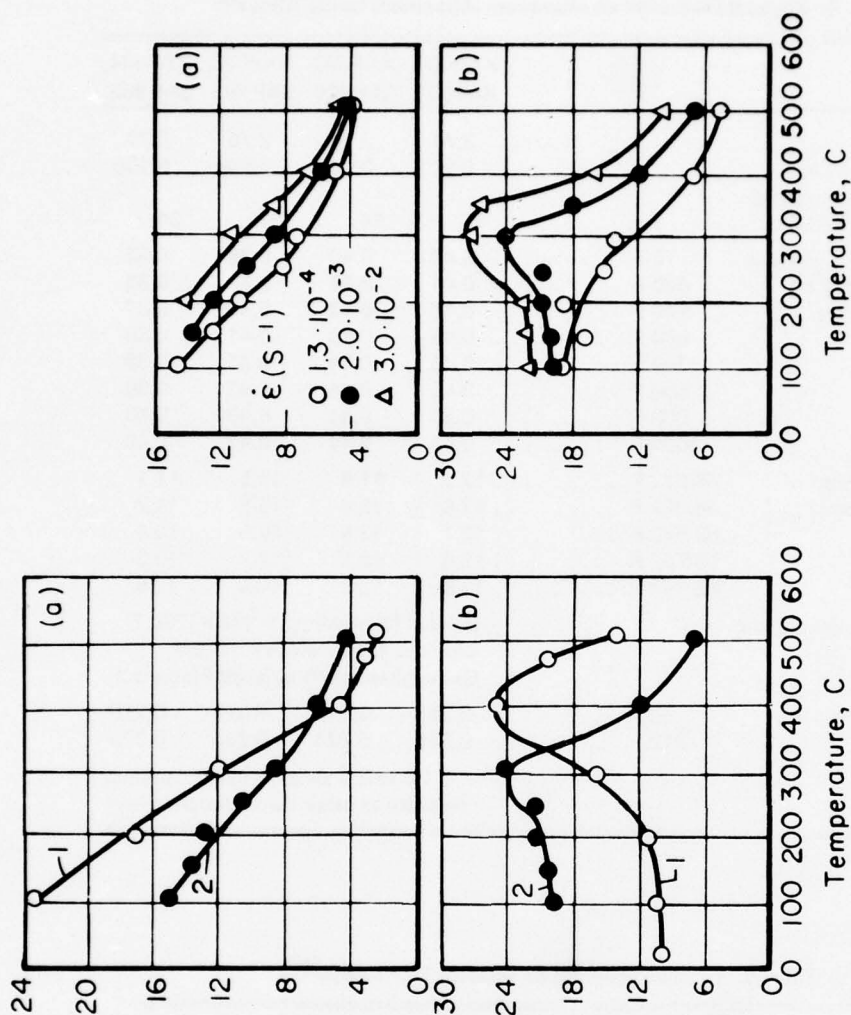


Figure 6. Comparison Between Tensile Behavior of ISML 960 (4% Al<sub>2</sub>O<sub>3</sub>) at Various Temperatures for As-Received (1) and Annealed 4 h, 600°C Before Testing (2); Extension Rate  $\dot{\epsilon} = 2 \cdot 10^{-3}$  sec<sup>-1</sup><sup>(4)</sup>

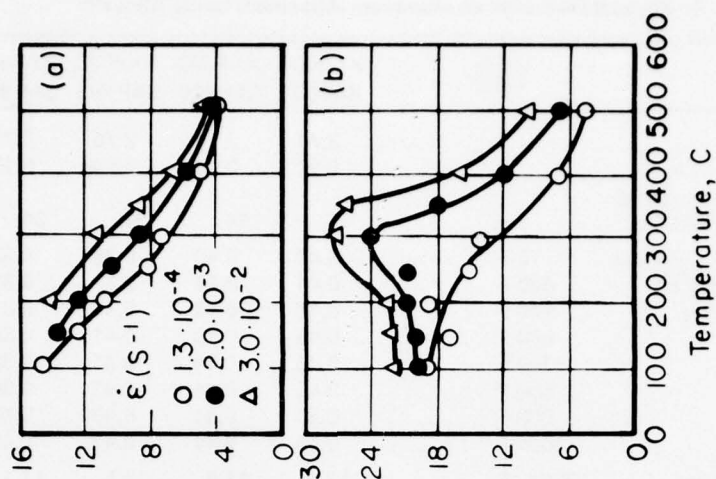


Figure 7. Effect of Temperature and Extension Rate on Tensile Properties of ISML 960 (4% Al<sub>2</sub>O<sub>3</sub>); Specimens were Annealed 4 h, 600°C Before Testing<sup>(4)</sup>



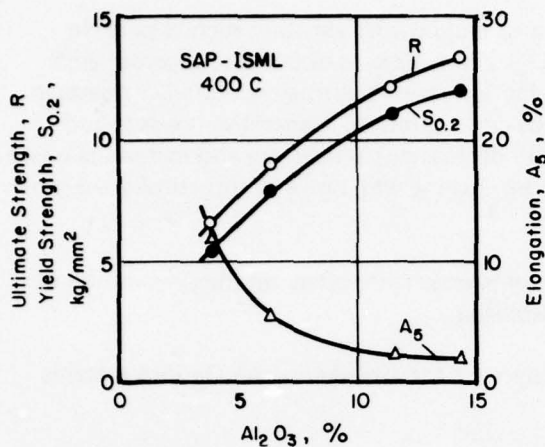


Figure 8. Tensile Properties of SAP Alloys at 400 C as a Function of  $\text{Al}_2\text{O}_3$  Content<sup>(5)</sup>

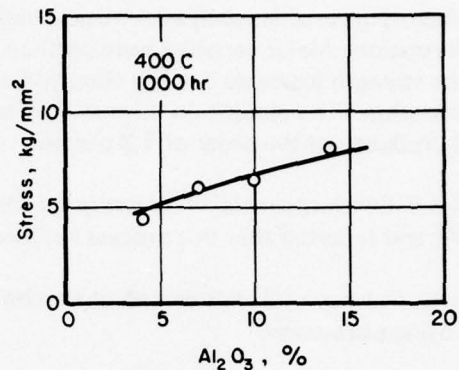


Figure 9. Stress to Produce Rupture in 1000 hours at 400 C as a Function of  $\text{Al}_2\text{O}_3$  Content<sup>(5)</sup>

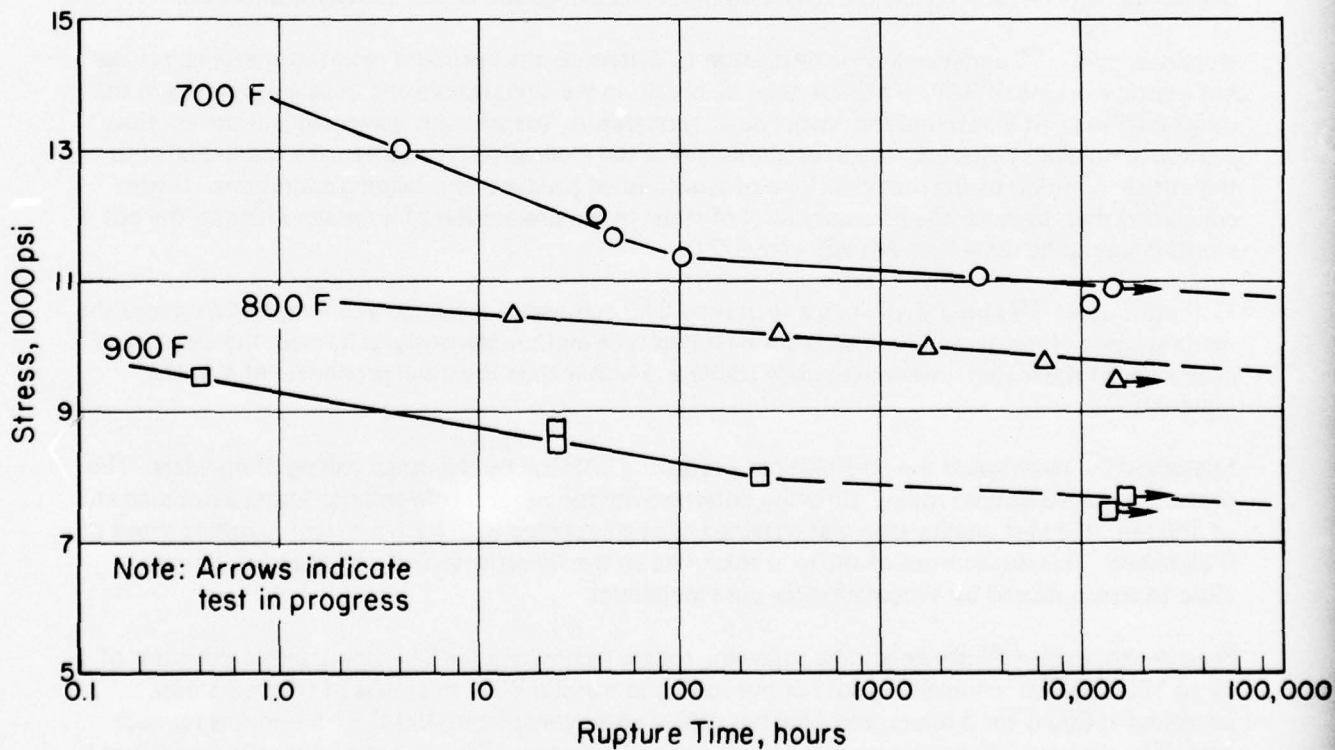


Figure 10. Stress-Rupture Curves For SAP 895 Alloy at 700, 800, and 900 F (371, 427, and 482 C)<sup>(7)</sup>

N. Hansen of the Danish Atomic Energy Commission has written extensively<sup>(8)</sup> on studies of dispersion-strengthened aluminum alloys and has included an extensive bibliography.

Hansen<sup>(9)</sup> has also investigated the effect of powder blending, and powder variables such as particle size, volume concentration, and type of oxide ( $\text{Al}_2\text{O}_3$ ,  $\text{SiO}_2$ ,  $\text{ZrO}_2$ ) used as dispersoid, together with manufacturing variables such as extrusion temperature, reduction ratio in extrusion, and heat treatment after extrusion. Major variables were particle size and oxide concentration. Generally, it was found that the strength increases and the elongation decreases with decreasing particle size and increasing oxide concentration. The elongation measured after extended creep testing was, however, practically the same for all products--of the order of 1-3 percent.

Matejka in Czechoslovakia<sup>(10)</sup> investigated the application of plasma technology on the preparation of ODS-Al and reported that this process has interesting possibilities.

Similarly, Polakovic<sup>(11)</sup> has described a technique and equipment for introducing  $\text{Al}_2\text{O}_3$  into metallic melts using ultrasound.

In 1963, Solomir<sup>(12)</sup> described the production of large SAP billets (0.5 meter in diameter and weighing over 400 lbs) by sintering them in a high vacuum without any protective sheath and then conveying them to the extrusion press in a transport chamber filled with inert gas. Hot upsetting was also carried out in an inert gas atmosphere. It was possible to obtain gas contents of less than 2 ml per 100 g of SAP which is about the same amount found in wrought aluminum alloys. He indicated that a similar but greatly simplified method of vacuum sintering produced a large amount of SAP with a gas content of 4-10 ml per 100 g. An important concern in this process was the distribution of the oxide since an uneven oxide dispersion lowers the tensile strength and elongation in the transverse direction.

Kursikov, et al. <sup>(13)</sup> undertook an investigation to determine the optimum temperature range for the hot plastic working of SAP. This was done by checking the compressive and tensile properties in the range 20-550 C. It was found that with rise in temperature, the strength decreased and the ductility showed anomalous behavior. It was established that the elongation anomalies were not linked with the initial condition of the material (type of semifinished product) and loading conditions. It was concluded that, to reach the necessary level of stress in the production of large sized blanks, the hot working should be done between 350 and 400 C.

Kurbatov, et al. <sup>(14)</sup> noted that when a re-pressed SAP compact was heated at a temperature above the melting point of the aluminum matrix for a limited time and subsequently deformed, the mechanical properties of the material were extremely stable and higher than the usual properties of the SAP materials.

Shelamov<sup>(15)</sup> investigated the possibility of producing SAP foil by the direct rolling of powders. The process consisted of cold rolling, sintering, intermediate rolling, and cold rolling. Using a roll diameter of 180 mm, the best quality strip was obtained at a roll opening of 2.3-2.5 mm with a rolling speed of 0.05 m/sec. This dependence of the strip thickness on the fill ratio of SAP was found to be very close to that obtained by Vinogradov for pure aluminum.

Severdenko, et al. <sup>(16)</sup> developed the following rolling technology for SAP strips with a thickness of up to 150 microns: compacting cold or hot rolling to a preliminary thickness of about 2.5 mm, annealing at 600 C for 3 hours, and final hot rolling with reheating to 450 C for 5 minutes for each pass. The area reduction per pass should not exceed 10 percent. Strips of several meters length and a width of up to 100 mm were produced.

Fridlyander, et al. <sup>(17)</sup> investigated the structure and recrystallization behavior of SAP 930 plate material. This work included the development of pole figures showing the textures that were developed during fabrication. Analysis of the pole figures and of the size of the coherent scattering regions showed that structural changes occur even after heating at 300 C for 100 hours. Primary recrystallization occurs under these conditions. Secondary recrystallization (new grains 1-10 microns in size) does not occur. Heating of the cold worked plate at 450 C leads to replacement of the deformation texture by the recrystallization texture.

Kolesnikov <sup>(18)</sup> determined optimum conditions for drawing and flanging (bending) of 1.5-mm-thick sheet of SAP-1. Understandably, he found that when the bending lines coincide with the rolling direction of the sheet, the minimum bend radius increases markedly. The relationship between the maximum drawing coefficient and the tool curvature radius was determined during die forming with heating.

Shelamov, et al., (see reference 120 of reference 19) have described their experiences in the production of clad sheets and pipes.

Gualandi, et al. <sup>(5)</sup> of the Instituto Sperimentale Metalli Leggeri (ISML) of Italy have described a number of their activities in producing a nuclear grade SAP. These activities were concerned with (1) the achievement of complete structural stability during prolonged heating through an effective degassing treatment during the processing of the material, with the attainment of better weldability as a consequence; (2) the improvement of the quality of the starting powder material in order to obtain the maximum uniformity of the semifinished products; (3) the development of methods to fabricate straight tubing with narrow dimensional tolerances and finned tubes with straight or helical fins; (4) the complete elimination of metallic impurities (e.g., iron) in order to achieve improved corrosion resistance, better formability, more homogeneous behavior toward organic materials, and smaller neutron absorption; and (5) an understanding of the structure of these materials.

Aastrup, et al. <sup>(20)</sup> have reviewed different welding methods as applied to sintered aluminum products. A major problem in joining is to prevent a decrease in high temperature strength by disturbing the specific distribution of dispersed particles. Gas content may be another important factor since the presence of a large amount of gas in the material is likely to result in a porous welding zone. The investigation by these authors was on 16-mm rod of SAP 930, SAP 895, and SAP 865, and also on some multifinned tubing. References are given on work done on the various methods which are grouped as follows:

- I) Direct joining of SAP to SAP
  - a) flash welding
  - b) magnetic-force welding
  - c) friction welding
  - d) hot-pressure welding
  - e) cold-pressure welding
  - f) ultrasonic welding
- II) Joining SAP to SAP using an intermediate layer
  - a) eutectic bonding—Ag-Al, Al-Si
  - b) brazing
- III) Joining SAP to aluminum alloys
  - a) all of the above processes
  - b) fusion welding.

Given the same material and specimen configuration, the zone adjacent to the bonding line will have a similar appearance regardless of the pressure-welding processes used. Mechanical properties of welds made by different pressure-welding methods are expected to be alike if carried out under optimum



conditions (see Figures 11 and 12). The mechanical properties measured probably indicate what can be expected in SAP welded by any pressure-welding process. That is, an ultimate tensile strength a little lower than the longitudinal strength of the parent material (about 90 percent for SAP 930) but well over the transverse strength of the parent material and a relatively poor elongation for the welded material.

Fusion welding can be used to join SAP and aluminum. With aluminum as a filler material, TIG and MIG welding can also probably be used for joining SAP to SAP. In all cases, success is largely dependent on close heat control and a process that prevents the arc forces from being directed onto the SAP materials.<sup>(20)</sup> For practical purposes, the authors recommend that attention be paid to the inferior high-temperature strength of unalloyed aluminum as compared with SAP. This necessitates particular emphasis on joint design in order to keep stresses low in the unalloyed aluminum part. However, the primary function of such a joint can be to provide tightness while the load is carried by other means. In fusion welding of SAP, a swelling of the parent material can be expected adjacent to the fused zone.

According to the data of Nikiforov (see reference 150 of reference 19), the use of AMg6 alloy wire in argon-arc welding can produce welded joints in dispersion-strengthened aluminum alloys with strengths of 30-35 kg/mm<sup>2</sup> (294-343 MPa) at room temperature. Good results were also obtained on soldering, particularly when both parts were of SAP. In contact welding (roller or spot), a good joint was produced when the parts to be welded were clad with some weldable aluminum alloy.

Kishnev, et al. <sup>(21)</sup> have described their experiences with argon-arc and diffusion-welded, finned SAP-1 tubes. The diffusion welding showed a number of advantages: (1) parts of complex configuration, including helically finned tubes, could be welded; (2) the welds were free of porosity; (3) the welded zone had the same corrosion properties as the parent metal; and (4) the structure and strength properties were virtually identical with those of the parent metal.

Hansen, in his 1967 paper<sup>(22)</sup>, reviewed the main properties of sintered aluminum products of interest when considering their application in nuclear technology. These include strength, elongation, corrosion resistance, homogeneity, purity, compatibility with fuel, and resistance to irradiation damage. He found that nuclear-grade SAP has acceptable properties for use as pressure tubes and canning material in organic reactors whereas for water-cooled reactors, the corrosion resistance was inadequate. He pointed out that manufacture of sintered aluminum products by various methods-milling, high temperature oxidation and powder blending-gave products with basically the same properties.

Cunningham<sup>(23)</sup> has also reported on work sponsored by the U.S. Atomic Energy Commission on the long-term irradiation of SAP material which was encouraging to the production of nuclear grades of SAP materials.

Ruedl and Kelly<sup>(24)</sup> studied damage and diffusion phenomena in aluminum and SAP alloys following bombardment with oxygen or an inert gas. It was found that there is a dose and dose-rate dependence for the appearance of damage in these materials following 9-keV oxygen and neon bombardments. The arrangement of the damage for low doses depends on whether the damage is produced by oxygen or neon. In the first case, the damage is more aligned, while in the second it is more random. The damage in oxygen-bombarded foils anneals out roughly in the temperature range for aluminum self-diffusion. The damage in neon-bombarded foils, on the other hand, persists to above 500 C for aluminum and to above 625 C for SAP. In addition, specimens heated above 500 C showed small bubbles and large undefined features. The latter were probably gas pockets or blisters near the metal-oxide-skin interface.

Hansen and Clauer<sup>(25)</sup> studied the characteristics of high-temperature dispersion hardening by fabricating an Al-Al<sub>2</sub>O<sub>3</sub> alloy having coarse elongated grains. Under these conditions, the contribution of grain boundary sliding is minimized and most of the deformation must occur within the dispersion-hardened

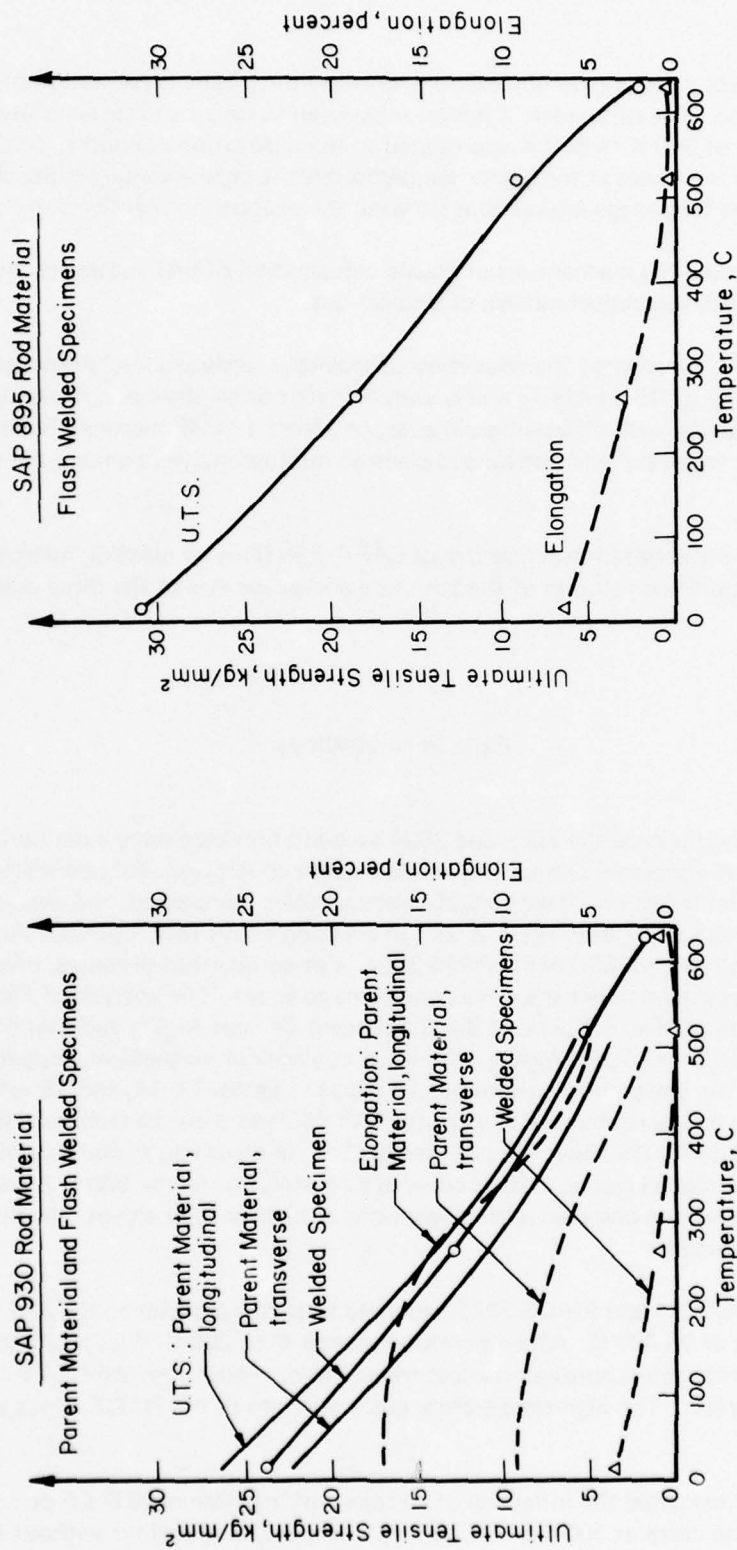


Figure 11. Ultimate Tensile Strength and Total Elongation Versus Temperature as Measured for Flash Welded SAP 930 6-mm Rod Material. Each Point Represents the Mean of Four Measurements. Typical Curves of Longitudinal and Transverse U.T.S. and Total Elongation for the Parent 16-mm Rod Material Included (20)

Figure 12. Ultimate Tensile Strength and Total Elongation Versus Temperature as Measured for Flash Welded SAP 895 6-mm Rod Material. Each Point Represents the Mean of Four Measurements (20)

matrix. The creep characteristics of an alloy containing 0.8 percent  $\text{Al}_2\text{O}_3$  were studied and related to theory.

Falzone, et al. <sup>(26)</sup> made comparative observations to study the plastic deformation of SAP 960, cold rolled and recrystallized. The difference in behavior between as-rolled and recrystallized SAP sheets in the temperature range of 300 K to 600 K was related to the dislocation networks. In the recrystallized samples and in the as-rolled ones at the higher temperatures, the experimental results are consistent with back stresses due to the long range interactions between the dislocations held back by the oxide particles.

Guyot<sup>(27)</sup> has also studied the mechanisms of plastic deformation of SAP materials, and compared his experimental results with theoretical models of dislocations.

Nechaev and Pustov<sup>(28)</sup> investigated the relaxation of vacancies, dislocations, and pores during the quenching and annealing of DS Al- $\text{Al}_2\text{O}_3$  alloys with different dimensions and distribution of oxide inclusions and, accordingly, with different grain sizes, i.e., from 1-1000 microns. Relative electrical resistance, hydrostatic weighing, and optical and electron microscopy were among the techniques used.

Earlier, Polyanskii<sup>(29)</sup> investigated the structure of SAP-1 thin films by electron microscopy. Paisov, et al. <sup>(30)</sup> have also reported on studies of the structure and properties of the three common types of SAP.

### Experimental Alloys

Recently, Wilcox<sup>(31)</sup> synthesized the 7075 and 2024 precipitation hardening aluminum alloys with a high volume fraction of dispersoid (about 12 volume percent of  $\text{Al}_2\text{O}_3$ ). Ribbon melt-spun 7075 and 2024 alloys were ball milled to fine flake ( $\sim 0.25$  micron thick), compacted, and extruded. These alloys were named PH-DS 7075 and PH-DS 2024. In addition alloys with 1 percent  $\text{Al}_2\text{O}_3$  of the same material were made and named MS 7075 and MS 2024. For comparison purposes, billets of commercial 7075 and 2024 were extruded under the same conditions as above. The analysis of PH-DS 7075 was 2.2 percent Mg, 1.5 percent Cu, 5.5 percent Zn, 0.1 percent Cr plus  $\text{Al}_2\text{O}_3$  and that of PH-DS 2024 was 1.3 percent Mg, 4.0 percent Cu plus  $\text{Al}_2\text{O}_3$ . The alloy contents of magnesium, copper, and zinc were very close to those of the corresponding commercial alloys. Figures 13, 14, and 15 summarize some of the data obtained and compare the new alloys with SAP 865 and with the commercial alloys in the strongest condition. The PH-DS alloys did not recrystallize on annealing at 500 C, while MS alloys recrystallized to fine equiaxed grains, 1-10 microns in diameter, during the 500 C anneal. Superplastic behavior of the MS alloys was observed with elongations as high as 185 percent, but these alloys exhibit only marginal superplasticity.

The as-extruded PH-DS 2024 and PH-DS 7075 had yield strengths superior to the SAP 865 alloy over the temperature range of 25-400 C. At temperatures greater than 250 C, the PH-DS alloys had higher strength than their commercial counterparts heat treated to optimum strength (7075-T6 and 2024-T81), but their ductility was low. The high-temperature creep strength of the PH-DS alloys was far superior to commercial alloys.

Reinolds, et al. <sup>(32)</sup> investigated the influence of additions of magnesium (0.8-4.5 percent) and Cu (0.6-1.7 percent) on the creep at 500 C of SAP alloys. Whereas, in the alloys without  $\text{Al}_2\text{O}_3$ , the addition of magnesium reduces the creep rate by approximately 100 times, the addition of Mg in com-



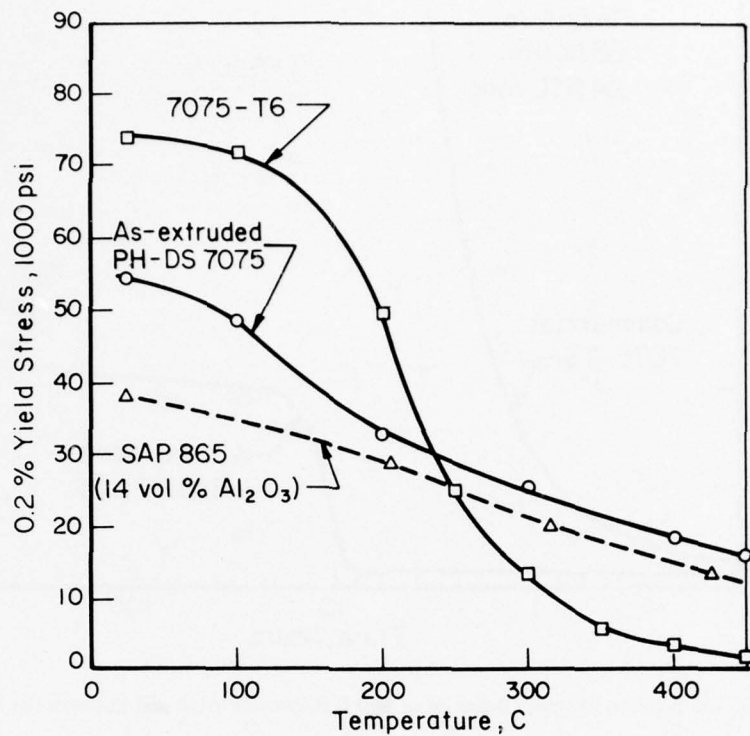


Figure 13. Yield Strength of As-Extruded PH-DS 7075 as a Function of Temperature, Compared with Data from the Literature on Commercial 7075-T6 and a SAP Alloy<sup>(31)</sup>

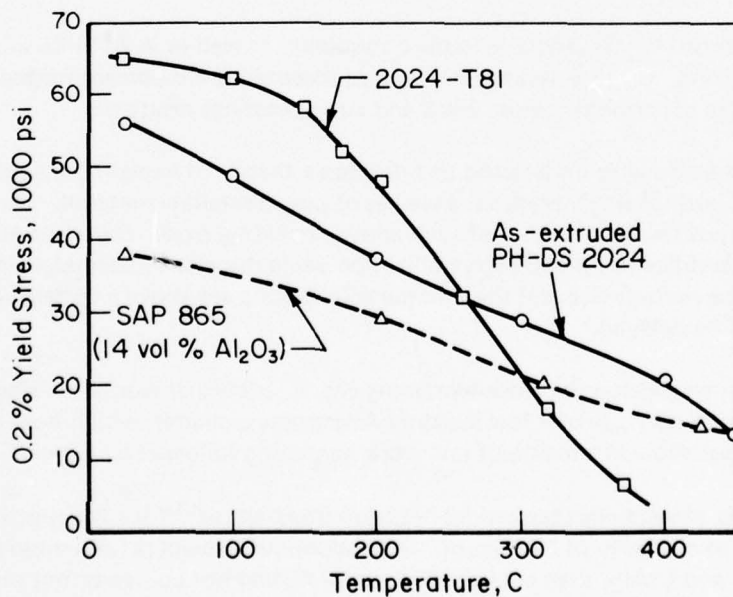


Figure 14. Yield Strength of As-Extruded PH-DS 2024 as a Function of Temperature, Compared with Data from the Literature on Commercial 2024-T81 and a SAP Alloy<sup>(31)</sup>

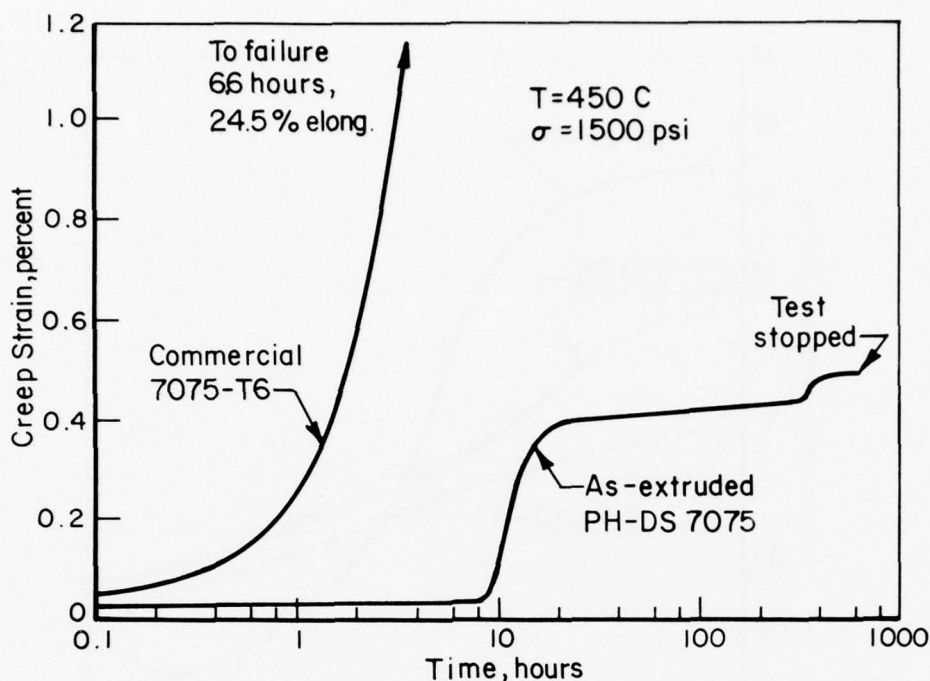


Figure 15. Comparison of Creep Behavior at 450 C Between PH-DS and Commercial 7075<sup>(31)</sup>

bination with  $Al_2O_3$  causes a drop in the creep rate of only 2.5 times. The overall influence of alloying of the matrix on the heat resistance of the alloys is, therefore, negative because of lowering of the melting temperature of the matrix. In the area of low and moderate temperatures, however, DS Al alloys with an alloyed dispersant have higher heat resistance than those with a non-alloyed matrix.

Pai, et al. <sup>(33)</sup> introduced  $Al_2O_3$  particles in pure aluminum as well as in Al-Si-Cu alloys, using superheated melts and stirring. Up to 4 percent  $Al_2O_3$  was accepted if 4.5 percent magnesium was also added. The melt was cast into permanent molds. Hard and strong castings resulted.

Much research has been done to understand and develop a theory to explain the hardening of dispersion-strengthened alloys, both of single crystals as well as of polycrystalline material. Hansen<sup>(34)</sup> has compared accelerated and delayed recrystallization of such alloys, including oxide dispersion-strengthened aluminum. He noted the oxide additions retarded recrystallization while dispersed intermetallics may accelerate recrystallization if the particle size and the interparticle spacing are above a certain value. If smaller, recrystallization will be delayed.

Matsuura, et al. <sup>(35)</sup> investigated the work-hardening characteristics of aluminum single crystals containing equiaxed silicon particles of a few hundred Angstroms diameter, which were obtained by aging. The stress-strain curves showed a region of low work hardening followed by a region of rapid hardening.

The addition of other dispersoids than oxides has been investigated<sup>(36)</sup> for the specific purpose of raising the modulus of elasticity of aluminum. Thus, aluminum powders (200 mesh size) were mixed with  $MnAl_6$ ,  $NiAl_3$ , and  $CrAl_3$ , then cold pressed, sintered, and hot coined or hot pressed and extruded. If the volume proportion of the dispersoid was substantial, it was possible to increase the modulus by 20-50 percent. More effective was the addition of fine TiC powder over the range of 5-40 weight percent (3-27 volume percent). A 15 weight percent addition resulted in a modulus of the order of  $13 \times 10^6$  psi ( $.09 \times 10^6$  MPa).

More recently, Misra and Upadhyaya<sup>(37)</sup> added up to 8 volume percent of TiC or WC to aluminum and by thermal-cyclic sintering achieved high densities. After hot deformation at 400 C, the Al-TiC alloys were consistently harder than the Al-WC alloys on the basis of equivalent volume percent of carbide.

Towner<sup>(38)</sup> found that a coarse atomized Al-FeAl<sub>3</sub> alloy had better combinations of ductility and strength than SAP alloys of medium oxide content at temperatures from 25-430 C.

The Aluminum Company of Canada recently described<sup>(39)</sup> some new alloys that utilize insoluble particles for dispersion or grain-boundary strengthening in combination with a fine grain size, i.e., from 0.5-3 microns. The insoluble particles are intermetallics, which are held to a size of about 0.3 micron in diameter by the plastic deformation of a rapidly solidified ingot of eutectic composition. The eutectics that are applicable contain brittle rod-like intermetallic phases of a small volume fraction (5-10 percent) and include the Al-Fe-Mn, Al-Mn-Ni, and Al-Fe-Si systems. The principal interest in these materials is for large volume markets (e.g., automotive sheet) where a relatively cheap alloy with an improved combination of strength and ductility at room temperature is needed rather than for specialized uses where good elevated-temperature properties are needed. Figure 16 illustrates the range of room-temperature tensile properties available in one of these candidate alloys.

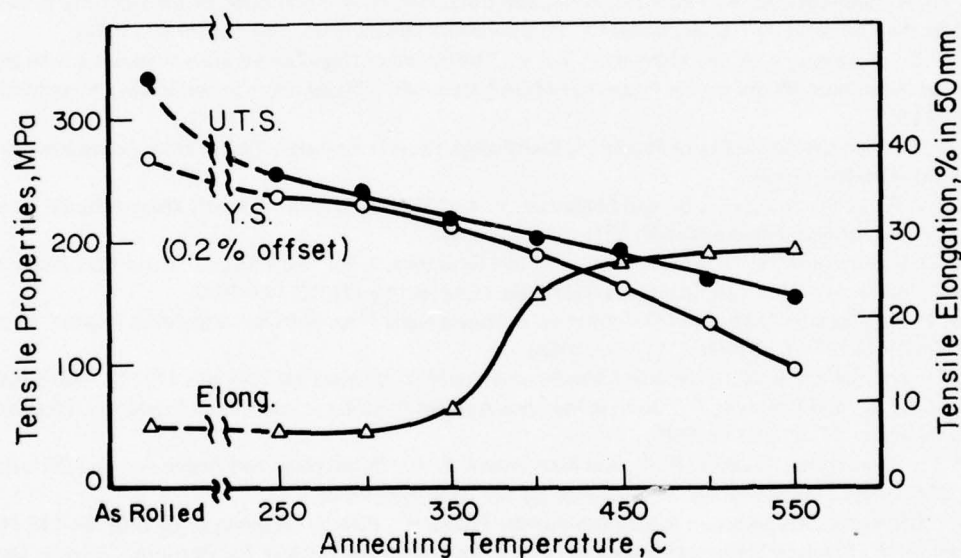


Figure 16. Room-Temperature Tensile Properties of Al-1.6Fe-1.9Ni-0.5 Alloy After Various 2-Hour Isochronal Anneals<sup>(39)</sup>



## REFERENCES

1. Rühle, M., "Neuartige Dispersionsgehartete Aluminiumlegierungen", *Metall*, **29** (3), 237-247 (1975).
2. Van Horn, K. R., *Aluminum*, Volume I, American Society for Metals (1967), pp 347-353.
3. Hansen, N., "Tensile Properties at Room Temperature and at 400 C of Commercial SAP", Riso Report 96 (1964). (AD 461 231)
4. Hammad, F. H., and Shafie-Taha, A., "Effect of Temperature and Extension Rates on the Tensile Properties of Some Sintered Aluminum Powder Alloys", *Aluminium*, **52** (3), 172-175 (1976).
5. Gualandi, D., and Jehenson, P., "Powder Metallurgy of Al-Al<sub>2</sub>O<sub>3</sub> Composites (SAP) for Nuclear Applications", *Modern Developments in Powder Metallurgy*, H. H. Hausner, Editor, Plenum Press (1966), pp 36-58.
6. Solomir, J. G., "Übersicht über die Pulvermetallurgie des Aluminium", *Z. f. Metallkunde*, **52** (10), 645-651 (1961).
7. Porembka, S. W., "Progress on USAEC/AECL Cooperative Program", Report No. BMI-X-266, Battelle Memorial Institute AEC Contract No. W-7405-eng-92 (December 1963).
8. Hansen, N., "Bibliography on DSM", Riso Report 48 (1962, 1964, and 1967). (AD 453 028 and AD 476 152)
9. Hansen, N., "Dispersion Strengthened Aluminum Products Manufactured by Powder Blending", *Powder Metallurgy*, **12** (23), 23-44 (1969).
10. Matejka, D., "Dispersion Strengthened Aluminum-Al<sub>2</sub>O<sub>3</sub> Produced by Plasma Spraying", *Kovove Mat.*, **12** (5), 667-675 (1974).
11. Polakovic, A., "Experimental Equipment for Introduction of Insoluble Particles into Metallic Melts by Help of Ultrasound", *Kovove Met.*, **11** (6), 726-728 (1973).
12. Solomir, J. G., "Progress in Sintered Aluminum Alloys", *Metal Progress*, 105-108 (January 1963).
13. Kursikov, Yu. N., Sitnikova, M. A., Fedorova, A. V., and Borzunov, A. A., "Variation of the Ductility of SAP Material Over the Temperature Range 20-550 C", *Poroshkovaya Metallurgiya*, **149** (5), 26-29 (1975).
14. Kurbatov, V. S., Shelamov, V. A., and Shmakov, Yu. V., "Influence of High-Temperature Annealing with the Melting of the Aluminum Matrix on the Properties of SAP Materials", *Transl. from Poroshkovaya Metallurgiya*, **57** (9), 711-713.
15. Shelamov, V. A., "On the Possibility of Producing SAP Foil by Powder Rolling", *Transl. from Poroshkovaya Metallurgiya*, **26** (2), 104-107 (1965).
16. Severdenko, V. P., Lozhechnikov, E. B., and Shelamov, V. A., "Rolling of Strips Directly from Sintered Aluminum Powder", *Soviet JI. of Non-Ferrous Metals*, **5** (1), 92-94 (1964).
17. Fridlyander, I. N., Barsukov, V. N., Stepanova, M. G., and Smirnova, I. N., "Fine Structure and Recrystallization of SAP-1 Plate", *Metallovedenie i Termicheskaya Obrabotka Metallov*, **13** (7), 13-14 (1971).
18. Kolesnikov, N. P., "Specific Features of Deformation in Sheets made from Sintered Aluminum Powder", *Tsvetnye Metally Soviet JI. Non-Ferrous Metals*, **41** (4), (1968).
19. Portnoy, K. I., and Babich, B. N., "Dispersion Hardened Materials", *Moscow Metallurgiya* (1974). (ADB 009 068)
20. Aastrup, P., Moe, A., and Knudsen, P., "Joining Methods Applied to Sintered Aluminum Products", *Metallurgical Society Conferences*, **47**, 813-844 (1968).
21. Kishnev, P. V., Charukhina, Kazakov, N. F., and Kuznetsova, E. A., "Production and Argon-Arc and Diffusion Welding of Finned SAP Tubes", *Poroshkovaya Metallurgiya*, **86** (2), 160-163 (1970).
22. Hansen, N., "Dispersion-Strengthened Aluminum Powder Products", *Powder Metallurgy*, **10** (20), 94-115 (1967).
23. Cunningham, G. W., "United States Experience in Powder Metallurgy for Nuclear Applications", *Powder Metallurgy*, **10**, 78-93 (1967).
24. Ruedl, E., and Kelly, R., "Damage and Diffusion in Aluminum and an Al-Al<sub>2</sub>O<sub>3</sub> Alloy Following Bombardment with Oxygen or Inert Gas", *Modern Developments in Powder Metallurgy*, **2**, 145-159 (1966).
25. Hansen, N., and Clauer, A. H., "Dispersion Strengthening at High Temperatures in Al-Al<sub>2</sub>O<sub>3</sub> Alloys", *The Micro-structure and Design of Alloys*, Proc. of the 3rd Conference on the Strengthening of Metals (1973), pp 321-325.
26. Falzoni, G., Gondi, P., Patuelli, C., and Tognato, R., "Plastic Deformation of DS SAP Alloys - Dislocation Emission and Sink Phenomena", *Metallurgical Trans.*, **4**, 2115-2122 (1973).
27. Guyot, P., "On the Mechanism of Plastic Deformation of SAP-Type Alloys", *Modern Developments in Powder Metallurgy*, H. H. Hausner, Editor, Volume 2 (1966), p 112.
28. Nechaev, Yu. S., and Pustov, Yu. A., "Study of the Relaxation of Defects in Alloy Composition During Quenching and Annealing", *Izvestiya VUZ Chernaya Metallurgiya*, (7), 133-140 (1975).
29. Polyanskii, V. M., and Spiridonov, V. B., "Electron Microscopic Investigation of the Structure of SAP", *Transl. from Metallovedenie i Termicheskaya Obrabotka Metallov*, (12), 37-39 (1963).
30. Paisov, A. I., Kolpashnikov, A. I., and Pan Ya-Chen, "Structure and Properties of SAP", *Soviet JI. Non-Ferrous Metals*, **III** (10), (1962).

# REFERENCES (Cont.)

31. Wilcox, B. A., "Microstructural Synthesis in Combined Precipitation Hardened - Dispersion Strengthened (PH-DS) Aluminum Alloys", AFML-TR-72-238 (December 1972). (MCIC-87255)
32. Reinolds, G. H., Lenel, F. V., and Ansell, G. S., Metal Trans., 2 (11), 3027-3034 (1971).
33. Pai, P. C., Ray, S., Prabhakar, K. V., and Rohatgi, K. V., reported in Foundry, 196 (April 1976).
34. Hansen, N., "Recrystallization accélérée et retardée dans les produits renforcés par des dispersions", Mem. Scient. Revue Metallurgie, 189-203 (March 1975).
35. Matsuura, K., Ishizaka, A., and Watanabe, K., "The Work Hardening of Aluminum Alloy Single Crystals Containing Silicon Particles", The Microstructure and Design of Alloys, Proc. of the 3rd Conference, 36, paper 59, 291 (1974).
36. MacDonald, N. F., and Ransley, C. E., "Preparation of High-Modulus Aluminum Alloys by Powder Metallurgy", Symposium on Powder Metallurgy, 1954, Special Report No. 58, The Iron and Steel Inst., London (1956), pp 242-252.
37. Misra, P. S., and Upadhyaya, G. S., "Properties of Sintered Aluminum Dispersed with TiC and WC", Intern. J. of Powder Metallurgy and Powder Technology, 11 (4), 129-133 (1975).
38. Towner, R. J., "Atomized Powder Alloys of Aluminum", Metal Progress, 73 (5), 70-76, 176, 178 (1958).
39. Morris, L. R., "Grain Boundary Strengthened Aluminum Sheet", Preprint of paper presented at the 4th International Conference on the Strength of Metals and Alloys (August 1976).

## GOLD

Fuschillo and Gimpl<sup>(1)</sup> have recommended a gold 2-volume-percent  $\text{ThO}_2$  alloy wire for applications requiring good tensile properties and hardness, combined with low resistivity and oxidation resistance at high temperatures. The alloys were prepared by dissolving gold in aqua regia to form a solution of  $\text{AuCl}_3$ . Dispersoid particles of  $\text{ThO}_2$  or  $\text{Al}_2\text{O}_3$  were then suspended in a dilute basic solution of the  $\text{AuCl}_3$  by stirring. Hydrazine was added causing the gold to precipitate and uniformly coat the oxide particles. When the reduction process was complete, the powdered alloy was filtered and vacuum dried. The alloy powders were then degassed in dry hydrogen at 900 C for 4 hours and pressed into 2.5-cm-diameter slugs, canned in copper, evacuated, and extruded at 650 C with a 30:1 reduction. Then they were cold rolled into wire with intermediate anneals.

The tensile properties of the alloys are summarized in Table 6. The best properties were obtained in a 3.4-volume-percent  $\text{ThO}_2$  alloy. The 3.5-volume-percent  $\text{Al}_2\text{O}_3$  alloy showed considerable particle growth when heated at 900 C. Recrystallization in the 3.4-volume-percent  $\text{ThO}_2$  alloy occurred about 200 C higher than for pure unalloyed gold. No appreciable grain growth was noted in the alloy after annealing at 100 C for 4 hours.

The electrical resistivity of the alloys was greater than predicted by a simple volume effect. This is attributed to impurities which were introduced and to work hardening during the processing steps. The slightly lower temperature coefficient of resistivity was attributed to the tendency of  $\text{ThO}_2$  to absorb impurities at high temperatures. The Au- $\text{Al}_2\text{O}_3$  alloy showed a greater increase in resistance for a given volume of oxide. This may be related to the lower free energy of formation of  $\text{Al}_2\text{O}_3$ , leading to a higher aluminum content in the gold.

Sautter<sup>(2)</sup> in 1963 investigated the electrodeposition of gold with dispersoids and since has studied the creep behavior of Au- $\text{Al}_2\text{O}_3$  alloys. In 1968<sup>(3)</sup>, he reported that a fine dispersion can introduce a threshold stress for creep initiation. A substantial increase in threshold stress was observed between pure gold and gold alloys strengthened with particles of 1-micron diameter. A later publication<sup>(4)</sup> confirmed the existence of porosity in these alloys. Finally, the role of surface energy on high-temperature creep strength was assessed.<sup>(5)</sup> The steady-state creep in the Au- $\text{Al}_2\text{O}_3$  alloys at very high temperatures and low stresses was found to proceed in two stages, both of which show a linear dependence between creep rate and applied stress. It was suggested that creep in the first region is associated with the movement of pinned grain boundaries while in the second region the effect of pore growth is also included. Equations describing the threshold stress as well as that for pore growth were derived from grain boundary and surface energy considerations. Good correlation was obtained with experimental results.



Table 6. Tensile Properties of Dispersion-Strengthened Gold Alloys<sup>(1)</sup>

Alloy	Test Temperature, C	Ultimate Tensile Strength		Yield Strength (0.2% offset)		Elongation, %
		psi	MPa	psi	MPa	
Au-3.4 vol. % ThO <sub>2</sub> Cold rolled 55%	25	31,500	217	26,500	183	2.7
	260	28,500	196	25,500	176	2.7
	537	17,900	123	16,300	112	2.0
Au-3.5 vol. % Al <sub>2</sub> O <sub>3</sub> Cold rolled 60%	25	35,000	241	32,000	220	1.4
	260	32,800	226	29,500	203	3.2
	537	11,100	76	8,900	61	5.1
Au-6.4 vol. % Al <sub>2</sub> O <sub>3</sub> Cold rolled 50%	25	35,000	241	33,000	227	1.0
	260	21,900	151	19,800	136	1.0
	537	8,400	58	7,100	49	2.1
Au made by powder metallurgy Cold rolled 60%	25	29,700	205	26,800	185	1.9
	260	16,100	111	—	—	4.2
	537	7,800	54	6,900	48	12.0

#### REFERENCES

1. Fuschillo, N., and Gimpl, M. L., "Electrical and Tensile Properties of Cu-ThO, Au-ThO<sub>2</sub>, Pt-ThO<sub>2</sub> and Au-Al<sub>2</sub>O<sub>3</sub>, Pt-Al<sub>2</sub>O<sub>3</sub> Alloys", J. Mater. Sci., **5**, 1078-1086 (1970).
2. Chen, E. S., and Sautter, F. K., "Interfacial Energy and the High Temperature Strength of Dispersion-Strengthened Gold-Al<sub>2</sub>O<sub>3</sub> Alloys", Watervliet Arsenal Technical Report WVT-7153 (August 1971). (MCIC-81948)
3. Sautter, F. K., "Electrodeposition of Dispersion-Strengthened Au-Al<sub>2</sub>O<sub>3</sub> Alloys", Watervliet Arsenal Technical Report RR-6321 (December 1963).
4. Sautter, F. K., and Chen, E. S., "Oxide Dispersion Hardening", Metallurgical Society Conferences, **47**, 495 (1968).
5. Sautter, F. K., and Chen, E. S., "Porosity in Gold-Alumina Alloys", J. Electrochem. Soc., **117**, 726 (1970).

## BERYLLIUM

Two dispersion-strengthened beryllium alloys are available commercially <sup>(1)</sup>—Berylco PS-20 (sheet) and PR-20 (plate). These alloys contain about 1.4 and 1 weight percent of BeO, respectively. Both alloys have found application in aerospace and nuclear reactors because of their low density, high specific strength, very high modulus of elasticity, and high neutron-scattering factor. Lockalloy <sup>(1)</sup>, a Be-37Al alloy may also be strengthened by the presence of 0.7 percent of BeO and Al<sub>2</sub>O<sub>3</sub>.

Actually, all industrial grades of beryllium are essentially dispersion hardened since they are made from powder containing from 0.7-1.5 percent BeO. Due to the unavoidable presence of oxide films, blanks produced from fine-grained powder have higher mechanical properties than those from large-grained powders. <sup>(2)</sup>

Webster, et al. <sup>(3)</sup> investigated the structure and creep properties of beryllium with various morphologies and compared them with PR-20 and ingot beryllium. For material given 10 percent reduction, the lowest recrystallization temperature (650 C) was found for the oxide-free ingot beryllium. This recrystallization temperature increased to 760 C for PR-20 with a coarse oxide dispersion. An experimental alloy with a finer dispersion recrystallized at 1085 C, after a 10 percent reduction. An anomalously high creep strength was found for the latter material—3700-3800 psi stress at creep rate of 10<sup>-2</sup> percent per second at 980 C. This was explained partly by the efficient oxide dispersion and also by the residual dislocation structure. After annealing at 1200 C, this alloy lost most of its substructure and its creep strength decreased significantly. The authors concluded that the creep strength of beryllium at 980 C is controlled by a dislocation substructure that is stabilized by a fine BeO dispersion, and the volume of liquid phase present in the grain boundaries. Further, the effectiveness of a BeO dispersion in stabilizing a dislocation substructure is inversely proportional to the BeO particle size. The volume of liquid phase present in the grain boundaries at 980 C is proportional to the total amount of aluminum and silicon in the alloy. <sup>(3)</sup>

This work was a sequel to previous work on the recrystallization of beryllium <sup>(4)</sup> where, in an alloy with a median size of oxide of 600 Angstroms, a dislocation substructure was maintained up to very near the melting point of beryllium. The extent to which the recrystallization temperature was raised was inversely proportional to the size of the oxide dispersion.

Moberley, et al. <sup>(5)</sup> studied the processing of beryllium and its alloys by powder metallurgy to produce isotropic material. The classical techniques produce anisotropic materials, which is undesirable for certain beryllium applications. The influence of oxide content on the properties of sintered blanks is presented in Table 7. Higher strengths were obtained, as expected, with the higher oxide content and finer grain size. The yield strength of the fine grain size FP-17 compacts is 10-20 percent higher than that of the SP 200 samples. At room temperature, all samples exhibited a maximum 2 percent elongation before fracture. After deformation leading to the rupture of the oxide grids and fragmentation of particles, elongations above 4 percent were obtained.

Since hardening with its own oxide does not give beryllium sufficient creep resistance at elevated temperatures, other dispersion agents seem to be needed. Watts <sup>(6)</sup> studied the stability of tungsten and ThO<sub>2</sub> dispersions in beryllium. The tungsten powder was produced by the decomposition of ammonium metatungstate and the ThO<sub>2</sub> from thorium nitrate. It was found that during hot pressing or sintering the beryllium containing ThO<sub>2</sub> reacted above 750 C producing ThBe<sub>2</sub>, while that containing tungsten produced two beryllides, WBe<sub>22</sub> and WBe<sub>12</sub>, above 850 C.

Interesting results have been achieved by dispersing Be<sub>2</sub>C in beryllium. Grant <sup>(7)</sup> reports some work done by Greenspan, who mixed beryllium powder with fine carbon black, then pressed, sintered, and extruded

Table 7. Strength and Ductility of Sintered Beryllium<sup>(5)</sup>

Test Temperature, C	Yield Strength (0.2% offset)		Ultimate Tensile Strength		Elongation, %
	psi	MPa	psi	MPa	
NP-50 (0.8% BeO)					
25	27,500	189	39,000	269	2.0
200	23,500	162	33,000	227	2.0
400	21,000	145	35,000	241	14.0
600	16,500	114	29,000	200	15.0
SP-200-C (1.8% BeO)					
25	34,000	234	44,000	303	2.0
200	30,500	210	41,500	286	2.5
400	25,000	172	34,500	238	4.0
600	20,000	138	26,500	183	6.5
FP-17 (1.8% BeO)					
25	38,000	262	51,000	351	2.0
200	35,000	241	47,000	324	2.5
400	30,000	207	45,000	310	8.5
600	24,000	165	32,500	234	6.0
P-50 (3.0% BeO)					
25	35,000	241	46,500	320	1.0
200	32,000	220	44,500	307	1.5

Table 8. Be<sub>2</sub>C Extruded Powder Product<sup>(7)</sup>

Material	Stress		Rupture Life, Hr
	psi	MPa	
650 C (1200 F)			
Pure beryllium	10,000	69	0.2
	5,000	34	1.6
	2,500	17	35.0
	1,500	10	455.0
Be + C powder product *	10,000	69	4.0
	7,500	51	22.0
	5,000	34	181.0
	3,000	21	2800.0
730 C (1350 F)			
Pure beryllium	2,000	14	0.95
	1,000	7	8.0
	700	5	22.0
	600	4	164.0
Be + C powder product *	5,000	34	2.55
	4,000	28	29.3
	3,000	21	860.0

\* Contains 0.8 percent C, equivalent to about 2.5 percent Be-C.



the material. The creep-test results at 650 C and 730 C are given in Table 8. As shown, the carbide-strengthened alloy has much superior rupture life to the pure beryllium at both test temperatures.

Lympny, et al. <sup>(8)</sup> explored the effects of aluminum, silicon, germanium, copper, silver, vanadium, ruthenium, samarium, and manganese in Be-BeO alloys. They found that by proper control of metallic alloy content, BeO level, and grain size, mechanical properties somewhat better than those found in hot-pressed beryllium metal were obtained. They also described the production of hardware by pressureless sintering, iso-pressing, and slip casting of powders with especially selected additions.

Moberly, et al. <sup>(9)</sup> studied the systems Be-BeO, Be-Be<sub>2</sub>C, Be-Si, Be-WBe<sub>22</sub>, and Be-Al<sub>2</sub>O<sub>3</sub>. Mechanical tests showed that strengthening was always obtained with the addition of a hard second phase dispersoid. Increasing the fraction of dispersoid increased the strength, but also decreased the ductility at the temperatures studied (25-600 C). The highest strength was obtained in beryllium which contained a homogeneous dispersion of 20 percent BeO. Two alloys, Be-20BeO and Be-15Be<sub>2</sub>C, exhibited good creep strength up to 750 C. Microstructural analysis showed that the dispersed particles limited the beryllium grain size. BeO was the most effective in this respect. It is of interest to develop DS-Be alloys with a low temperature ductility equivalent to or better than that of commercial purity polycrystalline Be.

Skorov has published results which suggest that dispersion-hardened beryllium has higher corrosion resistance than cast beryllium. <sup>(10)</sup> For example, accelerated local corrosion was observed on extruded specimens of Be-BeO alloys after 140-160 days' exposure in 320 C, pressurized water. However, specimens cast in a vacuum ruptured after less than two days.

#### REFERENCES

1. "Data Sheet Be-2, Berylco PS-20 (sheet) and PR-20 (plate)", Alloy Digest (August 1972), and "Data Sheet Be-1, Lockalloy", Alloy Digest (September 1971).
2. Davidenkov, N. N., Sidorov, B. A., Shestopalov, L. M., Mironov, N. F., Bogograd, N. M., Izhevov, L. A., and Kostogarov, S. B., "Study of the Mechanical Properties of Beryllium", Soviet Atomic Energy, 18 (6), 768-776 (1965).
3. Webster, D., Karlak, R. F., and Vidoz, A. E., "Dispersion Hardened Beryllium", The Microstructure and Design of Alloys, proceedings of the Third International Conference on the Strength of Metals and Alloys, Cambridge, England, August 1973 (1974), pp 326-329.
4. Webster, D., Crooks, D. D., and Vidoz, E., "The Effect of Oxide Dispersions on the Recrystallization of Beryllium", Metallurgical Trans., 4, 2841-2847 (1973).
5. Moberly, J. W., Goggin, W. R., and Brown, H. M., "Compacting and Pressureless Sintering of Beryllium Powders", Intern. J. Powder Metallurgy, 5 (2), 63-76 (1969).
6. Watts, C. R., "Stability of Tungsten and Thorium Dispersions in Beryllium", Int. J. Powder Metallurgy, 4 (3), 49-53 (1968).
7. Grant, N. J., and Preston, O., "Dispersed Hard Particle Strengthening of Metals", Trans. AIME, 209, 349-357 (1957).
8. Lympny, B. B., Theodore, J. G., Beaver, W. W., "Microalloying Be for Improved Sintering Characteristics & Mechanical Properties", Conference Internationale sur la metallurgie du Be, Grenoble (1965), pp 565-573.
9. Moberly, J. W., Sherby, O. D., and Shyne, J. C., "Investigation of Beryllium with Added Dispersoids", AFML-TR-69-247 (October 1969). (MCIC-76869)
10. Skorov, D. M., Metallovedeniye Reaktornykh Materialov, Moscow, Gosatomizdat Press (1962), p 22.

## COLUMBIUM

Columbium is amenable to carbide strengthening but this mechanism is regarded as being outside the scope of this review. Also, solid-solution strengthening (with or without additional carbide-precipitation strengthening) has provided a wide variety of columbium alloys which retain a good balance between moderate-to-high strength at elevated temperatures and good weldability. However, there apparently has been little incentive to develop dispersion-strengthened columbium alloys. A major reason is that columbium has a high solubility for oxygen and nitrogen and is seriously embrittled when saturated with these gases. Nonetheless, there have been a few dispersion-strengthening studies conducted on columbium within the past 10 years, and these are reviewed in the paragraphs which follow.

Osipov<sup>(1)</sup> investigated the influence of  $\text{Al}_2\text{O}_3$  on the creep activation energy of columbium. Creep tests were made in vacuum ( $\sim 10^{-5}$  torr) on specimens annealed at 1300 C for 4 hours prior to testing. Electron-beam zone-refined columbium of 99.99 percent purity was used for comparison. Creep rates determined on three alloys are given in Table 9. As shown, the steady-state creep may be lowered by 2 to 3 orders of magnitude under the test conditions by the presence of  $\text{Al}_2\text{O}_3$ .

Table 9. Creep Rates of Cb- $\text{Al}_2\text{O}_3$  Alloys<sup>(1)</sup>

Weight Percent $\text{Al}_2\text{O}_3$	Stress		Temperature, C	Creep Rate, percent/ minute x $10^3$	Weight Percent $\text{Al}_2\text{O}_3$	Stress		Temperature, C	Creep Rate, percent/ minute x $10^3$
	kg/mm <sup>2</sup>	MPa				kg/mm <sup>2</sup>	MPa		
0	9.2	90	850	3.30	1.90	9.5	93	1300	0.98
	9.2	90	920	20.70		9.5	93	1400	1.77
	3.2	31	1200	216.00		9.5	93	1450	4.90
1.62	3.0	29	1200	0.47	2.90	8.7	85	1200	1.34
	6.0	59	1200	1.30		8.7	85	1300	3.07
	3.0	29	1300	1.57		8.7	85	1350	7.90
	6.0	59	1300	4.28					
	10.6	104	1300	14.00					

Osipov, et al.<sup>(2)</sup> also investigated the electrical characteristics of Cb- $\text{Al}_2\text{O}_3$  thin films. The  $\text{Al}_2\text{O}_3$  and Cb were evaporated together in vacuum and condensed on a glass plate. Different evaporation conditions were used to produce films of different thickness, from 0.7 to 1.2 microns. Their resistivity varied with composition from 20 to  $8 \cdot 10^8$  ohm-cm. The changes of electrical resistivity and temperature coefficient with temperature were also determined for these films.

Best and Pfeiffer<sup>(3)</sup> investigated the superconducting behavior of cold worked wires of sintered, unalloyed columbium and columbium containing additions of  $\text{Al}_2\text{O}_3$  in amounts up to 2 weight percent.  $\text{Al}_2\text{O}_3$  was found to have a definite influence on the values of the residual resistivity, the magnetization behavior, and the critical current density, whereas the critical temperature,  $T_c$ , remained nearly unaffected. Primarily, the upper critical field,  $H_{c2}$ , is strongly influenced and increases to more than twice the value of that of pure columbium by the addition of 2 weight percent  $\text{Al}_2\text{O}_3$ .

#### REFERENCES

1. Osipov, K. A., and Miroshkina, E. M., "Influence of  $\text{Al}_2\text{O}_3$  on the Creep Activation Energy of Nb", Izv. AN SSSR Metally, (4), 1174 (1970).
2. Osipov, K. A., and Borovich, T. L., "Production and Properties of Nb- $\text{Al}_2\text{O}_3$  Films", Izv. SSSR Metally, (5), 180-183 (1972).
3. Best, K. J., and Pfeiffer, I., "Über die Supraleitfähigkeit von gesinterten Nb mit und ohne Zusatz von  $\text{Al}_2\text{O}_3$ ", Z. Metallkunde, 63 (3), 152-155 (1972). (10 references)



## COBALT

For the sake of convenience, dispersion-strengthened cobalt alloys have been somewhat arbitrarily classified in this review into three groups:

- DS-Co Alloys—dispersion-strengthened cobalt
- DS-Co-M Alloys, where M is a metal other than chromium
- DS-Co-Cr-Base Superalloys where chromium is the major alloying metal.

### DS Co Alloys

In 1959, Adkins, et al.<sup>(1)</sup> investigated some 35 Co-base alloys containing 0.1-10 volume percent of  $\text{Cr}_2\text{O}_3$ ,  $\text{TiO}_2$ ,  $\text{SiO}_2$ , and  $\text{Al}_2\text{O}_3$ . The tensile properties at room temperature of the strongest alloys are compared in Table 10. Figure 17 shows the creep properties of these alloys at 500 C. Each of the alloys showed considerably better creep resistance than unalloyed cobalt. Figure 17 also illustrates the effectiveness of decreasing the particle size of  $\text{TiO}_2$  from 2 to 0.02 microns on improving the creep resistance in Co- $\text{TiO}_2$  alloys.

**Table 10. Room-Temperature Tensile Properties of Cobalt and Cobalt Alloys Containing Non-Metallic Dispersions<sup>(1)</sup>**

Alloy Composition, volume percent	Ultimate Tensile Strength		0.2% Offset Yield Strength		Elongation in 1 inch, %
	psi	MPa	psi	MPa	
Co	111,000	765	57,000	393	12
Co - 1 $\text{Cr}_2\text{O}_3$	118,000	813	56,000	386	20
Co - 0.2 $\text{TiO}_2$	111,500	768	68,000	469	16
Co - 0.1 $\text{SiO}_2$	118,500	816	43,500	300	14

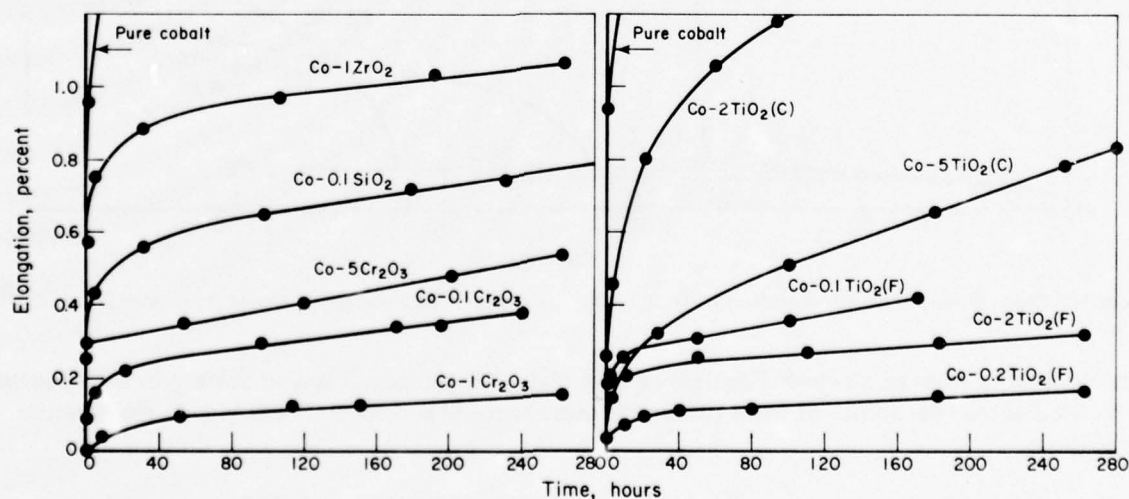


**Figure 17. Creep Curves of Cobalt and Various Cobalt Alloys Tested at 500 C under 12,000 psi<sup>(1)</sup>**  
 [(C) Average particle size about 2  $\mu$ ; (F) Average particle size about 0.02  $\mu$ ]

Palme<sup>(2)</sup> investigated the effect of these same oxides and also the effect of additions of some carbides. The room-temperature properties are shown in Table 11. Figure 18 shows the creep behavior of selected alloys at 500 and 650 C. Palme also tested additions of  $\text{Al}_2\text{O}_3$ ,  $\text{MgO}$ ,  $\text{ThO}_2$ ,  $\text{ZrO}_2$ ,  $\text{TiC}$ ,  $\text{TiN}$ , and boron.

Table 11. Room-Temperature Properties of Sintered Cobalt Samples With Various Additions<sup>(2)</sup>

Addition	Tensile Strength		Yield Strength		Elongation, %	Brinell Hardness	
	kg/mm <sup>2</sup>	MPa	kg/mm <sup>2</sup>	MPa		kg/mm <sup>2</sup>	MPa
none	79	774	40	392	17	205	2009
0.5% $\text{TiO}_2$	65	637	44	431	6	194	1901
0.5% $\text{Cr}_2\text{O}_3$	65	637	47	461	6	207	2029
1% WC	76	745	38	372	10	225	2205
5% WC	59	578	38	372	5	240	2352
1% VC	66	647	34	333	7	220	2156
5% VC	69	676	32	313	14	250	2450
2% $\text{TiO}_2$ (very fine)	69	676	47	461	5	213	2087

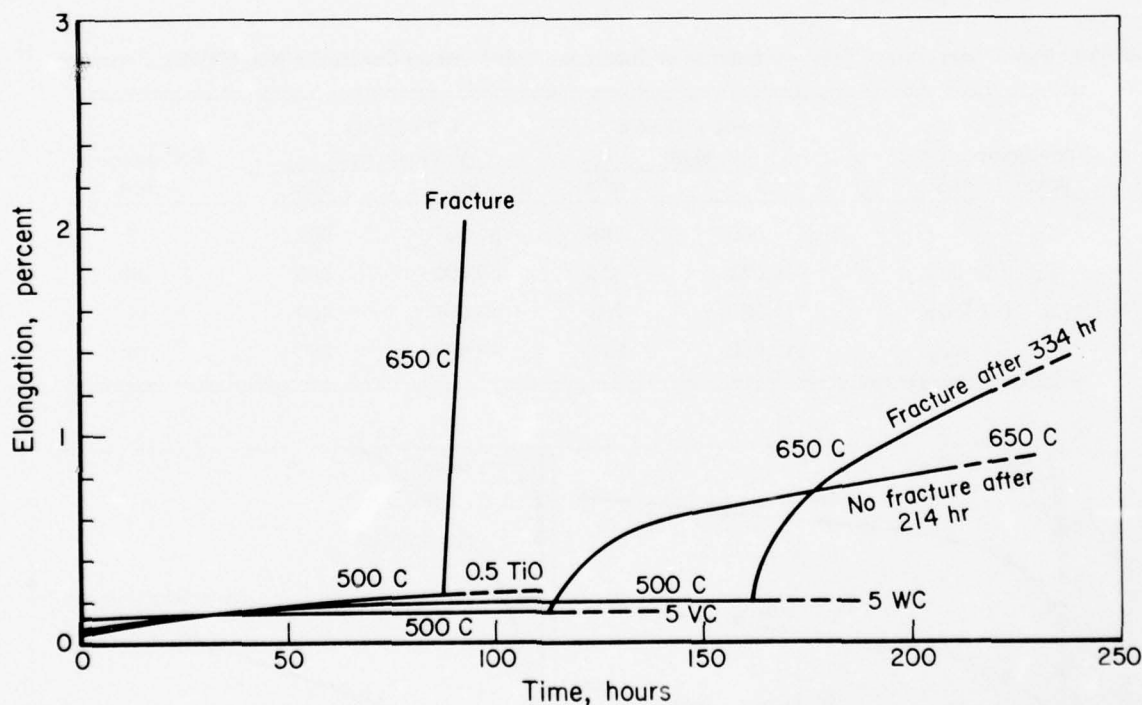


Figure 18. Creep Curves of Cobalt with Non-Metallic Additions Tested at 500 and 650 C Under 8 kg/mm<sup>2</sup> (78.4 MPa)<sup>(2)</sup>

Gatti<sup>(3)</sup> inferred from results with  $\text{Fe-Al}_2\text{O}_3$  alloys that  $\text{Al}_2\text{O}_3$  in cobalt would coarsen in the same way. He concluded that the ability of these systems to overage could restrict their use in high-temperature applications.

An E. I. du Pont de Nemours patent<sup>(4)</sup> gives as an example a DS Co-7 vol. %  $\text{ThO}_2$  alloy with a yield strength of 14 ksi (96 MPa) at 815 C (1500 F).

Esenwein, et al.<sup>(5)</sup> determined the effect of  $\text{La}_2\text{O}_3$  and  $\text{Al}_2\text{O}_3$  in amounts up to 20 volume percent on the hardness and strength of cobalt at temperatures up to 900 C.

Elyutin, et al.<sup>(6)</sup> found that dispersed particles of  $\text{Al}_2\text{O}_3$  in cobalt arrest the process of recrystallization to a considerable degree. They also suppress the grain-boundary peak of internal friction temperature curves, the effect being more evident in the case of sintered and hot-rolled specimens than in the as-sintered condition. In a later paper<sup>(7)</sup>, it was concluded that the  $\text{Al}_2\text{O}_3$  dispersoid accelerates self-diffusion, but that dispersoid agglomeration also occurs, slowing down the process.

Opara and Zhuk<sup>(8)</sup> studied the oxidation behavior of sintered binary cobalt alloys, containing additions of 1-10 weight percent of  $\text{MgO}$ ,  $\text{ZrO}_2$ , and  $\text{Al}_2\text{O}_3$ , in air at 900 C, 1000 C, and 1100 C. The Co-MgO alloys were the only ones which displayed lower weight gains than unalloyed cobalt.

Bufferd and Grant<sup>(9)</sup> prepared a Co-10 vol. %  $\text{Al}_2\text{O}_3$  alloy and determined its stress-rupture life at 815 C, as shown in Figure 19.

Thibaudon, et al.<sup>(10)</sup> prepared dispersions of refractory carbides and nitrides ( $\text{Cr}_3\text{C}_2$ ,  $\text{TiC}$ ,  $\text{VC}$ ,  $\text{CrN}$ ,  $\text{Ti(O-N)}$ ,  $\text{VN}$ ) in cobalt by chemical means. A gas-solid reaction was used in conjunction with mixtures of  $\text{H}_2\text{-CH}_4$ , or  $\text{H}_2\text{-NH}_3$ . Through the use of high-quality starting materials it was possible to obtain products which were characterized by a very homogeneous distribution of the dispersoid in the dispersant.

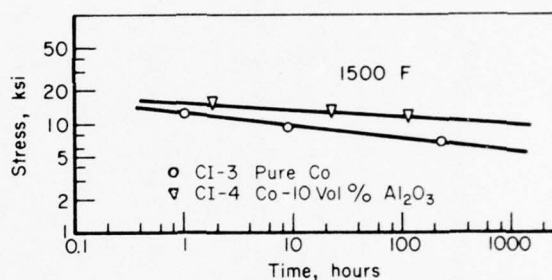


Figure 19. Stress-Rupture Curves for Pure Cobalt and a Co- $\text{Al}_2\text{O}_3$  Alloy at 1500 F (816 C)<sup>(9)</sup>

Towner, et al.<sup>(11, 12)</sup> investigated DS ferromagnetic materials having a high Curie temperature, such as cobalt at 1121 C, as a potential creep-resistant, soft, magnetic material for high-temperature power systems. They prepared and evaluated a series of cobalt alloys containing additions of  $\text{Al}_2\text{O}_3$ ,  $\text{BeO}$ , and  $\text{ThO}_2$ . Properties of these alloys are shown in Table 12.

In further work<sup>(13)</sup>, a Co-0.25Zr-7.5 $\text{ThO}_2$  alloy and a Co-10 vol. %  $\text{ThO}_2$  alloy exhibited the highest creep strength associated with adequate magnetic properties. However, Fe-27 Co-base alloys were favored over the cobalt-base alloys because their saturation magnetization values at 1200 and 1600 F were 25 percent higher.

### DS Co-M Alloys<sup>(a)</sup>

As a part of a larger study, Mincher<sup>(14)</sup> prepared a series of Co-30Ni- $\text{ThO}_2$  alloys. The 30 percent nickel was added to suppress the allotropic transformation of cobalt to room temperature.<sup>(b)</sup> The compositions and tensile properties of swaged bars of the four alloys investigated are given in Table 13 and the stress-rupture properties in Table 14. Figure 20 gives the logarithmic variation of tensile strength with  $\text{ThO}_2$  content in the two alloys. Figure 21 shows the variation of stress rupture and tensile strength at 1095 C as a function of secondary work.

(a) M designates metals other than chromium.

(b) High-purity cobalt at room temperature is hexagonal close-packed (h.c.p.) while above 419 C it is face centered cubic (f.c.c.).



Table 12. Properties of Dispersion-Strengthened Extrusions<sup>(12)</sup>

Powder or Extrusion No.	Nominal Composition weight %	Coercive Force, H <sub>c</sub> (oersteds)	Saturation Magnetization, B <sub>s</sub> (kilogauss)	Creep Properties(a)		Tensile Properties(e)				At 1200 F				At 1600 F						
				At 10 ksi Stress	At 15 Ksi Stress	Ultimate Tensile Strength MPa	Yield Strength 0.2% Offset MPa	Elongation In 4D, %	Ultimate Tensile Strength kSi	Yield Strength 0.2% Offset MPa	Elongation In 4D, %	Ultimate Tensile Strength kSi	Yield Strength 0.2% Offset MPa	Elongation In 4D, %						
Internally Oxidized Powders																				
(Extruded)																				
8.	Co + 4.7Al <sub>2</sub> O <sub>3</sub>	8.0	12.6	0.40	Failed in 10.8 hr 2.6% Strain	30	207	21	145	16	38	262	30	207	17	21	145	12	83	15
9.	Co + 3.6BeO	6.4	12.9	Failed in 11.8 hr 2.7% Strain	—	34	234	21	145	35	54(d)	372	35(d)	241	41(d)	13	90	7	48	28
18.	Fe + 26Co + 3.9BeO	4.9	16.4	Failed during loading, 6.5% Strain	—	30	207	17	117	30	48	331	31	214	24	12	83	4	28	36
Composite Powders																				
(Extruded)																				
3.	Co + 11.2ThO <sub>2</sub> (0.01-0.06 μ)	16.8	12.8	0.24	Failed in 0.15 hr 0.33% Strain	19	131	19	131	2	26	179	26	179	4	13	90	(f)		0
3.	Co + 11.2ThO <sub>2</sub> (0.01-0.06 μ)	10.3	12.9	0.21	Failed in 7.5 hr 0.40% Strain	25	172	20	138	6	30	207	24	165	8	20	138	16	110	3

Notes: (a) All experimental alloy specimens aged 100 hours at 760 C (1400 F) in vacuum (pressure of  $1 \times 10^{-5}$  torr or less) before creep testing in vacuum (pressure of  $1 \times 10^{-6}$  torr or less).  
 (b) All experimental alloy specimens aged 100 hours at the test temperature in vacuum (pressure of  $1 \times 10^{-5}$  torr or less) before tensile testing in vacuum (pressure of  $1 \times 10^{-5}$  torr).  
 (c) Approximate values obtained by extrapolation of vacuum creep data on Larson Miller plot.  
 (d) Average of two tests. Other tensile test values represent one test.  
 (e) No tensile tests made at 760 C (1400 F). Values are average of 649 C (1200 F) and 871 C (1600 F) test results.  
 (f) Failed before reading 0.2% offset.

Table 13. Tensile Properties of Swaged Bar of the Co-2ThO<sub>2</sub> and Co-30Ni-2ThO<sub>2</sub> Alloys<sup>(14)</sup>

Alloy	R.T.			1400 F (760 C)			2000 F (1093 C)		
	U.T.S.		El., %	U.T.S.		El., %	U.T.S.		El., %
	ksi	MPa		ksi	MPa		ksi	MPa	
Co-2ThO <sub>2</sub>	136.1	937	8	24.1	166	16	12.1	83	9
Co-2ThO <sub>2</sub> -0.2Zr	145.2	1000	13	35.4	244	24	20.3	140	13
Co-30Ni-2ThO <sub>2</sub>	147.5	1016	20	37.9	261	6	16.9	116	13
Co-30Ni-2ThO <sub>2</sub> -0.2Zr	165.4	1140	15	49.1	238	16	20.4	141	9

Table 14. Stress-Rupture Behavior of the Co-ThO<sub>2</sub> and Co-30Ni-ThO<sub>2</sub> Alloys at 2000 F (1093 C)<sup>(14)</sup>

Alloy	Rupture Life, hours	
	at 8,000 psi (55 MPa)	at 15,000 psi (103 MPa)
	Stress	Stress
Co-2ThO <sub>2</sub>	0.6	—
Co-30Ni-2ThO <sub>2</sub>	4.3	—
Co-4ThO <sub>2</sub>	> 21.0	> 22.0
Co-30Ni-4ThO <sub>2</sub>	> 100.0	4.9
Co-2ThO <sub>2</sub> -0.2Zr	> 100.0	> 100.0
Co-30Ni-2ThO <sub>2</sub> -0.2Zr	> 100.0	4.7

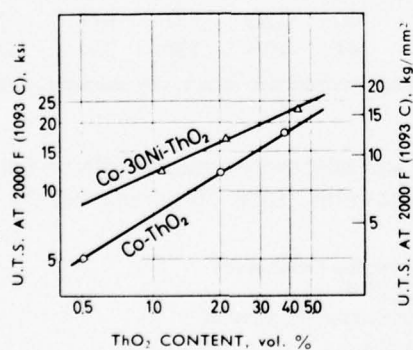


Figure 20. Logarithmic Variation of Tensile Strength with Thoria Content of Co and Co-30Ni Base Alloys<sup>(14)</sup>

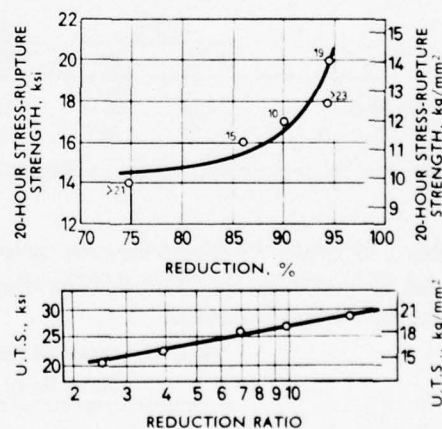


Figure 21. Variation of Mechanical Properties of Co-30Ni-2ThO<sub>2</sub>-0.2Zr Alloy as a Function of Secondary Work<sup>(14)</sup>

Above: 20-hour stress-rupture strength at 2000 F (1093 C)  
(numbers indicate actual life in hours)  
Below: Tensile strength at 2000 F (1093 C), showing logarithmic relationship with reduction ratio

As shown, the strength of the cobalt alloys at elevated temperatures was improved by a dispersion of ThO<sub>2</sub> particles. Increases in strength were achieved by increasing either the ThO<sub>2</sub> content or the extent of secondary work. Additional strengthening was obtained in certain compositions by the addition of 0.2 percent zirconium. Rupture strengths in vacuum for a 100-hour life at 1095 C was greater than 15 ksi (10.5 kg/mm<sup>2</sup>) for some of the compositions. Under these conditions, the Co-30Ni-2ThO<sub>2</sub>-0.2Zr alloy showed a rupture life of 19 hours with a load of 20 ksi (14.1 kg/mm<sup>2</sup>). These high strengths were associated with a fibrous structure of elongated grains.

Drapier, et al.<sup>(15)</sup> recently studied the structural stability of 3 oxide-dispersion-strengthened cobalt alloys after holding them 1 hour in a vacuum at temperatures of 1100-1425 C and cooling rapidly. As-swaged, the Co-4ThO<sub>2</sub>, Co-2ThO<sub>2</sub>-0.2Zr, and Co-10Ni-2ThO<sub>2</sub>-0.2Zr alloys showed a characteristic fibrous microstructure with some ThO<sub>2</sub> clusters aligned in the swaging direction.

Extensive recrystallization occurred in the Co-2ThO<sub>2</sub>-0.2Zr alloy after holding for 1 hour at 1400 C. Since a 10 percent nickel addition is not sufficient to stabilize the f.c.c. phase down to room temperature, the f.c.c.→h.c.p. allotropic transformation of the recrystallized matrix occurs extensively during cooling from the high-temperature treatment, as was the case for the Co-ThO<sub>2</sub> alloys.

The Co-10Ni-2ThO<sub>2</sub>-0.2Zr alloy underwent extensive recrystallization in the 1050-1150 C range. Substantial grain growth was observed, which was attributed to the higher deformation energy stored in this alloy during its secondary working. For both alloy bases, grain growth is accompanied by the formation of substantial amounts of h.c.p. cobalt on cooling from high temperature. The fact that, in the as-swaged condition, all alloys exhibited essentially a f.c.c. structure is mainly due to their fine grain size.

Selected short-time tensile properties of the alloys are summarized in Table 15.

Table 15. Selected Short-Time Tensile Properties of Thorium-Dispersed Alloys<sup>(15)</sup>

Alloy	Tested at R.T.					Tested at 1093 C (2000 F)				
	U.T.S.		Y.S.		Elong., %	U.T.S.		Y.S.		Elong., %
	MPa	ksi	(0.2% offset) MPa	(0.2% offset) ksi		MPa	ksi	(0.2% offset) MPa	(0.2% offset) ksi	
Co-2ThO <sub>2</sub> -0.2Zr	1133	164.4	1031	149.6	6	155	22.5	137	19.9	9
Co-10Ni-2ThO <sub>2</sub> -0.2Zr	1409	204.5	1409	204.5	1.0	141	20.4	138	20.1	3.3

Cheney and Smith<sup>(16)</sup> found that the technique of spray drying and selectively reducing offers a better process for preparing Co-15Mo-4ThO<sub>2</sub> alloys than does vapor deposition. Table 16 summarizes the hardness data they obtained.

Table 16. Effect of Composition and Processing on the Hardness of Spray-Dried and Reduced Cobalt Alloys<sup>(16)</sup>

Composition	Hardness, R <sub>A</sub>		
	Sintered Billets	Hot-Worked Sheet	Cold-Worked Sheet
Co	55	55	64
Co-4ThO <sub>2</sub>	67	57	60
Co-15Mo	68	70	72
Co-15Mo-4ThO <sub>2</sub>	74	68	—



Hancock, et al.<sup>(17)</sup> compared the behavior of 60Co-Ni-2.5 vol. percent  $\text{Al}_2\text{O}_3$  alloy and a Ni-2.5 vol. percent  $\text{Al}_2\text{O}_3$  alloy. They noted that the cobalt-base alloy had lower interfacial energy with the  $\text{Al}_2\text{O}_3$  than did the nickel-base alloy. This reduction in interfacial energy has important consequences in terms of the work-hardening behavior and ductility of the material, reportedly increasing the ductility markedly.<sup>(18)</sup>

In 1955, Baxter, et al.<sup>(19)</sup> investigated the wetting and bonding of  $\text{Al}_2\text{O}_3$  with cobalt and some 10 binary cobalt alloys listed in Table 17. Practically no wetting tendency was noted for the  $\text{Al}_2\text{O}_3$  with any of these materials.

**Table 17. Bond Strengths and Contact Angles of Cobalt Alloys on Alumina<sup>(19)</sup>**

Bond Strength	Cobalt Alloy	Contact Angle (to nearest 5)
Slight adherence	Pure Cobalt	125
	20% Copper	115
Non-adherence	10% Molybdenum	140
	5% Vanadium	120
	10% "	110
	10% Tungsten	130
	5% Manganese	115
	10% "	120
	10% Tantalum	125
	5% Copper	130
	10% "	120
	35% Chromium	130
	5% Aluminum	—

#### DS Co-Cr-Base Superalloys

A recent definition of cobalt-base superalloys is "an alloy developed for very high-temperature service generally considered to be in excess of 815 C where relatively high stresses (tensile, thermal, vibratory, and shock) are encountered and where oxidation resistance is frequently required".<sup>(20)</sup>

Several cobalt alloys, based on the original Vitallium composition of Co-30Cr-7W-0.5C, were among the first superalloys to be used in the first aircraft gas-turbine engines. In this cobalt-base alloy, the chromium serves the same purpose as in iron- and nickel-base superalloys, which is to promote oxidation resistance in addition to increasing hot strength. Nickel is also useful in cobalt-base superalloys both for its ductilizing behavior and for increasing solubility of the refractory metals. Additions of the refractory metals tungsten and molybdenum are desirable for solid-solution strengthening.

Adkins and Jaffee<sup>(1)</sup> were among the first to attempt the dispersion strengthening of Co-Cr alloys by adding 0.2 percent  $\text{TiO}_2$  and 0.1 percent  $\text{SiO}_2$  to a Co-20Cr base. However, these additions were not beneficial to the alloys' strength properties.

A more complex alloy base and more sophisticated processing procedures were later employed by Mincher and Arnold<sup>(21)</sup> who also used thorium as the dispersoid. Minor alloying additions of zirconium,

manganese, tantalum, and columbium were also investigated. After various screening evaluations, the following alloys were selected<sup>(22)</sup> for scale-up studies:

Co-20Ni-18Cr-2ThO<sub>2</sub>  
Co-20Ni-18Cr-4ThO<sub>2</sub>  
Co-20Ni-30Cr-2ThO<sub>2</sub>  
Co-20Ni-20Cr-10W-2ThO<sub>2</sub>

A summary of the processing and resultant typical tensile properties of these alloys is given in Table 18. Figure 22 identifies maximum tensile strengths and 100-hour rupture strengths after heat treatment for 1 hour at 1315 C or 1370 C. Creep data are listed in Table 19.

All alloys exhibited sensitivity to strain rate at 1095 C tensile testing, but the alloy containing 30 percent chromium was least affected. Hot-corrosion testing was conducted at 1150 C in a high-velocity oxidizing-sulfidizing gas flow for exposures up to 200 hours. Weight-loss data from these tests indicated superior behavior for the Co-20Ni-18Cr-2ThO<sub>2</sub> alloy compared to the oxidation-resistant Hastelloy X nickel-base alloy.

The thermal stability of these alloys is shown in Figure 23. From this work, the Co-20Ni-18Cr-2ThO<sub>2</sub> and Co-20Ni-30Cr-2ThO<sub>2</sub> alloys were selected for further development to evaluate their applicability to turbine-vane airfoils.<sup>(23)</sup> Both alloys exhibited tensile properties commensurate with turbine-vane operation, but the 30Cr alloy was stronger at room temperature, whereas, at 1095 C, the reverse was true. Thermal fatigue testing was carried out using the cyclic conditions illustrated in Figure 24. In these tests, the 18Cr alloy was superior (see Table 20). Conclusions from this work,<sup>(23)</sup> which included engine testing, were as follows:

1. "Both the Co-20Ni-30Cr-2ThO<sub>2</sub> and the Co-20Ni-18Cr-2ThO<sub>2</sub> compositions, when worked in a controlled manner to uniformly recrystallized structures, are potentially advantageous material selections for turbine-vane applications in advanced gas turbines. On the basis of the standard guide-vane-performance parameters (particularly resistance to bowing, oxidation and corrosion resistance, and thermal fatigue at leading edges), the engine test showed the TD Co-Cr alloys investigated to be superior to all established guide-vane materials in current production engines. The alloy with lower chromium content will require protective coating for sustained service; however, the protective coating need for the higher chromium alloy would be minimal."

"Use of the 18Cr composition would be dictated for high-temperature/high-stress applications. The observed cracking may be controlled by a better design that specifically accounts for the physical and mechanical properties. The cracking that did occur did not degrade engine performance and was most probably due to unusually high thermal stresses created by a non-optimum cooling scheme."

2. "Both experimental alloys can be fabricated into usable form by extrusion. The working conditions must be controlled such that uniform recrystallization can occur during annealing, if maximum alloy strength is to be obtained."
3. "High-temperature tensile and creep-rupture strength are proportional to grain structure for both alloys. A recrystallized, coarse-grain alloy produces highest tensile strength, creep resistance, and creep-rupture life. A cold-worked, or fine-grain condition will not achieve commensurate levels."
4. "Both alloys are stable after final annealing at 1370 C (2500 F) with respect to ThO<sub>2</sub> dispersion and grain growth. Inert phase coalescence was not evident during the anneal or for prolonged exposures up to 1315 C (2400 F), the highest temperature studied."
5. "When processed to the optimum conditions observed in this program, the high-temperature strength of the experimental Co-20Ni-18Cr-2ThO<sub>2</sub> surpassed those of known cast, cobalt-base alloys. In similar manner, the Co-20Ni-30Cr-2ThO<sub>2</sub> alloy high-temperature strength equalled those of the cast Co systems."

Table 18. TD Cobalt Scale-Up - Summary of Processing (22)

Alloy	Billets Evaluated	Results (a)	Preferred Processing Route	Processing Difficulties and Potential Problem Areas	Typical Tensile Properties Obtained							
					U.T.S.		2% Y.S.		El., %	R.A., %		
					ksi	MPa	ksi	MPa				
Co-10Ni-2ThO <sub>2</sub> -0.2Zr	7	1) Sound, stable, high strength CG bar produced (3/4" Ø)	CG material-work at 1000 F, Rx	1) Obtaining uniform ZrH <sub>2</sub> distribution	CG-RT	186	1281	184	1268	1.5	0.8	
					1400 F	31	214	26	179	25	35	
		2) Sound, stable, high strength FG bar produced at smaller size (0.5" Ø)	FG material-work at 1500 F, large reduction	2) Obtaining reproducible Rx behavior	2000 F	20	138	20	138	3	8	
					FG-RT	157	1082	96	661	15	15	
Co-20Ni-18Cr-2ThO <sub>2</sub>	4	1) Sound, stable, high strength CG bar produced (~1" Ø)	Recrystallize, extrusion work at 1800 F	1) Obtaining reproducible Rx behavior	1400 F	30	207	28	193	21	87	
					2000 F	22	152	21	145	7	8	
		1) Sound, stable, high strength CG bar produced (~1.25" Ø)	Recrystallize extrusion, work at 1800 F	2) Uniform working throughout bar cross section	RT	148	1020	94	648	14	15	
					1400 F	49	338	48	331	19	38	
Co-20Ni-18Cr-4ThO <sub>2</sub>	6	1) Sound, stable, high strength CG bar produced (~1.25" Ø)	Recrystallize extrusion, work at 1800 F	1) Obtaining reproducible Rx behavior	2000 F	23	158	22	152	13	28	
					RT	168	1157	117	806	12	10	
		1) Bar produced with shallow OD cracks, sound center (~1.1" Ø)	Recrystallize extrusion, work at 2000 F	2) Inability to work uniformly throughout bar cross section	1400 F	55	379	49	338	10	8	
					2000 F	20	138	19	131	5	4	
Co-20Ni-30Cr-2ThO <sub>2</sub>	6	1) Bar produced with shallow OD cracks, sound center (~1.1" Ø)	Recrystallize extrusion, work at 2000 F	1) Obtaining powder free of contaminant causing ThO <sub>2</sub> agglomeration	RT	185	1275	147	1013	19	19	
					1400 F	62	427	60	413	4	3	
		1) No sound bar produced by secondary working	Not determined	2) Inability to work uniformly throughout bar cross section	2000 F	16	110	15	103	5	6	
					RT	185	1275	147	1013	19	19	
Co-20Ni-20Cr-10W-2ThO <sub>2</sub>	4	1) No sound bar produced by secondary working	Not determined	3) Cracking of bar (related to No. 2)	2000 F	18.3	126	17.8	123	4	5(b)	
					RT	185	1275	147	1013	19	19	
		1) No sound bar produced by secondary working	Not determined		1400 F	62	427	60	413	4	3	
					2000 F	16	110	15	103	5	6	
Co-20Ni-20Cr-10W-2ThO <sub>2</sub>	4	1) No sound bar produced by secondary working	Not determined	2) Catastrophic cracking of bar (related to No. 1)	2000 F	18.3	126	17.8	123	4	5(b)	
					RT	185	1275	147	1013	19	19	
		1) No sound bar produced by secondary working	Not determined		1400 F	62	427	60	413	4	3	
					2000 F	16	110	15	103	5	6	

(a) CG designates coarse-grain and FG designates fine-grain structure.

(b) Test from cracked bar.



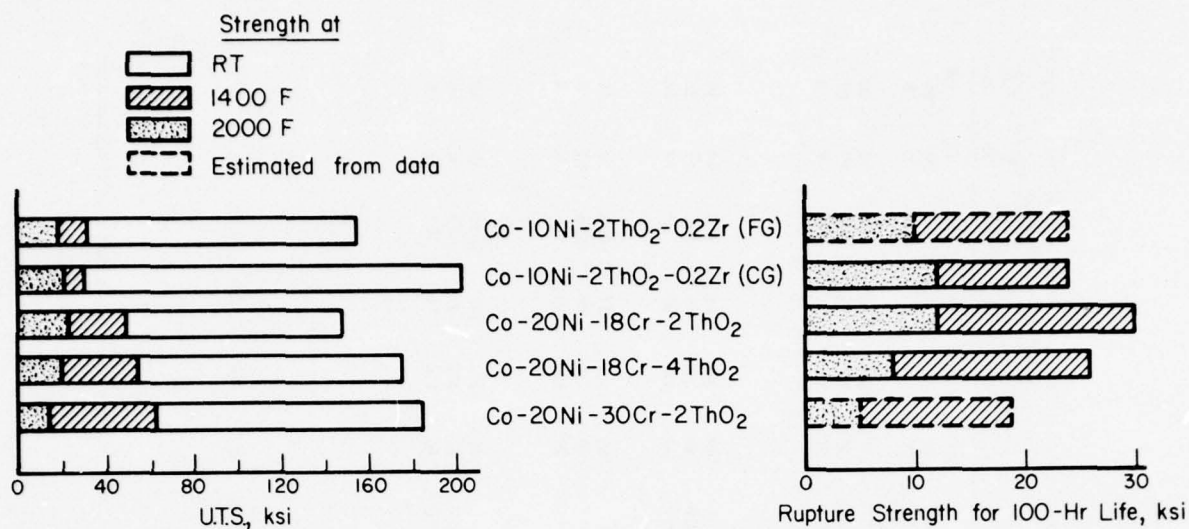


Figure 22. TD Cobalt Alloys-Comparison of Strength Levels After Heat Treatment of 1 Hour at 2500 F (1371 C) for Co-10Ni Alloys and 1 Hour at 2400 F (1316 C) for Co-20Ni-18Cr and Co-20Ni-30Cr Alloys<sup>(22)</sup>

Table 19. 2000 F (1013 C) Creep Data<sup>(22)</sup>

Alloy	Billet No.	Stress, ksi	Failure		Time for Creep of 0.2%, hours
			Time, hours	El., %	
Co-10Ni-2ThO <sub>2</sub> -0.2Zr (coarse grain)	2503-2	14.0	18.7	4.0	1.5
		10.0	454.6+		69.9
		12.0	80.4	3.5	16.8
		14.0	4.6	3.0	2.0
		14.0	6.9	6.0	1.5
Co-20Ni-18Cr-2ThO <sub>2</sub>	2801-4	14.0	1.5	3.5	1.0
		12.0	97.5	4.3	10.0
Co-20Ni-18Cr-4ThO <sub>2</sub>	2707-2	12.0	0.7	2.3	—
		10.0	3.7	3.5	3.4

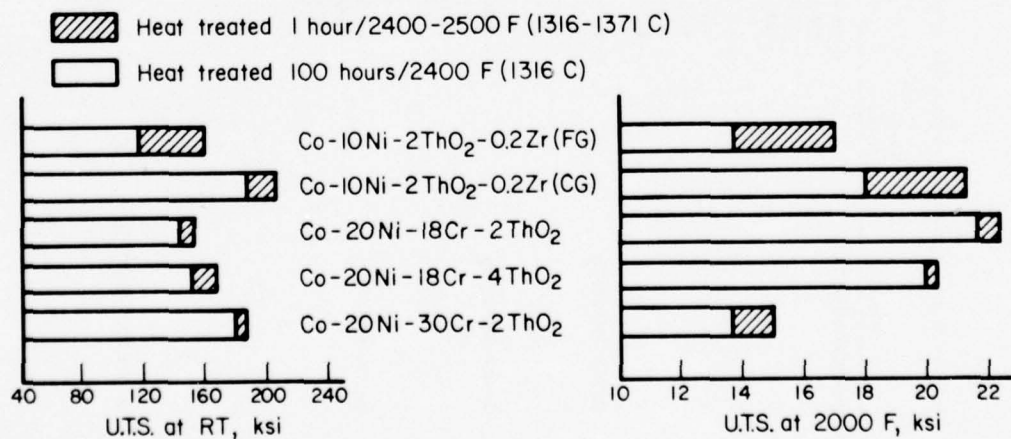


Figure 23. Thermal Stability<sup>(22)</sup>

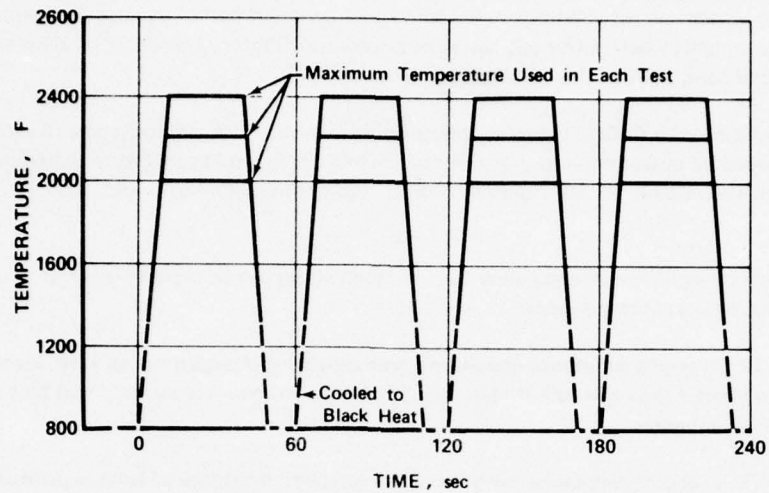


Figure 24. Time-Temperature Cycle Used in Thermal Fatigue Testing<sup>(23)</sup>

Table 20. Results of Thermal Fatigue Testing<sup>(23)</sup>

Solid Airfoils			
Temperature, F	Cycles to First Cracking		
	TD Co (18Cr)	TD Co (30Cr)	
2000	1000 <sup>(a)</sup>	1000 <sup>(a)</sup>	
+2400	577	71	
2200	1000 <sup>(b)</sup>	1000 <sup>(b)</sup>	
Vane Assemblies			
Temperature, F	Cycles to First Cracking		
	TD Co (18Cr)	TD Co (30Cr)	MAR M-302
2000	1000 <sup>1</sup>	1000 <sup>1</sup>	1000 <sup>1</sup>
+2400	150	48	52

(a) Discontinued, no cracking, temperature raised to 2400 F.

(b) Discontinued, no cracking.

6. "The oxidation and hot-corrosion resistance of the low Cr alloy was as good as other current Co compositions; however, for sustained operation, a protective coating is necessary. For the high Cr alloy, the oxidation resistance was sufficiently great as to warrant consideration of an uncoated application in turbine environments where sulfur-salt reactions are noncontributory. Under conditions where salt ingestion is significant, a protective coating is again necessary."
7. "Vapor deposition of a CoCrAlY coating composition provides adequate resistance to each of the alloys such that successful operation in severe corrosive environments can be realized. Coating stability with base metal was acceptable for 100 hours at 1205 C. Pack-cementation aluminide coatings were not adequate."
8. "Braze joining of each experimental alloy to cast cobalt alloys can be accomplished successfully using a standard cobalt braze composition."
9. "Under the TF 30 engine endurance conditions, bow resistance of experimental vane assemblies of each alloy was better than cast Bill-of-Material. The lower chromium alloy exhibited best resistance to trailing-edge deformation."
10. "Under the TF 30 engine endurance conditions, the corrosion resistance of both experimental alloys uncoated was as good as that of coated Bill-of-Material. The higher chromium composition was noticeably superior."
11. "Under the TF 30 engine endurance conditions, the corrosion resistance of the experimental assemblies, coated with CoCrAlY, was sufficient to anticipate satisfactory operation several times that of coated Bill-of-Material. Coating degradation because of base metal was minimal."

Because of the favorable potential of these alloys in gas-turbine engines, further work was done to examine the feasibility of making these alloys by mechanical attrition.<sup>(24)</sup> This also permitted substitution of  $Y_2O_3$  in place of the  $ThO_2$ , previously used for these alloys.

The optimum blend of starting powders to produce a Co-20Ni-18Cr-1 $Y_2O_3$  base composition was determined. Using this blend, four different alloys were produced: two contained 1 percent and 2 percent  $Y_2O_3$  and no Al, and two contained 1 percent and 4 percent Al with 1 percent  $Y_2O_3$ , respectively. A full-scale property evaluation was performed for each alloy composition on extrusions produced at four different temperatures with a reduction ratio of 16:1. Only the aluminum-containing alloys were found to undergo secondary recrystallization to elongated grains of high aspect ratio. This required annealing treatments in the range of 1405-1420 C. In stress rupture, only the Co-20Ni-16Cr-4Al-1 $Y_2O_3$  composition met the program goal of 1095 C/55 MPa/100 hr. It was found to be capable of 1095 C/69 MPa/100 hr. However, this alloy had the poorest overall oxidation resistance which was attributed to the fact that the experimental lot contained only 2.78 percent Al instead of 4 percent.

This work is being continued under Air Force Contract F33615-75-C-5061.<sup>(25)</sup> The follow-on work includes an effort to increase the alloy's aluminum content up to 4.5 percent, and to vary the oxide level and extrusion ratios as well as heat treatment. (At the time, the most promising amount of oxide appeared to be 1.75 percent.) At the time of this review, no material had yet been produced which showed the required combination of properties.<sup>(25)</sup>

Drapier, et al.<sup>(26)</sup> determined the creep-rupture properties of several Co-Ni-Cr alloys containing  $ThO_2$  additions and compared them with properties of TD-Ni and other DS-Co alloys as shown in Figure 25. The results obtained for the Co-20Ni-18Cr- $ThO_2$  alloys creep tested at 1093 C are compared in Table 21. Somewhat unexpectedly, the rupture life was found to decrease and the secondary creep rate increase as the  $ThO_2$  content was raised from 2 to 4 percent. This anomalous behavior was attributed to the non-uniform deformation of the 4 percent  $ThO_2$  material during secondary working.



The 100-hour rupture strengths for two of these DS-Co alloys at 760 and 1093 C are compared with those of two commercial cast superalloys in Figure 26. Figure 27 compares the hot-corrosion resistance of these alloys. The importance of corrosion resistance – oxidation and hot corrosion (or sulfidation) – has encouraged considerable research on Co-base as well as ODS-Co alloys. Unfortunately, because of time limitations, it was necessary to restrict this review to highlighting only a few of the more recent studies in this area.

Table 21. Creep-Rupture Properties of Co-20Ni-18Cr-ThO<sub>2</sub> Alloys at 1093 C<sup>(26)</sup>

Alloy	Stress,		Rupture Life, hr	Elong., %	R. in A., %	Secondary Creep Rate, %/hr
	MPa	ksi				
Co-20Ni-18Cr-2ThO <sub>2</sub>	98	14.2	1.93	1.60	5.37	0.5136
	69	10.0	30.17	3.00	2.21	0.00198
	59	8.5	453.9	n.d.	n.d.	0.00107
Co-20Ni-18Cr-4ThO <sub>2</sub>	98.1	14.2	0.11	3.57	1.46	22.22
	69	10.0	0.70	1.45	2.93	0.1760
	49	7.1	573.6	1.96	0.98	0.0012

n.d. Not determined.

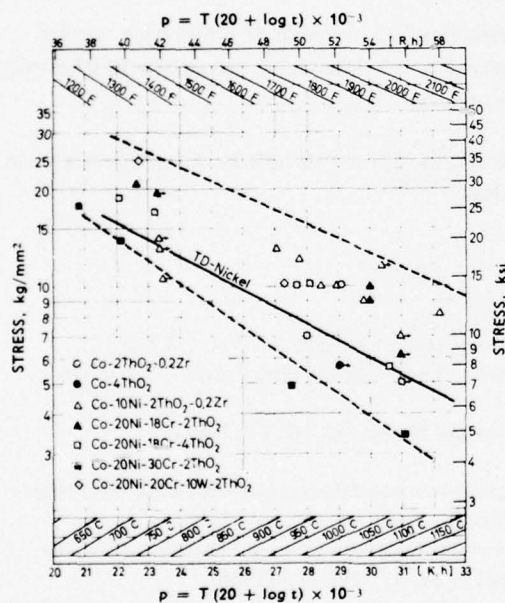


Figure 25. Larson-Miller Plot of Creep-Rupture Strength of TD-Cobalt Alloys<sup>(26)</sup>

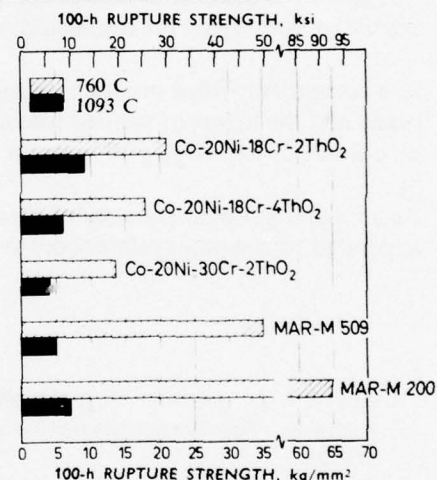


Figure 26. Comparison of Creep-Rupture Strength of TD-Cobalt Alloys with That of Two Commercial Superalloys<sup>(26)</sup>

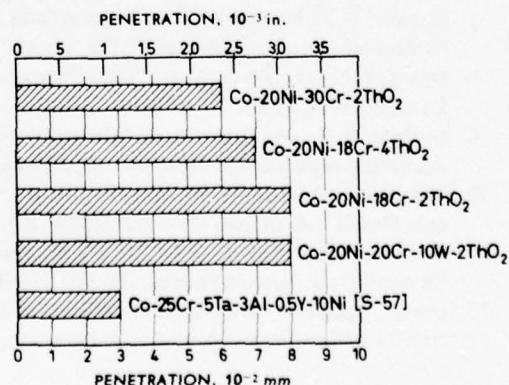


Figure 27. Hot Corrosion of Chromium-Containing TD-Cobalt Alloys and S-57 After 500 Hours Exposure in Contaminated Combustion Gases at 950 C<sup>(26)</sup>

Wallwork and Hed<sup>(27)</sup> suggested a system of superimposing oxide maps over the ternary phase diagrams in order to select oxidation resistant compositions. On this basis, they predicted that a Co-10Cr-9Al alloy would be suitable for the temperature range 1100-1200 C due to the formation of a protective  $\text{CoAl}_2\text{O}_4$  spinel or  $\text{Al}_2\text{O}_3$  scale. Specimens of such an alloy were prepared and did show small weight gains on exposure to 100 torr oxygen pressures at these temperatures, but severe spalling occurred on thermal cycling.

Wright, et al.<sup>(28)</sup> investigated the effects of oxide dispersions on the high-temperature oxidation and hot corrosion of DS-Co alloys. They determined the effects of  $\text{Y}_2\text{O}_3$  and  $\text{CeO}_2$  dispersoids on the oxidation of  $\text{Cr}_2\text{O}_3$  forming alloys. Co alloys containing 3 vol. %  $\text{Y}_2\text{O}_3$  and as little as 13 percent chromium were found to oxidize at almost the same rates, and to produce scale morphologies similar to a Co-21Cr-3 vol. %  $\text{Y}_2\text{O}_3$  alloy. The most notable effect of a dispersion of  $\text{Y}_2\text{O}_3$  particles on  $\text{Al}_2\text{O}_3$  forming Co-Cr-Al alloys was to improve the scale adhesion. A mechanism was proposed to explain the observed phenomena.

Springer and Wright<sup>(29)</sup> studied the high-temperature oxidation of Co-21Cr-3 vol. %  $\text{Y}_2\text{O}_3$  which was oxidized in oxygen at 100 torr in the temperature range 900-1200 C. The selective oxidation of chromium to form a continuous protective  $\text{Cr}_2\text{O}_3$  was promoted by the dispersoid addition. Also, the rate of growth of  $\text{Cr}_2\text{O}_3$  was reduced compared to dispersoid free alloys and the adhesion of the  $\text{Cr}_2\text{O}_3$  was greatly improved. It is believed that the scale forming reaction is at the metal-scale interface in the alloys containing the dispersoid, whereas it is at the scale- $\text{O}_2$  interface in dispersoid-free alloys.

In a current Air Force program, Giggins and Pettit<sup>(30)</sup> are investigating oxide-scale adherence mechanisms and the effect of applied loads. In one future task, they plan to determine the adhesion of  $\text{Al}_2\text{O}_3$  on a Co-20Cr-6Al- $\text{Al}_2\text{O}_3$  alloy under cyclic conditions of exposure.

As a further guide to the subject of corrosion at high temperatures, a few references to recent work are appended to the other references for this section of this review.<sup>(31-37)</sup>

## REFERENCES

1. Adkins, E. F., and Jaffee, R. I., "Application of Dispersion Hardening to Co", *Cobalt*, **3**, 27-30 (1959).
2. Palme, R., "Non-Metallic Dispersions in Cobalt and its Alloys. Part I. Dispersions in Pure Cobalt", *Cobalt*, 15-20 (1960).
3. Gatti, A., "Notes on the Stability of  $\text{Al}_2\text{O}_3$  in Fe, Ni, and Co", *Powder Metallurgy*, **10**, 77 (1962).
4. U. S. Patent 3,019,103 (filed in 1957).
5. Esenwein, R., Gerlach, J., and Pawlek, F., "Herstellung und Eigenschaften von Mischkörpern aus kobaltüberzogenen Verbundpulvern", *Journées Internationales des Applications du Cobalt*, Paper No. 17 (June 1964).
6. Elyutin, V. P., Mozhukin, E. I., and Balasubramanian, F. O., "Recrystallization and Internal Friction Phenomena in the Dispersion-Hardened System Co- $\text{Al}_2\text{O}_3$ ", *Indian Inst. Metals Trans.* **17**, 196-198 (1964).
7. Elyutin, V. P., Mozhukin, E. I., and Yakovlev, S. G., "Self Diffusion of Co in Co and Co- $\text{Al}_2\text{O}_3$  Compositions Obtained by Powder Metallurgy Methods", *Fiz. Metal. i Metalloved.*, **19** (3), 389-396 (1965).
8. Opara, B. K., and Zhuk, N. P., "High Temperature Resistance of Dispersion-Strengthened Cobalt", *Zashchita Metallov*, **1** (1), 99-103 (1965).
9. Bufferd, A. S., and Grant, N. J., "Oxide Dispersion Strengthening of Cobalt-Base Alloys", *Journées Intern. des Applications du Cobalt*, Paper No. 18, 251-261 (June 1964).
10. Thibaudon, D., Roubin, M., and Paris, R. A., "Obtention de Dispersions de Carbures et de Nitrures dans le Cobalt et le Nickel", *Jl. of Less Common Metals*, **29**, 171-182 (1972).
11. Towner, R. J., Pavlovic, D. M., Detert, K., and Bufferd, A. S., "Effect of Dispersoids on Magnetic Properties of Fe, Co and Ni", *J. Applied Physics*, **39**, 601 (1968).
12. Towner, R. J., and Pavlovic, D. M., "Effect of Dispersoid Parameters on High-Temperature Behavior of Cobalt and Iron-27 % Co Alloys", *Jl. of Applied Physics*, **40** (3), (1969).

# REFERENCES (Cont.)

13. Kueser, P. E., and Towner, R. J., "Dispersion Strengthened Magnetic Materials for Applications in the 1200 to 1600 C Range", NASA Cont. Rep., 135-286 (March 1970).
14. Mincher, A. L., "Dispersion-Strengthened Cobalt Alloys", *Cobalt*, **32**, 119-123 (1966).
15. Drapier, J. M., Coutsouradis, D., and Habraken, L., "Structure and Properties of Dispersion-Strengthened Cobalt Alloys", *Cobalt*, **53**, 197-205 (1971).
16. Cheney, R. F., and Smith, J. S., "Development of Dispersion-Strengthened Ni and Co-Base Alloys", Sylvania Electric Products, Final Report on Contract AF 33(615)-1697 (July 1965). (AD-A012 095).
17. Hancock, J. W., Dillamore, I. L., and Smallman, R. E., "Void Nucleation and Growth During Low Temperature Deformation of Ni-Co-Al<sub>2</sub>O<sub>3</sub> Alloys", *High Temperature Materials*, 6th Plansee Seminar, 1968 (published 1969), pp 467-480.
18. Hancock, J. W., Dillamore, I. L., and Smallman, R. E., "The Creep of Dispersion-Strengthened Ni-Co Alloys", *Metal Science JI.*, **6**, 152-156 (1972).
19. Baxter, J. R., and Roberts, A. L., "Development of Metal-Ceramics from Metal-Oxide Systems", *Iron and Steel Inst. Spec. Rep. No. 58* (1954), pp 315-324.
20. *American Metal Market*, (December 19, 1975), p 14.
21. Mincher, A. L., and Arnold, D. B., "Development of Dispersion-Strengthened Co-Base Alloys", AFML TR-68-95, Contract No. AF 33(615)-67-C-1093 (April 1968). (MCIC 72365)
22. Mincher, A. L., "Research on Dispersion Strengthened Co-Base Alloys", AFML-TR-65-442, Contract No. AF 33(615)-1680 (January 1966). (MCIC 63461)
23. Cox, A. R., and Hecht, R. J., "Evaluation and Performance of TD-Co Alloys as Guide Vanes in Gas Turbine Engines", AFML-TR-70-273, Contract AF 33(615)-69-C-1668 (December 1970). (MCIC 79515)
24. Klarstrom, D. L., and Grierson, R., "Feasibility of Making an Oxide Dispersion-Strengthened Co-Base Alloy by Mechanical Attrition", AFML-TR-74-34, Contract No. AF 33(615)-73-C-5150 (March 1974). (MCIC 89506)
25. Grierson, R., "Investigation of Processing-Microstructure-Property Relationships of Oxide Dispersion-Strengthened Co-Alloy Extrusions", IR-73510173 (II), Contract AF 33(615)-75-C-5061 (September 1975). (MCIC 96079)
26. Drapier, J. M., Coutsouradis, D., and Habraken, L., "Structure and Properties of Dispersion-Strengthened Co Alloys", *Cobalt*, **53**, 197-205 (December 1971).
27. Wallwork, G. R., and Hed, A. Z., "Selection of An Alloy Composition in the Ternary Co-Cr-Al System for Oxidation Resistance", *Oxidation of Metals*, **3** (3), 243-250 (1971).
28. Wright, I. G., Wilcox, B. A., and Jaffee, R. I., "Oxidation and Hot Corrosion of Ni-Cr and Co-Cr Alloys Containing Rare Earth Oxide Dispersions", Final Report, Contract N00019-72-C-0190 (1973). (MCIC 85696)
29. Stringer, J., and Wright, I. G., "The High-Temperature Oxidation of Co-21 Wt. % Cr-3 Vol. % Y<sub>2</sub>O<sub>3</sub> Alloys", *Oxidation of Metals*, **5** (1), 59 (1972).
30. Giggins, C. S., and Pettit, F. S., "Oxide Scale Adherence Mechanisms", Contract AF 33(615)-72-C-1702, Progress Report (April 1975). (MCIC 93380)
31. Barnett, W. J., Bailey, P. G., Klingler, L. J., "A Manufacturing Process for TD Co-Ni-Cr-Sheet", AFML-TR-72-116 (July 1972). (AD906 873)
32. Triffleman, B. H., and Irani, K. K., "Process Development for a Dispersion-Strengthened Co-Base Alloy", NASA CR-72591, Contract NAS 3-11161 (December 1969).
33. Triffleman, B. H., "Development of Procedures for Producing Dispersion-Strengthened Co-Base Alloys by the Flash Drying Selective Reduction Process", Contract NAS 3-7272 (December 1967).
34. "Dispersion Strengthened Material Evaluation Program-Feasibility for Structural Mechanical Fasteners 1400-2200 F", Standard Pressed Steel Co., Contract AF 33(615)-3220 (November 1966).
35. Bufferd, A. S., and Grant, N. J., "Oxide Dispersion Strengthening of Co-Base Alloys", *Journées des Applications du Cobalt*, Paper No. 18, 251-261 (June 1964).
36. Kobrin, L., "Dispersions Lock Strength in Metals", *The Iron Age*, 69-72 (November 26, 1964).
37. Palme, R., "Non-Metallic Dispersions in Co and Its Alloys. Part 2. Sintered High-Temperature Co-Cr Alloys", *Cobalt*, **6**, (1960).



## CHROMIUM

The main reason for interest in chromium as a structural material lies with its combination of high melting point, low density, and moderately good oxidation resistance, especially as compared with iron, cobalt, and nickel. Unfortunately, the ductility of chromium is adversely affected by trace amounts of carbon and nitrogen so that the ordinary commercial grades of the metal are normally brittle at room temperature. Also, the metal is further embrittled during high-temperature air exposure. The effect of various alloying element additions and of impurities has been presented in some detail in a book<sup>(1)</sup> and two articles<sup>(2, 3)</sup>.

Some promising chromium alloys have been made by dispersion hardening. Some of these incorporated oxide additions and were produced by powder metallurgy methods. These will be described in this section. However, some authors define DS alloys as those produced by precipitation of a compound insoluble in the solid chromium solid solution, such as carbides, nitrides, or borides.<sup>(1)</sup> These alloys will not be discussed in this review.

### Cr-MgO Alloys

The development of successful DS chromium alloys began when Scruggs<sup>(4)</sup> announced a ductile Cr-6MgO-0.5Ti alloy which was designated as "Chrome 30". This alloy was characterized by its consistently high degree of room-temperature tensile ductility, and its surprisingly high tolerance for impurities. The alloy also showed improved oxidation resistance relative to unalloyed chromium at 1800 F (982 C).

This work at the Bendix Corporation was continued through a series of several research and development programs under sponsorship of the Air Force and the Bureau of Naval Weapons. An excellent accounting of these is available in an earlier MCIC review by Maykuth and Gilbert.<sup>(5)</sup> In brief, it was shown that the high-temperature strength of the Cr-MgO alloys could be improved with minor additions of vanadium, columbium, and tantalum. The effects of numerous powder-metallurgical processing variables were also explored. The major compositions of interest were identified as follows:

Chrome 30: Cr-6MgO-0.5Ti<sup>(a)</sup>  
Chrome 30A: Cr-6MgO-0.5Ti  
Chrome 90: Cr-3MgO-2.5V-0.5Si  
Chrome 90S: Cr-3MgO-2.5V-1Si-0.5Ti-2Ta-0.5C

The strength and ductilities of these alloys are compared in Figures 28 and 29 with each other and to those of several other high-strength, chromium-base alloys. The latter include the solid-solution strengthened Alloy E (Cr-2Ta-0.5Si-0.5Ti) and the solid-solution-plus-precipitation-strengthened alloys C-207 (Cr-7.5W-0.8Zr-0.2Ti-0.1C-0.15Y) and CI-41 [Cr-7.1Mo-2Ta-0.09C-0.1(Y + La)].

Generally, for all alloy types, the alloys with highest strengths also show the highest ductile-to-brittle transition temperatures. Also, the DS Cr-MgO alloys show lower strengths but better low-temperature ductility than the solid-solution or precipitation-strengthened alloys.

NASA investigators<sup>(6)</sup> have also studied the properties of a Cr-5MgO alloy to determine the capabilities and limitations of this material for structural applications at elevated temperature. The room-

---

(a) Prepared using chemically precipitated MgO. All others used fused MgO.

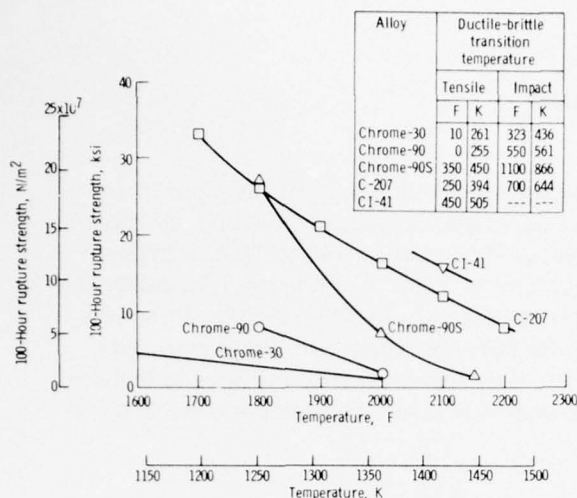


Figure 28. Strength and Ductility of Selected Chromium Alloys<sup>(3)</sup>

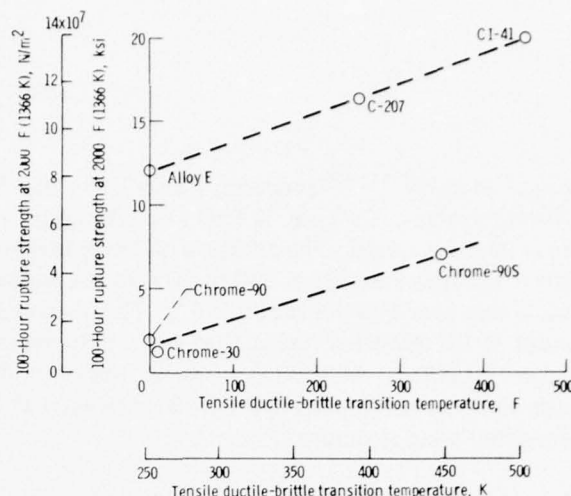


Figure 29. Trade-Off Between Strength and Ductility of Chromium Alloys<sup>(3)</sup>

temperature tensile strength and yield strength were 40 and 35 ksi, respectively, and the tensile elongation was 3 percent. Preoxidation at 1095 C did not affect the strength, but preoxidation at and above 1205 C caused a loss in room-temperature strength and ductility. The elevated-temperature strength dropped rapidly and at 1095 C the tensile strength was only 25 percent of the room-temperature value. At 1425 C, the tensile strength was only 7 percent of the room-temperature strength.

Khodkin, et al.<sup>(7)</sup> also investigated the properties of chromium containing 3 to 9 percent MgO in both the as-sintered and wrought conditions. As-sintered, the alloys were porous and brittle in room-temperature bending. After deformation, the Cr-5MgO alloy had a tensile strength in the range of 25-33 kg/mm<sup>2</sup> (245-323 MPa), with an elongation of 3 percent. After annealing at 900-1000 C, these properties increased to 40 kg/mm<sup>2</sup> and 20 percent. After annealing at 1200-1300 C, the alloy showed a tensile strength of 30-35 kg/mm<sup>2</sup> (294-343 MPa) and an elongation of 10 percent.

In a study of the oxidation behavior of Cr-MgO alloys<sup>(8)</sup>, the Bendix investigators discovered that impurities contained in the MgO—particularly iron, silicon, and calcium—had profound effects. The purest MgO at a level of 3 percent showed the least resistance to contamination and spalling of scale. A fused grade of MgO, in which selected impurities were added during manufacture to aid in melting, was found to give best results. A 0.15 percent CaO addition to a very pure Cr-3MgO alloy reduced substantially the rate of oxidation and promoted adherence of the protective scale. Additions of 0.1 percent each of Fe<sub>2</sub>O<sub>3</sub> and SiO<sub>2</sub> were found to reduce room-temperature ductility to almost zero. In general, best oxidation resistance was achieved with the Chrome 30 and 90 compositions which could be exposed for several hours at temperatures of about 1230 C in air and rapidly air cooled to room temperature without suffering detachment of the protective oxide layer.

The NASA studies on Cr-5MgO indicated that oxidation rates in static air were rapid above 1205 C.<sup>(6)</sup> Yttrium additions did not improve this alloy's resistance to oxidation. The oxide film formed on the surface was composed of Cr<sub>2</sub>O<sub>3</sub> and MgCr<sub>2</sub>O<sub>4</sub>, which spalled. In dynamic oxidation tests at 1760 C for 5 minutes, the material eroded and melted. Machining, forming, and joining of this sheet material were also studied.

Khodkin<sup>(9)</sup> also explored the effect of MgO additions on the oxidation kinetics of chromium. He further demonstrated that a Cr-5MgO alloy showed good thermal stability after 450 cycles of heating to 1300 C and quenching in water, or 200 cycles of heating with an acetylene torch to 1500-1550 C and cooling with a jet of compressed air.

## Cr-ThO<sub>2</sub> Alloys

Veigel, et al.<sup>(10, 11, 12)</sup> prepared DS Cr-ThO<sub>2</sub> powder by hydrogen reduction of CrI<sub>2</sub> vapor in a "flame" reactor. Cr-3 vol. % ThO<sub>2</sub> powders were consolidated by hot isostatic pressing, rolled to sheet, and evaluated. The addition of ThO<sub>2</sub> lowered the DBTT, e.g., from 140 to 15 C in the as-rolled condition and from 140 to 50 C in the annealed (1 hour at 1200 C) condition. The dispersion was stable over 100 hours at 1427 C. The yield and ultimate strengths of the Cr-3ThO<sub>2</sub> alloy were about 10 ksi (69 MPa) higher than corresponding values for pure chromium over the temperature range 150-200 C. At 1093 C, however, the strength of the alloy was essentially the same as that for pure chromium. Annealing the Cr-3ThO<sub>2</sub> alloy at 1316 and 1427 C for 100 hours resulted in an elongated grain structure.

Arias<sup>(13)</sup> also investigated the properties of Cr-ThO<sub>2</sub> alloys, which he prepared using the unique procedure of ball milling the chromium powder in an environment of hydrogen halides. The reason for using these gases is first, to exclude oxygen and nitrogen as possible contaminants on the chromium powder's surface, and second, to use the chromium halides (which form by reaction) as ball-milling aids. His most extensive work was carried out using hydrogen iodide as the ball-milling medium to explore the effects of processing variables on the properties of a Cr-4 vol. % ThO<sub>2</sub> composition.<sup>(14, 15)</sup> With this milling technique, he was able to achieve a uniform distribution of thoria in particle sizes from 0.02 to 0.2 micron. The effects of various processing variables on the yield strength of the Cr-4ThO<sub>2</sub> alloy as a function of temperature are shown in Figure 30. By isostatically hot pressing and hot rolling the alloy, he was able to achieve impressive combinations of strength and ductility in the Cr-4ThO<sub>2</sub> composition. These are compared in Figure 31 with similar values for selected alloys which were prepared by arc melting. As shown, the strength of the Cr-4ThO<sub>2</sub> alloy is superior to these other materials at temperatures up to about 800 C. Also, the alloy maintains a reasonably low DBTT (-8-24 C) in this test condition.

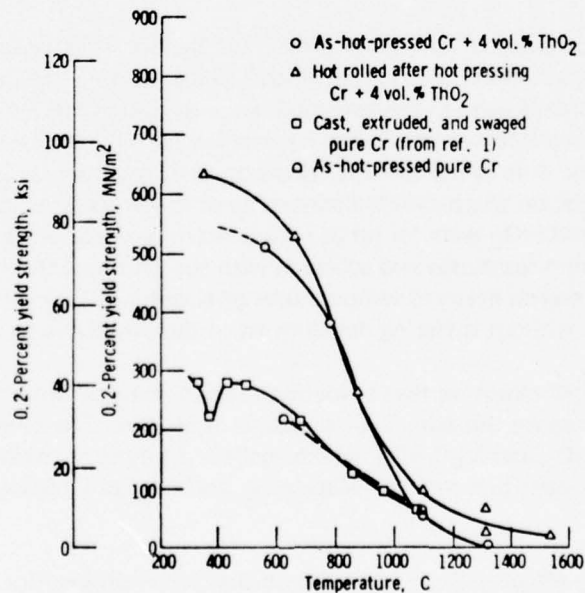


Figure 30. Effect of Temperature on the Yield Strength of Cr-4ThO<sub>2</sub><sup>(15)</sup>



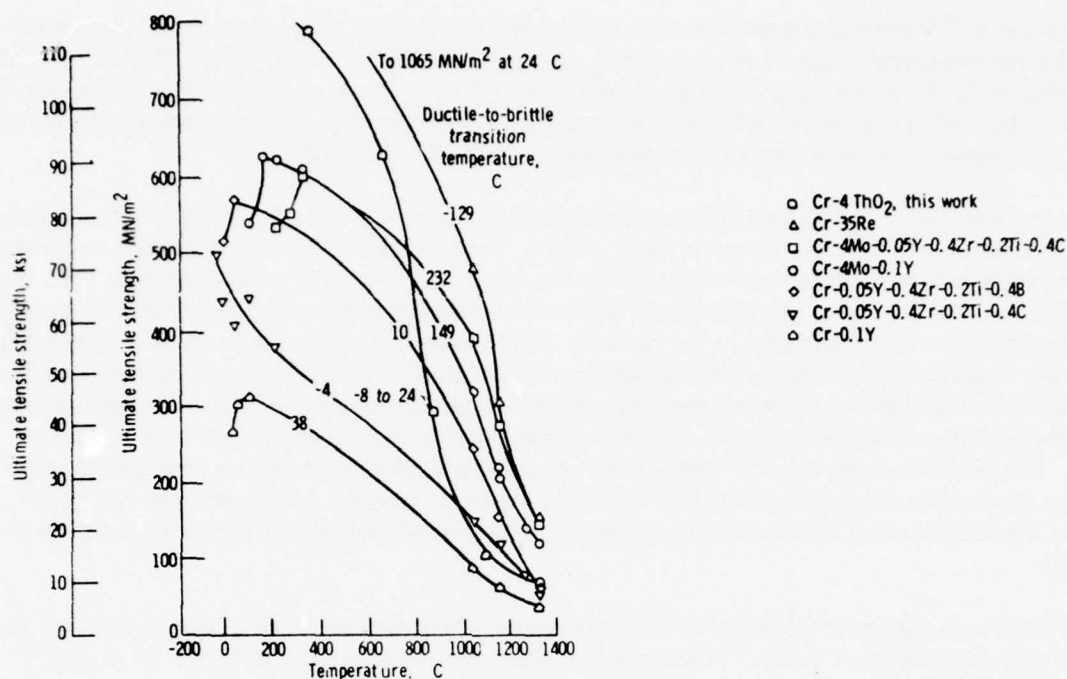


Figure 31. Effect of Temperature on the Ultimate Tensile Strength of Selected Chromium-Base Alloys<sup>(15)</sup>

Hed, et al.<sup>(16)</sup> investigated the high-temperature oxidation of a Cr-3.12 wt. % ThO<sub>2</sub> alloy at 1100 and 1200 C in oxygen at 100 torr for 25 hours. The rate of oxidation as compared with chromium was significantly reduced by the ThO<sub>2</sub> dispersion. The morphology of the scale showed that oxygen can diffuse slowly through the oxide scale, at least after it detaches from the metal. The continuous oxide formed on the DS Cr-ThO<sub>2</sub> alloy had a rather smaller grain size than that formed on pure Cr.

### Other Chromium Alloys

Recent Russian work includes that of Antsiferov and Maksimova<sup>(17)</sup> who dispersed  $\alpha$ -Al<sub>2</sub>O<sub>3</sub>, ZrO<sub>2</sub>, and MgO in chromium powder having a particle size of 90 percent less than 10 microns. The average particle size of the oxides was approximately 1 micron. The mixtures were stirred mechanically in alcohol for 36 hours and dried by stirring. They contained 1,3,5, and 7 wt. % Al<sub>2</sub>O<sub>3</sub> or ZrO<sub>2</sub> and 1,3, and 5 wt. % MgO. Increasing the sintering temperature from 1500 to 1600 C resulted in an increase in the particle size of the dispersoid. The relative density of the sintered compacts was approximately 80 percent. The bending strength of plate samples and their room-temperature toughness was tested.

Kaputkin, et al.<sup>(18)</sup> calculated the potential reactivity of chromium with several oxides under conditions where they were either separated from any outside environmental effects or exposed to wet hydrogen. In the first case, the reactivity of the oxides with chromium at 1000 K (727 C), in decreasing order, was MgCrO<sub>4</sub>, Al<sub>2</sub>O<sub>3</sub>, MgO, and ZrO<sub>2</sub>. At 2000 K (1727 C), the order was MgO, MgCr<sub>2</sub>O<sub>4</sub>, Al<sub>2</sub>O<sub>3</sub>, and ZrO<sub>2</sub>. With hydrogen present at 1000 K, the order was MgO, Al<sub>2</sub>O<sub>3</sub>, ZrO<sub>2</sub>, and MgCr<sub>2</sub>O<sub>4</sub>, and at 2000 K, MgCr<sub>2</sub>O<sub>4</sub>, MgO, Al<sub>2</sub>O<sub>3</sub>, and ZrO<sub>2</sub>.

Samsonov, et al.<sup>(19)</sup> studied the spark-erosion resistance of chromium alloys containing binary additions of 4 volume percent each of  $\text{Al}_2\text{O}_3$ ,  $\text{Sc}_2\text{O}_3$ ,  $\text{Cr}_2\text{O}_3$ ,  $\text{TiO}_2$ ,  $\text{ZrO}_2$ ,  $\text{HfO}_2$ ,  $\text{AlN}$ ,  $\text{TiN}$ ,  $\text{ZrN}$ ,  $\text{HfN}$ ,  $\text{CbN}$ ,  $\text{VN}$ ,  $\text{TaN}$ , and  $\text{Cr}_2\text{N}$ , with special emphasis on the Cr-AlN alloys. It was concluded that the erosion resistance of the alloys is determined by their hardness, strength, ductility, grain size, and electrical resistivity. The highest erosion resistance was obtained in a Cr-8AlN composition.

Wagner and Erickson<sup>(20)</sup> tried two different electroplating techniques to produce DS chromium alloys containing particles of BC, SiC, glass frit,  $\text{ZrO}_2$ ,  $\text{Al}_2\text{O}_3$ , and diamond dust. One technique involved reliance on the random occlusion of mechanically dispersed particles in the plating solution. The other technique involved the use of particles plated with a ferromagnetic coating and a magnetic cathode for magnetic attraction of the particles to the cathode. Coatings were plated on steel Falex pins and subjected to a modified test procedure with unplated steel V-blocks and oil. From the test data, coefficients of friction and wear properties were determined for each coating. The first technique produced randomly occluded particles which increased the coating coefficient of friction and wear of Falex blocks. The second technique, with magnetically attracted particles, produced an unsatisfactory distribution of particles along the surface of the pins during electroplating. Little variation was noted between the coefficient of friction of the chromium plate with and without particles occluded by this technique.

Several other investigators have explored the properties of chromium containing large amounts (more than 20 volume percent) of oxides. These reported alloy systems include Cr- $\text{UO}_2$ <sup>(21)</sup>, Cr- $\text{Al}_2\text{O}_3$ <sup>(22)</sup>, and Cr- $\text{Cr}_2\text{O}_3$ <sup>(23, 24, 25)</sup>. Inasmuch as these materials are more properly considered as cermets rather than as DS chromium alloys, these works are not reviewed in this report. A brief review of these studies is available in Reference 5.

## REFERENCES

1. Sully, A. H., and Brandes, E. A., Chromium, Plenum Press, New York (1967).
2. Rogers, J. A., and Brown, A.R.G., "The Development of Cr-Base Alloys for Use at High Temperatures", Metals and Materials, 246-258 (August 1967).
3. Klopp, W. D., "Recent Developments in Cr and Cr Alloys", J. of Metals, 23-32 (November 1969).
4. Scruggs, D. M., "Chromium Composites are Ductile", Materials in Design Engineering, 115-117 (December 1962).
5. Maykuth, D. J., and Gilbert, A., "Chromium and Chromium Alloys", DMIC Report 234, 20-24 (1966).
6. Manning, C. R., and Royster, D. M., "Investigation of Mechanical Properties and Metallurgical Characteristics of a Metallic Cr-MgO Composite", NASA TN D-1735 (1963).
7. Khodkin, V. I., Semina, L. V., and Gerasimova, M. I., "New Chromium-Base Material With MgO Additives" (1968). (MCIC 80539)
8. Watkins, R. V., "Optimization and Evaluation of Chromium Composites", Bendix Corporation Report (February 1968). (MCIC 71802)
9. Khodkin, B. I., "Dispersion Hardened Materials", Reference 206 in Portnoy and Babich, Moscow Metallurgiya, 127-199 (1974).
10. Veigel, N. D., Wilcox, B. A., Blocher, J. M., Clauer, A. H., Seifert, D. A., Meiners, K. E., Browning, M. F., and Pfeifer, "Development of a Chromium-Thoria Alloy", NASA-Cr-72901 (March 1971).
11. Veigel, N. D., Blocher, J. M., and Browning, M. F., "Preparation and Properties of Thoriated Chromium", Third Chemical Vapor Deposition Proceedings, 200-213 (1972).
12. Wilcox, B. A., Veigel, N. D., and Clauer, A. H., "Ductile-Brittle-Transition of Thoriated Cr", Met. Trans. (January 1972).
13. Arias, A., "Feasibility of Producing Dispersion Strengthened Cr by Ball Milling in Hydrogen Halides", Powder Metallurgy, 12 (23), 45-78 (1969).
14. Arias, A., "Properties of DS-Cr-4 Vol. %  $\text{ThO}_2$  Alloys Produced by Ball Milling in Hydrogen Iodide", NASA TN D-7512 (January 1974).
15. "Production of Cr Base Alloys by Ball Milling in HI", Metallurgical Trans. 6B, 631-640 (1975).

# REFERENCES (Cont.)

16. Stringer, J., Hed, A. Z., Wallwork, G. R., and Wilcox, B. A., "The Effect of ThO<sub>2</sub> Dispersion on the High Temperature Oxidation of Cr", *Corrosion Science*, 12, 625-636 (1972).
17. Antsiferov, V. N., and Maksimova, T. N., "The Effect of Dispersed Oxide Inclusions on Certain Properties of Sintered Cr", *Poroshkovaya Metallurgiya*, 73 (1), 34-36 (1969).
18. Kaputkin, E. Y., Kenigfest, A. M., Mozhukhin, E. I., Rabovskiy, V. S., and Khodkin, V. I., "Reaction Between Dispersed Oxide Inclusions and Cr", *Izvest. Akad. Nauk SSSR Metally*, (5), 159-164 (1974).
19. Samsonov, G. V., Alfintseva, R. A., and Verkhoturov, A. D., "Erosion Resistance of DS M Based on Refractory Metals", *Soviet Powder Metallurgy and Metal Ceramics*, 14 (10), 831-833 (1975).
20. Wagner, L. H., and Erickson, R. P., "Electrodeposition of Cr With Codeposited Particles", SWERR-TR 72-29 (May 1972). (AD 747 767)
21. Lever, R. C., "Metallic Fuel Element Materials", General Electric Company Report APEX-913 under Air Force Contract AF 33(600)-38062 and AEC Contract AT(11-1)-171 (June 20, 1962).
22. Schifferli, L. M., "A Review of Some Chromium-Alumina Refractory Composites", paper presented at 9th Meeting of the Refractory Composites Working Group, Worcester, Massachusetts (August 1964).
23. Stone, H.E.N., and Lockington, N. A., "Chromium Oxide-Chromium Cermets", *Nature*, 203, 70 (1964).
24. Stone, H.E.N., and Lockington, N. A., "Preparation and Some Properties of Chromic Oxide-Chromium Cermets Made by Partial Reduction of the Oxides", *Powder Met.*, 7 (14), 113-124 (1964).
25. Stone, H.E.N., and Lockington, N. A., "Preparation and Some Properties of Cr<sub>2</sub>O<sub>3</sub> Cermets. II. Preparation Directly from Mixtures of Oxide and Metal, and of Oxide, Metal, and Graphite", *Powder Met.*, 8 (15), 81-91 (1965).



## COPPER

To initiate this review on the dispersion-strengthening of copper, both the MCIC files and those of the Copper Development Association, Inc., were searched. These searches yielded a total of 128 references, extending as far back as 1959, on studies or articles concerning the dispersion strengthening or dispersion hardening of copper. These included a 1966 review (containing 38 references) of the subject<sup>(1)</sup> which had been prepared under the auspices of the Defense Metals Information Center, a precursor to MCIC. A more recent review by Marsden<sup>(2)</sup> covered the period of 1967 to 1972 (with 14 references).

Unfortunately, it was not possible in the time available for this study to locate and review each of these 128 references. As a compromise, abstracts and/or summaries of 51 of the most recent references were selected and reviewed to determine the most outstanding new accomplishments in this subject area. From these, 18 were chosen as primary references. The balance of 33 references were classified for reader assistance according to the types of dispersoid investigated and are identified in the last table of this section. The remaining 77 unused references have been attached as a bibliography as a possible additional information source for the reader.

In 1969, Desy<sup>(3)</sup> compared the properties of dispersion-strengthened copper prepared by seven other investigators who used various methods as shown in Table 22. A considerable spread in the strengths occurred, even for alloys containing about the same volume percent of the same dispersoid, e.g., alumina. This, of course, is due to processing differences. Desy strongly favored the coprecipitation process whose advantages were illustrated by comparing the disadvantages of the other methods. The mechanical mixing method, for example, has the following disadvantages:

1. It is difficult to produce a good dispersion without agglomeration of the oxide particles, which tends to cause segregation and lamination in the working direction of the fabricated material.
2. Mixing of powders on a large scale may prove to be difficult.
3. Dispersoid particle spacings are limited by the copper particle size.
4. The size of the dispersoid is limited by the powders that are available.
5. The relative sizes of the copper and oxide particles must be carefully regulated for best mechanical properties.
6. The dispersoid particles are generally present only at the grain boundaries of the copper, a condition which reduces ductility.

The internal oxidation method, as conventionally used, has the following disadvantages:

1. This process is limited by the diffusion rate of oxygen in solid copper. Thin sheet, wire, or powder must generally be used.
2. Control of the particle size is difficult. The initial precipitate particles tend to grow as the process proceeds.
3. There is a tendency for the diffusing oxygen to form copper oxides in the grain boundaries. This means that the material is subject to hydrogen embrittlement if brazed in a hydrogen atmosphere.

The coprecipitation method has the following advantages:

1. The process could be adapted to commercial operations involving leaching of primary or secondary copper sources.
2. The process produces well-dispersed particles in the optimum size range for strengthening.
3. Concentration of oxide can easily be varied.
4. The process is adaptable to a variety of oxides.
5. The plastic deformation that is required to produce the optimum properties can be introduced during the compaction and extrusion of the powder, and by subsequent cold work.

Table 22. Comparison of Dispersion-Strengthened Copper Prepared by Various Methods<sup>(3)</sup>

Materials			Room Temperature Properties				100-Hour Rupture Strength at 450 C, psi	Electrical Conductivity, % of IACS <sup>(a)</sup>
Source	Method of Preparation	Oxide Content, vol. %	Tensile Strength, psi	Yield Strength, psi	Reduction in Area, %	Elongation, %		
<u>Desy—1969</u>								
Aqueous solutions of mixed nitrates of copper and aluminum or yttrium	Coprecipitation	2.0 alumina	46,200 <sup>(b)</sup>	33,800 <sup>(b)</sup>	53 <sup>(b)</sup>	23 <sup>(b)</sup>	15,000	93 <sup>(e)</sup>
		2.0 yttria	57,500 <sup>(c)</sup>	50,900 <sup>(c)</sup>	66 <sup>(c)</sup>	19 <sup>(c)</sup>	14,500	93 <sup>(e)</sup>
<u>Zwilsky and Grant—1961</u>								
1 micron copper powder with 0.018 micron alumina powder	Mechanical mixing	7.5 alumina	88,500 <sup>(b)</sup>	69,900 <sup>(b)</sup>	7 <sup>(b)</sup>	5 <sup>(b)</sup>	23,500	69.4
		2.5 alumina	35,300 <sup>(b)</sup>	27,400 <sup>(b)</sup>	68 <sup>(b)</sup>	20 <sup>(b)</sup>	8,000	78.7
<u>Preston and Grant—1961</u>								
Powdered copper-aluminum alloy	Internal oxidation	3.5 alumina	76,000 <sup>(b)</sup>	65,100 <sup>(b)</sup>	31 <sup>(b)</sup>	13 <sup>(b)</sup>	38,000	64
<u>Jackson—1963</u>								
Aqueous solutions of mixed nitrates of copper and aluminum	Coprecipitation	0.6 alumina	44,800 <sup>(d)</sup>	—	—	24 <sup>(d)</sup>	—	99
<u>Iler, Pasfield, and Yates—1964</u>								
Aqueous solution of copper nitrate with colloidal zirconium oxide	Coprecipitation	2.5 zirconia	45,000 <sup>(e)</sup>	—	—	25 <sup>(e)</sup>	—	—
<u>McDonald—1966</u>								
Copper-0.10 wt. % beryllium alloy	Internal oxidation	0.8 beryllia	80,000 <sup>(f)</sup>	63,000 <sup>(f)</sup>	50 <sup>(f)</sup>	12 <sup>(f)</sup>	44,000 <sup>(g)</sup>	85
<u>Das, Chevrette, and Freedman—1964</u>								
Thin strips of copper-aluminum alloy	Internal oxidation	2.5 alumina <sup>(h)</sup>	44,000 <sup>(i)</sup>	29,000 <sup>(i)</sup>	—	12 <sup>(i)</sup>	—	—
<u>London—1963</u>								
Copper-thorium alloy added to molten copper-boron alloy	Liquid metal process	2.0 thorium boride <sup>(j)</sup>	36,130 <sup>(k)</sup>	19,330 <sup>(k)</sup>	—	38 <sup>(k)</sup>	8,000 <sup>(l)</sup>	—
		4.0 thorium boride <sup>(j)</sup>	42,400-46,400 <sup>(k)</sup>	—	38-40 <sup>(k)</sup>	26 <sup>(k)</sup>	—	—

(a) International Annealed Copper Standard.

(b) As-extruded.

(c) As-extruded and swaged 64 percent.

(d) Annealed ½ hour at 780 C.

(e) Annealed at 400 C.

(f) Annealed at 704 C.

(g) Tested at 399 C.

(h) Composition estimated.

(i) Annealed 1 hour at 1000 C plus 22 hours at 475 C.

(j) Reference does not state whether composition is by weight or by volume.

(k) As hot rolled.

(l) Tested at 400 C.

As with several other metals, aluminum oxide has been strongly favored as a dispersoid strengthener in copper because of its high free energy of formation which leads to good stability and compatibility with the matrix. The most notable recent advances with producing DS Cu-Al<sub>2</sub>O<sub>3</sub> alloys are those which were achieved by workers in the Metals Group of the Glidden-Durkee Division of the SCM Corporation. These investigators developed a new variation<sup>(4, 5)</sup> of internal oxidation which is carried out by using an oxidant consisting of an intimate mixture of cuprous oxide and a carefully controlled amount of Al<sub>2</sub>O<sub>3</sub>. After reduction, the in situ reduced copper oxide forms dispersion-strengthened copper because of the presence of the Al<sub>2</sub>O<sub>3</sub> during consolidation. The oxidant may be produced by any method of making DS copper where the intermediate product can be used as the source of oxygen for internal oxidation. It may also be made by complete oxidation of the appropriate copper-aluminum alloy or dispersion-strengthened alloy.

As a result of this effort, four commercial grades of DS Cu-Al<sub>2</sub>O<sub>3</sub> alloys were introduced by Glidden Metals<sup>(6,7,8)</sup> in 1973. These contain nominally 0.1, 0.2, 0.35, and 0.6 weight percent Al<sub>2</sub>O<sub>3</sub> and carry the designations of Glidcop AL-10, 20, 35, and 60, respectively. Figure 32 relates these compositions to their nominal room-temperature tensile properties in the as-extruded condition. Since that time, the Copper Development Association has assigned these alloys the copper number 157 and offers data sheets for three alloys: C-157-10, -20, and -35, respectively.<sup>(9)</sup> Physical properties for three of these alloy grades are given in Table 23.

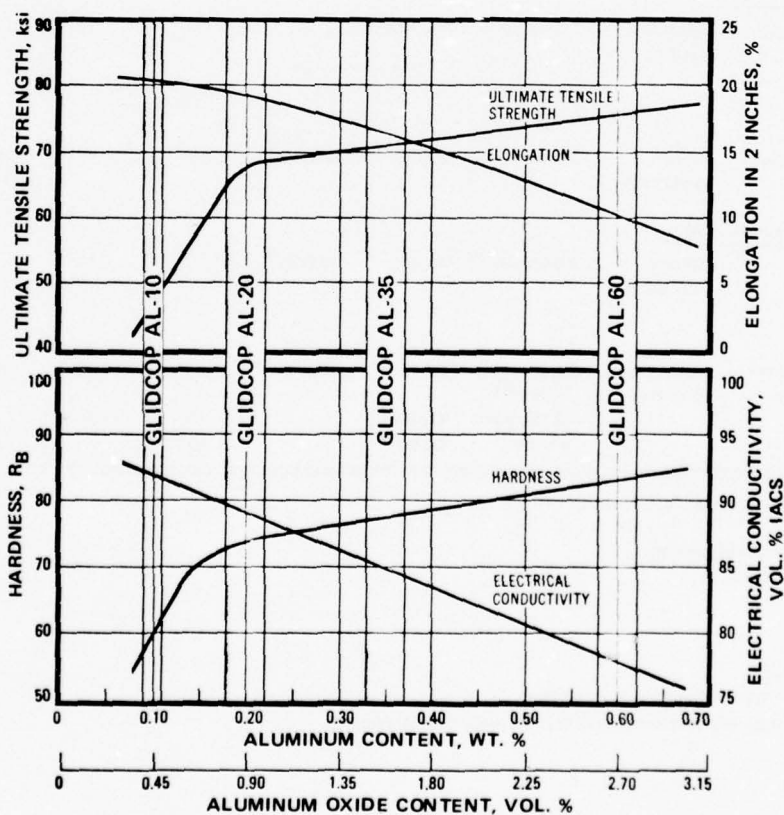


Figure 32. Nominal Tensile Properties of Four Commercial DS Cu-Al<sub>2</sub>O<sub>3</sub> Alloy Grades, As Extruded<sup>(6)</sup>



Table 23. Physical Properties of GlidCop Alloys<sup>(6)</sup>

Properties	Grades		
	AL-10	AL-35	AL-60
Melting Point, F . . . . .	1980	1980	1980
Density,			
at 68 F, lb/cu in . . . . .	0.3191	0.3183	0.3176
at 28 C, g/cm <sup>3</sup> . . . . .	8.82	8.80	8.78
Electrical Conductivity,			
at 68 F, % IACS . . . . .	90	85	80
at 20 C, megmho-cm . . . . .	0.522	0.493	0.464
Thermal Conductivity,			
at 68 F, BTU/ft <sup>2</sup> /ft/hr/F . . . . .	208	196	186
at 20 C, Cal/cm <sup>2</sup> /cm/sec/C . . . . .	0.86	0.81	0.77
Electrical Resistivity,			
at 68 F, Ohms (circ. mil/ft) . . . . .	11.56	12.22	13.00
at 20 C, microhm-cm . . . . .	1.92	2.03	2.16
Coefficient of Thermal Expansion			
(120-850 F) in/in/F . . . . .	10.8x10 <sup>-6</sup>	11.1x10 <sup>-6</sup>	11.3x10 <sup>-6</sup>
(50-450 C) cm/cm/C . . . . .	19.5x10 <sup>-6</sup>	20.0x10 <sup>-6</sup>	20.4x10 <sup>-6</sup>
Modulus of Elasticity			
psi . . . . .	15.5x10 <sup>6</sup>	17.8x10 <sup>6</sup>	19.9x10 <sup>6</sup>
GN/m <sup>2</sup> . . . . .	107	123	137

These alloys maintain high tensile strength at elevated temperatures as illustrated by the data in Figure 33 which compares these values to those for OFHC copper and for Cu alloys 150 and 182. Similarly, the DS Cu-Al<sub>2</sub>O<sub>3</sub> alloys maintain their strength after elevated temperature exposure as illustrated by the data in Figure 34. Some stress-rupture properties of the Cu-0.35Al<sub>2</sub>O<sub>3</sub> alloy are shown in Figure 35.

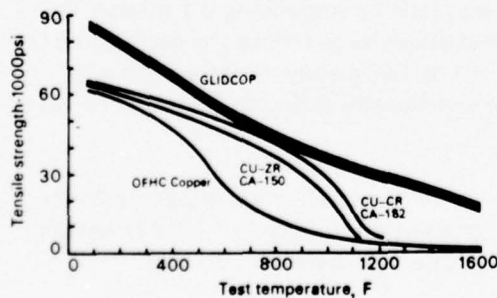


Figure 33. Tensile Strengths of Selected Copper Alloys at Various Test Temperatures<sup>(10)</sup>

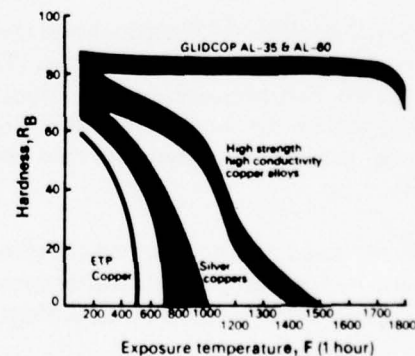


Figure 34. Hardness of Selected Copper Alloys as Affected by Exposure Temperature<sup>(10)</sup>

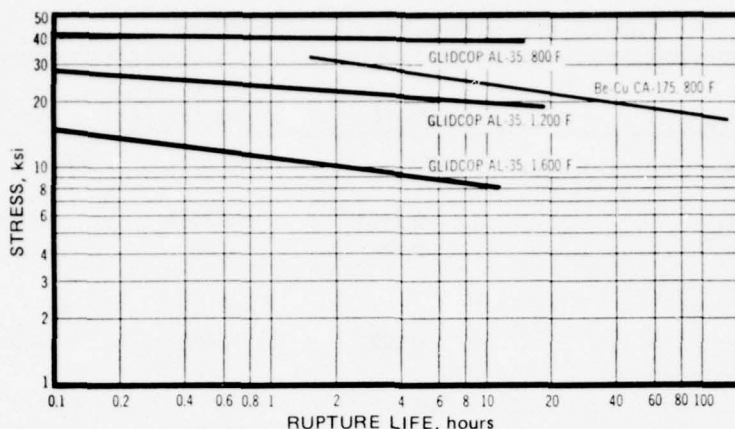


Figure 35. Stress-Rupture Life of DS Cu-0.35Al<sub>2</sub>O<sub>3</sub> Alloy at Elevated Temperatures<sup>(6)</sup>

Nadkarni, et al.<sup>(5)</sup> have reported the properties for a series of DS Cu-Al<sub>2</sub>O<sub>3</sub> alloys prepared using the patented Glidden procedure. In this instance, the oxidants were prealloyed copper-aluminum powders. Properties were determined after hydrogen reduction and extrusion. Details on the effects of processing variables, including extrusion ratio and effects of cold-working reductions and annealing treatments, were explored and are reported. Properties for a DS Cu-1.57 vol. % Al<sub>2</sub>O<sub>3</sub> alloy, which corresponds to the GlidCop Al-35 grade, were reported extensively. Figures 36, 37, and 38 compare the tensile strength, stress-rupture strength, and thermal plus electrical conductivities of this alloy, respectively, with those for pure copper and Cu-0.15Zr and Cu-0.7Cr alloys.

Peterson, et al.<sup>(11)</sup> investigated a Cu-1 vol. % ThO<sub>2</sub> alloy which was fabricated from spray-dried and subsequently consolidated powders. The ThO<sub>2</sub> particle dispersion quality improved during subsequent cold working of the alloy. However, it was found that the character of the dispersions is largely determined during the powder formation and consolidation process. The texture formation resulting from hot consolidation and secondary processing cannot be considered significant in determining the alloy's mechanical response. Although cold forming may prove a necessary step in the production of structural geometries of the alloy, no appreciable improvement of properties was achieved by this processing over the hot-consolidated alloy forms.

Fuschillo and Gimpl<sup>(12,13,14)</sup> used a novel chemical-precipitation technique to prepare several DS Cu-ThO<sub>2</sub> alloys for electrical-property studies. These alloys were made by suspending 0.1 micron ThO<sub>2</sub> particles in a solution of cupric acetate. Hydrazine was added dropwise to reduce the acetate and precipitate copper on the thorium. The resistivity of a Cu-2.2 vol. % ThO<sub>2</sub> alloy, prepared this way (then pressed, sintered, extruded, and cold swaged) was not significantly different from that for pure copper.<sup>(14)</sup>

Hansen<sup>(15)</sup> reviewed the literature on the effect of dispersoids on recrystallization as well as on the structure and mechanical properties after recrystallization. In addition to polycrystalline materials, DS-single crystals in the systems of Cu-0.8Al<sub>2</sub>O<sub>3</sub>, Cu-SiO<sub>2</sub>, and Cu-B<sub>4</sub>C were also covered.

Graham, et al.<sup>(16)</sup> made a series of unusual alloy compositions by coprecipitation and blending. Table 24 lists the compositions and hardness for these alloys both as-extruded and after annealing at 750 C for 1 hour. Air oxidation and tarnishing tests were made on all of these alloys, but none showed a tarnishing rate that was significantly different from that for high-conductivity copper although all of the DS alloys did show improved oxide-scale adhesion.

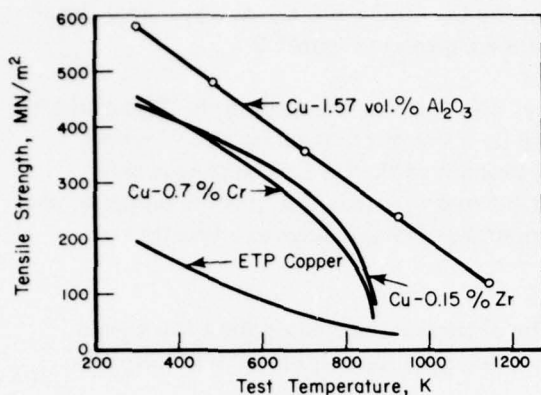


Figure 36. Elevated-Temperature Tensile Strength of Cu-1.57 Vol. %  $\text{Al}_2\text{O}_3$  Alloy, Cu-0.15Zr, Cu-0.7Cr, and Electrolytic Tough-Pitch Copper<sup>(5)</sup>

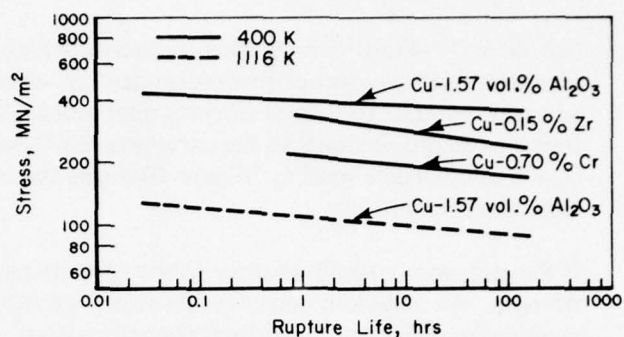


Figure 37. Stress-Rupture Data for DS Copper and Precipitation-Hardened Copper Alloys<sup>(5)</sup>

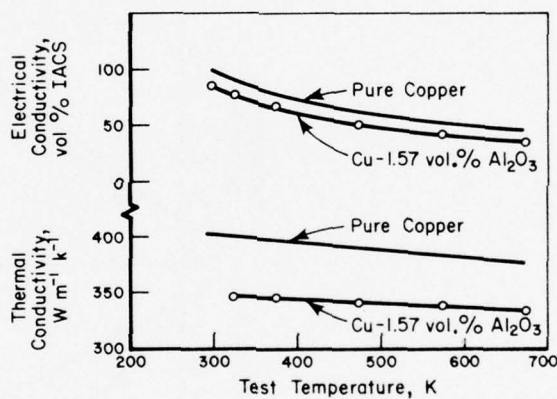


Figure 38. Thermal and Electrical Conductivities of DS Copper and Pure Copper<sup>(5)</sup>

Table 24. Hardness of Miscellaneous Dispersion-Strengthened Alloys<sup>(16)</sup>

Alloy Composition	HV 10 Hardness	
	As-Extruded	Annealed
Cu-8Al-4 vol. % $\text{Al}_2\text{O}_3$	242	220
Cu-7Al-2 vol. % $\text{Al}_2\text{O}_3$	186	213
Cu-2Be-2 vol. % $\text{Al}_2\text{O}_3$	186	173
Cu-24Ni-2.5 vol. % $\text{Al}_2\text{O}_3$	166	158
Cu-2.2 vol. % $\text{Al}_2\text{O}_3$	133	124
Cu-1.5 vol. % $\text{SiO}_2$	115	110
Cu-2.2 vol. % $\text{ThO}_2$	104	103



Poniatowski and Clasing<sup>(17)</sup> prepared and evaluated alloys in the Cu-Al<sub>2</sub>O<sub>3</sub> and Cu-BeO systems. Some stress-rupture properties for these alloys at three temperatures are given in Figure 39.

Donald and Pollard<sup>(18)</sup> have recently fabricated copper alloys using glass as the dispersoid. These alloys, approaching 95 percent of theoretical density, were obtained by a simple compacting and sintering sequence without the use of working operations. The yield strength of the DS Cu-glass alloys was found to be proportional to the parameter  $d/pD_s$  where  $d$  is the mean particle size,  $p$  is the porosity, and  $D_s$  the interparticle spacing. Figure 40 shows the tensile properties of these alloys as a function of dispersoid content.

If the glass was crystallized prior to the alloy preparation, the dispersions decreased the alloy's yield strength. An enhanced densification effect was obtained by using glass supersaturated with Cu<sub>2</sub>O in conjunction with mildly oxidized copper powder.

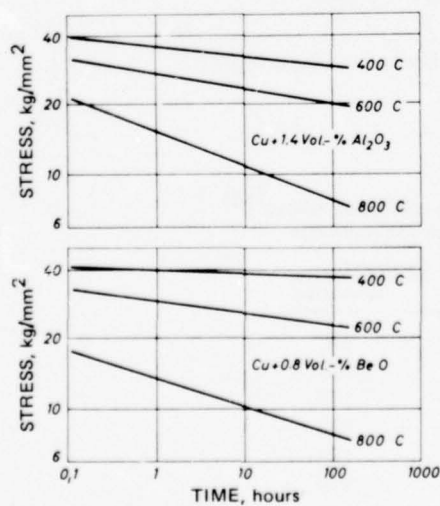


Figure 39. Stress-Rupture Curves for Annealed Copper Alloy Wires of 2-mm Diameter<sup>(17)</sup>

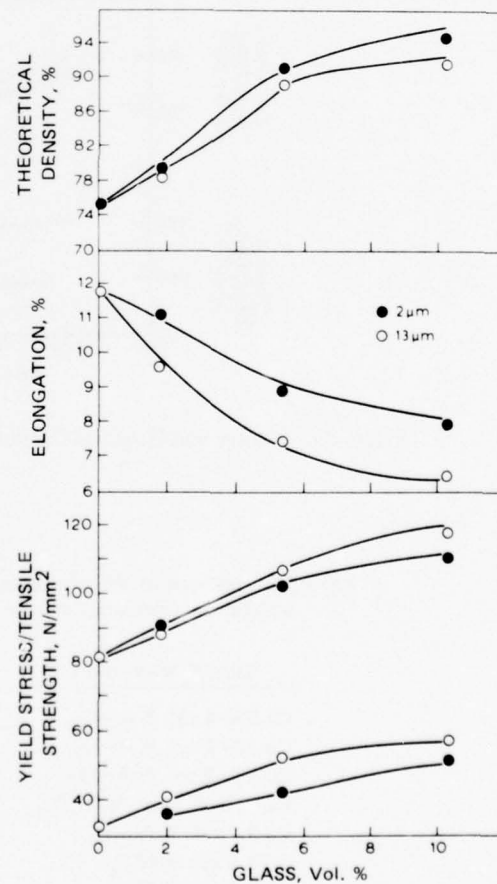


Figure 40. Effect of Glass Concentration of Mechanical Properties and Density Using Oxide-Saturated Glass and Oxidized Copper Powder<sup>(18)</sup>

In addition to the preceding studies, 33 additional references on the dispersion strengthening of copper and copper alloys were reviewed. For reader assistance, the types of dispersoids used in these studies have been listed by author and technique in Table 25. A bibliography of 77 un-cited references is also given following the numbered references.

**Table 25. Additional References to Dispersion-Strengthened Copper and Copper Alloys**

**I. Single crystals:**

- a) Cu-Al<sub>2</sub>O<sub>3</sub> - Gould (19,20); Hazzeldine (21); Lloyd (22); Dorey (23)
- b) Cu-BeO - Gould (20)
- c) Cu-SiO<sub>2</sub> - Mori (24); Hashimoto (25); Atkinson (26,27); Shewfelt (28); Lloyd (29)
- d) Cu-Cr-SiO<sub>2</sub> - Lloyd (29)

**II. Internal oxidation:**

- a) Cu-Al<sub>2</sub>O<sub>3</sub> - Chopra (32); Daneliya (33); Woolhouse (34); Schilling (35)
- b) Cu-Be - Jones (36)
- c) Cu-Si - Jones (36)
- d) Cu-Cr-Si - Palmer (37)
- e) Cu-Ni-Al - Schilling (35)

**III. Other techniques:**

- a) Cu-Al<sub>2</sub>O<sub>3</sub> - Schilling (35,38); Kueser (39); Schreiner (40); Denisenko (41,42); Burton (44); Crosby (45); Dorey (23); Daneliya (33)
- b) Cu-ThO<sub>2</sub> - Scheithauer (48)
- c) Cu-MgO - Goodwin (49); Rao (50)
- d) Cu-ZrO<sub>2</sub> - Denisenko (41); Pashkova (51)
- e) Cu-Y<sub>2</sub>O<sub>3</sub> - Crosby (45)
- f) Cu-SiO<sub>2</sub> - Hashimoto (25); Schreiner (40); Ohmann (43)
- g) Cu-Cr<sub>2</sub>O<sub>3</sub> - Pashkova (51)
- h) Cu-TiO<sub>2</sub> - Schreiner (40)
- i) Cu-carbides (Ti, Zr, etc.) - Motyazhev (46)
- j) Cu-Cr - Ohmann (43)
- k) Cu-Co - Parker (47); Ashton (31)
- l) Cu-W - Borok (30)
- m) Cu-24Ni-Al<sub>2</sub>O<sub>3</sub> - Schilling (35)
- n) Cu-Al-Al<sub>2</sub>O<sub>3</sub> - Schilling (38)

**REFERENCES**

1. Hodge, W., "Dispersion Strengthening of Cu", DMIC Technical Note (January 1966).
2. Marsden, T. B., "Dispersion Hardening by Oxides", *The Metallurgist and Materials Technology*, 6 (6), 251-258 (1974).
3. Desy, D. H., "Dispersion-Strengthened Cu", Bureau of Mines R.I. 7228 (1969).
4. Nadkarni, A. V., and Klar, E., U.S. Patent 3,779,714 (December 18, 1973).
5. Nadkarni, A. V., Klar, E., and Shafer, W. M., "A New Dispersion-Strengthened Cu", *Metals Engineering Quarterly*, 10-14 (August 1976).
6. "GlidCop", Metals Group, Trade Brochure No. 04177, Glidden-Durkee Div. SCM Corporation (1973).

# REFERENCES (Cont.)

7. P/M Newsletter, 51-52 (June 1973).
8. "Glidden Claims Commercial Version of DS-Cu", Amer. Metal Market (June 12, 1973).
9. Copper Development Association, personal communication.
10. "Strengthened Copper", Engineering (June 1974).
11. Peterson, L. G., Kimmel, E. R., and Queeney, R. A., "Consolidation by Hot-Rolling and Properties of a Dispersion-Hardened Cu Alloy", Powder Met. Inter., 5 (2), 65-70 (1973).
12. Fuschillo, N., and Gimpl, M. L., "Electrical Conductivity and Tensile Strength of DS-Cu", JI. Applied Physics, 42 (13), 5513-5516 (1971).
13. Fuschillo, N., and Gimpl, M. L., "Electrical and Tensile Properties of Cu-ThO<sub>2</sub>, Au-ThO<sub>2</sub>, Pt-ThO<sub>2</sub> and Au-Al<sub>2</sub>O<sub>3</sub> Pt-Al<sub>2</sub>O<sub>3</sub> Alloys", JI. of Materials Science, 1078-1086 (1970).
14. Gimpl, M. L., and Fuschillo, N., "Dispersion-Hardened Alloys Made by Vapor Plating and Chemical Precipitation Techniques", Oxide Dispersion Strengthening, Metallurgical Society Conference, 47 (1968), pp 719-740.
15. Hansen, N., "Accelerated and Delayed Recrystallization", Mem. Sci. Rev. Metall, 72 (3), 189-203 (1975).
16. Graham, R. L., Edge, D. A., and Moore, D. C., "Dispersion-Hardened Copper and Copper Alloys from Chemically Prepared Powders", JI. Inst. of Metals, 99, 81-92 (1971).
17. Poniatowski, M., and Clasing, M., "Dispersionsgehartete Werkstoffe auf Silber- und Kupferbasis", Z. Metallkunde, 59 (3), 165-170 (1968).
18. Donald, I. W., and Pollard, G., "Fabrication and Properties of Some Dispersion-Strengthened Copper-Glass Alloys", Powder Metallurgy, 18 (35), 32-46 (1975).
19. Gould, D., and Hirsch, P. B., "The Bauschinger Effect, Work-Hardening and Recovery in DH-Cu Crystals", Phil. Mag., 30 (6), 1353-1377 (1974).
20. Gould, D., and Humphreys, F. J., "Some Aspects of the Work Hardening of Copper Crystals Containing Dispersions of Al<sub>2</sub>O<sub>3</sub> and BeO", Proc. of the Third International Conference on the Strength of Metals, Inst. of Metals, Paper 61 (1973), p 301.
21. Hazzledine, P. M., and Hirsch, P. B., "A Coplanar Orowan Loops Model for Dispersion Hardening", Phil. Mag., 30 (6), 1331-1351 (1974).
22. Lloyd, C. H., and Loretto, M. H., "The Properties of Copper Alloys Containing Shearable and Non-Shearable Particles", Proc. of the Third International Conference on the Strength of Metals, Inst. of Metals (1973), p 306.
23. Dorey, G., "Yield in Dispersion-Hardened Copper Alloys", Technical Report 68230, Royal Aircraft Establishment (September 1968).
24. Mori, T., and Narita, K., "Decrease of Back Stress and Softening of Work Hardened Cu-SiO<sub>2</sub> Crystals by Recovery", Acta Metallurgica, 23, 85 (1975).
25. Hashimoto, O., and Haasen, P., "Abgleitungslawinen bei der Wechselbeanspruchung Dispersionsgehartete Kupfer Einkristalle", Zt. Metallkunde, 65 (3), 178-183 (1974).
26. Atkinson, J. D., Brown, L. M., and Stobbs, W. M., "The Work Hardening of Copper-Silica IV. The Bauschinger Effect and Plastic Relaxation", Phil. Mag., 30 (6), 1247-1280 (1974).
27. Atkinson, J. D., Brown, L. M., and Stobbs, W. M., "Recovery and Bauschinger Effect in Cu-SiO<sub>2</sub>", Proc. of the Third International Conference on the Strength of Metals, Inst. of Metals, Paper No. 8 (1973), pp 36-39.
28. Shewfelt, R.S.W., and Brown, L. M., "High Temperature Strength of DS Cu Single Crystals", Proc. of the Third International Conference on the Strength of Metals, Inst. of Metals Paper No. 63 (1973), p 311.
29. Lloyd, G. J., and McElroy, R. J., "A Model for the Quantitative Interpretation of High Temperature Relaxation Phenomena - The Effect of Anelasticity", Phil. Mag., 32, 231-244 (July 1975).
30. Borok, B. A., Gel'tman, I. S., and Dzeladze, "Dispersion Hardening of Copper by Tungsten", Fizika i Khimiya Obrabotki Materialov, (3), 68-74 (1970).
31. Ashton, J. D., Woo, O. T., and Ramaswami, B., "Fatigue Deformation of Cu Single Crystals Containing Noncoherent Cobalt Particles", Metallurgical Trans., 6A, 1957-1959 (1975).
32. Chopra, O. K., and Niessen, P., "Intergranular Failure After Annealing of Deformed Cu-Al<sub>2</sub>O<sub>3</sub> Alloys", Materials Science and Engineering, 19, 87-94 (1975).
33. Daneliya, E. P., Rozenberg, V. M., and Teplitskii, "Structure and Properties of Internally Oxidized Cu-Al Alloys", Izv. VUZ. Tsvetn. Metall, (3), 153-155 (1975).
34. Woolhouse, G. R., and Brown, L. M., Studies of Coherency in Internally Oxidized Copper Alloys", JI. Inst. Metals, 98, 106-110 (1970).
35. Schilling, W. F., and Grant, N. J., "Oxide Dispersed Copper Alloys by Surface Oxidation", Metallurgical Trans., 1 (8), 2205-2210 (1970).



## REFERENCES (Cont.)

36. Jones, R. L., "The Tensile Deformation of Copper Single Crystals Containing BeO Particles", *Acta Metallurgica*, 17 (3), 229-235 (1969).
37. Palmer, I. G., "Internal Oxidation of Some Copper-Chromium-Silicon Alloys", *Metal Science JI.*, 6, 30-32 (1972).
38. Schilling, W. F., and Grant, N. J., "High Temperature Behavior of Cu-Al<sub>2</sub>O<sub>3</sub> Alloys", *Powder Met. Intl.*, 5 (3), 117-121 (1973).
39. Kueser, P. E., "High-Temperature Electrical Materials", *Machine Design*, 38 (26), 222-228 (1966).
40. Schreiner, H., and Ohmann, H., "Dispersion-Hardened Materials With Copper as a Base Metal", *Modern Developments in Powder Met.*, 5, 125-136 (1971).
41. Denisenko, E. T., Polushko, A. P., Filatova, N. A., Kostenko, A. D., Natanson, E. M., and Rybchinskii, M. I., "Effect of Various Factors on the Properties of Copper Hardened with Dispersed Oxides", *Poroshkovaya Metallurgiya*, 106 (10), 49-54 (1971).
42. Denisenko, E. T., Voinitskii, A. G., Kostenko, A. D., Polushko, A. P., and Filatova, N. A., "Some Deformation Regularities of Copper Containing Al<sub>2</sub>O<sub>3</sub> Inclusions", *Problemy Prochnosti (Strength of Metals)*, 2 (11), 54-57 (1970).
43. Ohmann, H., Schreiner, H., and Dietz, H., "The Internal Oxidation of Copper Alloys — A Diffusion Problem", *Metall*, 24 (11), 1180-1191 (1970).
44. Burton, B., "The Influence of Al<sub>2</sub>O<sub>3</sub> Dispersions in the Diffusion-Creep Behavior of Polycrystalline Copper", *Metal Science JI.*, 5, 11-15 (1971).
45. Crosby, R. L., and Desy, D. H., "Dispersion-Strengthening in Copper-Alumina and Copper-Yttria Alloys", *Report of Investigations 7266* (June 1969).
46. Motyazhev, V. I., Boiko, P. A., Vitryanyuk, V. K., and Sleptsov, "Preparation of Fine Composite Powders Containing Carbides of the Transition Metals", *Poroshkovaya Metallurgiya*, 87 (3), 23-27 (1970).
47. Parker, J. D., and Wilshire, "The Effect of a Dispersion of Cobalt Particles on High-Temperature Creep of Copper", *Metal Science*, 8, 248 (1975).
48. Scheithauer, W., Cheney, R. F., and Kopatz, N. E., "The Manufacture, Properties, and Applications of High-Conductivity High-Strength Cu-ThO<sub>2</sub>", *Paper presented at the CDA-ASM Conference on Copper*, Cleveland, Ohio (October 16-19, 1972).
49. Goodwin, R. J., "Dispersion-Hardened Copper Wire", *Jl. Inst. Metals*, 98, 257-264 (1970).
50. Rao, T. H., and Vasu, K. I., "Oxidation of Copper-Magnesia Composite Alloys", *Trans. Indian Inst. Metals*, 23 (3), 8-15 (1970).
51. Pashkova, O. A., Makarova, N. I., Zhuk, N. P., and Opara, B. K., "Resistance of Dispersion-Hardened Copper to Oxidation at High Temperatures", *Tsvetnaya Metallurgiya*, (4), 136-140 (1970).

## BIBLIOGRAPHY ON DISPERSION STRENGTHENING OF COPPER

- Lloyd, G. J., McElroy, R. J., and Martin, J. W., "Some Creep Studies on Internally Oxidized Cu-Al Crystals", *Proc. of the Third International Conference on the Strength of Metals*, Inst. of Metals, Paper No. 37 (1973), p 185.
- Haussler, G., Daut, H. H., and Tenzler, U., "Grundlagen der Dispersionsverfestigung von Kupfer u bisherige Anwendung - Auscheidungshärtung", *Neue Hütte*, 17 (4), 193-196 (1972).
- "Advances in Aerospace Materials—Processing Technology", *Metal Progress*, 105 (3), 41-44 (1974).
- Fickett, F. R., "Oxygen Annealing of Copper: A Review", *Matls. Science and Eng.*, 14 (3), 199-210 (1974).
- Kenyon, N., and Hrubec, R. J., "Brazing of a Dispersion Strengthened Nickel Base Alloy Made by Mechanical Alloying", *Welding JI.*, 53 (4), 1458-1528 (1974).
- "Metals in the Electrical/Electronics World", *Insulation/Circuits*, 20 (2), 24-27 (1974).
- Sell, H. G., and King, G. W., "Bubble Strengthening - A New Materials Concept", *Res. Dev.*, 23 (7), 18-21 (1972).
- Kupcis, O. R., Ramaswami, B., and Woo, O. T., "The Effect of Particle Size on the Yield Stress of Cu-Al<sub>2</sub>O<sub>3</sub> Crystals", *Acta Metallurgica*, 21 (8), 1131-1137 (1973).

## BIBLIOGRAPHY (Cont.)

- "Dispersion Strengthened Copper is Available", *Mats. Eng.* 78 (1), 32 (1973).
- Fleck, R. G., and Taplin, D.M.R., "Superplasticity in a Commercial Copper Dispersion Alloy", *Canadian Met. Quarterly*, 11 (2), 299-302 (1972).
- Cocks, G. J., "Work-Hardening in a Commercial Copper Dispersion Alloy", *Jl. Inst. Metals*, 101, 178-180 (1973).
- "New Copper Provides Long-Sought Properties", *Machine Design*, 45 (16), 18 (1973).
- Komatsu, N., and Grant, N. J., "Particle Coarsening in a Copper-Silica Alloy", *Trans. Met. Soc. AIME*, 230 (4), 1090-1096 (1964).
- Williams, D. N., Roberts, J. W., and Jaffee, R. I., "Formation of a Dispersion in Copper by Reaction in the Melt", *Trans. Met. Soc. AIME*, 218 (3), 574-575 (1960).
- Freeman, R.F.A., "The Surface Tension of Copper and Its Alloys", Second Annual Report, R347/6 to INCRA, New York, New York (September 1972).
- Mitchell, P. R., and Hanna, K. R., "Some Effects of Dispersed Phases of Engineering Properties of Wrought Copper Alloys", *Jl. Australian Inst. Metals*, 14 (2), 73-83 (1969).
- Lawrence, G. D., and Foerster, G. S., "Dispersion Hardened Metals made by Atom-Quenching", *Intl. Jl. Powder Met.*, 6 (4), 45-51 (1970).
- Matsuda, Y., Maeda, Y., Hitotsuyanagi, H., and Furukawa, T., "On the Dispersion Strengthened Copper-Alumina Alloy", *Sumitomo Electric Tech. Rev.*, (6), 78-88 (1965).
- Sylwestrowicz, W. D., "Plane of Crack Propagation in Stress Corrosion Fracture in Copper Beryllium", *Corrosion*, 26 (12), 552-558 (1970).
- Takahashi, S., and Yoshioka, M., "On Temperature Dependence of Mechanical Properties of Dispersion Strengthened Cu-Al<sub>2</sub>O<sub>3</sub> Alloys", *Jl. Japan Inst. Metals*, 35 (8), 739-745 (1971).
- Temple, S. G., "Recent Developments in Properties and Protection of Copper For Electrical Uses", *Met. Rev.* 11, 47-60 (1966).
- Priester, P., Fargette, B., Whitwham, D., Diner, O., and Herenguel, J., "Properties Imparted by the Dispersion-Type Structure Produced by Heat Treatment of Cu-0.8 Percent Cr Alloy", *Memoires Scientifiques de la Rev. de Metallurgie*, 68 (10), 677-686 (1971).
- Miller, R. J., "Performance and Properties of Copper Alloy 194", Paper Presented at the CDA-ASM Conference on Copper, Cleveland, Ohio (October 16-19, 1972).
- Davies, P. W., Dunstan, G. R., Evans, R. W., and Wilshire, B., "Fracture Behavior of Copper During Hot Deformation", *Jl. Inst. Metals*, 99, 195-197 (1971).
- Exner, H. E., "Analysis of Grain- and Particle-Size Distributions in Metallic Materials", *Intl. Met. Rev.*, 17, 25-42 (1972).
- Fox, A., and Swisher, J. H., "Superior Hook-Up Wires for Miniaturized Solderless Wrapped Connections", *Jl. Inst. Metals*, 100, 30-32 (1972).
- Aleksander, C., "Sintered Copper-Iron-Aluminum Oxide Alloys", *Rudy I Metale Niezylazne*, 15 (9), 462-467 (1970).
- Ashby, M. F., and Smith, G. D., "Structures in Internally Oxidized Copper Alloys", *Jl. Inst. Metals*, 91, 182-187 (1962-63).
- "DS Grade Replaces OFHC in Electronic Applications", *Metal Progress*, 99 (1), 9 (1971).
- Mueller, L. A., Snider, W. E., and Koutnik, E. A., "Flexible Electrical Conductors for High-Temperature Switchgear", NASA Tech. Brief 70-10569 (October 1970).

## BIBLIOGRAPHY (Cont.)

- Ruhle, M., "Production and Properties of Dispersion-Strengthened Copper—Part 1", *Metall*, (5), 465-471 (1970).
- Mueller, L. A., and William, E. S., "Flexible Electrical Conductors for High-Temperature Switchgear", Report No. NASA TM X-1986, (April 1970).
- Clark, A. F., Childs, G. E., Wallace, G. H., "Electrical Resistivity of Some Engineering Alloys at Low Temperatures", *Cryogenics*, 10 (4), 295-305 (1970).
- Liesner, C., and Wassermann, G., "Deformation Behavior and Mechanical Properties of Composite Materials of Copper with Alpha-Alumina", *Zeitschrift für Metallkunde*, 60 (11), 827-835 (1969).
- Lenel, F. V., Ansell, G. S., and Morris, R. C., "Sintering of Loose Spherical Copper Powder Aggregates Using Silica as Markers", *Metallurgical Transactions*, 1 (8), 2351-2354 (1970).
- Elman, I. B., and Hopper, H., "Comparative Evaluation of Die Materials for Brass Die Casting", Paper No. 803, presented at the Fourth National Die Casting Exposition and Congress, Cleveland, Ohio (November 14-17, 1966).
- Spengler, H., and Dihlmann, M., "Silver Alloys as Contact Spring Materials for Electrotechnical Purposes", *Metall*, 22 (7), 694-696 (1968).
- Grant, N. J., and Schilling, W. F., "Improved Method of Producing Oxide-Dispersion-Strengthened Alloys", NASA Tech. Brief 69-10536 (October 1969).
- Bouchard, K. G., "Vacuum Breakdown Voltages of Dispersion-Strengthened Copper Vs. Oxygen Free, High-Conductivity Copper", *Jl. of Vacuum Science and Tech.*, 7 (2), 358-360 (1970).
- Bondar, M. P., "Effect of Silicon on the Properties of Internally Oxidized Cu-0.2% Al Alloy", *Fizika Metallov i Metallovedeniye*, 27 (5), 650-654 (1969).
- Williams, D. N., Roberts, J. W., and Jaffee, R. I., "Eutectic Alloying of Copper. . . A New Concept in Dispersion Hardening", *Metal Progress*, 78 (2), 108-109 (1960).
- Lewis, M. H., and Martin, J. W., "Yielding and Work-Hardening in Internally Oxidized Copper Alloys", *Acta Metallurgica*, 11 (11), 1207-1214 (1963).
- Preston, O., and Grant, N. J., "Dispersion Strengthening of Copper by Internal Oxidation", *Trans. Met. Soc. AIME*, 221 (2), 164-173 (1961).
- Whitman, C. I., "Copper for Aerospace", Paper for presentation at the Non-Ferrous Metal in Aerospace Symposium of the AIME Metallurgical Society, New York (November 1, 1962).
- "Literature Survey on Copper-Base Cermets", Report No. 87, the International Copper Development Council, Brussels, Belgium (October 29, 1965).
- McIntire, H. O., "Trends in Powder Metallurgy", *Battelle Tech. Rev.*, 17 (1), 16-21 (1968).
- Safranek, W. H., "A Survey of Electroforming for Fabricating Structures", *Plating*, 53 (10), 1211-1216 (1966).
- Rumberger, W. M., "Investigation of Materials for Use in Copper Alloy Die Casting Dies", prepared for International Copper Research Association, Inc., Project 59, Annual Report (March 1966).
- Dorey, G., "The Effect of Temperature on the Yield Properties of an Internally Oxidized Copper-Aluminum Alloy", Tech. Report No. 65126 (June 1965).
- Wolf, S. M., "Properties and Applications of Dispersion-Strengthened Metals", *Jl. of Metals*, 19 (6), 22-28 (1967).
- Chin, L.L.J., Grant, N. J., "Stored Energy in Oxide Dispersion Strengthened Copper Alloys", Tech. Report, Contract NONR 3963(18) (April 1967).
- Andrews, A. J., and Das, D. K., "DSC Dispersion Strengthened Copper", *Electronic Progress*, XI (1), 6-12 (1967).



#### BIBLIOGRAPHY (Cont.)

Hoffmann, J. E., and Mantell, C. L., "Mechanisms of the Codeposition of Aluminas with Electrolytic Copper", Trans. Met. Soc. AIME, 236 (7), 1015-1024 (1966).

Getz, A. J., and Hoffmann, J. E., "Electrodeposition of Copper with Dispersed Non-Metallics", Final Report INCRA Project No. 31(B), U.S. Metals Refining Company, Carteret, New Jersey (May 19, 1966).

"Cube-Alloy Dispersion Hardened Copper", Technical Data Sheet No. 39-1, Handy and Harman Company, New York, New York (February 1965).

Bufford, A. S., Dr., "Dispersion Strengthened Metals/ Stronger at High Temperatures", Matls. Eng., 65 (4), 98-103 (1967).

Raghavan, R. V., "Strengthening of Copper by Dispersions of Aluminum Oxide", Trans. Indian Inst. Metals, 16, 195-200 (1963).

Ashby, M. F., "Deformation of Internally Oxidized Copper-Based Alloys", Symposium on Electron Microscopy and Strength of Crystals (1961), pp 891-897.

"Preliminary Investigation of Electrodeposition of Dispersion-Hardening Copper Refractory Oxide Alloys", International Copper Research Association, Inc., INCRA Project No. 31, Final Report (1964).

Ratcliff, N. A., "A Laboratory Extrusion Press for Copper Alloys", Metallurgia, Manchr., 68, 193-194 (1963).

Kueser, P. E., "High Temperature Materials for Rotating Electrical Machinery", Materials in Design Engineering, 65 (3), 80-82 (1967).

Pendleton, W. W., "Electrical Conductors for High Temperature Operation", Wire and Wire Products, 41 (6), 908-912, 953-955 (1966).

Yamazaki, M., and Grant, N. J., "Alumina Dispersion-Strengthened Copper-Nickel Alloys", Trans. Met. Soc. AIME, 233, 1573-1580 (1965).

Lenel, F. V., "A Study of the Material Transport Mechanism in Sintering", A Paper submitted to Symposium su la Metallurgia des Poudres, Paris (June 15-17, 1964).

Farthing, T. W., "Improved die Materials for the Pressure Diecasting of Brass", Paper Presented at a Symposium on Copper Alloy Casting held at Brimingham, England, by the CDA, Paper 10 (April 26, 1966).

Savitskiy, E. M., and Vlasov, A. I., "Hardening Copper with Fine-Dispersed Particles", Tsvetnye Metally, 2, 81-85 (1962).

Smith, G. C., "The Preparation, Structure, and Properties of Alloys Containing Dispersed Nonmetallic Phases", Powder Metallurgy, 11, 102-132 (1963).

Grimwade, M. F., and Jackson, K., "The Preparation and Properties of Copper, Nickel, and Iron Containing a Dispersed Oxide Phase", Powder Metallurgy, 10, 13-33 (1962).

Lewis, M. H., Seebohm, R. H., and Martin, J. W., "The Structure and Properties of Some Internally Oxidized Alloy Powder Compacts", Powder Metallurgy, 10, 87-107 (1962).

Valentich, J., "New Values for Thermal Coefficients", Product Engineering, 36 (15), 63-71 (1965).

McDonald, A. S., "A Dispersion Hardened Copper for Electrical Uses", Metal Progress, 89 (4), 70-72 (1966).

Brimhall, J. L., Klein, M. J., and Huggins, R. A., "Influence of a Finely Dispersed Second Phase on Recrystallization", Tech. Report No. 15, Contract No. NONR-225(34) for the Office of Naval Research (February 1965).

Brimhall, J. L., and Huggins, R. A., "Electron-Microscopic Observations of Deformed Internally Oxidized Alloys", Trans. Met. Soc. AIME, 1076-1084 (June 1965).

White, J. E., "Alloy and Dispersion Strengthening by Powder Metallurgy", JI. of Metals, 17 (6), 587-593 (1965).

BIBLIOGRAPHY (Cont.)

Early, J. G., Lenel, F. V., and Ansell, G. S., "The Material Transport Mechanism During Sintering of Copper-Powder Compacts at High Temperatures", Trans. Met. Soc. AIME, 230 (7), 1641-1650 (1964).

London, G. J., "Dispersion Strengthened Copper-Thorium Boride and Copper-Alumina Alloys Produced by Melting and Casting", Report No. R 59SD407, Contract No. AF 04(647) 269 for USAF Ballistic Missiles Division (August 6, 1959).

"Dispersion Strengthened Copper Property Mix", Iron Age, 212 (7), 69-70 (1973).

## IRON AND STEEL

A modest effort has been expended in studying the effects of dispersoids on iron-base alloys. As a matter of convenience in this review, these efforts have been separated into two alloy groups, i.e., iron-base and iron-chromium-base alloys. The latter include stainless iron and steels in addition to superalloys.

### DS Fe Alloys

Alumina has been by far and away the most popular dispersoid used in iron-base alloys.

In 1959, Gatti<sup>(1)</sup> prepared several Fe-Al<sub>2</sub>O<sub>3</sub> alloys using four different techniques: a) oxidation-reduction of an Fe-8Al alloy, b) coprecipitation of Fe(OH)<sub>3</sub> and Al(OH)<sub>3</sub>, c) colloidal mixing of Fe<sub>2</sub>O<sub>3</sub> and Al<sub>2</sub>O<sub>3</sub>, and d) colloidal mixing of iron powder and Al<sub>2</sub>O<sub>3</sub>. The alloy compositions and tensile properties obtained are shown for different temperatures in Table 26. Stress-rupture curves for the same alloys at 650 C are given in Figure 41. In the coprecipitated alloys, considerable clumping of Al<sub>2</sub>O<sub>3</sub> occurred. The more random dispersions produced by oxidation-reduction and colloidal mixing of oxides produced stronger, more ductile alloys.

**Table 26. Tensile Properties of Fe-Al<sub>2</sub>O<sub>3</sub> Alloys As-Extruded<sup>(1)</sup>**

Specimen Designation	Test Temp., F	0.2% Yield Strength,		Tensile Strength,		Elong. in 0.82 in., %
		ksi	MPa	ksi	MPa	
Blank	RT	16.3	112	31.2	215	27
0% Al <sub>2</sub> O <sub>3</sub>	1200	4.0	28	5.6	39	24
	1500	2.2	15	2.5	17	17
	1800	2.6	18	3.0	21	8
Oxidation-reduction 16% Al <sub>2</sub> O <sub>3</sub>	RT	66.5	458	73.5	506	1
	1200	26.5	183	27.2	187	5
	1500	9.5	65	9.5	65	2.2
	1800	9.0	62	9.2	63	1.5
Coprecipitate 16% Al <sub>2</sub> O <sub>3</sub>	RT	50.3	347	50.3	347	0
	1200	32.0	220	32.2	222	0.5
	1500	12.1	83	12.1	83	5
	1800	5.5	38	5.5	38	3
Fe <sub>2</sub> O <sub>3</sub> + Al <sub>2</sub> O <sub>3</sub> 8% Al <sub>2</sub> O <sub>3</sub>	RT	43.0	296	52.0	358	2.5
	1200	13.5	93	14.4	99	15
	1500	5.0	34	5.1	35	10
	1800	4.8	33	4.9	34	4
Fe + Al <sub>2</sub> O <sub>3</sub> 8% Al <sub>2</sub> O <sub>3</sub>	RT	41.5	286	44.7	308	4.5
	1200	10.5	72	11.4	79	20
	1500	4.0	28	4.2	29	11
	1800	4.4	30	5.2	36	2

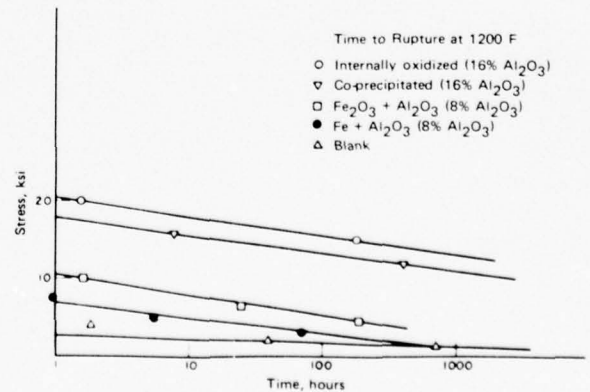


**Figure 41. Initial Stress vs Time to Rupture of Fe-Al<sub>2</sub>O<sub>3</sub> Alloys, Tested at 1200 F (649 C)<sup>(1)</sup>**



Later, Gatti<sup>(2)</sup> investigated the stability of  $\text{Al}_2\text{O}_3$  in iron by mixing the fine oxide powders and reducing the mixtures with pure, dry hydrogen at about 500 C. The powders were ball milled, pressed into slugs and canned, and then hot extruded into rods at 700-800 C. The coarsening of the  $\text{Al}_2\text{O}_3$  with increasing temperature and time was observed. It was concluded that the growth of  $\text{Al}_2\text{O}_3$  particles in iron results from coalescence, with large grains growing at the expense of the smaller grains.

Bovarnick and Flood<sup>(3)</sup>, following the lead of du Pont with TD-nickel alloys, produced a series of Fe- $\text{Al}_2\text{O}_3$  alloys by thermal decomposition of homogeneous solution with subsequent selective reduction in hydrogen. On an equivalent volume percent basis, these investigators obtained greater strengthening effects, both in tension and stress rupture, from the  $\text{Al}_2\text{O}_3$  additions made using their technique as compared with Gatti's<sup>(1)</sup> earlier alloys. Figure 42 compares the stress-rupture data from both investigations. Some room-temperature tensile strength values determined by Bovarnick on these materials are given as follows:

$\text{Al}_2\text{O}_3$ Content, %	Tensile Strength, MPa	Yield Strength, MPa
0.41	549	431
2.8	657	480
6.25	696	608

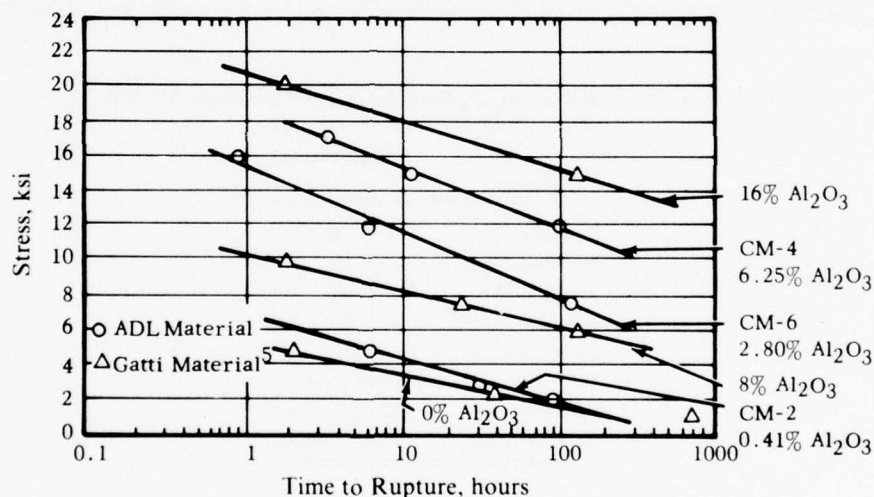


Figure 42. Stress-Rupture Lives of Fe- $\text{Al}_2\text{O}_3$  Alloys at 1200 F (649 C)<sup>(3)</sup>

Copeland and McBee<sup>(4)</sup> found it is feasible to form  $\text{Al}_2\text{O}_3$  dispersoids (0.1 micron or less) in Fe-Al alloy sheet containing 1 and 2 percent aluminum by internal oxidation in wet hydrogen. The technique was also applied to samples of Fe-2Al powder made from selected particle sizes. Tensile and stress-rupture properties were determined on the powder alloys after sintering and extrusion. As shown in Figure 43, the strongest of the Fe-Al/ $\text{Al}_2\text{O}_3$  specimens displayed a stress-rupture strength at 800 C that approached that of type 310 stainless steel. Tensile strength at 800 C depended upon the Al-O<sub>2</sub> weight ratio of these elements in the extrusions and reached a maximum of 17 ksi.

Internal oxidation of iron-aluminum alloys had been reported earlier by Meijering<sup>(5)</sup>, but his alloys did not show appreciable hardening, probably because of the coarse dispersion obtained.

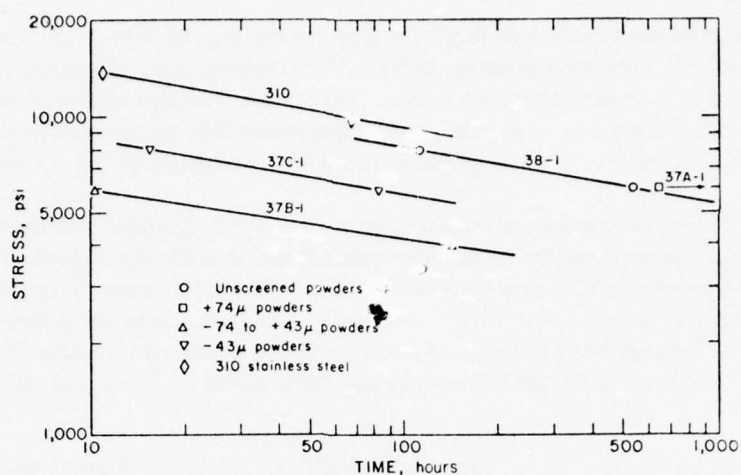


Figure 43. Stress-Rupture Lives of Fe-Al/Al<sub>2</sub>O<sub>3</sub> Specimens Prepared by Internal Oxidation and Tested at 800 C<sup>(4)</sup>

Navara and Easterling<sup>(6)</sup> investigated the adhesion of Al<sub>2</sub>O<sub>3</sub> particles with the matrices of numerous iron-base alloys. The compositions of these and the calculated contact angles between the Al<sub>2</sub>O<sub>3</sub> particles and the matrices are given in Table 27. The alloy Fe-40Ni matrix exhibited such poor adhesion with the Al<sub>2</sub>O<sub>3</sub> particles that virtually all of them were separated by the deformation used.

Table 27. Contact Angles for Al<sub>2</sub>O<sub>3</sub> Particles in Eight Iron-Base Alloys<sup>(6)</sup>

Dispersant	Contact Angle, degrees
Fe-40Ni	0
Fe-40Ni-5Mn	15
Fe-40Ni-5Mo	65
Fe-10Co	60
Fe-5Cr	80
Fe-15Cr	No decohesion
Fe-5Mo	No decohesion
Fe-40Ni-10Cr	No decohesion

Imai and Hirostani<sup>(7)</sup> investigated the hardness and sintering behavior of iron containing Al<sub>2</sub>O<sub>3</sub>, SiO<sub>2</sub>, and MgO additions in amounts up to 15 volume percent. Al<sub>2</sub>O<sub>3</sub> was found to be the most suitable of the three dispersoids tried. Thus, an alloy containing 10 volume percent of Al<sub>2</sub>O<sub>3</sub> which had been sintered and cold-worked to a 50-percent reduction did not soften even when heated above the A<sub>3</sub> temperature. Later, Imai<sup>(8)</sup> reported on work done over a 12-year span on dispersion-strengthened iron alloys. Some stress-rupture tests for the strongest alloys prepared are compared in Figure 44.

Imai found that dissolved oxygen in the matrix plays an important role in oxide particle growth. If oxygen is contained in large amounts, FeO precipitates in the matrix reacting with Al<sub>2</sub>O<sub>3</sub> to form the spinel FeO-Al<sub>2</sub>O<sub>3</sub>, a compound that starts to melt at about 1300 C. Imai considered these alloys interesting, but cautioned that several metallurgical problems remained. One problem is the need to minimize the growth rate of the dispersoid in the dispersant. Another is a need to minimize the inter-particle distance. These are both problems that are common to all dispersion-strengthened metals. The stress-strain curve from Imai's study shown in Figure 45, illustrates that when the dispersoid spacing

of an Fe-18Al<sub>2</sub>O<sub>3</sub> alloy increases the yield decreases. Imai varied the dispersoid spacing by using the different annealing schedules indicated on the figure.

Zwilsky, et al.<sup>(9)</sup> investigated DS-iron alloys containing  $\alpha$ -Al<sub>2</sub>O<sub>3</sub>,  $\gamma$ -Al<sub>2</sub>O<sub>3</sub>, MgO, and ThO<sub>2</sub>. The best results were obtained for the alloy containing 10 volume percent of the  $\gamma$ -Al<sub>2</sub>O<sub>3</sub>, as shown in Figure 46.

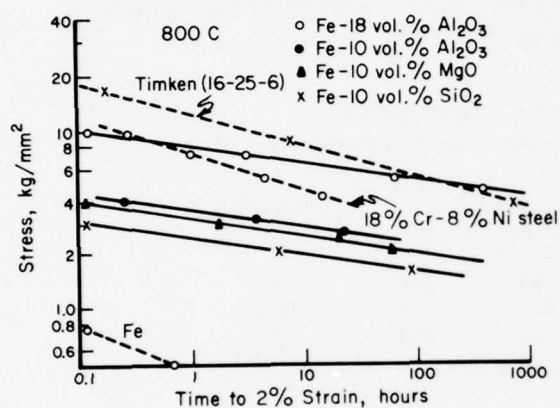


Figure 44. Log Stress vs. Log Time to 2 Percent Strain for Dispersion-Strengthened Irons at 800 C<sup>(8)</sup>

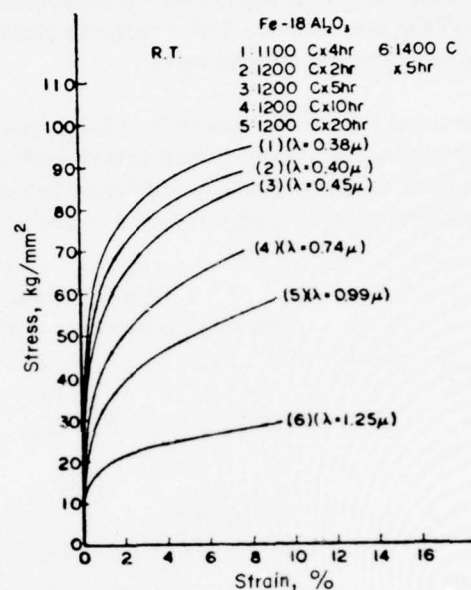


Figure 45. Stress-Strain Curves for Dispersion-Strengthened Irons with Various Mean Free Path<sup>(8)</sup>

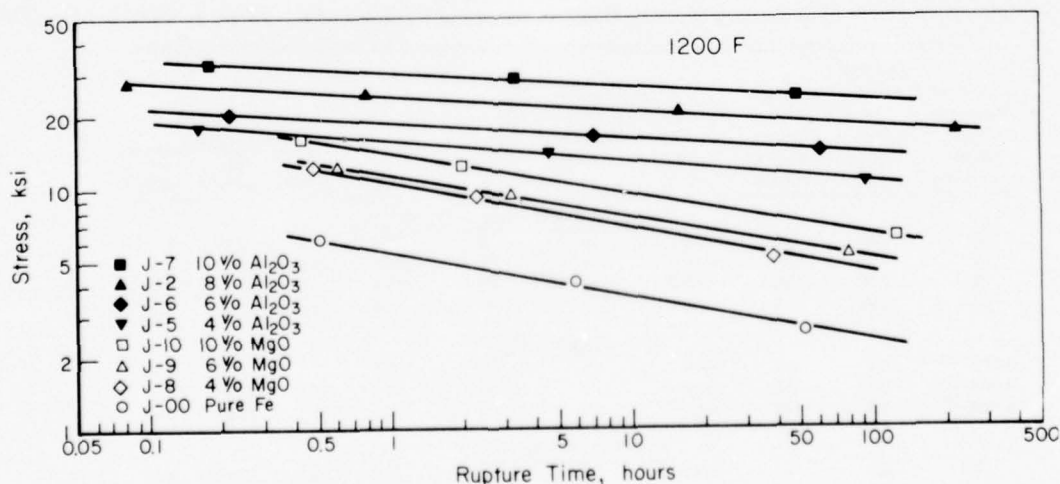


Figure 46. Stress-Rupture Lives for Fe-Al<sub>2</sub>O<sub>3</sub> and Fe-MgO Alloys Compared to Pure Iron<sup>(9)</sup>  
(All materials extruded at 840 C)

Mitsche<sup>(10)</sup> has explored the effects of sintering environment (vacuum versus hydrogen) on the hardness and structure of iron alloys containing up to 5 volume percent  $\text{Al}_2\text{O}_3$  or  $\text{CaO}$ .

Singh and Houseman<sup>(11)</sup> studied the effect of various dispersoids including  $\text{Al}_2\text{O}_3$ ,  $\text{TiO}_2$ , and  $\text{ZrO}_2$  on the densification of carbonyl iron during sintering in the 1350-1490 C range. The presence of the oxide particles inhibited the degree of densification of the iron matrix to an extent that generally increased with the amount of the dispersoid.  $\text{ZrO}_2$  was by far the most effective inhibitor, e.g., as little as 0.5 percent  $\text{ZrO}_2$  virtually prevented densification at temperatures up to 1490 C. In the Fe- $\text{TiO}_2$  system,  $\text{Fe}_2\text{TiO}_5$  was formed. These particles increased densification at lower temperatures, but hindered the process at higher temperatures.

Place and Lund<sup>(12)</sup> prepared Fe- $\text{ThO}_2$  alloys containing up to 1.7 percent  $\text{ThO}_2$  by the coprecipitation technique. Room-temperature tensile properties for these alloys are given in Table 28. Later<sup>(13)</sup>, the same investigators reported properties obtained in the temperature range 77-373 K. A peak in work-hardening rate was observed in the temperature range 250-300 K.

Table 28. Tensile Properties of Fe- $\text{ThO}_2$  Alloys<sup>(12)</sup>

Material	0.2% Proof Stress		U.T.S.		Elongation, percent
	kg/mm <sup>2</sup>	MPa	kg/mm <sup>2</sup>	MPa	
Fe	17.8	174	24.6	241	29.0
Fe-0.9 $\text{ThO}_2$	29.4	288	41.3	405	14.5
Fe-1.7 $\text{ThO}_2$	34.2	335	47.8	468	11.4

Towner and Pavlovic<sup>(14)</sup> measured the coercive force ( $H_c$ ) at room temperature and 425-870 C on a series of Fe-27Co extrusions. The alloys were dispersion strengthened with boron,  $\text{ZrO}_2$ , and  $\text{ThO}_2$  particles ranging from 0.1-1.6 microns in average diameter. Table 29 gives some of the data obtained on specimens with different dispersoids and after different working conditions.

Table 29. Calibration Study of Secondary Working-Coercive Force and Hardness of Fe+27 Wt. % Co-Base Alloys<sup>(13)</sup>

Amount of Dispersed Phase, percent by volume	Average	Average Inter-Particle Spacing, microns	Secondary Work <sup>(c)</sup>			Hardness at Room Temp., R <sub>C</sub>	Coercive Force, H <sub>c</sub> , oersteds		
	Effective Size of Dispersed Particles, microns		Secondary Working Temp., F	Secondary Working Cycles, No.	Cumulative Reduction in Area, %		At 800 F	At 1200 F	At 1600 F
Fe-25.6Co-1B-4.2Zr Alloy									
20	0.90	3.6	None	0	0	30.5	14.8	9.9	4.1
20	0.90	3.6	1000	8	56	40.3	25.0	14.0	2.8
20	0.90	3.6	1250 <sup>(a)</sup>	28	95	36.4	17.2	12.3	5.3
20	0.90	3.6	800	8		39.8	36.5	13.3	2.6
Fe-24.5Co-8.3 Zr Alloy									
6.4ZrO <sub>2</sub> <sup>(b)</sup>	0.3	3.0	None	0	0	29.5	11.1	7.1	1.9
6.4ZrO <sub>2</sub> <sup>(b)</sup>	0.3	3.0	1000	8	56	39.4	27.9	13.3	6.0
6.4ZrO <sub>2</sub> <sup>(b)</sup>	0.3	3.0	1250 <sup>(a)</sup>	28	95	37.5	18.9	13.3	6.7
Fe-24.5Co-9.3ThO <sub>2</sub> Alloy									
7.5	0.3	3.7	None	0	0	21.2	11.0	7.4	4.1
7.5	0.3	3.7	1000	8	56	31.5	20.6	11.2	5.9
7.5	0.3	3.7	1250 <sup>(a)</sup>	28	95	26.7	14.8	11.1	6.3

(a) The secondary working temperature had to be increased from 1000 F to 1250 F in order to achieve the indicated number of cycles.

(b) Also present was 14 vol. % of large, elongated particles of Fe-Co-Zr constituent.

(c) Each cycle of secondary working consisted of approximately a 10-percent reduction in area followed by a 10-minute anneal at the swaging temperature.



Previously, Towner, et al.<sup>(15)</sup> had determined the coercive force and saturation induction of iron that had been dispersion strengthened with 0.02 to 0.10 volume fraction of  $\text{Al}_2\text{O}_3$  or  $\text{ThO}_2$ . These properties were measured at temperatures up to 80-98 percent of the critical temperature. Saturation magnetization values at a given temperature level were found to decrease in direct proportion to the volume fraction of non-magnetic phase present.

### DS Fe-Cr Alloys

Chromium imparts several important properties to iron-base alloys. These include strengthening plus oxidation and corrosion resistance over a wide range of temperatures. To be effective at high temperatures, the chromium content must be between 13 and 30 weight percent.

Daikoku, et al.<sup>(16,17)</sup> used liquid-phase sintering followed by hot working to produce two  $\text{Al}_2\text{O}_3$ -strengthened grades of Fe-13Cr ferritic steels, which both showed higher creep strengths than those of wrought steels without the  $\text{Al}_2\text{O}_3$ . Table 30 lists the compositions of the alloy steel powder matrices used for these materials, which also contained 1 volume percent each of  $\gamma\text{-Al}_2\text{O}_3$ . Figure 47 compares the stress-rupture properties of these alloys with those for analogous melted and wrought compositions. Representative 650 C tensile properties for the two Fe-13Cr- $\text{Al}_2\text{O}_3$  grade steels are given in Table 31.

Table 30. Chemical Composition of Alloy Steel Powders Used for  $\text{Al}_2\text{O}_3$  Strengthening<sup>(17)</sup>

Powder	C	Si	Mn	S	P	Cr	Al	Mo	Ti
AISI 406	0.03	0.64	0.69	0.017	0.013	12.91	2.86	—	—
13CrMoTi Steel	0.04	1.35	0.15	0.02	0.022	12.91	0.14	1.91	0.41

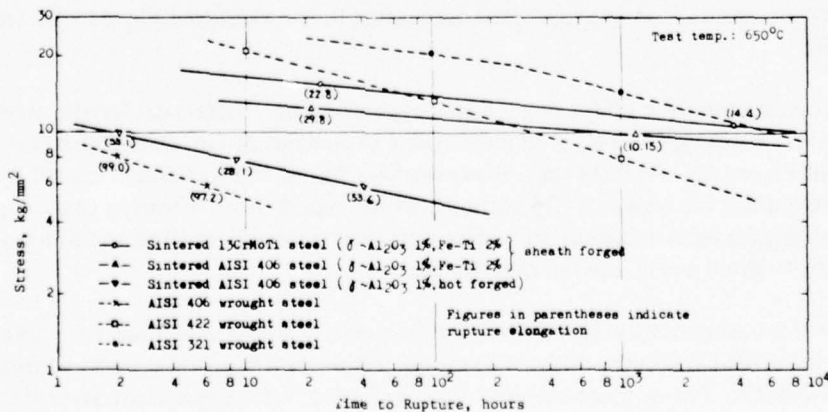


Figure 47. Stress-Rupture Lives of  $\text{Al}_2\text{O}_3$ -Strengthened Steels<sup>(17)</sup>

**Table 31. Representative 650 C Tensile Properties of Al<sub>2</sub>O<sub>3</sub>-Strengthened Steels<sup>(17)</sup>**

Matrix	0.2% Proof Stress,		Ultimate Tensile Strength		Elongation, %	Reduction of Area, %
	kg/mm <sup>2</sup>	MPa	kg/mm <sup>2</sup>	MPa		
AISI 406	22.5	221	32.2	316	14.4	18.4
13CrMoTi Steel	24.2	237	34.2	335	33.8	57.9

In Russia, Borok, et al.<sup>(18)</sup> reported work done on a Kh13M2 steel (13Cr-2Mo) strengthened with Al<sub>2</sub>O<sub>3</sub>. With 3 percent of Al<sub>2</sub>O<sub>3</sub> added, the rupture stress of this steel at 700 C was increased approximately 50 percent, i.e., from 4 to 6-7 kg/mm<sup>2</sup> (3.9 to 5.9-6.9 MPa).

As shown earlier in Table 27, Navara and Easterling<sup>(6)</sup> found that the adhesion of Al<sub>2</sub>O<sub>3</sub> particles in a matrix of Fe-Cr alloys containing more than 10 percent Cr was good. For an alloy of Fe-5Cr-Al<sub>2</sub>O<sub>3</sub>, however, the contact angle was poor.

Denisenko and Van Asbroeck<sup>(19)</sup> investigated Fe-13Cr-2TiO<sub>2</sub> steels produced by powder mixing. The TiO<sub>2</sub> was chosen because it had proved superior as a dispersed phase at high temperature to Al<sub>2</sub>O<sub>3</sub>, MgO, SiO<sub>2</sub>, and ZrO<sub>2</sub>. The compositions of the steels investigated are given in Table 32.

**Table 32. Chemical Compositions of TiO<sub>2</sub>-Strengthened Steels<sup>(19)</sup>**

Steel No.	Amounts of Elements, Wt. %						
	C	O <sub>2</sub>	Cr	Mo	W	TiO <sub>2</sub>	Fe Ti
264	<0.005	1.480	10.8	0.01	0.01	(2.0)	— —
265	<0.005	1.450	11.3	0.06	0.56	(2.0)	— —
266	<0.005	1.465	11.2	1.99	—	(2.0)	— —
267	<0.005	—	(13)	(2.0)	(1.0)	(2.0)	— —

Tensile tests conducted at 700 C showed that the TiO<sub>2</sub> additions had no significant effects on the strength of these steels. The TiO<sub>2</sub> additions were, however, effective in improving the creep strength of the alloys, with the magnitude of improvement decreasing as the average TiO<sub>2</sub> particle size increased from 1 to 5 microns.

De Wilde, et al.<sup>(20)</sup> investigated the effect of powder preparation parameters on ferritic steels corresponding nominally to Fe-13Cr-2Mo-1W. The mechanical properties at 700 C as a function of TiO<sub>2</sub> content are shown in Figure 48. As indicated, these workers found a considerable spread in the strength and ductility values for a given TiO<sub>2</sub> content, which results from differing process parameters. In general, highest strengths were achieved only after optimizing the ball-milling and mixing practices and by decreasing the original oxide powder particle size.

Wright and Wilcox<sup>(21)</sup> investigated the possibilities of mechanical alloying, as used for nickel-base alloys, in preparing a Fe-16Cr-2.6Y<sub>2</sub>O<sub>3</sub> alloy. Figure 49 compares the yield strength of this alloy with that of TD-Ni and TD-NiCr. The authors believed that improved high-temperature strengths for their Fe-16Cr-2.6Y<sub>2</sub>O<sub>3</sub> alloy might be realized by achieving higher "grain aspect ratios" through improved thermomechanical processing. The isothermal and cyclic oxidation characteristics of these alloys were

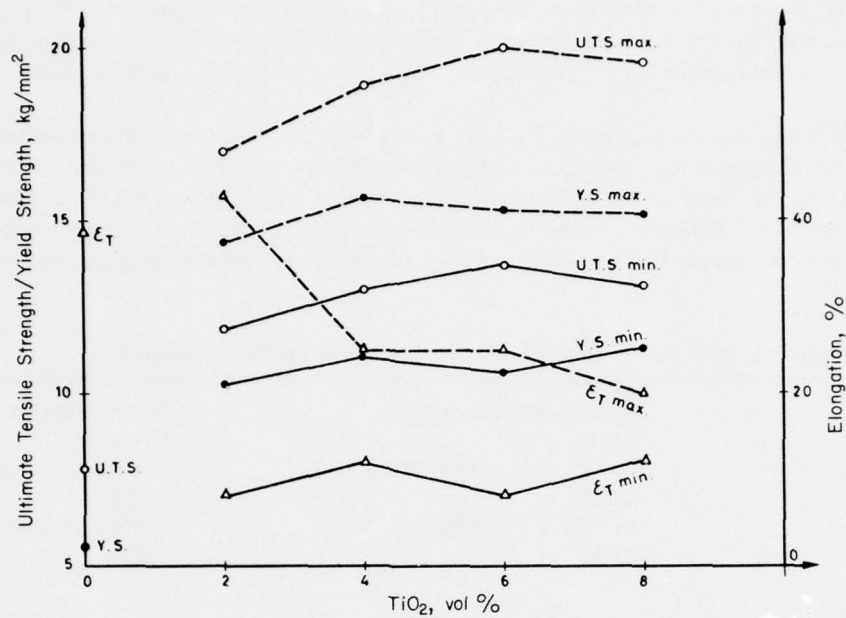


Figure 48. Effect of Processing Parameters on the Tensile Properties of a TiO<sub>2</sub>-Strengthened Ferritic Steel<sup>(20)</sup>

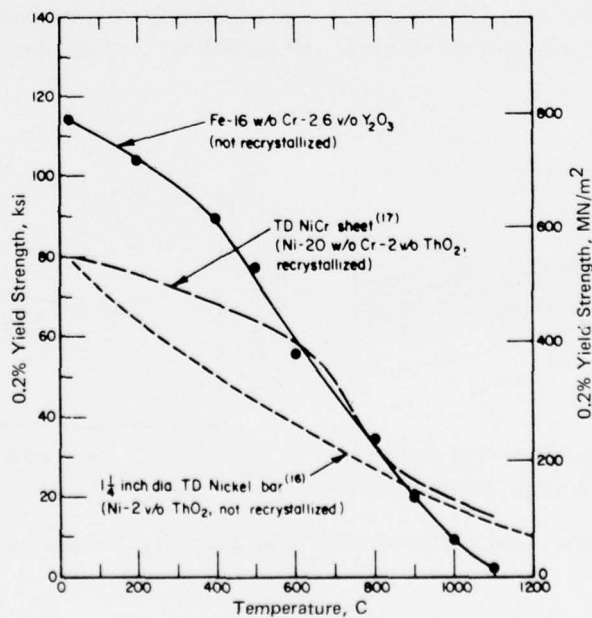


Figure 49. Yield Strength of Fe-16Cr-2.6Y<sub>2</sub>O<sub>3</sub> as a Function of Temperature, Compared With TD Nickel and TD NiCr<sup>(21)</sup>

also determined and compared at 1100 C in 100 torr ( $1.33 \times 10^4$  N/m<sup>2</sup>) oxygen.<sup>(21,22)</sup> In general, the weight changes observed for the Fe-Cr-Y<sub>2</sub>O<sub>3</sub> alloy were similar in magnitude to those for the TD-NiCr material and much improved over those for dispersion-free alloys of Fe-18Cr and Ni-20Cr.

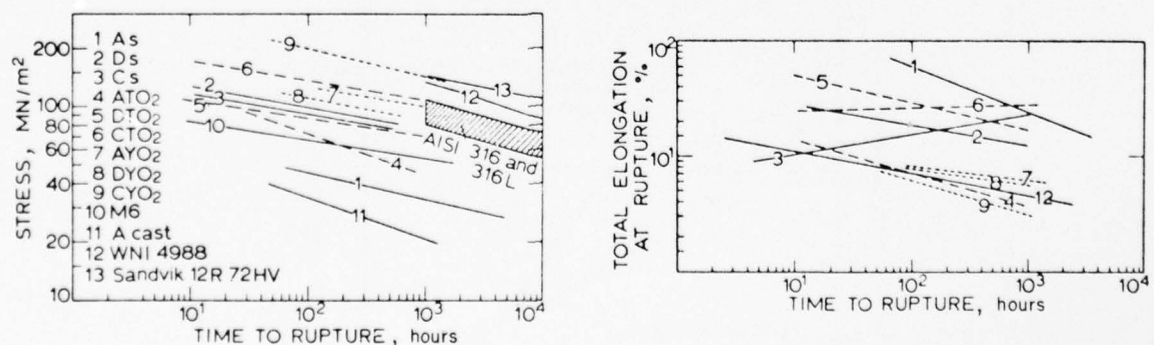
Snykers and Huet<sup>(23)</sup> investigated a series of Fe-13Cr alloys trying to improve high-temperature creep properties in the 700 C range and so permit the use of these alloys as possible canning materials for fast-reactor fuel elements. First improvements were achieved by adding 2.5 to 5 percent titanium to the conventional Fe-13Cr-1.5Mo alloy. Additional strengthening was obtained by additions of TiO<sub>2</sub> and Y<sub>2</sub>O<sub>3</sub>. The nominal compositions and code names for the alloys investigated are given in Table 33.

Table 33. Nominal Compositions and Code Names of the Ferritic Alloys<sup>(23)</sup>

Fe-13Cr-2Mo-1W	Fe-13Cr-2Mo-1W-2TiO <sub>2</sub>	Fe-13Cr-2Mo-1W-2Y <sub>2</sub> O <sub>3</sub>
A(s)	ATO2	AYO2
Fe-13Cr-3.5Ti-1.5Mo	Fe-13Cr-3.5Ti-1.5Mo-2TiO <sub>2</sub>	Fe-13Cr-3.5Ti-1.5Mo-2Y <sub>2</sub> O <sub>3</sub>
D(s)	DTO2	DYO2
Fe-13Cr-5Ti-2Mo	Fe-13Cr-5Ti-2Mo-2TiO <sub>2</sub>	Fe-13Cr-5Ti-2Mo-2Y <sub>2</sub> O <sub>3</sub>
C(s)	CTO2	CYO2
Fe-13Cr-2.5Ti-2Mo		
M6 (cast)		

(s) Indicates sintered alloy.

Creep-rupture lives for these materials at 700 C are compared in Figure 50 with those for some more conventional steels. As shown, rupture times comparable with the strongest austenitic steels were obtained without impairing the ductility of the alloys. The strengthening without loss of ductility in the alloys containing molybdenum and titanium was attributed to the coherent phase. These alloys were found to have excellent properties in the areas of irradiation embrittlement and sodium corrosion and were therefore proposed as canning material candidates for fast-reactor fuel elements.



Miyazaki, et al.<sup>(24)</sup> investigated the growth of oxide particles in a Fe-25Cr-28Ni alloy during annealing at 1100-1300 C. Three volume percent each of  $\alpha$ -Al<sub>2</sub>O<sub>3</sub>, MgO, Er<sub>2</sub>O<sub>3</sub>, TiO<sub>2</sub>, and ZrO<sub>2</sub> were investigated as dispersoids. In general, the oxide particles were coagulated by annealing the alloys in air as well as in a hydrogen stream, although the rates of growth were smaller in hydrogen than in air.



Sands, et al.<sup>(25)</sup> investigated the effects of  $\text{Al}_2\text{O}_3$ ,  $\text{ThO}_2$ , and  $\text{ZrO}_2$  additions to an austenitic stainless steel base consisting of Fe-22Cr-22Ni-0.07C. The compositions, creep rates, and rupture times for these materials after testing at 650 C are given in Table 34. The stress-rupture properties are also compared in Figure 51. As shown, the  $\text{TiO}_2$ -containing alloy had superior strength to the other dispersion-strengthened alloys as well as to a wrought alloy except at very short times (less than 10 hours). The authors speculated that the better creep resistance of the  $\text{TiO}_2$ -containing alloy was due to the lower solubility of  $\text{TiO}_2$  in a (Fe, Cr, Ni) oxide, which is present to some degree in all of these materials.

Table 34. Results of Creep Tests on Dispersion-Strengthened Austenitic Steel Alloys at 650 C<sup>(25)</sup>

Specimen	Dispersoid	Extrusion Ratio	Stress, tons/in <sup>2</sup>	Time to Rupture, h	Total Elongation, %	Creep Rate, in/in/hr
AA	None	Forged	10	93	30.1	$17.5 \times 10^{-4}$
			12	95	37.2	
			14	9.6		
1	None	15:1	6	16.5	3.2	$17.5 \times 10^{-4}$
			8	3.5	4.3	
			12	0.5	5.1	
7	5% Alumina-1	15:1	5	290		$42 \times 10^{-6}$
			7	121		
			8	209	8.1	
			9	31		$14 \times 10^{-4}$
			10	38	6.5	
			12	7.6	6.5	
5	10% Alumina-2	15:1	8	600(UB)	—	$56.5 \times 10^{-6}$
			10	103	4.0	$12.5 \times 10^{-5}$
			12	26	3.3	$96 \times 10^{-5}$
9	12% Alumina-1	28:1	5	500(UB)		$80 \times 10^{-6}$
			8	3.6	7.7	
			10	0.7	6.6	
			12	0.2	3.7	$80 \times 10^{-6}$
8	15% Alumina-1	15:1	6	422	6.5	
			8	62	5.0	
			10	23	4.3	$17 \times 10^{-6}$
			12	5.6	5.0	
10	10% Titania	15:1	12	950(UB)		
			14	324	6.2	$90 \times 10^{-6}$
			15	79	1.8	$15 \times 10^{-5}$
			16	43	2.1	$30 \times 10^{-5}$
			18	9	2.1	
4	10% Zirconia	15:1	6	14	5.0	
6	10% Thoria	15:1	10	0.4	5.4	

(UB) Unbroken.

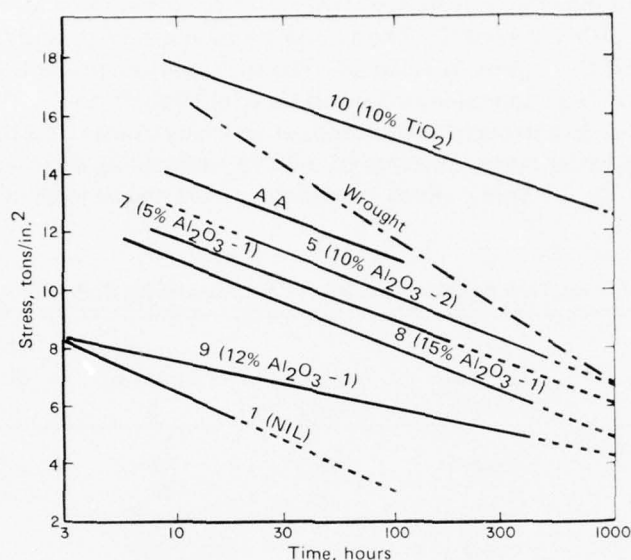


Figure 51. Stress-Rupture Properties of Dispersion-Strengthened Austenitic Steel Alloys, Tested at 650 C<sup>(25)</sup>

Imai, et al.<sup>(7,8)</sup> investigated the growth of MgO, TiO<sub>2</sub>, and Al<sub>2</sub>O<sub>3</sub> particles in a matrix of Fe-15Cr-10Ni-2Mo. A linear relationship between the logarithm of particle diameter and the heating time was observed.

The exceptional, high-temperature, oxidation resistance of FeCrAlY alloys has been known since 1964.<sup>(26)</sup> The high-temperature strength properties of these alloys, however, were low and this precluded their application in hot-structural parts. Starting in 1970, workers in the Aircraft Engine Group of General Electric have conducted a continuing series of investigations<sup>(27-32)</sup> aimed at improving the strength of FeCrAlY alloys in the hope that these alloys could serve in the uncoated condition for jet-engine applications in the 2000-2500 F (1093-1371 C) temperature range. Most of this effort has been devoted to exploiting the promise of oxide-dispersion strengthening these alloys, which are expected to offer the following unique combination of properties<sup>(32)</sup>:

- Outstanding oxidation and hot-corrosion resistance up to at least 2400 F (1315 C) in static and dynamic gas flame—at least to Mach 1;
- High melting temperatures ranging from 2650-2700 F (1454-1482 C);
- Creep and rupture strength approximately equal to that of TD-NiCr sheet;
- Relatively low densities of about 0.25 lb/in<sup>3</sup>; and
- High anisotropy, which may allow orienting the low modulus direction in the major stress axis to greatly enhance thermal fatigue life.

Initial efforts in this program<sup>(27,28,29)</sup> centered around the oxide dispersion strengthening of two matrix chemistries—Fe-25Cr-4Al-1Y (Alloy 2541) and Fe-15Cr-5Al-1Y-1Cb (Alloy 1551-1Cb). Oxide additions were made by the SAP technique, i.e., preoxidation of atomized alloy matrix powder followed with densification by extrusion. In later research<sup>(30)</sup>, the study of matrix chemistries was extended to include Fe-15Cr-6Al-2Y (Alloy 1562), Fe-20Cr-6Al-2Y (Alloy 2062), and Fe-25Cr-6Al-2Y (Alloy 2562). Oxide additions as great as 8 volume percent were explored in most of these matrices.

By the end of 1973, the rupture strengths achieved in these ODS (Oxide Dispersion Strengthened)-FeCrAlY alloys were equivalent to those achieved in ODS NiCr sheet. However, they were still inferior

to ODS NiCr extrusion properties, which were 75 to 100 percent higher. The properties of ODS FeCrAlY sheet compare very favorably to those of TD NiCr at Larsen Miller parameters above 72, as illustrated in Figure 52.<sup>(30)</sup>

The static oxidation resistance of Alloys 2541 and 1551 was not affected by additions of 1-4 volume percent oxide. Long-time, hot-corrosion testing at 1600 F (871 C) and 1800 F (982 C) indicate that the ODS FeCrAlY Alloy 2541 has extremely good hot corrosion resistance. After almost 10,000 hours exposure to a hot, corrosive environment, corrosive attack on this alloy was an order of magnitude less than on any commercially available nickel or cobalt-base alloy.<sup>(32)</sup> Figure 53 shows a comparison between FeCrAlY, TDNiCr, and Hastelloy X in cyclic 2100 F (1148 C) Mach 1 oxidation.

One of the major conclusions of the 1973 program was that attaining adequate high-temperature strength and thermal-fatigue resistance in ODS FeCrAlY alloys was not likely by utilizing the pre-oxidation (SAP) process of making the powders.<sup>(32)</sup> Accordingly, under Contract No. N62269-73-C-0575, the program has been redirected to achieve a dispersoid distribution equivalent to that in current ODS nickel-base alloys. Thus, chemical-oxide-dispersion strengthening and mechanical alloying are being used to prepare powder alloy mixtures containing 21-25 weight percent chromium, 4-5 weight percent aluminum, and 0.4-1.6 weight percent  $Y_2O_3$ . It is hoped that these improved powder making processes plus carefully controlled thermo-mechanical processing will lead to an alloy with suitable properties as a jet-engine vane material.

The last report of this work available to MCIC<sup>(32)</sup> reported that the alloy powders had been extruded to bar stock and rolling studies were in process to achieve the desired recrystallization textures.

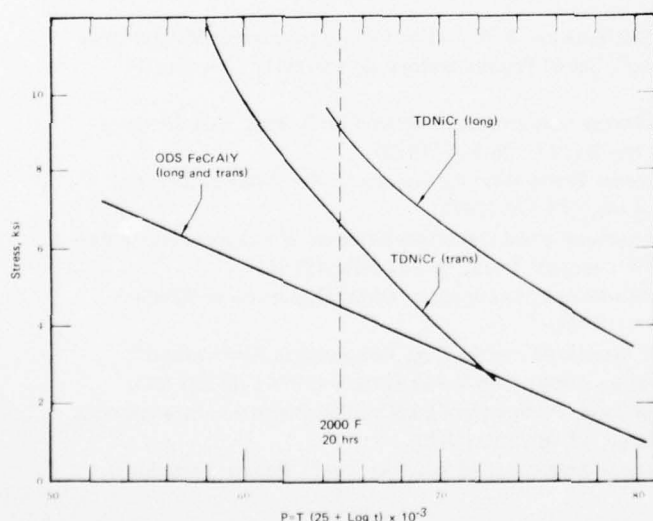


Figure 52. Stress-Rupture Comparison of Fe-25Cr-4Al-1Y Alloy + 4 % Oxide Sheet and TDNiCr Sheet<sup>(30)</sup>

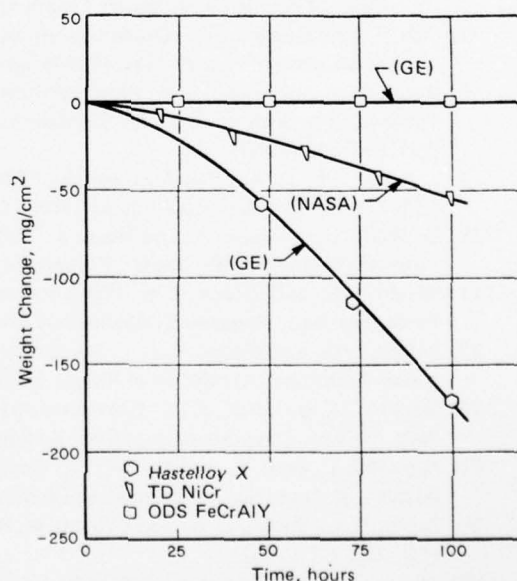


Figure 53. Cyclic Oxidation Behavior of FeCrAlY 2541, Hastelloy X, and TDNiCr in 2100 F/Mach 1 Gases<sup>(32)</sup>

## REFERENCES

1. Gatti, A., "Iron-Alumina Materials", *Trans. Metallurgical Soc. of AIME*, **215**, 753-755 (1959).
2. Gatti, A., "Notes on the Stability of  $Al_2O_3$  in Iron, Nickel, and Cobalt", *Powder Metallurgy*, **10**, 77 (1962).
3. Bovarnick, B., and Flood, H. W., "Dispersion Strengthening Principles for an Improved Iron Powder", *Progress Powder Metallurgy*, **20**, 64-81 (1966).
4. Copeland, M. I., and McBee, W. C., "Dispersion Strengthening of Internally Oxidized Fe-Al Alloys", *Bureau of Mines R. I.* 7686 (1972).
5. Meijering, J. L., *Plansee Proceedings 1955* (1956), pp 405-410.
6. Navara, E., and Easterling, K. E., "Observations on the Decohesion of Oxide Particles in a Deformed Iron-Base Matrix", *Jernkont. Ann.*, **155**, 438-441 (1971).
7. Imai, Y., and Hirostani, H., "A Study on the Dispersion-Strengthened Steel", *Science Reports of the Research Inst. Tohoku Univ., Series A*, **12**, 169-174 (1960).
8. Imai, Y., Kubota, H., and Miyazaki, T., "Physical and Mechanical Properties of Dispersion Strengthened Alloys", *Powder Metallurgy and Material Strengthening Proc. of Intern. Symp. at Indian Institute of Technology, Kharagpur, India*, Oxford & IBH Publishing Co. (1970), pp 77-85.
9. Zwilsky, K. M., Nelson, R. C., and Grant, N. J., "Dispersion Strengthening of Iron", *Met. Soc. Conf.*, **28**, Gordon & Breach Publications, New York (1963), pp 327-349.
10. Mitsche, R., "Eigenschaftsänderungen in Metallischen Systemen durch Dispersionsbildung am Beispiel von Eisenlegierungen", *Schweizer Archiv*, **31** (7), 209-217 (1965).
11. Singh, B. N., and Houseman, D. H., "The Influence of Oxide Particles on the Sintering Characteristics of Carbonyl Iron", *Powder Metallurgy International*, **3**, 26-30 (1971).
12. Place, T. A., and Lund, J. A., "Preparation of  $ThO_2$  Dispersion Hardened Iron", *Int. J. of Powder Metallurgy*, **6** (2), 59-66 (1970).
13. Place, T. A., and Lund, J. A., "Low-Temperature Mechanical Properties of Thoria Dispersion-Strengthened Iron", *Metallurgical Trans.*, **3**, 1613-1619 (1972).
14. Towner, R. J., and Pavlovic, D. M., "Effect of Dispersoid Parameters on High-Temperature Behavior of Co and Fe-27Co", *Jl. of Applied Physics*, **40** (3), 1583-1585 (1969).
15. Towner, J. E., Pavlovic, D. M., Detert, K., and Bufferd, A. S., "Effect of Dispersoids on Magnetic Properties of Iron, Cobalt, and Nickel", *Jl. of Applied Physics*, **39**, 601 (1968).
16. Daikoku, T., and Ikenaga, M., "Study on Dispersion Strengthening of Ferritic 13 Percent Chromium Steels", *Jl. Japan Soc. of Powders and Powder Metallurgy*, **18**, 307 (1972).
17. Oda, T., and Daikoku, T., "Dispersion Strengthened Ferritic Heat-Resisting Steels", *Modern Developments in Powder Metallurgy*, Plenum Press (1971), pp 159-168.
18. Borok, B. A., Lobashev, B. P., Dzheladze, Zh. I., and Shishkhanov, T. S., "Manufacture by Powder Metallurgical Techniques of Semi-Products for Subsequent Processing", *Soviet Powder Metallurgy and Metal Ceramics*, **59** (11), 876-886 (1967).
19. Denisenko, E. T., and Van Asbroeck, P., "Sintered 13 Percent Chromium Steel for Fast Reactor Fuel Element Cans", *Soviet Powder Metallurgy and Metal Ceramics*, No. 9 (117), 95-101 (1972).
20. De Wilde, L., Massaux, H., and Noels, J., "Effect of Powder Preparation Parameters on the Oxide Dispersion Strengthening of Ferritic Steels", *Powder Metallurgy*, **4** (4), 173-176 (1971).
21. Wright, I. G., and Wilcox, B. A., "Observations on Strengthening and Oxidation Behavior of a Dispersion Hardened Fe-Cr-Base Alloy Prepared by Mechanical Alloying", *Metallurgical Trans.*, **5**, 957-960 (1974).
22. Wright, I. G., and Wilcox, B. A., "The Oxidation of Fe-Cr Alloys Containing an Oxide Dispersion or Reactive Metals Additions", *Oxidation of Metals*, **8** (5), 283-301 (1974).
23. Snykers, M., and Huet, J. J., "Dispersion-Strengthened Ferritic Alloys for High Temperature Applications", *Proc. of Conf. Creep Strength in Steel & High-Temperature Alloys*, The Metals Society (1974), pp 237-241.
24. Miyazaki, T., Imai, Y., and Kawati, T., "Coagulation of Oxide Particles in Fe-25Cr-28Ni Dispersion Strengthened Alloys", *Jl. Japan Soc. of Powders and Powder Metallurgy*, **18** (6), 223 (1972).
25. Sands, R. L., Phelps, L. A., and Morgan, W. R., "Dispersion-Strengthened Stainless Steel", *Powder Metallurgy*, **10**, 158-170 (1962).
26. Wukusick, C. S., and Collins, J. F., "An Iron-Chromium-Aluminum Alloy Containing Yttrium", *Materials Research Standards*, 637-646 (December 1964).
27. Allen, R. E., "Strengthening of Fe-Cr-Al-Y Oxidation Resistant Alloys", *General Electric Final Report*, Naval Air Systems Command Contract N00019-69-C-0149 (January 1970).



#### REFERENCES (Cont.)

28. Allen, R. E., "Strengthening of Fe-Cr-Al-Y Oxidation Resistant Alloys", General Electric Company Final Report, Naval Air Systems Command Contract N00019-70-C-0232 (January 1971).
29. Allen, R. E., and Perkins, R. J., "Strengthening of Fe-Cr-Al-Y Oxidation Resistant Alloys", General Electric Company Final Report, Naval Air Systems Command Contract N00019-71-C-0100 (April 1972).
30. Allen, R. E., and Perkins, R. J., "Strengthening of Fe-Cr-Al-Y Oxidation Resistant Alloys", General Electric Company Final Report, Naval Air Systems Command Contract N00019-72-C-0271 (May 1973).
31. Allen, R. E., and Perkins, R. J., "ODS Fe-Cr-Al-Y Component Manufacturing Development", General Electric Company Final Report, Naval Air Systems Command Contract No. N00019-72-C-0397 (November 1973).
32. Bailey, P. G., and Bauer, H. J., Jr., "Strengthening of Fe-Cr-Al-Y Oxidation Resistant Alloys", General Electric Company Quarterly Report No. 3, Naval Air Systems Command Contract N62269-73-C-0575 (November 1974).

## MAGNESIUM

Researchers at the Dow Chemical Company<sup>(1,2,3)</sup> have reported extensively on various techniques for the dispersion strengthening of magnesium. Magnesium presents special problems because it has little tendency to wet materials and is very reactive. Generally, MgO was found to be the best dispersoid as contrasted with oxides of other metals.

It was found that the following processes worked well to produce DS magnesium: a) extrusion of ultrafine powder, b) screw extrusion of powder mixtures, c) atomization of two-phase alloys, and d) interference hardening. The properties of materials produced by these processes are listed in Table 35.

**Table 35. Properties of Dispersion-Hardened Magnesium Extrusions<sup>(1)</sup>**

Composition	Fabrication Data	Shape	Extrusion <sup>(a)</sup>		Elonga- tion, %	Yield Strength				Tensile Strength	
			Temp., F	Speed, fpm		Tension ksi MPa	Compression ksi MPa			ksi MPa	
Mg (EMP)	<1 $\mu$ powder	1/8 in. diam.	1100	$\leq 1$	1	35	241	36	248	40	276
ZK10 + 2MgO	Screw extruded	3/8 by 3/4 in.	820	4	7	35	241	22	152	42	289
Mg-1Zn-1.6Si	Atomized, 35/65 mesh	1/16 by 3/4 in.	600	5	3	43	296	36	248	50	345
Mg-1Zn-1.6Si	Atomized, 35/65 mesh	1/16 by 3/4 in.	600	100	7	34	234	22	152	42	289
Mg-1Zn-1.6Si	Atomized, -100 mesh	1/16 by 3/4 in.	600	100	4	45	310	29	200	49	338
AK11	Interference hardened <sup>(b)</sup>	1/16 by 3/4 in.	600	100	8	44	303	45	310	51	351
AK11	Interference hardened <sup>(b)</sup>	1/16 by 7/8 in.	900	70	10	48	330	36	248	51	351

(a) 1/8 in. diam. wire was extruded from 3/4 in. container; others, from 3 in. container.

(b) Atomized magnesium-zirconium pellets were coated with aluminum flake powder, compacted at 650 F and heat treated 16 hr. at 780 F.

Like other metals, magnesium can be dispersion strengthened by fabricating from ultrafine powder. The MgO film on the powder is fragmented during working and the resulting particles are dispersed along the powder boundaries. Since the powder is very fine and is severely elongated during extrusion, oxide particles become well-dispersed in the metal matrix. The strength of extruded magnesium powder (EMP) is high, but its ductility is low. As shown in Figure 54, the yield strength of EMP compares favorably at room temperature with SAP (dispersion strengthened aluminum) and HM31A (Mg-3Th-1.5Mn), a commercial magnesium alloy designed for applications at elevated temperatures. However, as testing temperature is increased, the yield strength of the EMP alloy falls rapidly, crossing the yield-strength line of SAP at only 200 F (85 C). The microstructure of EMP was similar to that of SAP although the oxide was not as well dispersed. Though the MgO in magnesium does not prevent recrystallization, it does inhibit grain growth. The fine grain size (2 to 5  $\mu$ ) of EMP is primarily responsible for its high strength, particularly in compression. (Wrought magnesium tends to twin in compression at a much lower stress than it yields in tension. Reducing the grain size acts to inhibit twinning, thus decreasing the difference in yield strengths.)

Screw extruding a mixture of a dispersoid with coarse metal powder (or pellets) may be the easiest way of dispersion strengthening magnesium. In this method, the powder particles are very severely

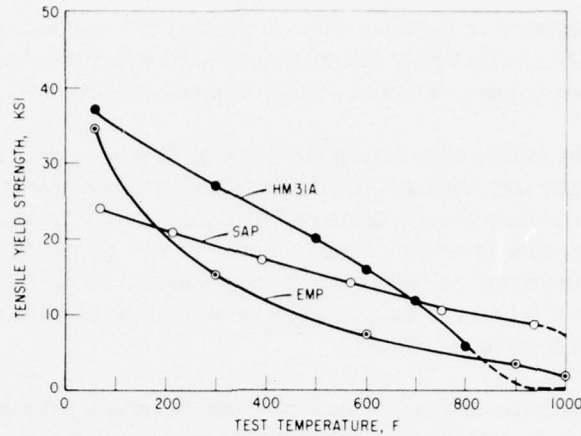


Figure 54. Effect of Temperature on the Yield Strength of EMP, SAP, and HM31A<sup>(1)</sup>

worked and the additive becomes well dispersed throughout the metal matrix. The addition of 2 percent MgO inhibits grain growth and provides good properties, Table 35. Higher strength can be obtained at the expense of ductility by increasing the concentration of MgO.

Another method tried by the Dow investigators was atomization of a molten magnesium alloy and extrusion of the powders. This technique works well and silicon is an excellent choice for the dispersoid because it has appreciable liquid solubility (about 1.3 percent at the eutectic) and essentially no solid solubility. Pellet extrusions of Mg-Si, therefore, contain a fine, uniform dispersion of Mg<sub>2</sub>Si. Table 35 shows the excellent properties obtained with the pellets of Mg-1Zn-1.6Si alloy. The zinc is included to improve ductility.

Interference hardening is the most effective technique for producing DS magnesium. In this method, a dispersion of an intermetallic compound which is essentially insoluble in the base metal in both the solid and the liquid states is used. In Table 35, AK11 is a DS alloy of magnesium made by diffusing aluminum into pellets of Mg-Zr. Very finely dispersed Al-Zr particles are formed, and these particles act so as to inhibit grain growth during subsequent fabrication (extrusion) even under severe processing conditions. This alloy has the highest specific strength of any metal capable of being extruded into complex (multihollow) shapes. The yield strength of this alloy is compared with those of numerous commercial aluminum alloys in Figure 55, which shows yield strength as a function of solidus temperature, which, in turn, is a rough measure of extrudability.

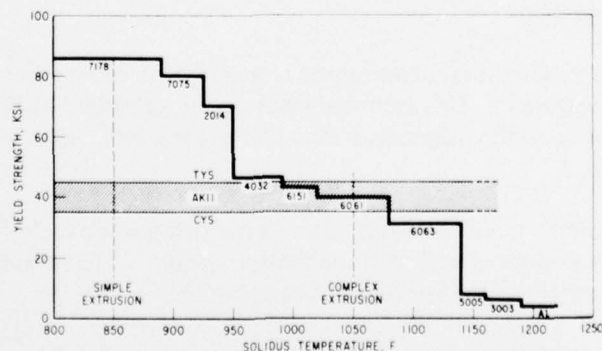


Figure 55. Properties of Aluminum Extrusion Alloys and AK11<sup>(1)</sup>

In the late 1950's Busk<sup>(2)</sup> reported that the Dow Metal Products Company extruded relatively fine (150-800 microns) pellets of ZK60 (Mg-6Zn-0.7Zr minimum) into structural shapes. This alloy, (P)ZK60B, had the highest strength specifications of any magnesium alloy at the time.

Meerson<sup>(4)</sup> has summarized the results of Ivanov, et al.<sup>(5)</sup> on some work with DS Mg-MgO alloys. In this work, magnesium powder was subjected to additional oxidation to regulate its MgO content. During sintering, the powder particles become separated by oxide films. Consequently, in working the sintered blanks, it was necessary to employ large reductions and high temperatures in order to intensify the deformation of the metal particles and the disintegration of the oxide films so that the latter could be transformed into submicroscopical inclusions in a dense metallic matrix. Table 36 lists some tensile properties of the alloy obtained.

In contrast to most other magnesium alloys, DS Mg-MgO materials retain their strength after heating to high temperatures. Thus, the tensile strength of the Mg-1MgO materials remained unchanged (30 kg/mm<sup>2</sup>, 42,670 psi) after heating for 100 hours at 450 C. Table 37 presents the creep characteristics of some of the DS Mg-MgO materials. Increasing the MgO content from 0.1 to 0.3 percent sharply reduced the creep strain. The Mg-MgO and Mg-5MgO materials ruptured in 100 hours at 350 C under a stress of about 2 kg/mm<sup>2</sup> (2845 psi), which is higher than the short-time strength of unalloyed magnesium at this temperature. In spite of their high mechanical properties, DS Mg-MgO materials lack adequate corrosion resistance at 400-450 C.

Table 36. Mechanical Properties of Mg+MgO Materials<sup>(4)</sup>

Composition	20 C			400 C		
	U.T.S. kg/mm <sup>2</sup>	MPa	Elong., %	U.T.S. kg/mm <sup>2</sup>	MPa	Elong., %
MgO	18	176	4	1	10	30
Mg+0.3MgO	27	265	1.5	5	49	10
Mg+1MgO	30	294	2	6	59	8
Mg+5MgO	31	304	2	7	69	7.5

Table 37. Creep of Mg+MgO Materials at 350 C and Stress of 1.2 kg/mm<sup>2</sup> (11.8 MPa)<sup>(4)</sup>

Composition	Strain, %					
	1 hr	2 hr	3 hr	50 hr	100 hr	250 hr
Mg+0.1MgO	4	8	13	—	—	—
Mg+0.3MgO	—	—	—	1	1.5	2

The mechanism of creep in DS Mg-MgO alloys has been studied by various investigators.<sup>(6,7,8)</sup> Early French work<sup>(6)</sup> and a recent investigation<sup>(7)</sup> have shown that a dispersion of about 1 percent MgO produces a marked creep strengthening at temperatures up to 500 C (0.85 T<sub>m</sub>) and also changes the stress and temperature dependence of the creep rate. There is considerable controversy on the subject between Crossland, et al.<sup>(8,9)</sup> and Milicka and coworkers<sup>(10,11)</sup> on the role played by MgO particles on the creep behavior of magnesium.

The internal oxidation of magnesium alloys containing rare earth and other reactive elements was also explored by Dow investigators.<sup>(1)</sup> This technique was not as successful as the methods described earlier due to the high reactivity of the magnesium base and the low solid solubility of magnesium for oxygen.

Planz<sup>(12)</sup> tried to develop DS magnesium alloys by using a melting-casting technique in which Y<sub>2</sub>O<sub>3</sub>, Pr<sub>6</sub>O<sub>11</sub>, Nd<sub>2</sub>O<sub>3</sub>, B<sub>2</sub>O<sub>3</sub>, or BeO were mixed with the molten metal. The method was not successful, however, as the magnesium either reduced or rejected these oxides.

In a recent rocket flight, the feasibility of making Mg-ThO<sub>2</sub> DS material in a low-gravity space environment was demonstrated.<sup>(13)</sup> The process consisted of melting a mixture of ThO<sub>2</sub> blended with



magnesium powder. The space casting was found to be sounder than ground-cast samples and free of internal gas voids. Further, earth-prepared samples showed clusters of dispersoids which were not observed in the space-prepared samples.

Alloying with beryllium improves the high-temperature oxidation resistance of magnesium.<sup>(4)</sup> Beryllium is only slightly soluble in magnesium. However, by processing magnesium-beryllium powder mixtures, DS-magnesium materials containing a few percent of beryllium could be prepared.<sup>(6)</sup> Such alloys were found to exhibit high and stable oxidation resistance. Moreover, when dispersed oxides were added, the material reportedly acquired high heat resistance. After plastic working, the microstructure of these materials contained uniformly distributed grains of two phases. The strength of the Mg-Be/BeO/MgO materials was slightly higher than that for Mg-MgO alloys.

Zelenskii, et al.<sup>(14)</sup> recently reported on the properties of DS Mg-Be alloys containing from 0.2-2 percent beryllium. The properties of the sintered alloys depended strongly upon the method of preparation of the starting powders, their particle size and distribution. One of the most effective methods found for the preparation of these alloys was to vaporize the alloy component in a vacuum and to condense them on the same plate. These sintered DS Mg-Be alloys resist oxidation in air and CO<sub>2</sub> at a temperature of ~580 C for more than 10,000 hours, thus they were claimed to be superior in heat resistance to all existing magnesium alloys.

Huseby, et al.<sup>(15)</sup> studied initial and strain-aging yield points of a Mg-25B alloy in which the boron particles varied in size from submicron to 40 microns. The initial yield point with the as-extruded alloy was not observed below the  $\approx 0.75T_m$  because of a change in crystallographic texture. It was concluded that the kinetics of strain-aging were complex.

## REFERENCES

1. Foerster, G. S., "Dispersion Hardening of Magnesium", *Metals Engineering Quarterly*, **12** (1), 22-27 (1972).
2. Busk, R. S., "Pellet Metallurgy of Magnesium", *Metal Industry*, 275-277, 280 (September 30, 1960); 298-300 (October 7, 1960).
3. Busk, R. S., and Leontis, T. E., "The Extrusion of Powdered Magnesium Alloys", *Trans. AIME*, **188**, 297-306 (1950).
4. Meerson, G. A., "Sintered Materials for Atomic Engineering", *Soviet Powder Metallurgy and Metals Ceramics*, 899-904 (1967).
5. Ivanov, V. E., Zelenskii, V. F., Faifer, S. I., et al., *Proceedings of an International Conference on New Nuclear Materials*, Volume 2, International Atomic Energy Agency Press, Vienna (1963), p 183.
6. Biais, R., Bitran, M., Dabosi, F., Millet, P., and Pegoud, J., "Structural and Mechanical Properties of Sintered Magnesium Products at Elevated Temperatures", *Powder Metallurgy*, **10** (20), 116-144 (1967).
7. Vickers, W., and Greenfield, P., *Jl. Nuclear Materials*, **27** (73), (1968).
8. Crossland, I. G., and Jones, R. B., "Dislocation Creep in Magnesium", *Metal Science Jl.*, **6**, 162-166 (1972).
9. Crossland, I. G., "Remarks Regarding 'High Temperature Creep in Magnesium Strengthened by MgO Particles' by Milicka, et al.", *Zt. Metallkunde*, **65**, 161-162 (1974).
10. Milicka, K., Cadek, J., and Rys, P., Reply to Above, *Zt. Metallkunde*, **65**, 162 (1974).
11. Milicka, K., Cadek, J., and Rys, P., "High Temperature Creep in Magnesium Strengthened by MgO Particles", *Zt. Metallkunde*, **64**, 581-585 (1973).
12. Planz, E. J., "Development of Dispersion-Hardened Magnesium Alloys", Univ. of Alabama, Final Report on Contract DAAH01-71-C-0258 (January 1972) (AD 743 248).
13. Anonymous, "Space Casting Shows Promise", *Industrial Research*, **13** (June 1976).
14. Zelenskii, V. F., Savchenko, V. I., and Bovkunenko, A. S., "Mechanical Properties of Sintered Mg-Be Alloys", *Soviet Powder Metallurgy and Metals Ceramics*, **138** (6), 90-95 (1974).
15. Huseby, I. C., Hsu, S. E., McNelley, T. R., Edwards, G. R., Francois, D., Shyne, J. C., and Sherby, O. D., "Yield Points and Strain Aging in Hexagonal-Based Particulate Composites", *Metallurgical Transactions*, **6A**, 2005-2008 (1975).

## MOLYBDENUM

One of the first attempts at dispersion strengthening of molybdenum was carried out by Bruckart, et al.<sup>(1)</sup> who used small additions (0.1-2 percent) of various oxides and creep deformation as a measure of strengthening. Of the additions employed, titanium dioxide was found to be the most effective at 980 C, as shown in Figure 56, which summarizes the results of this study.

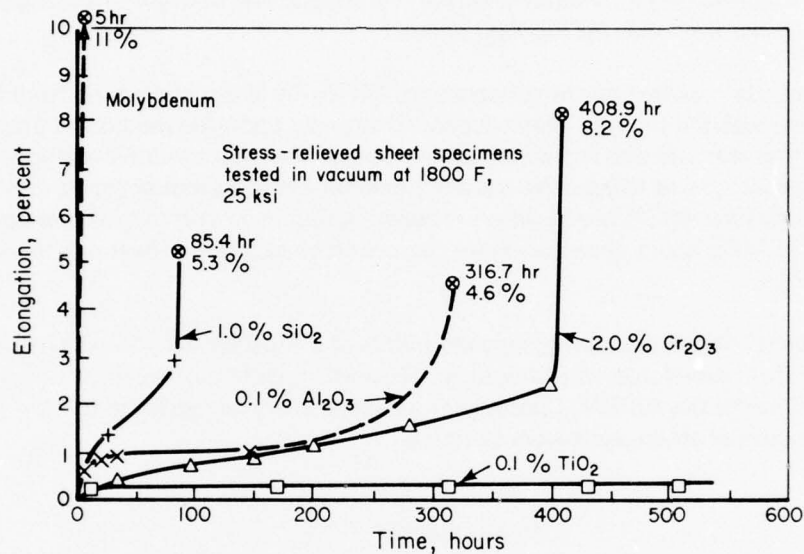


Figure 56. Effects of Dispersions of Small Quantities of Various Oxides on the Creep of Molybdenum at 980 C<sup>(1)</sup>

In 1965, White<sup>(2)</sup> reported on his investigation on the dispersion of various oxides, nitrides, and borides in molybdenum after vacuum annealing 1 hour at temperatures from 1650 C to 2205 C (3000 F to 4000 F). Table 38 gives the Knoop hardnesses measured. He concluded that of the nitrides, BN was

Table 38. Knoop-Hardness Values of Molybdenum Alloys<sup>(2)</sup>

Material	As-Hot Pressed	1-Hour Vacuum-Annealing Temp., F		
		3000	3500	4000
Pure Molybdenum	210	180	172	165
Mo+2.5 vol. %:				
BN	200	175	172	165
ZrN	208	200	181	190
HfN	206	200	202	196
LaB <sub>6</sub>	220	238	215	235
ZrB <sub>2</sub>	211	185	175	185
TaB <sub>2</sub>	205	200	185	185
Y <sub>2</sub> O <sub>3</sub>	239	242	210	218
MgO	242	218	220	202
ZrO <sub>2</sub>	237	216	195	191
ThO <sub>2</sub>	236	209	199	195

incompatible with molybdenum at temperatures of 1650 C because of swelling and blistering; ZrN underwent solution above 1925 C. The refractory borides LaB<sub>6</sub>, ZrB<sub>2</sub>, and TaB<sub>2</sub> were found to be of questionable utility in a molybdenum matrix because of the apparent formation of a low-melting eutectic. The effectiveness of Y<sub>2</sub>O<sub>3</sub> as a dispersoid was lost owing to instability above 1925 C. MgO containing alloys exhibited a surface loss of MgO due to volatilization during vacuum annealing at as low as 1925 C. A relatively high degree of stability up to 2205 C was exhibited by HfN, ZrO<sub>2</sub>, and ThO<sub>2</sub> as dispersed phases. A dispersion of ultrafine ThO<sub>2</sub> resulted in excellent resistance to grain growth and in particle stability up to 2205 C.

White and Barr also evaluated thoria as a dispersoid in molybdenum,<sup>(3)</sup> both as a simple binary addition and also in combinations with titanium, zirconium, and carbon. The temperature range of interest was from 1370 C to 2205 C, with particular attention to temperatures just above 1650 C. The alloys investigated and tensile properties obtained are listed in Table 39. Table 40 lists the hot-hardness values of these plus a few other alloys.

**Table 39. Elevated Tensile Properties of Molybdenum-Base Alloys<sup>(3)</sup>**

Alloy	Temp., F	Tensile Strength		0.2% Offset Yield Strength		Elong., %
		ksi	MPa	ksi	MPa	
Mo (0.004 C)	2000	21.3	147	19.9	137	3
	2500	4.4	30	2.9	20	3
	3000	2.4	17	1.1	8	0
	3500	.57	4	—	—	4
Mo+2.5ThO <sub>2</sub> (0.005 C)	2500	19.6	135	14.3	99	1
	3000	10.2	70	—	—	3
	3500	7.8	54	4.9	34	3½
TZM (Mo-0.5Ti -0.1Zr -0.021 C)	2000	29.1	200	28.6	197	43
	2500	9.7	67	—	—	80
	2500	8.7	60	6.4	44	101
	3000	4.8	33	2.9	20	125
	3500	1.5	10	—	—	136
TZM+2½ThO <sub>2</sub> (Mo-0.5Ti -0.1Zr -0.024 C)	2000	29.4	202	29.1	200	48½
	2500	7.8	54	5.9	41	111
	3000	4.6	32	2.2	15	104
	3500	1.0	7	—	—	88

**Table 40. Hot-Hardness Values of Molybdenum-Base Materials<sup>(3)</sup>**

Material and Composition	Diamond Pyramid Hardness		
	2000 F	2500 F	3000 F
Mo	45.8	23.8	15.3
Mo+2.5ThO <sub>2</sub>	41.4	32.3	24.0
Mo+5ThO <sub>2</sub>	84.9	56.4	32.2
TZM	37.7	25.9	17.1
TZM+2.5ThO <sub>2</sub>	37.9	24.5	15.6
Mo+2Ta+0.1C+2.5ThO <sub>2</sub>	48.9	30.8	16.4
Mo+1Cb+0.1C+2.5ThO <sub>2</sub>	58.8	37.4	21.7
Mo+2Hf+1Ti+1Zr+0.1C+ 2.5ThO <sub>2</sub>	—	26.0	11.2

It was found that a 2.5 percent  $\text{ThO}_2$  addition markedly improved the elevated-temperature tensile strength of molybdenum from 1370 C to 1930 C. In addition, it afforded a pronounced resistance to recrystallization and grain growth in this temperature range. Additions of less than 1 percent of elemental titanium or zirconium powders to molybdenum billets hot pressed under an argon atmosphere provided a marked improvement in both fabricability and elevated-temperature elongation. This is apparently a partial result of the titanium and zirconium in removing oxygen by forming stable oxide inclusions. On the other hand, these same additions to the thoriated molybdenum resulted in considerable degradation of the  $\text{ThO}_2$  distribution resulting from a solid-state reaction occurring primarily between the  $\text{ThO}_2$  and the reaction-metal additions. The resulting dispersed-phase distribution afforded no improvement in elevated-temperature mechanical properties relative to TZM alloys of the same matrix composition.

Mitchell<sup>(4)</sup>, on internal nitriding of a Mo-1Hf solid solution alloy (atomic percent), found a homogeneous dispersion of coherent plate-like HfN precipitates. This alloy – actually a precipitation hardened alloy – presented high-temperature tensile strength substantially superior to that currently available in commercial Mo-base alloys such as TZM and TZC. However, a severe particle-coarsening occurred at high temperatures in regions of the nitrided alloy containing a high density of small, fully coherent, HfN particles.

In Russia, there has been also considerable work done on DS molybdenum alloys. Altfinseva, et al.<sup>(5)</sup> studied the effects of temperature, in the range 20-1500 C, upon the hardness of molybdenum and its alloys with additions of 4 volume percent of  $\text{Al}_2\text{O}_3$ ,  $\text{TiO}_2$ ,  $\text{ZrO}_2$ ,  $\text{HfO}_2$ , AlN, TiN, ZrN, and HfN. The particle sizes of these were: (A) 0.5-2 and 0.5-3 microns, and (B) 0.5-1 micron. The addition of oxides and nitride in the coarser sizes gave no property improvements. With rising temperature, the hardness of the alloys decreases in the same way as does the hardness of unalloyed molybdenum (see Figure 57). The presence of dispersoids  $\text{TiO}_2$  and  $\text{Al}_2\text{O}_3$  increased the hardness of molybdenum over the whole temperature range, the increase being particularly marked for the alloy containing  $\text{TiO}_2$  (106 kg/mm<sup>2</sup> at 300 C and 78 kg/mm<sup>2</sup> at 900 C). Nitrides of the same particle size and added in the same amounts as oxides were more effective in increasing the hardness (see Figure 57). In the temperature range from 20-900 C, the greatest increase in hardness was due to additions of AlN. At temperatures above 900 C, the addition of ZrN caused the greatest increase in hardness. A pronounced fall in hardness of these alloys occurred above 1100 C. At 800 C, the Mo-4AlN alloy had the highest hardness, 120 kg/mm<sup>2</sup> (827 MPa), which is almost twice the hardness of unalloyed molybdenum.

Figure 58 shows the temperature dependence of hardness of molybdenum with additions of oxides and nitrides of 0.5-1 micron particle size. The increase in the hardness of Mo due to additions of nitrides with particles 0.5-1 micron is again greater than that due to the oxide dispersoids. The greatest improvement in hardness was due to TiN with a hardness of 390 kg/mm<sup>2</sup> (2687 MPa) at 20 C, 138 kg/mm<sup>2</sup> (951 MPa) at 1000 C, and 30 kg/mm<sup>2</sup> (207 MPa) at 1500 C. On microscopic examination, the Mo-4TiO<sub>2</sub> alloy showed more than half of the particles with 1 micron size, while in the alloy containing HfO<sub>2</sub> oxide particles of 2-3 micron size predominated, which would explain the higher hardness of the former alloy.

Later, Altfinseva, et al.<sup>(6)</sup> determined the stress-rupture strength of several Mo-AlN alloys with the results shown in Figure 59.

Samsonov, et al.<sup>(7)</sup> investigated certain regularities in the variation of the spark erosion and strength characteristics of a series of DS molybdenum alloys with special emphasis on the molybdenum-AlN series (see Figure 60). The AlN particles were between 0.5-1 micron size. Erosion resistance of molybdenum alloys with 4 percent additions of  $\text{Al}_2\text{O}_3$ ,  $\text{Sc}_2\text{O}_3$ ,  $\text{Cr}_2\text{O}_3$ ,  $\text{TiO}_2$ ,  $\text{ZrO}_2$ ,  $\text{HfO}_2$ , TiN, ZrN, HfN, CbN, VN, TaN, and  $\text{Cr}_2\text{N}$  was also studied.



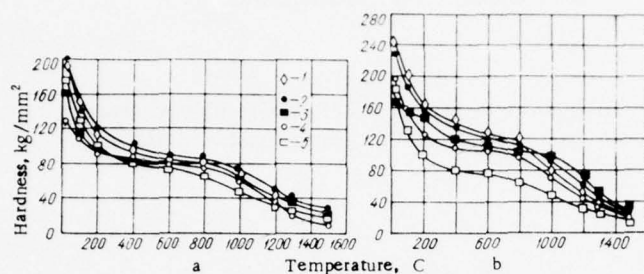


Figure 57. Effect of Temperature Upon Hardness of Molybdenum Alloys With Additions of Oxides (a) and Nitrides (b) of Particle Sizes 0.5-3 and 0.5-2  $\mu$ : 1) Mo+Al<sub>2</sub>O<sub>3</sub> and Mo+AlN; 2) Mo+TiO<sub>2</sub> and Mo+TiN; 3) Mo+ZrO<sub>2</sub> and Mo+ZrN; 4) Mo+HfO<sub>2</sub> and Mo+HfN; 5) Mo<sup>(5)</sup>

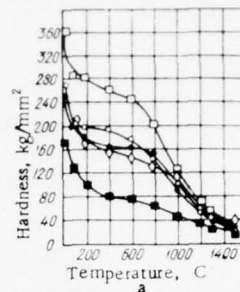
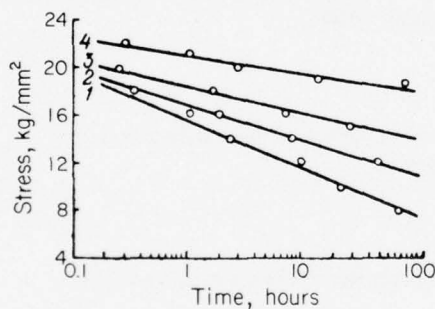


Figure 58. Temperature Dependence of Hardness of Molybdenum With Additions of Oxides (a) and Nitrides (b) of 0.5-1  $\mu$  Particle Size. Curve Designations as Figure 57 (5)



1-Mo; 2-Mo-4AlN (volume percent, pressed and sintered); 3-Mo-2AlN (volume percent, pressed, sintered, and deformed); 4-Mo-2AlN (volume percent, activated sintering and rolling)

Figure 59. Stress-Rupture Lives of Selected Molybdenum Alloys at 1100 C<sup>(6)</sup>

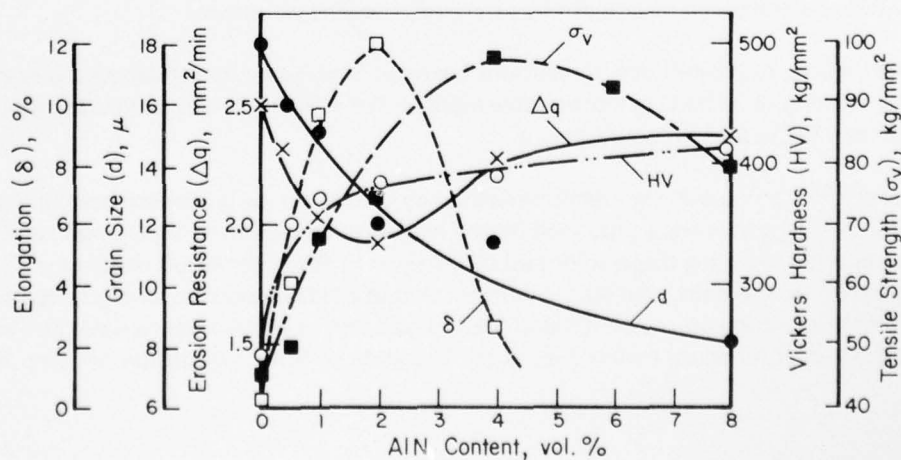


Figure 60. Variation of Erosion Resistance, Elongation, Tensile Strength, Hardness, and Grain Size of Molybdenum Alloys With Aluminum-Nitride Content<sup>(7)</sup>

Strashinskaya, et al.<sup>(8)</sup> conducted X-ray diffraction studies on molybdenum alloyed with various dispersoids after heating in the range of 1500-2200 C. The following results were found:

#### Mo-HfC

A Mo-3HfC alloy, after heating at 1500 C, contained all the HfC lines, but after heating at 2200 C, no HfC lines remained. HfC lines were found in all patterns of molybdenum with 5 and 10 percent HfC additions. The molybdenum lattice parameter remained unchanged at 3.15 angstroms after heating to 2200 C.

#### Mo-TaC

An alloy with a 10 percent TaC addition showed all TaC lines on heating up to 2200 C. The molybdenum lattice parameter was unchanged.

#### Mo-ZrC

A five percent addition of ZrC showed ZrC lines up to 1500 C, but not at 2200 C. With a 10 percent addition, ZrC lines were present even after heating at 2200 C.

#### Mo-ZrN

With a 3 percent ZrN addition, some lines of ZrN disappeared after heating at 2200 C; with 10 percent ZrN, all lines remained after 2200 C heating, but a new phase, Mo<sub>2</sub>N, appeared after heating above 1800 C.

#### Mo-ZrO<sub>2</sub>

For ZrO<sub>2</sub>, a 3 percent addition showed no ZrO<sub>2</sub> lines above 1500 C. With 5 percent, some weak lines were detected above 1500 C, and with 10 percent, all the main lines of monoclinic ZrO<sub>2</sub> were visible.

#### Mo-CaO, Mo-La<sub>2</sub>O<sub>3</sub>, and Mo-Nd<sub>2</sub>O<sub>3</sub>

Seven percent additions were added to Mo and heated to 1500 and 2000 C. The patterns showed seven to nine lines of the oxides. No lines of a new phase were detected.

#### Unalloyed Molybdenum

Heating at 1500 and 2200 C did not affect the lattice parameter. After heating at 2200 C, however, some line broadening was observed which was linked with thermal stresses developed on cooling the samples.

Dubok<sup>(9)</sup> investigated the possibility of reactions between Sc<sub>2</sub>O<sub>3</sub> and molybdenum. Since none was observed after heating to 2100 C in a protective medium for 4 hours, it was concluded that this oxide may be useful as a dispersoid in molybdenum.

Poltavtsev, et al.<sup>(10)</sup> carried out high-temperature X-ray studies on molybdenum containing Al<sub>2</sub>O<sub>3</sub> and ZrO<sub>2</sub>. The Mo-Al<sub>2</sub>O<sub>3</sub> alloys were produced by the hydrogen reduction of MoO<sub>3</sub> and aluminum chlorhydrate, and the resulting dispersoids had dimensions of the order of 50 angstroms. The purpose of the investigation was to study the elastic deformation in oxide-dispersion-strengthened alloys. It was shown, that, depending on the elastic and thermal properties of the materials of the matrix and the dispersoid, the molybdenum matrix may occur in a state of isotropic tension or compression.

## REFERENCES

1. Bruckart, W. L., Craighead, C. M., and Jaffee, R. I., "Investigations of Mo and Mo Base Alloys Made by Powder Metallurgy Techniques", WADC Tr 54-398 (January 1955).
2. White, J. E., "Observations on the Effect of Vacuum Heat Treatment (Up to 4000 F) on Dispersions of Various Oxides, Nitrides, and Borides in Mo", *Powder Metallurgy*, 8 (15), 64-80 (1965).
3. White, J. E., and Barr, R. Q., "Dispersion Strengthened Molybdenum and Molybdenum-Base Alloys", *Metallurgical Society Conferences*, 41, 541-555 (1967).
4. Mitchell, J. B., "Mechanisms of Growth and Loss of Coherency of HfN Particles in Mo", *Acta Metallurgica*, 19, 1063-1077 (1971).
5. Altfinseva, R. A., and Borisenko, V. A., "Temperature Dependence of the Hardness of Dispersion Strengthened Molybdenum", *Soviet Powder Metallurgy & Metal Ceramics*, 12 (10), 830-833 (1973).
6. Altfinseva, R. A., Borisenko, V. A., and Lemeshko, A. M., "Strength of Dispersion-Hardened Mo Alloys", *Fiz-Khim Mekh. Mater.*, 1 (4), 77-81 (1975).
7. Samsonov, G. V., Altfinseva, R. A., and Verkhoturov, A. D., "Erosion Resistance of Dispersion-Hardened Materials Based on Refractory Metals", *Soviet Powder Metallurgy and Metal Ceramics*, 14 (10), 831-833 (1975).
8. Strashinskaya, L. V., and Stashevskaya, I. A., "An X-Ray Diffraction Study of the Reactions of Molybdenum and Tungsten With Disperse Inclusions", *Soviet Powder Metallurgy and Metal Ceramics*, 13 (5), 420-422 (1975).
9. Dubok, V. A., and Tyutkalo, L. I., "High Temperature Compatibility of Refractory Metals With Scandium Oxide", *Soviet Powder Metallurgy and Metal Ceramics*, 1, 83-87 (1968).
10. Poltavtsev, N. S., Pryanchikov, E. N., Sagalovich, V. V., Slezov, V. V., and Khrebtov, V. L., "Isotropic Elastic Deformation in Two Phase Alloys", *Sov. Phys. Solid State*, 16 (7), 1234 (1975).

## NICKEL

Research on dispersion-strengthened nickel possibly goes back to the early 1950's when Baxter<sup>(1)</sup> investigated the contact angles between  $Al_2O_3$  and nickel and some binary nickel alloys. Grant<sup>(2)</sup> in 1956 showed that considerable property improvements in nickel were possible by incorporating a 10 volume percent addition of  $Al_2O_3$ . Interest in these materials grew rapidly and, by 1962, du Pont<sup>(3)</sup> announced the first commercial, DS nickel material which was designated as TD-Ni and contained 2 volume percent of  $ThO_2$ . This material was prepared by a proprietary co-precipitation process and aroused considerable interest. Much work has since been done to understand the alloy and strengthening mechanisms involved. Shortly thereafter, Sherritt Gordon offered an equivalent product, DS-Ni, which contained 3.5 volume percent of  $ThO_2$ . Since then, two similar commercial compositions were announced in the U.S.S.R.<sup>(4)</sup> These carry the VDU-1 and VDU-2 designations, which correspond to compositions in the Ni- $ThO_2$  and Ni- $HfO_2$  systems, respectively.

Even though the oxide-dispersion-strengthened (ODS) nickel alloys showed outstanding hot strength, their relatively poor oxidation resistance discouraged applications at elevated temperatures. The natural consequence of this was alloy development to improve high-temperature, oxidation behavior. Du Pont was again amongst the first to develop the second generation of these alloys, which was TD-NiC and contained 20 weight percent chromium with 2 volume percent of  $ThO_2$ . Fansteel purchased the rights to produce this alloy in 1968 and continued the development of commercial mill products from it. In 1972, the Stellite Division of the Cabot Corporation acquired Fansteel's rights.

The most recent exciting development associated with these alloys was the "mechanical alloying" process developed by Benjamin and his coworkers at International Nickel.<sup>(5,6,7)</sup> This has since formed the basis for the commercial production of nickel alloys that are strengthened by the combination of oxide dispersion and gamma prime precipitation, e.g., the MA753 and 754 designations. The compositions for these are given in Table 41, which also contains the compositions, designations, and present commercial status of ODS nickel alloys in the U.S.

**Table 41. Designations, Compositions, and Current Status of Commercial, Dispersion-Strengthened Nickel Alloys**

Alloy Designation	Producer	Composition	Status
TD-Ni	du Pont/Fansteel	2 vol. % $ThO_2$	Discontinued
DS-Ni	Sherritt Gordon	3.5 vol. % $ThO_2$	Discontinued
TD-NiC	du Pont/Fansteel	20Cr, 2 vol. % $ThO_2$	
DS-NiCr	Sherritt Gordon	20Cr, 2 vol. $ThO_2$	Discontinued
MA-753	International Nickel	20Cr, 1.5Al, 2.5Ti, 1.3 vol. % $Y_2O_3$	
MA-754	International Nickel	20Cr, 0.3Al, 0.5Ti, 0.6 vol. % $Y_2O_3$	Commercial
MA-953	International Nickel	Ni-Fe-Cr-Al	Development
HDA-8077	Stellite	16Cr, 4Al, 1.3 vol. % $Y_2O_3$	Semi-commercial
YDNCrAl	Special Metals		Semi-commercial
DSNCrAl	Sherritt Gordon		Development

Numerous applications-oriented studies have been conducted for these alloys.<sup>(8,9)</sup> In addition to a study of their use as a skin material in the Space Shuttle, the following alloys have been examined for the applications indicated below in aircraft, gas-turbine engines:



TD-Ni sheet for flame holder  
 TD-Ni sheet vanes  
 TD-NiCr sheet for flame holder  
 TD-NiCr sheet vanes  
 TD-NiCr extrusion vanes  
 DS-NiCr extrusion vanes  
 MA-754 vanes and shrouds

Many papers and reports have been issued since the first comprehensive review of these materials<sup>(10)</sup> was published in 1965. As a matter of convenience, in this review, this literature has been grouped and will be treated in the following subject categories:

- I. Ni alloys, where the dispersoid is
  - A.  $\text{ThO}_2$
  - B.  $\text{Al}_2\text{O}_3$
  - C.  $\text{HfO}_2$
  - D. Other
- II. Ni-M alloys, where M is other than chromium
- III. Ni-Cr alloys
  - A. Experimental Ni-Cr- $\text{ThO}_2$  alloys
  - B. Commercial Ni-20Cr02 $\text{ThO}_2$  alloys
  - C. Other Ni-Cr alloys
- IV. Ni-Cr-Al alloys
- V. Superalloys
- VI. Oxidation and Hot-Corrosion Resistance

### Ni- $\text{ThO}_2$ Alloys

Ruscoe, et al.<sup>(11)</sup> investigated the dependence of dispersoid parameters, microstructure, and crystallographic texture on the room-temperature and high-temperature properties of an ODS-Ni-2 $\text{ThO}_2$  alloy. The dependence of these variables upon thermomechanical processing is shown in Figures 61 and 62 and Table 42.

Table 42. Properties of ODS-Ni-2 Vol. %  $\text{ThO}_2$ <sup>(12)</sup>

Temperature		Ultimate Tensile Strength	
F	K	ksi	MPa
77	298	80	551
1200	922	43	296
1600	1144	32	220
2000	1366	20	138

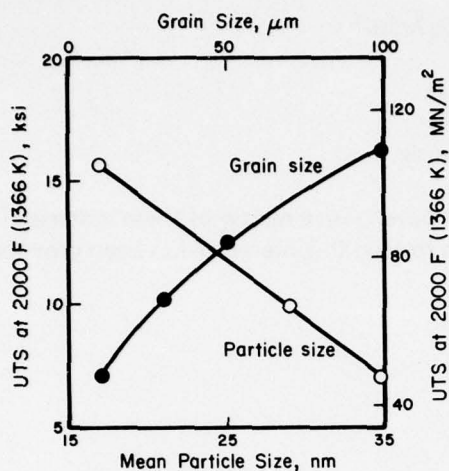


Figure 61. Tensile Strength of Ni/ThO<sub>2</sub> Strip at 2000 F (1366 K) as a Function of Grain Size and Dispersoid Particle Size<sup>(11)</sup>

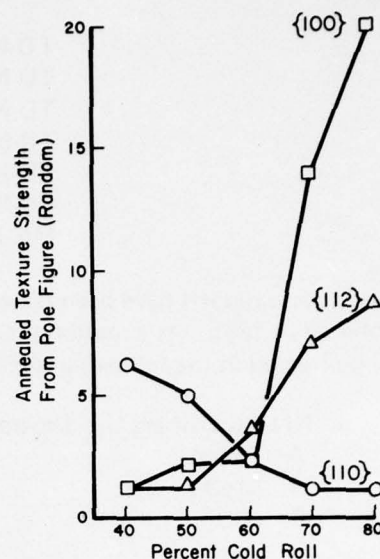


Figure 62. Annealed Texture as a Function of Cross Cold-Roll Reduction for Ni/2ThO<sub>2</sub> Sheet<sup>(11)</sup>

Quatinetz, et al.<sup>(12)</sup> conducted an investigation to determine the possibilities of producing DS nickel by thermomechanical processing of comminuted and blended composites. Ni-4 vol. % ThO<sub>2</sub> and NiO-4 vol. % ThO<sub>2</sub> were so prepared. The products were then cold pressed, sintered, hot rolled, and subjected to 7, 14, or 21 cold-roll and anneal cycles. A number of the sheet materials produced were stronger in the 1095 C tensile and stress-rupture properties than both the processed reference powder and the best available commercial TD-Ni sheet. In general, the strengths of the materials produced increased as the number of cold-roll and anneal cycles increased from 7 to 21.

Marty, et al.<sup>(13)</sup> prepared TD-Ni by wetting a powdered nickel compound in suspension within a methyl polymethacrylate with a solution of a thorium salt, the pyrolysis of which gives at 550 C, and above a stoichiometric ThO<sub>2</sub>. The Ni-ThO<sub>2</sub> was worked by extrusion. Thermomechanical treatment was re-temperatures.

Cheney, et al.<sup>(14)</sup> investigated the properties of ODS-Ni-2ThO<sub>2</sub> sheet made from powders produced by spray drying and selective reduction. Small ThO<sub>2</sub> particle size (200 Angstroms) and strongly developed crystallographic texture were both necessary for good strength at 1095 C. The sheet with about 400-Angstroms-diameter ThO<sub>2</sub> had little texture and poor strength. The thermomechanical processing of the alloys greatly influenced their strength because of the effects on texture, grain structure, and the spatial distribution of the ThO<sub>2</sub>.

Arias<sup>(15)</sup> showed that dispersion strengthening of nickel can be produced by a postulated nonreactive milling mechanism, using water as the nonreactive milling fluid. The tensile properties of this ODS-Ni-1.8 vol. % ThO<sub>2</sub> at 1093 C are reproduced in Table 43.

Norris, et al.<sup>(16)</sup> found that the mechanical aspects of cold rolling Ni-ThO<sub>2</sub> strip are similar to those for pure nickel, the only significant differences arising from the varying rates of work hardening. Several series of Ni-ThO<sub>2</sub> powders were fabricated to strip by hot rolling, cold rolling 20 to 80 percent, and annealing to recrystallization. Strip which has been cold rolled parallel to the hot-rolling direction: 1) developed a {120} {001} texture, and texture strength increased with increasing cold reduction; 2) had strength characteristics at 1095 C that correlated with the grain aspect ratio; 3) exhibited

Table 43. Tensile Properties of ODS-Ni-1.8 Vol. % ThO<sub>2</sub> at 1095 C<sup>(15)</sup>

Ultimate Tensile, Strength		0.2% Yield Strength		Elongation, %
MPa	ksi	MPa	ksi	
141.5	20.5	131	19	3.7
124.1	18.0	113.1	16.4	5.0
122.3	17.9	118.3	17.2	3.9

increasing strength at 1095 C along the rolling direction; 4) had anisotropy in strength at 1095 C and in tensile elongation at room temperature; and 5) had high-anisotropic, room-temperature, elastic moduli.

Strip for which the cold rolling direction was perpendicular to the hot-rolling direction: 1) developed a {100} <001> texture; 2) had strength characteristics at 1095 C which correlated with grain size; 3) exhibited minimum strength levels for intermediate rolling reductions of 40-60 percent that yielded weakly textured microstructures; 4) had nearly isotropic strength at 1095 C and tensile elongation at room temperature; and 5) had lower and isotropic room-temperature elastic moduli. It was also shown that the texture composition was determined by the characteristics of the dispersoid distribution.

Babich, et al.<sup>(17)</sup> investigated the recrystallization of extruded ODS-Ni-2.8 vol. % ThO<sub>2</sub> after cold drawing and annealing. The material was characterized by a large temperature range between recovery, occurring at 400-600 C, and recrystallization, which developed at 1200-1400 C. During recrystallization, structural heterogeneities occurred which were stable up to 1400 C (0.97 T<sub>m</sub>). The number of large grains depended on the degree of prior deformation and the annealing temperature. A large degree of deformation (83 percent) prevented the formation of large recrystallized grains.

Petrovic and Ebert<sup>(18)</sup> investigated the primary recrystallization of commercial TD-Ni. While it occurs readily after rolling transverse to the bar axis and annealing (800 C), it is completely inhibited by longitudinal rolling and swaging deformations, even for very high (1320 C) annealing temperatures. Coarse grain formation is the result of abnormal grain growth (or secondary recrystallization), which follows primary recrystallization. The coarse grains may be up to 500 times the size of the initial as-received state.

Hotzler, et al.<sup>(19)</sup> established that ODS-Ni-ThO<sub>2</sub> recrystallized prematurely during annealing when its surface was exposed to impurity atoms of certain elements having low melting temperatures, such as sulfur, selenium, lead, and bismuth.

In TD-Ni, high internal stress remains captive, according to Lasalmonie and Strudel<sup>(20)</sup>, and cannot contribute to recovery or recrystallization as in pure metals.

Footner and Alcock<sup>(21)</sup> investigated the growth rates of dispersed ThO<sub>2</sub> particles in nickel as a function of time at 1350 C in gases of two separate partial oxygen pressures. The diffusion coefficient and solubility of thorium in nickel placed in contact with ThO<sub>2</sub> were also determined under the same conditions.

The dissolution of ThO<sub>2</sub> in nickel in atmospheres of controlled oxygen partial pressure between 1295 and 1400 C was investigated by Alcock and Brown<sup>(22)</sup>. It was concluded that the rate-determining step in the dissolution process was the diffusion of thorium atoms in nickel and that the presence of oxygen in solution in the metal enhanced this process.



Durber and Davies<sup>(23)</sup> examined some strain characteristics of TD-Ni alloys containing up to 3 vol. % ThO<sub>2</sub>, which were prepared by sequentially powder blending, hot compacting, and wire swaging. Room temperature tensile tests and cyclic temperature tests between 77 and 293 K were made. The flow stress was found to increase with decreasing interparticle spacing as predicted by theory. The presence of the inert dispersoid is considered to decrease the temperature sensitivity of the flow stress.

Ansell<sup>(24)</sup> carried out studies directed toward providing an analytical rationale for the sensitivity-insensitivity of DS systems to process history. Thermal shock was found to have little effect on room-temperature properties of TD-Ni. The effect of thermal cycling on high-temperature behavior was also studied. Here, preloaded specimens of TD-Ni were tested in creep and stress rupture as a function of initial heating rate. Those specimens heated rapidly to temperature, e.g., 5,500 F/sec to 1100 F (3050 C/sec to 595 C), exhibited much faster creep rates and shorter stress-rupture lives than those heated to temperature using slower heating rates, e.g., 30.5 C/sec.

Murr, et al.<sup>(25)</sup> investigated the substructure of TD-Ni following simultaneous, explosive shock loading at pressures of 80, 180, 240, and 460 kbars. Well-defined dislocation cells having average diameters of 0.8, 0.3, 0.2, and 0.1 micron for the respective pressure levels were observed in pure nickel, but were not developed to the same extent in annealed TD-Ni due to the presence of the ThO<sub>2</sub> having a mean particle diameter of 340 Angstroms. Deformation microtwins having an average width of 175 Angstroms occupied approximately 1 vol. % of the nickel substructure at 460 kbars while twinning was inhibited by the ThO<sub>2</sub> particle distribution in the TD-Ni.

Murr<sup>(26)</sup> measured the absolute (mean) interfacial free energies in TD-Ni and TD-NiC at 1200 C utilizing techniques of scanning and transmission electron microscopy. It was concluded that the apparent difference in particle/matrix interfacial strength between TD-Ni and TD-NiC results from a more complex mechanism than simple interfacial decohesion involving phase separation.

Thompson<sup>(27)</sup> investigated the compatibility of ODS-Ni-2ThO<sub>2</sub> with both hydrogen charging and tests in high-pressure hydrogen gas. The former were conducted at 194 K as well as at room temperature. The ODS-Ni showed small ductility losses with no change in fracture morphology.

Ikawa, et al.<sup>(28)</sup> made a study of the weldability of TD-Ni. They found that the joint efficiencies of solid-state-bonded joints made by a one-step bonding method were about 100 percent. The joint efficiencies were superior to those of fusion-welded joints, but the reduction of area in such joints was inferior to that in the base metal. The joint efficiencies of solid-state-bonded joints made by two-step bonding method were also 100 percent and the reduction of area in such joints was 80-100 percent of those in the base metal.

### Ni-Al<sub>2</sub>O<sub>3</sub> Alloys

Dzneladze and his coworkers described<sup>(29)</sup> the preparation of Ni-Al<sub>2</sub>O<sub>3</sub> alloys from carbonyl nickel and Al<sub>2</sub>O<sub>3</sub>, made by calcining Al<sub>2</sub>(SO<sub>4</sub>)<sub>3</sub>. An alloy containing 0.2 percent Al<sub>2</sub>O<sub>3</sub> was prepared in wire form. Room and elevated-temperature tensile properties were determined as a function of temperature and wire reduction, with the results shown in Table 44.

Severdenko, et al.<sup>(30)</sup> investigated the possibility of intensifying the comminution of oxides in strip rolled directly from Al<sub>2</sub>O<sub>3</sub>-containing nickel powder by subjecting this material to rerolling and the application of ultrasonic vibration. It was concluded that the application of ultrasonic vibrations during rolling intensified the comminution of dispersed oxides making it possible to increase the alloy's strength and ductility at elevated temperatures.



Table 44. Tensile Properties of Ni-0.2Al<sub>2</sub>O<sub>3</sub> Wires<sup>(29)</sup>

Wire Diam., mm	Reduc- tion, %	Tensile Strength, MPa				Yield Strength, MPa As Drawn	Elongation, %			
		As Drawn	500 C	600 C	700 C		As Drawn	500 C	600 C	700 C
3	35	637	392	382	382	637	5.3	41	39	38
2	55	686	402	402	402	686	5.0	57	59	59
1	75	784	431	421	412	784	4.6	46	42	43

Buchta and Schatt<sup>(31)</sup> tensile tested electrolytically deposited Ni-Al<sub>2</sub>O<sub>3</sub> alloys. For low oxide concentrations, the stress found at 0.2 percent plastic elongation was in good agreement with the Orowan stress. The Fisher mechanism evidently accounted for the hardening process only up to 2 percent deformation. The Ashby model gave the best agreement and could be used from about 2.5 percent deformation upwards.

Broszeit, et al.<sup>(32)</sup> also produced layers of Ni-Al<sub>2</sub>O<sub>3</sub> electrolytically. The hardness of the layers for alloys containing up to 10 percent Al<sub>2</sub>O<sub>3</sub> were determined as were wear test data.

Hancock, et al.<sup>(33)</sup> investigated the work-hardening behavior of Ni-2.5 vol. % Al<sub>2</sub>O<sub>3</sub> alloy to study the influence of matrix stacking-fault energy on plastic instability and ductility. Kulikov, et al.<sup>(34)</sup> investigated alloys of nickel with 1, 3, and 5 percent of  $\alpha$ -Al<sub>2</sub>O<sub>3</sub> and their loss of strength on annealing.

Sergenkova and Berezutskii<sup>(35)</sup> found that an addition of one percent titanium to DS-Ni-Al<sub>2</sub>O<sub>3</sub> markedly inhibited the growth of Al<sub>2</sub>O<sub>3</sub>. In a previous paper, Sergenkova<sup>(36)</sup> had reported that on the basis of metallographic examination the Al<sub>2</sub>O<sub>3</sub> particles started to grow on annealing at 1000 C. This growth was slight, but noticeable. The fastest growth started at 1200 C.

Perry and Smallman<sup>(37)</sup> studied the effect of heating a Ni-2.5 vol. % Al<sub>2</sub>O<sub>3</sub> 0.1 weight % Mg alloy in vacuo at 1200 C for times up to 225 hours. The magnesium addition was clearly found to increase the growth rate of Al<sub>2</sub>O<sub>3</sub> particles. At 1200 C, there was no apparent tendency for the growth rate to level off even after 225 hours. The results at 1200 C differ from those reported for coarsening at 1300 C where the addition of magnesium initially increased the coarsening rate of Al<sub>2</sub>O<sub>3</sub>. After 16 hours, however, the magnesium almost completely restricted coarsening.<sup>(38)</sup>

Sergenkova, et al.<sup>(39)</sup> have explored the effects of Al<sub>2</sub>O<sub>3</sub>, ZrO<sub>2</sub>, HfO<sub>2</sub>, and SiO<sub>2</sub> in quantities up through 10 vol. % on the hot hardness and stress rupture strength of nickel at temperatures up through 800 C. Of these dispersoids, Al<sub>2</sub>O<sub>3</sub> appeared most effective in improving the stress-rupture life. Figure 63 summarizes these data.

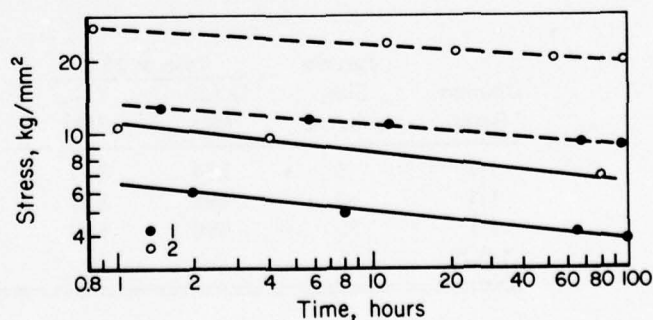


Figure 63. Effects of Al<sub>2</sub>O<sub>3</sub> on the Stress-Rupture Life of Nickel at 600 C (dotted lines) and 800 C (solid lines). 1 = Ni + 3 vol. % Al<sub>2</sub>O<sub>3</sub>, 2 = Ni + 10 vol. % Al<sub>2</sub>O<sub>3</sub><sup>(39)</sup>

## Ni-HfO<sub>2</sub> Alloys

Plechev, et al.<sup>(40)</sup> prepared a Ni-2 weight % HfO<sub>2</sub> alloy using carbonyl nickel. The HfO<sub>2</sub> was introduced into the nickel by chemical precipitation from hafnium oxychloride. The blanks were pressed hydrostatically and then sintered in a hydrogen atmosphere at 1100 C. After sintering, the blanks were heated to 1050 C and extruded into rods. The dense material was subjected to cold forging with an overall reduction of 65 percent. Recrystallization annealing was performed for 1 hour in a vacuum of 10<sup>-5</sup> mm of mercury at 1400 C. The mechanical properties at room temperature and 1100 C of this material are given below.

	20 C	1100 C
Tensile Strength, MPa	427	45
0.2% Yield Strength, MPa	178	42
Elongation, %	49.4	4.75

For this alloy, the mechanothermal treatment produced a dislocation structure which is stable up to 0.8 T<sub>m</sub>.

Timofeyeva and coworkers published a series of three papers describing work on DS-Ni-HfO<sub>2</sub> alloys. In the most recent<sup>(41)</sup>, the alloys were produced with nickel powders of 1000-5000 Angstroms containing 3.5 weight % HfO<sub>2</sub> produced by chemical precipitation of the components from aqueous nitrate solutions by (NH<sub>4</sub>)<sub>2</sub>CO<sub>3</sub>, followed by filtration, drying, and heating with selective reduction. The particle size of the HfO<sub>2</sub> was 200-400 Angstroms. The influence of the sintering temperature on the structure and consolidation was studied. It was found that HfO<sub>2</sub> significantly retards the growth rate of nickel grains and the shrinkage during isothermal heating at 1673 K. In another investigation<sup>(42)</sup>, nickel powder was mixed with a master alloy of nickel powder containing up to 20 vol. % HfO<sub>2</sub>, produced by chemical coprecipitation as indicated above. The effect of particle size on the dispersant was investigated using powders of 5, 40, and 70 microns. Dilution ratios of 1.02 to 1.9 were also explored. The strength properties obtained are shown in Table 45. These properties were determined on specimens that had been sintered at temperatures between 800 and 1000 C for 2 hours in hydrogen and after thermomechanical treatment.

Table 45. Mechanical Properties at Various Temperatures of the Alloy Ni + 2 Vol. % HfO<sub>2</sub> Produced by Dilution<sup>(42)</sup>

Dilution Ratio	Particle Size, microns	Tests at 20 C		Tests at 1100 C			
		U.T.S., MPa	Y.S., MPa	U.T.S., MPa	Y.S., MPa	U.T.S., MPa	Y.S., MPa
				Without Annealing		Annealing 1200 C for 2 Hours	
1:1	5	564	541	98	87	100	88
1:1	40	595	557	74	62	73	61
1:1	70	566	539	73	—	78	73
1:0.75	5	—	—	91	78	92	—

It is typical of DS-Ni produced by dilution that over a fairly wide dilution range, annealing at 1200 C causes very little change in mechanical strength at 1100 C. This indicates the great structural stability of the cold-deformed alloy.

In the third study, Timofeyeva<sup>(43)</sup> investigated the behavior of HfO<sub>2</sub> particles in nickel during isothermal annealing. The alloy investigated contained 3.5 vol. % HfO<sub>2</sub>. The average particle sizes of

nickel tested were 0.075, 0.350, and 0.550 micron, and, of  $\text{HfO}_2$ , 0.5, 1.6, and 3.5 microns. It was found that after prolonged isothermal annealing, in particular at 1300 C, recrystallization occurred that was more complete the higher the nonuniformity and the more evenly the  $\text{HfO}_2$  particles were dispersed.

Portnoy, et al.<sup>(44)</sup> investigated Ni- $\text{HfO}_2$  alloys containing 1-4 percent  $\text{HfO}_2$ . After sintering, samples were extruded to a ratio of 25:1. Stress-rupture data for these materials are reproduced in Figure 64. The authors concluded that the concentration of dispersoid may be changed within fairly broad limits without substantially changing the long-term strength at high temperatures.

Babich, et al.<sup>(45)</sup> obtained the mechanical properties shown in Table 46 for a DS-Ni-2.5 $\text{HfO}_2$  alloy which was cold drawn 80 percent and annealed for 1 hour at 1400 C. Raising the compact sintering temperature reduced not only the high-temperature tensile and yield strength of the rods, but also their long-time strength. Thus, over the sintering temperature range 800-1200 C, the value of the stress to rupture in 100 hours at 1100 C fell from 8 to 6.5 kg/mm<sup>2</sup> (78 to 64 MPa), while at a sintering temperature of 1300 C the 100-hour strength of cold-drawn and annealed rods at 1100 C did not exceed 4.5 kg/mm<sup>2</sup> (44 MPa).

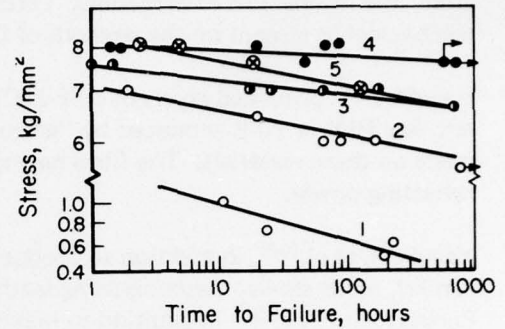


Figure 64. Variation of Stress-Rupture Time for Pure Nickel and Its Alloys with Hafnium Dioxide at 1100 C. 1) Pure Nickel; 2) with 1.15 $\text{HfO}_2$ ; 3) 2.2 $\text{HfO}_2$ ; 4) 3.15 $\text{HfO}_2$ ; 5) 4.10 $\text{HfO}_2$ <sup>(44)</sup>

Table 46. Mechanical Properties of Ni-2.5 $\text{HfO}_2$  Rods After Cold Drawing and Annealing<sup>(45)</sup>

Sintering Temp., C	At 20 C						At 1100 C					
	Y.S.		U.T.S.		Elong., %	R. in Area, %	Y.S.		U.T.S.		Elong., %	R. in Area, %
	kg/mm <sup>2</sup>	MPa	kg/mm <sup>2</sup>	MPa			kg/mm <sup>2</sup>	MPa	kg/mm <sup>2</sup>	MPa		
800	35.2	345	54.6	535	21	63	11.1	109	11.7	115	7	13
1000	32.0	314	51.4	504	23.5	58	10.3	101	10.8	106	8	14.5
1200	27.1	265	49.2	482	26	54	9.9	97	10.7	105	11	16
1300	18.7	183	46.6	457	38.5	56	—	—	8.2	80	11	11

Yagubets, et al.<sup>(46)</sup> produced plates of DS-Ni-1.8 $\text{HfO}_2$  by electrolytic deposition of plates, assembly of plates into packets followed by diffusion welding (by rolling), and annealing to achieve degassing. The properties of the material produced are listed in Table 47. This paper includes a detailed discussion of the factors which influence the strength characteristics of electrochemically-produced, dispersion-strengthened metals.

Table 47. Some Properties of Nickel Containing Hafnium Dioxide Particles<sup>(48)</sup>

Material	Ultimate Tensile Strength				Hardness	
	20 C		1100 C		kg/mm <sup>2</sup>	MPa
	kg/mm <sup>2</sup>	MPa	kg/mm <sup>2</sup>	MPa		
Nickel (0.1 mm foil)	30	294	—	—	110	1078
Nickel with 1.8% $\text{HfO}_2$ (electrolysis)	59.5	583	—	—	199	1950
Nickel with 1.8% $\text{HfO}_2$ (rolled and annealed at 1200 C for 2 hours)	35	343	2.8	27	—	—



## Other Dispersoids In Unalloyed Nickel

Sastry and Vasu<sup>(47)</sup> investigated the low-temperature deformation behavior of DS-Ni 4 vol. % ZrO<sub>2</sub> to study the mechanism of hardening. Later Denisenko, et al.<sup>(48)</sup> investigated the effect of thermo-mechanical treatment on the strength of DS-Ni-ZrO<sub>2</sub>.

Gawrilov<sup>(49)</sup> produced layers of Ni-P-ZrO<sub>2</sub> and Ni-B-ZrO<sub>2</sub> by "chemical" deposition where the dispersant was Ni-P or Ni-B produced by "electroless" deposition. Some corrosion and oxidation tests were made on these materials. The films having 1 to 2 g/l of the P-ZrO<sub>2</sub> in the suspension showed superior reflecting power.

Yagubets, et al.<sup>(46)</sup>, in addition to producing electrochemical composites of DS-Ni-HfO<sub>2</sub> (as described earlier), made similar materials using lanthanum chromite and Pr<sub>2</sub>Zr<sub>2</sub>O<sub>7</sub> as the dispersoid. Similarly, Portnoy, in 1971,<sup>(50)</sup> in addition to making DS-nickel alloys with ThO<sub>2</sub>, Al<sub>2</sub>O<sub>3</sub>, and HfO<sub>2</sub>, also made alloys containing 3 percent ZrO<sub>2</sub> and 3 percent TiO<sub>2</sub>.

Schafer, et al.<sup>(51)</sup> investigated DS-Ni-MgO alloys using nickel powders of 1, 0.4, 0.2 micron average particle size in combination with 0.05 micron MgO powder. The mixtures were vacuum hot pressed and extruded at 1050 C. There was a general tendency toward oxide-particle growth during processing. A small amount of oxide (7 to 10 percent) considerably improved the 980 C stress-rupture strength, but further oxide additions (12 to 28 percent) resulted in a decrease in strength.

Arias<sup>(15)</sup> used nonreactive milling to produce a Ni-1.8 vol. % Y<sub>2</sub>O<sub>3</sub> alloy whose average tensile properties at 1093 C (2000 F) were as follows:

Ultimate Strength		Yield Strength		Elongation, percent
ksi	MPa	ksi	MPa	
19.3	133.3	17.7	122.1	3.1

DS-Ni-BeO alloys produced by powder-metallurgy techniques were investigated by Grewal, et al.<sup>(52)</sup>. The investigation was undertaken to gain a better understanding of the relationship between the structural changes brought about by various thermomechanical treatments in a Ni-1 vol. % BeO alloy and the accompanying changes in high-temperature properties. The authors concluded that the thermo-mechanical treatments were beneficial to both room- and elevated-temperature properties. Whereas cold work following extrusion is generally beneficial to high-temperature, creep-rupture strength, intermediate annealing can further improve strength. There is an optimum annealing temperature that must depend on the structure of the particular alloy. Whereas cold work modifies the total structure, with decreasing benefits at room temperature beyond about 30 percent further reduction, it can continue to improve the 982 C strength to much higher deformation.

The use of intermediate annealing treatments on top of cold work significantly modifies the dislocation density and distribution and substructural arrays without any visible change in the grain aspect ratio (GAR). The authors feel that this clearly demonstrates that the GAR is not the primary structural variable controlling high-temperature strength.

Kaufman<sup>(53)</sup> explored the use of splat cooling to dispersion strengthen nickel. His search for suitable dispersoids did not lead to any substance having as good particle size stability as ThO<sub>2</sub>. Thus, various high-melting borides were not chemically stable in nickel. Also, the refractory carbides of titanium, zirconium, hafnium, columbium, and tantalum, in submicron size, grew rapidly at temperatures as low as 900 C. TaC appears to have the best size stability. Th<sub>2</sub>Ni<sub>17</sub>, Y<sub>2</sub>Ni<sub>17</sub> have about the same size stability as TaC even though they have a much lower solid solubility in nickel than TaC. Substantial



hardening was also observed at lower temperatures of the alloys with TaC, Th<sub>2</sub>Ni<sub>17</sub>, and Y<sub>2</sub>Ni<sub>17</sub>. However, this strength dropped rapidly above 500 C. Some dispersion hardening was exhibited by the alloys containing 5 vol. % TaC, 1 weight % Th, and 15 vol. % Y<sub>2</sub>Ni<sub>17</sub>, but their strength at 900 C was not as good as that of TD-Ni. A splat-cooled alloy of 20 vol. % Th<sub>2</sub>Ni<sub>17</sub> was internally oxidized at 500 C to form 6.5 vol. % ThO<sub>2</sub>. This material contained submicron sized particles and showed a variation of strength with increasing temperature comparable to that of TD-Ni.

Thibaudon, et al.<sup>(54)</sup> prepared dispersions of refractory carbides (Cr<sub>3</sub>C<sub>2</sub>, TiC, VC, TiO<sub>x</sub>, V<sub>2</sub>O<sub>3</sub>) and nitrides in nickel. A gas-solid reaction was used in conjunction with mixtures of H<sub>2</sub>-CH<sub>4</sub> or H<sub>2</sub>-NH<sub>3</sub> to reduce and carburize, or reduce and nitride, respectively, the raw materials. Through the use of high-quality starting materials, the authors believe it is possible to obtain products that are characterized by a very homogeneous distribution of the dispersoid in the matrix.

Rudio, et al.<sup>(56)</sup> developed a technique for manufacturing extruded rods containing dispersions of glass particle mixtures. Four groups of these were prepared as listed below:

Group	Glass Compositions Represented
I	SiO <sub>2</sub> , Al <sub>2</sub> O <sub>3</sub> , MgO, TiO <sub>2</sub> , CeO <sub>3</sub>
II	SiO <sub>2</sub> , Al <sub>2</sub> O <sub>3</sub> , B <sub>2</sub> O <sub>3</sub> , PbO
III	SiO <sub>2</sub> , Al <sub>2</sub> O <sub>3</sub> , Li <sub>2</sub> O, ZrO <sub>2</sub> , CaO, B <sub>2</sub> O <sub>3</sub> , PbO, As <sub>2</sub> O <sub>3</sub>
IV	SiO <sub>2</sub> , Al <sub>2</sub> O <sub>3</sub> , CaO, MgO, FeO, Fe <sub>2</sub> O <sub>3</sub> , TiO <sub>2</sub> , Na <sub>2</sub> O, K <sub>2</sub> O

The use of silicate materials which react chemically with nickel substantially increased the specific load, i.e., the stress required to extrude the material. The use of glass rather than graphite lubrication decreased the specific load.

#### DS Ni-M Alloys\*

Cheney, et al.<sup>(14)</sup> prepared Ni-15Mo-ThO<sub>2</sub> sheet with varying volume fractions and sizes of ThO<sub>2</sub>, and investigated the metallurgical conditions affecting the strengths at 1090 C. The yield strengths at 1093 C were: Ni-15Mo = 13.1 ksi (90 MPa); Ni-15Mo-0.03ThO<sub>2</sub> = 13.8 ksi (95 MPa); Ni-15Mo-0.3ThO<sub>2</sub> = 21.3 ksi (147 MPa); and Ni-15Mo-3.0ThO<sub>2</sub> = 23.2 ksi (160 MPa). Ultimate strengths were usually within 2-4 ksi (14-28 MPa) of the yield strengths and elongations were 2-6 percent. The stress-rupture data of the above materials are given in Table 48.

Table 48. Stress-Rupture Properties of Ni-15Mo-ThO<sub>2</sub> Sheet<sup>(14)</sup>

Material	Stress		Rupture Time, hrs	Elongation, %
	ksi	MPa		
Ni-15Mo-0.3ThO <sub>2</sub>	16	110	0.05	5
Ni-15Mo-0.3ThO <sub>2</sub>	12	83	0.30	6
Ni-15Mo-0.3ThO <sub>2</sub>	9	62	11.7	3
Ni-15Mo-0.3ThO <sub>2</sub>	7	48	128.8	4
Ni-15Mo-3ThO <sub>2</sub>	12	83	467.9	—
Ni-15Mo-3ThO <sub>2</sub>	14	96	58.6	—

\* M designates metals other than chromium.

In a previous paper<sup>(56)</sup>, a Ni-15Mo-4ThO<sub>2</sub> alloy had been investigated. The strength of the alloys Ni-15Mo and Ni-15Mo-4ThO<sub>2</sub> was reported good at room temperature [150 ksi (1034 MPa)]. The molybdenum strengthens the alloy to at least 760 C. Strengths at higher temperatures were at least equivalent to those of TD-Ni. Excessive cold working with no intermediate anneals lowered the ultimate tensile strength of the alloy at 980 C from 18 ksi (124 MPa) to about 3 ksi (21 MPa). Repeated cold deformation followed by intermediate anneals at 1200 C increased the strength at 980 C to at least 21 ksi (145 MPa).

Walsh and Donachie<sup>(57)</sup> investigated the interdiffusion between TD-Ni and W. A large Kirkendall effect in TD-Ni/W diffusion couples indicated that nickel is the more rapidly moving species.

Hancock, et al.<sup>(58)</sup> studied the creep behavior of Ni-30Co-2.5Al<sub>2</sub>O<sub>3</sub> alloys in the temperature region between 770 and 1000 K.

Glasgow<sup>(59)</sup> produced a complex ODS alloy, WAZ-D, by mechanical alloying. This alloy was compared with cast WAZ-20 which is strengthened by both a high, refractory-metal content and 70 vol. % of gamma prime. The composition of the alloys tested are given in Table 49. The ODS-WAZ-D alloy was responsive to variables of alloy content, of attritor processing, of consolidation by extrusion, and of heat treatment. The best material produced had large, highly elongated grains. It exhibited strengths generally superior both to comparable cast and directionally solidified alloys as illustrated in Table 50. The ODS alloy also exhibited high-temperature, stress-rupture life considerably superior to any known cast superalloy. For example, its rupture life in vacuum at 1150 C under a stress of 102 MPa was approximately 1000 hours. Tensile and rupture ductility were low as was intermediate-temperature rupture life. Very low creep rates were noted and some specimens failed with essentially no third-stage creep. Comparison of ODS-WAZ-D to the conventionally cast WAZ-20 and to directionally solidified WAZ-20 indicates that oxide-dispersion strengthening may be beneficially added to even the strongest of superalloy compositions.

Table 49. Composition of Complex Nickel-Base Alloys<sup>(59)</sup>

Alloy	Ni	W	Al	Fe	Zr	B	C	O	N	Y
WAZ-D (17W)	Bal	16.6	7.3	4.3	0.6 <sup>1</sup>	N.D. <sup>2</sup>	0.05	0.56 <sup>3</sup>	0.09	0.8
WAZ-D (8W)	Bal	7.7	6.8	4.5	0.5 <sup>1</sup>	N.D. <sup>2</sup>	0.08	0.51 <sup>3</sup>	0.02	0.8
WAZ-20	Bal	18	6.0	—	1.5	0.0003	0.11	—	—	—

1. Analysis believed in error; added Zr was 0.95%.

2. Not determined, 0.015 added.

3. For 3.5 ml/min O<sub>2</sub>, 40-hour runs.

**Table 50. Results of Tensile Tests of Large, Elongated-Grain, ODS-WAZ-D (17W) and Comparable Data For Cast WAZ-20<sup>(59)</sup>**

Temp., C	Ultimate Tensile Strength		Reduction in Area, %	Elong. %
	ksi	MPa		
<u>ODS-WAZ-D (17W)</u>				
RT	228	1572	3	7
RT	227	1565	3	5
760	131	903	2	1
1095	42	290	2	2
1205	32	221	2	3
1260	18	124	0	1
1315	12	80	0	1
<u>WAZ-20, Conventionally Cast</u>				
RT	108	745	—	4
760	109	752	—	4
1095	44	303	—	4
1205	20	138	—	5
<u>WAZ-20, Directionally Solidified</u>				
RT	130	896	—	13
760	120	827	—	4
1095	44	303	—	12
1205	20	138	—	8

## Ni-Cr Alloys

### Experimental Ni-Cr-ThO<sub>2</sub> Alloys

Marty, et al.<sup>(60)</sup> described the production of dispersion-strengthened Ni-Cr alloys by mixing the chromium powder mechanically with Ni-ThO<sub>2</sub> powder. The sintering-diffusion process was carried out in a halogen-hydrogen atmosphere at a temperature range of 900-1200 C. This yielded a very porous Ni-Cr-ThO<sub>2</sub> alloy which had to be densified by extrusion. Thermomechanical treatment must follow to ensure good mechanical properties at high temperatures.

Wilcox, et al.<sup>(61)</sup> studied the creep behavior over the range 700-1100 C on three Ni-Cr-1 vol. % ThO<sub>2</sub> base alloys that contained 13.5, 22.6, and 33.7 weight % chromium, respectively. Similarly, Arunachalam and Lippett<sup>(62)</sup> investigated stress relaxation in nickel-chromium alloys containing 20 to 34 percent chromium and 1 to 2 percent ThO<sub>2</sub>. Their results fit well with the assumption that more than a single rate-controlling mechanism is operating in this alloy system.

Lund and Nix<sup>(63)</sup> investigated the high-temperature creep of single crystal ODS Ni-Cr and concluded that creep is controlled by self-diffusion, as for the case of pure metals and solid solutions. The ductility of the single crystals was much greater than that for polycrystals. At very high temperatures ( $\geq 1200$  C), the solubility of ThO<sub>2</sub> in Ni-20Cr is sufficient to cause a significant decrease in the creep resistance of the material.



On the basis of these and earlier similar studies, it was quickly decided that a chromium content of about 20 percent was near optimum for dispersion-strengthened, nickel-base alloys. In the case of the nickel-thoria system, the Ni-20Cr-2 vol. % ThO<sub>2</sub> alloy not only shows much superior oxidation resistance but also much higher mechanical properties at elevated temperatures than for the Ni-2 vol. % ThO<sub>2</sub> alloy.

#### Commercial Ni-20Cr-2ThO<sub>2</sub> Alloys

As noted earlier, two commercial Ni-20Cr-2ThO<sub>2</sub> alloys were developed in the early 1960's. The first of these was the TD-NiCr alloy developed by du Pont (later assigned to Fansteel, then Stellite) and the other was Sheritt Gordon's DS-NiCr alloy.

From the outset, great interest was shown in this material, particularly as a sheet alloy aimed at high-temperature applications. NASA was quick to recognize the potential of this alloy as a skin material for its Space Shuttle vehicle and supported much of the sheet development work. For TD-NiCr, a combination of powder-metallurgy techniques and thermomechanical processing was used.<sup>(64)</sup> For DS-NiCr, pack chromizing of thin Ni-2ThO<sub>2</sub> sheet was selected.<sup>(65)</sup> Extensive data were ultimately reported<sup>(66)</sup> on the tensile properties (for both longitudinal and transverse directions) of several sizes of TD-NiCr sheets (0.010- to 0.060-in. thick). Poisson's ratio was reported as 0.333 for longitudinal and 0.338 for the transverse directions. The modulus of elasticity was given as  $24 \times 10^6$  psi ( $165.36 \times 10^6$  MPa) at room temperature and  $4 \times 10^6$  psi ( $27.56 \times 10^6$  MPa) at 1315 C. Fatigue, creep, and stress-rupture properties were also determined. Little or no creep strain was evident until a critical stress level was applied. Then nonlinearity of creep strain versus stress was observed for a given time increment, probably the result of grain-boundary damage. Data were also obtained on linear thermal expansion, thermal conductivity, specific heat, and total hemispherical emittance. This evaluation, in addition to the above property characterization, also included sheet manufacture<sup>(67)</sup> forming and joining.<sup>(68)</sup>

Bearing strength, sharp notch, thermal diffusivity, and electrical resistivity were also determined in another study.<sup>(69)</sup>

Kane, et al.<sup>(70)</sup> investigated the recrystallization characteristics and the elevated-temperature mechanical properties of TD-Ni and TD-NiCr. They also developed a satisfactory etching technique for these materials. A thermal-oxidation etch gave good detail of grain boundaries over the entire range of grain sizes of the TD-NiCr produced (0.001 to 0.5 mm). No microstructural changes were found as result of this thermal etching technique.

Wilson, et al.<sup>(71)</sup> conducted tensile and creep-rupture tests for smooth and sharp edge-notched specimens of 0.38-mm-thick TD-NiCr sheet at 538 to 982 C with the results shown in Figure 65. Plotting stress versus minimum creep rate showed that the mechanism controlling creep changes between 538-650 C.

Murr<sup>(25)</sup> compared the substructures and properties of TD-NiCr with other material following explosive-shock deformation. No evidence of deformation twinning was observed in the TD-NiCr microstructure because of the inhibition afforded by the ThO<sub>2</sub> particle distribution in the annealed material.

Ansell<sup>(24)</sup> investigated the role of process history, phase morphology, and interface strength upon the mechanical properties of TD-NiCr. Using a thermal-shock method, the bond strength in TD-NiCr was quantitatively measured and found to be approximately four times that for TD-Ni. Thermal shock caused a significant drop in the room-temperature yield strength of TD-NiCr.



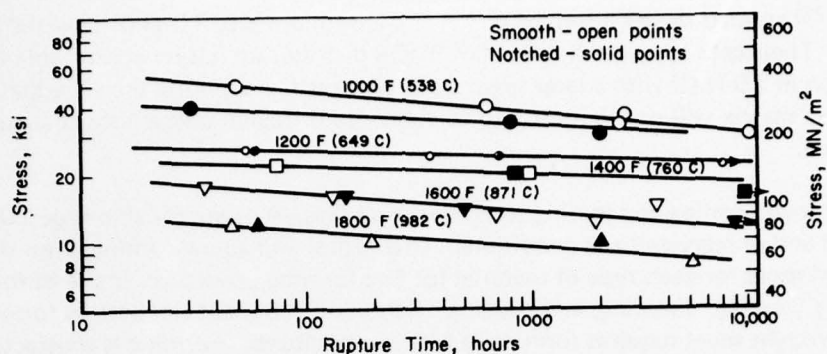


Figure 65. Stress Versus Rupture-Time Data at Temperatures From 1000 to 1800 F (538-982 C) Obtained From Smooth and Notched Specimens of 0.015-in. (0.38 mm) Thick, Stress-Relieved, TD-NiCr Sheet<sup>(71)</sup>

Wittenberger<sup>(72)</sup> correlated the mechanical properties for thin TD-NiCr sheet with the structural characteristics of the material. Emphasis was placed on tensile stress-rupture and creep behavior as related to microstructure and sheet thickness. Measurements of the mechanical properties of two heats of 0.051-cm thick and two heats of 0.025-cm thick TD-NiCr sheet indicated that elevated-temperature tensile, stress-rupture, and creep strength are primarily dependent on grain aspect ratio (GAR) and sheet thickness. In general, it was found that the strength properties increased with increasing GAR and increasing sheet thickness. Grain size for TD-NiCr sheet with an average grain size between 100 and 300 microns did not appear to be an important strength factor at elevated temperatures.

This study of TD-NiCr sheet also revealed that: 1) the thin sheet apparently has nil tensile ductility at elevated temperatures, 2) even very small amounts of prior creep deformation (0.1 percent) at elevated temperatures (1144 K) can produce severe creep damage which is responsible for the low residual tensile properties, and 3) there appears to be a threshold stress for creep.

Raymond and Neumann<sup>(73)</sup> investigated the high-temperature stability of ThO<sub>2</sub> in TD-NiCr made by du Pont and ODS-Ni-20Cr-2ThO<sub>2</sub> made by the Curtiss Wright Corporation. It was found that both materials were structurally stable up to 980 C. However, only the former material was unaffected by 1-hour anneals up to 1315 C as manifested by the retention of the room-temperature hardness and the (100) fiber texture.

Allen<sup>(74)</sup> developed a solid-state, crystal-growing process, which is capable of producing either columnar-oriented crystals or monocrystals from as-extruded TD-NiCr. Stress-rupture testing of columnar-grained bars, in which the (001) planes are perpendicular to the stress axis, indicated that this material is approximately twice as strong as the same as-extruded product given a conventional, recrystallization heat treatment. Stress-rupture ductilities were also improved to 6-7 percent elongation versus 1-2 percent in conventionally processed bar.

Murr<sup>(26)</sup> investigated the interfacial energetics in TD-NiCr and concluded, as for TD-Ni, that the apparent difference in particle/matrix interfacial strength results from a more complex mechanism than simple interfacial decohesion involving phase separation. Franklin, et al.<sup>(75)</sup> also investigated the particle/matrix interface strength of TD-NiCr. They concluded that the addition of Cr to the Ni matrix in ThO<sub>2</sub> dispersed alloys increases the particle/matrix interface strength thereby reducing or eliminating the strength differential effect. However, rapid heating to 980 C can produce sufficient stress to cause decohesion of the interface thus decreasing the yield stress for short times at temperature after initial heating.

Pawar and Tenney<sup>(76)</sup> studied the diffusion of nickel and chromium into TD-NiCr over the 900-1100 C temperature range. Their data suggests that 2 vol. % ThO<sub>2</sub> distribution has no appreciable effect on the rates of diffusion in TD-NiCr with a large grain size. This further supports the view that an inert dispersoid in an alloy matrix will not in itself lead to enhanced diffusion unless a short-circuit diffusion structure is stabilized.

Torgerson<sup>(77)</sup> developed forming and joining techniques and property data for thin-gage TD-NiCr sheet in the recrystallized and unrecrystallized conditions. Theoretical and actual forming-limit data are presented for several gages for each type of material for five forming processes: brake forming, corrugation forming, joggling, dimpling, and beading. Recrystallized sheet can best be formed at room temperature, but wrought sheet requires forming at high temperatures. Forming is satisfactory with most processes for the longitudinal orientation but poor for the transverse. Dimpling techniques require further development. Data on joining techniques and joint properties were presented for four joining processes: resistance seam welding (solid state), resistance spot welding (solid state), resistance spot welding (fusion), and brazing. Resistance seam welded (solid state) joints with 5t (i.e., five times the sheet thickness) overlap were stronger than parent material for both material conditions when tested in tensile-shear and stress rupture. Brazing studies resulted in development of the NASA 18 braze alloy (Ni-16Cr-15Mo-8Al-4Si) with several properties superior to baseline TD-6 braze alloy including lower brazing temperature, reduced reaction with TD-NiCr, and higher stress-rupture properties.

Moore<sup>(78)</sup>, by using specially processed TD-NiCr sheet in both 0.4-mm and 1.6-mm thicknesses and carefully selected welding procedures, produced solid-state, resistance spot welds which, after post-heating at 1200 C, were indistinguishable from the parent metal. Stress-rupture shear tests of single-spot lap joints in 0.4-mm sheet showed that these welds were as strong as the parent material. Similar results were obtained in tensile-shear tests at room temperature and 1100 C and in fatigue tests. Conventional fusion spot welds in commercial sheet were unsatisfactory because of poor stress-rupture shear properties resulting from metallurgical damage to the parent metal.

Holko<sup>(79)</sup> reported on an improved diffusion-welding technique. In the most preferred form, it consists of diffusion welding 320-grit-sanded-plus-chemically-polished surfaces of unrecrystallized TD-NiCr at 760 C under 140 MPa pressure for 1 hour followed by post heating at 1180 C for 2 hours. Compared to previous work, this improved technique is claimed to have the advantages of shorter welding time, lower welding temperature, lower welding pressure, and a simpler and more reproducible surface-preparation procedure. Weldments were made that had parent-metal, creep-rupture, shear strength at 1100 C.

Holko and Moore<sup>(80)</sup> also described a vacuum-hot-press welding procedure to produce lap welds. The best preweld surface preparation procedure involved sanding with 600-grit paper and subsequent electropolishing. A two-step weld cycle was found to work best consisting of 207 MPa and 705 C for 1 hour; and 15 MPa and 1190 C for 2 hours.

Metcalf<sup>(81)</sup> proposed joining of TD-NiCr sheet by Solar's continuous-seam, diffusion-bonding process, but structural instability limited stress-rupture life.

Kenyon and Hrubec<sup>(82)</sup> examined 13 brazing alloys, some commercial and some experimental. Brazing was carried out in dry hydrogen and in vacuum. It was found that brazed joints with 1050 C tensile strengths corresponding to approximately 80 percent of base-metal strength can be made with the brazing alloys tested.

While most of the developmental effort on the DS-Ni-Cr alloys concerned sheet product, some attention was also given to other wrought products. Filippi<sup>(83)</sup>, for example, carried out an extensive study on forged TD-NiCr. The high-temperature tensile and stress-rupture properties were evaluated and related to thermomechanical variables and microstructure on 0.38-cm-thick, channel-die-forged plates. Forging temperature and final annealed condition had pronounced influences on grain size which, in turn, was related to high-temperature properties. Conditions which served to optimize high-temperature strength were:

1. Forging in the temperature range of 1255 to 1475 K followed by annealing at 1615 K
2. An increase of total forging reduction
3. Forging to continue the deformation inherent in the starting material
4. A low forging speed, and
5. Prior deformation by extrusion.

The author concludes that the results demonstrated that the mechanical properties of TD-NiCr sheet developed for space-shuttle applications can be achieved in forged material. It was believed that further improvement of optimally forged material might possibly be increased further by shock treatment.

Roach and Wolf<sup>(84)</sup> determined the effect of manufacturing variables on the strength of TD-NiCr fasteners. No manufacturing sequence prevented head failure in forged tension bolts. However, shear fasteners were produced that did not demonstrate a head-critical condition and possessed the anticipated optimum shear properties.

Barnett and Bailey<sup>(85)</sup> produced TD-NiCr tubing by extrusion using filled-billet techniques of dense hollows to near target size. After a recrystallization heat treatment, these were then cold finished by drawing.

Recently, Johnson and Kilpatrick<sup>(86)</sup> summarized the results obtained in the space-shuttle program to evaluate ODS-Ni-base alloys for use in the metallic, radiative, thermal-protection system operating at surface temperatures to 1205 C (2200 F). TD Ni-20Cr characteristics of material used in this study were compared with TD-Ni-Cr produced in previous development effort. Cyclic load, temperature, and pressure effects, as well as residual strength, were investigated. The effects of braze reinforcement in improving the efficiency of spot-welded joints were evaluated on joint samples and through simulated mission tests. Initial tests of subsize, heat-shield panels included simulated meteoroid-impact tests. It was found that properties of the TD Ni-20Cr sheet material used in this program were similar to those of previous quantities of TD Ni-20Cr with the exception that lower tensile elongation at failure was observed from tests of sheet used in this program for test temperatures of 650 C and higher. Degradation of tensile properties resulting from a programmed cycle of stress, temperature, and low environmental air pressure were more pronounced in the long transverse direction than in the longitudinal (rolling) direction. Observed tensile-strength degradations did not significantly affect heat-shield weights because compressive buckling stresses in the thin-gage panels were critical for design strength. Braze-reinforcement of spot-welded, seam-welded, or diffusion-bonded joints provided significant improvement in fatigue, stress-rupture, and short-time joint strengths.

#### Other Ni-Cr Alloys

Antsiferov and Sal'nikov<sup>(87)</sup> investigated the recrystallization of a DS-Ni-20Cr-3ZrO<sub>2</sub> alloy. They observed that the beginning of recrystallization temperature after a 30 percent plastic deformation was lowered.



Antsiferov, et al.<sup>(88)</sup> also determined the behavior of  $ZrO_2$  and  $Al_2O_3$  particles in an 80Ni-20Cr matrix and grain growth of the matrix on annealing at 900 and 1150 C. With increasing duration of annealing, a metallographically visible growth of recrystallization nuclei begins, resulting in a coarsening of fine particles of the dispersoid. Annealing in air as opposed to hydrogen produces less coarsening of the dispersoid. These same workers also published two other papers<sup>(89,90)</sup> describing the effects of processing on the elevated-temperature strength properties of alloys made by adding  $Al_2O_3$  or  $ZrO_2$ , in amounts up to 8 weight %, to a Ni-20Cr ("Nichrome" base). Representative tensile properties for some of these alloys in an as-extruded condition are given in Table 51.

Table 51. Tensile Properties of Extruded Ni-20Cr- $Al_2O_3$  and Ni-20Cr- $ZrO_2$  Alloys<sup>(89)</sup>

Alloy No.	Oxide, wt. %	Relative Density, %	Testing Temperature, C					
			20			800		
			U.T.S.	Elong., %	U.T.S.	Elong., %	U.T.S.	Elong., %
			kg/mm <sup>2</sup>		kg/mm <sup>2</sup>		kg/mm <sup>2</sup>	
1	Nichrome	98.5	72.7	13.6	34.1	11.2	334	11.2
2	1% $Al_2O_3$	97.8	59.6	5.2	36.7	8.0	360	8.0
3	2% $Al_2O_3$	96.9	64.5	12.0	33.2	6.0	325	6.0
4	3% $Al_2O_3$	96.3	60.6	5.6	30.0	5.4	294	5.4
5	4% $Al_2O_3$	97.5	54.8	0.8	31.3	4.0	307	4.0
6	8% $Al_2O_3$	98.2	33.0	0.0	24.8	4.8	243	4.8
7	1% $ZrO_2$	98.5	66.1	9.2	35.6	10.0	349	10.0
8	2% $ZrO_2$	97.0	59	3.6	37.8	8.0	370	8.0
9	3% $ZrO_2$	99.0	64.9	6.8	36.7	8.4	360	8.4
10	4% $ZrO_2$	98.2	62.6	4.4	32.7	2.8	320	2.8
11	8% $ZrO_2$	97.0	40.0	0.4	26.0	1.6	255	1.6

Bunshah<sup>(91)</sup> has described the use of a high-rate, physical, vapor-deposition process to synthesize alloys corresponding to the Ni-20Cr- $Y_2O_3$  and Ni-20Cr-TiC compositions.

Meerson, et al.<sup>(92)</sup> observed that the introduction of  $HfO_2$  slows down the increase in density with rise in pressure for mixtures of nickel and chromium powders.

Timbres and Norris<sup>(93)</sup> reported on the investigation of Ni-Cr-Mo- $ThO_2$  and Ni-Cr-W- $ThO_2$  alloys. The purpose was to solution strengthen the dispersant. Increases in tungsten content up to 25 percent increased the low-temperature strength but decreased the strength at 1095 C. Changes in strength level were correlated with the grain size in the wrought alloys and it was concluded that the strength of the alloys was controlled more by microstructural factors than by contributions from solid-solution strengthening. A similar pattern appeared to exist with Ni-Cr-Mo- $ThO_2$  alloys.

### Ni-Cr-Al Alloys

The DS-Ni-Cr-Al alloys represent a third generation of dispersion-strengthened nickel alloys. The first two generations, represented by DS-Ni and DS-NiCr alloys with  $ThO_2$  as the dispersoid, possessed good mechanical properties but their resistance to high-temperature, dynamic oxidation was limited. The third generation sought to overcome this deficiency, primarily by the addition of aluminum. The addition of aluminum, however, complicates the response of these materials to thermomechanical processing and makes it more difficult to obtain the required mechanical properties.



Fansteel, then Stellite, as well as Sherritt Gordon, have worked on Ni-Cr-Al-ThO<sub>2</sub> alloys since the late 1960's. In some of the earlier work, Timbres and Norris<sup>(93)</sup> subjected a Ni-16Cr-5Al-2ThO<sub>2</sub> alloy to a series of thermomechanical-processing studies to optimize its mechanical properties. A reproducible process was defined that yielded the desired, coarse-grain microstructure and fine, dispersoid size in wrought strip. This process included roll consolidating powder compacts at 1095 C followed by rolling (in a series of 10 percent reductions to a total reduction of 77 percent) at 1205 C, and annealing at 1315 C. The short-time tensile properties at room temperature and 1095 C in the longitudinal and transverse direction were similar (130 ksi and 13 ksi, or 896 MPa and 90 MPa, respectively) but the transverse, stress-rupture and room-temperature ductility properties were lower than those in the longitudinal direction. All properties with the exception of room-temperature ductility were above the target specifications for the program. Substitution of prealloyed powders for blended elemental powders in preparing the alloys was not successful due to poor powder compactability and to high oxide content.

Gangler<sup>(94)</sup>, in discussing new materials in the aerospace industry, described two candidate alloys developed for heat-shield applications. These were Ni-16Cr-3.5Al-2ThO<sub>2</sub> and Ni-16Cr-5.0Al-2ThO<sub>2</sub>. The lower aluminum level appeared to provide the optimum combination of oxidation resistance, ductility, and strength for the space-shuttle heat shield. The higher, 5-percent aluminum level was believed more desirable to provide oxidation protection for longer times for such applications as gas turbines. Typical strength properties of the high-aluminum version are compared with those for the DS-Ni-20Cr-2ThO<sub>2</sub> alloy in Table 52. At 1093 C they are quite similar.

Table 52. Typical Properties for ODS NiCr & ODS NiCrAl Sheet<sup>(94)</sup>

Property	ODS NiCrAl (Ni-16Cr-5Al+2ThO <sub>2</sub> )		ODS NiCr (Ni-20Cr+2ThO <sub>2</sub> )	
	MPa	ksi	MPa	ksi
U.T.S., R.T.	700	110	900	130
Y.S., R.T.	550	80	690	100
U.T.S., 1336 K (1093 C)	110-120	16-18	110-120	16-18
100-Hour Stress	60	8	60	8
Rupture at 1336 K (1093 C)				

Klarstrom and Grierson<sup>(95)</sup> investigated the optimum alloy composition, in terms of gas-turbine-vane applications, within the Ni-16Cr-Al-Y<sub>2</sub>O<sub>3</sub> system to produce extruded vane blanks. The primary objectives of the program were:

- High-temperature strength - stress for a 100-hour life at 1366 K of 82.7 MPa parallel to the extrusion direction and 4.4 MPa in the long transverse direction
- Oxidation resistance - less than 0.076 mm metal recession after 500-hour exposure to high-velocity gas (Mach 1) at 1366 K under cyclic test conditions
- Crystal texture - low-modulus texture with the <100> crystallographic direction parallel to the extrusion direction
- Ductility - minimum of 5 percent tensile elongation at 1366 K
- Fabricability - alloy powder directly extrudable to vane blank or shape
- Stability - dispersoid stability comparable to commercial Ni-Cr-ThO<sub>2</sub> alloys
- Melting point - >1630 K.

The primary parameter used to define the optimum composition was the materials' dynamic oxidation resistance. This investigation resulted in an alloy, Ni-16Cr-4.75Al-1.8Y<sub>2</sub>O<sub>3</sub>, with excellent resistance

to dynamic oxidation plus low susceptibility to thermal fatigue cracking at and above 1644 K. To obtain complete recrystallization, samples were heated from 1477 to 1616 K over a period of 2 hours, held for 1 hour at the maximum temperature, and then cooled. Two experimental heats containing nominal additions of 0.9 and 1.8 percent tantalum for control of carbide formation were also produced and extruded. Modulus values were in the desired low range ( $\sim 137,900$  MPa, or  $20 \times 10^6$  psi) for the two tantalum-free extrusions and unacceptably high ( $\sim 200,000$  MPa, or  $29 \times 10^6$  psi) for the two tantalum-containing extrusions. Results of longitudinal tensile test for the optimized alloy are given in Table 53, and stress-rupture data in Table 54. It was concluded that the scaled-up, tantalum-free extrusions have properties that either exceed or are close to the target properties. However, further optimization of oxide level and heat treatment appears to be necessary. Another topic requiring additional study is the effect of long-time, high-temperature exposure on the alloys' mechanical properties.

**Table 53. Longitudinal Tensile Test Results for Full-Size Extrusions of the Ni-16Cr-4.75Al-1.8Y<sub>2</sub>O<sub>3</sub> Alloy<sup>(95)</sup>**

Extrusion No.	0.2% Y.S.		U.T.S.		Elongation, %	R.A., %
	ksi	MPa	ksi	MPa		
<u>Room Temperature</u>						
AT-262	133.6	921	181.7	1781	5.2	11.9
	129.8	894	166.2	1629	5.2	7.6
AT-264	125.2	863	156.4	1078	5.9	6.5
	124.8	860	162.2	1118	6.2	7.6
<u>1600 F (871 C)</u>						
AT-262	53.3	369	53.3	369	12.2	27.6
	61.2	422	61.2	422	6.8	14.5
AT-264	50.7	349	50.7	349	6.6	16.4
	57.1	393	57.1	393	9.2	21.5
<u>2000 F (1093 C)</u>						
AT-262	16.1	111	16.1	111	6.5	12.4
	15.8	109	15.8	109	6.0	10.5
AT-264	15.5	107	15.5	107	7.6	18.5
	16.0	110	16.0	110	5.6	10.4

**Table 54. 1366 K (2000 F) Stress-Rupture Data for Extrusions of the Ni-16Cr-4.75Al-1.8Y<sub>2</sub>O<sub>3</sub> Alloy<sup>(95)</sup>**

Extrusion No.	Specimen Orientation	Time at Stress to Rupture, Hours/MPa	Elong., %	R.A., %
AT-262	L	100/82.7 + 9.3/89.6	6.5	12.2
	L	73.4/82.7	2.6	3.9
	T	100/34.5 + 0.2/41.4	4.8	3.9
	T	82.7/34.5	4.7	3.5
AT-264	L	100/82.7 + 2.8/89.6	5.9	8.6
	L	6.8/82.7	8.2	14.7
	T	65.5/34.5	4.9	4.3
	T	110.3/34.5	14.5	5.3

Previously, Stellite had evolved Haynes Development Alloy 8077, which had the nominal composition of Ni-16Cr-4Al-1.33 Y<sub>2</sub>O<sub>3</sub>.<sup>(96)</sup> The melting point was >1370 C. Selected tensile properties are shown in Table 55. The bendability was 180 degrees around a mandrel of twice the sheet thickness. The stress-rupture capability at 1095 C with a load of 10 ksi (69 MPa) was more than 20 hours. The texture was (200) in the sheet plane and (100) in the rolling direction. The thermal fatigue resistance of the alloy at 1095 C is compared with that for dispersion-strengthened and commercial superalloys in Figure 66.

Table 55. Tensile Properties of HDA 8077 Alloy<sup>(96)</sup>

Temperature, F		Yield Strength		Ultimate Strength		Elong., %
		ksi	MPa	ksi	MPa	
RT	L	75.1	517	106.1	731	29.3
	T	72.2	497	100.8	695	34.0
1200	L	66.4	457	87.6	604	16.6
	T	64.9	447	80.6	555	16.6
1600	L	26.5	183	35.6	245	13.2
	T	27.1	187	37.9	261	26.7
2000	L	11.7	81	14.1	97	10.8
	T	12.0	83	12.8	88	11.1

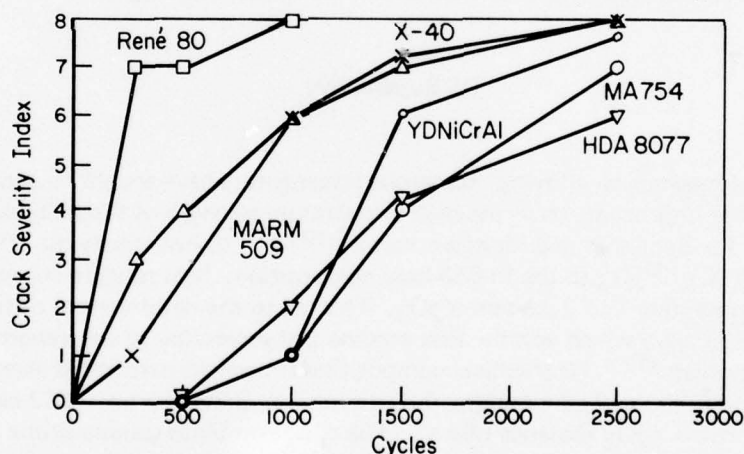


Figure 66. Comparative Performance of Selected Alloys in Thermal Fatigue Resistance Using a 2000 F (1093 C) Wedge-Specimen Test<sup>(96)</sup>

Trela, et al.<sup>(97)</sup> investigated methods of controlling the grain size and grain shape of the "NiCrAlY" Ni-16Cr-4Al-(2-3)Y<sub>2</sub>O<sub>3</sub> alloy, which was found to respond quite differently to thermal and thermo-mechanical processing. Specifically, it was not amenable to the control of grain size and shape by these processes in the same way as are TD-Ni and TD-NiCr. Thus, the NiCrAlY did not recrystallize rapidly and incur immediate abnormal grain growth on annealing, after substantial cold working, as does TD-Ni. Also, it was not amenable to grain-size control by classical nucleation and grain-growth mechanism like TD-NiCr. Rather, the NiCrAlY<sub>2</sub>O<sub>3</sub> appeared to be quite sluggish in its nucleation of new recrystallized grains on annealing following cold working. These new grains usually were fine



and equiaxed. In addition, the NiCrAlY was sluggish in the growth of newly recrystallized grains that form when the cold-worked material is annealed.

Gyorgak<sup>(98)</sup> evaluated the following five braze filler metals for joining TD-NiCrAl:

Designation	Composition, weight percent <sup>(a)</sup>						Flow Temperature, C
	Cr	W	Mo	Si	Al	Fe	
TD-6	15.1	4	15.9	4.5	—	6.1	1265
B-2	19.8	—	30.1	0.6	4.2	—	1288
NASA-18	15.9	—	15.6	4.5	8.6	—	1280
NASA-21	16.4	12.6	—	5.4	7.0	—	1260
NASA-22	15.9	15.5	—	1.9	4.3	—	1320

(a) Balance nickel.

In general, he found all of the alloys to be suitable and tolerant of slight variations in brazing procedures. Brazed butt joints and T-joints prepared by three sources using the filler metals TD-6, B-2, and NASA-18 exhibited essentially equivalent brazing characteristics in terms of braze remelt temperature, reactivity, wettability, and flow. The 1100 C, stress-rupture properties of brazed butt joints using the filler material TD-6, B-2, and NASA-18 produced by three sources were essentially equivalent, having a rupture strength of about 21 megapascal for a 100-hour life. Butt joints brazed with NASA-22, exhibited about 50 percent greater rupture strength than the other filler metals. However, this advantage was only evident for times up to about 300 hours, beyond which all of the brazed butt joints had similar stress-rupture strengths. It was pointed out that alloys containing aluminum must have clean surfaces when being brazed with filler metals that are not self-fluxing.

### DS Superalloys

Since the discovery of mechanical alloying, numerous investigators have sought to exploit this technique in seeking further improvements in the high-temperature strength of superalloys. It was not surprising, therefore, for Benjamin and his coworkers<sup>(99,100,101)</sup> to investigate the effects of additions of up to 4.5 vol. % of  $Y_2O_3$  to the In-853 base composition. Best rupture strengths at 1900 F occurred for alloys containing 1 to 2 percent  $Y_2O_3$ . This led to the development of International Nickel's Inconel MA753 alloy which was the first commercial superalloy to be prepared using the mechanical alloying process.<sup>(100)</sup> Its chemical composition (in weight percent) is given nominally as 20 chromium, 1.6 aluminum, 2.65 titanium, 0.07 zirconium, 0.008 boron, 0.062 carbon, 0.83 total oxygen, and 1.3  $Y_2O_3$  (balance nickel). The alloy combines gamma-prime precipitation strengthening and dispersion strengthening with good oxidation and sulfidation resistance. The tensile and rupture properties are given in Table 56, while Table 57 lists the alloy's fatigue properties at various temperatures. It was observed that the fatigue strength of MA753 at high temperatures decreased when a testing frequency of 800 cycles per minute was employed. At 1227 K, gamma prime is dissolved in the alloy and thus plays no part in the behavior. The temperature dependence of the elastic modulus on Inconel MA753 has been investigated by Malu, et al.<sup>(103)</sup> who also studied its activation energy for creep.

Cairns, et al.<sup>(104)</sup> applied "zone annealing" to IN-MA753 and an experimental alloy (alloy B) having the composition 15 chromium, 4.5 aluminum, 2.5 titanium, 2 tantalum, 0.5 molybdenum, 4 tungsten, 0.15 zirconium, 0.01 boron, 1.1  $Y_2O_3$ , balance nickel. It was found that grain size and aspect ratio are increased by using a moving hot zone to accomplish grain growth. These effects in grain aspect ratio lead to higher stress-rupture strength over the entire temperature range tested: 1033-1310 K.

**Table 56. Tensile and Stress-Rupture Properties of Inconel MA753<sup>(102)</sup>**

Test Temp., K	0.2% Offset Yield Strength		Ultimate Tensile Strength		Elong., %	Reduction in Area, %	Rupture Stress for 100 h Life	
	ksi	MPa	ksi	MPa			ksi	MPa
R.T.	139.7	963.2	169.6	1169.3	7.0	9.5	—	—
811	116.1	800.5	145.3	1003.2	5.0	8.5	123.3	850.1
1033	87.9	606.0	97.4	671.5	12.0	23.0	48.0	330.9
1227	23.1	159.3	26.5	183.7	15.0	27.0	19.4	133.8

**Table 57. Fatigue Strengths of Inconel MA753 for Various Test Temperatures<sup>(a)</sup>(102)**

Type of Fatigue Loading	Test Temp., K	10 <sup>7</sup> Cycle Fatigue Strength,		Fatigue Ratio <sup>(b)</sup>
		ksi	MPa	
Reversed Bending	R.T.	81.1	559.2	0.48
Axial (R=0.1) <sup>(c)</sup>	R.T.	48.2	332.3	0.28
Axial (R=-1.0)	R.T.	68.5	472.3	0.40
Reversed Bending	811	69.2	477.1	0.48
Reversed Bending	1033	62.0	427.5	0.64
Axial (R=0.1)	1033	32.8	226.1	0.34
Axial (R=-1.0)	1033	56.0	386.1	0.58
Reversed Bending	1227	34.2	235.8	1.29

(a) Testing frequency = 8000 cpm.

(b) Fatigue ratio = 10<sup>7</sup> cycle fatigue strength/ultimate tensile strength.

(c) R=minimum stress/maximum stress.

On alloy B the stress for 1000-hour life was increased by 15 to 17 percent at all temperatures tested. The zone-annealed material was superior to commercial alloys such as 713 C, and has a 125 C temperature-capability improvement over IN-100 for a 1000-hour rupture life of 103.5 MPa. It was found that grain aspect ratio tends to increase with decreasing zone travel rate. The parameters of the moving hot zone must also be consistent with requirements to minimize annealing during heat up and with achieving complete grain coarsening.

Kramer<sup>(105)</sup> mechanically alloyed Udimet 700 with 2.5 vol. % Y<sub>2</sub>O<sub>3</sub> and also IN-738 with 2.5 vol. % Y<sub>2</sub>O<sub>3</sub>, compacting the powders by isostatic hot pressing, with best results at 1200 C for 1 hour with 1000-bars pressure.

Gessinger<sup>(106)</sup> used mechanical alloying to produce a DS-IN-738 alloy containing 1.5 weight % Y<sub>2</sub>O<sub>3</sub>. He observed that annealing of the extruded alloy bars above the recrystallization temperature of 1160 C can be described by three stages of recrystallization: fine-grain, isotropic coarse-grain, and fibrous coarse-grain growth. The three stages of grain growth were explained in terms of recovery, differences in nucleation rate and dispersoid concentration in the two normal directions, and release in stored cold work. DS IN-738, heat treated to a coarse, elongated grain structure has both high intermediate-temperature strength and high elevated-temperature strength. Its creep strength at 1000 C exceeds that of cast or directionally solidified IN-738 after 300-hours service. However, depletion of surface zones of chromium, aluminum, and titanium contributes to the initiation of creep failure at 1000 C.

Glasgow and Quatinitz<sup>(107)</sup> used mechanical alloying to prepare an alloy of B-1900 containing 1 vol. %  $Y_2O_3$ . Some elevated-temperature, stress-rupture data for this material are compared with those for cast B-1900 in Table 58.

**Table 58. Results of 760 and 1095 C Stress-Rupture Tests of Smooth and Notched Specimens of ODS B-1900 and Comparable Data for Cast B-1900<sup>(107)</sup>**

Temp., C	Grain Aspect Ratio	Smooth or Notched Specimen <sup>(a)</sup>	Stress, MPa	Rupture Time, hr	Elong., %	Reduction in Area, %
<b>ODS B-1900</b>						
760	5.5	S	552	224	1.8	2.8
	3	S	"	98	1.5	3.6
	5.5	N	"	174	(b)	(b)
	3	N	"	11	(b)	(b)
760	5.5	S	517	396	1.3	2.1
	3	S	"	186	.9	2.0
	3	S	"	177	1.2	3.0
	5.5	N	"	140	(b)	(b)
1095	3	N	"	13	(b)	(b)
	5.5	S	68.9	143	4.1	3.9
	3	S	68.9	9	1.4	2.5
	5.5	S	62.1	145	1.5	2.1
1095	3	S	"	22	2.4	2.9
	3	S	"	41	3.5	3.6
	3	N	"	30	(b)	(b)
	3	S	55.2	44	2.8	3.7
1095	3	S	55.2	38	2.0	3.3
	3	N	55.2	80	(b)	(b)
<b>Cast B-1900</b>						
760 <sup>(c)</sup>	—	S	621	100	(d)	(d)
	—	S	517	1000	(d)	(d)
1095	—	S	62.1	100	(d)	(d)
	—	S	33.8	1000	(d)	(d)

(a) Smooth, S; notched, N (stress concentration factor, 3).

(b) Not meaningful.

(c) Data extrapolated from higher temperature data.

(d) Not available.

The newest and most commercially advanced mechanically alloyed superalloy is Inconel MA754<sup>(108,109)</sup> whose nominal composition is 20 chromium, 0.3 aluminum, 0.5 titanium, 0.05 carbon, 0.6  $Y_2O_3$ , balance nickel. Some properties of the alloy are: density 8.3 gm/cm<sup>3</sup>; solidus (melting point) 1399 C; and modulus of elasticity at 20 C (70 F) 144.8 GPa (21 x 10<sup>6</sup> psi). The low elastic modulus indicates a predominantly (100) texture in the direction of major grain elongation. This has been shown to give superior thermal fatigue resistance. Some stress rupture properties are given in Table 59.

Reportedly, Inconel MA754 is being used for vanes and shrouds in General Electric's F-101 engine where metal temperatures are approximately 2000 F (1093 C).<sup>(110)</sup>



**Table 59. Longitudinal and Long Transverse Stress-Rupture Properties of Inconel\* Alloy MA754 at 2000 F (1093 C)(109)**

Direction of Tests	Stress to Produce Rupture in					
	20 hr		100 hr		1000 hr	
	ksi	MPa	ksi	MPa	ksi	MPa
Longitudinal	20.0	138	19.0	131	17.9	123
Long Transverse	8.0	55	6.1	42	4.2	29

\* Registered trademark of The International Nickel Company, Inc.

### Oxidation and Hot-Corrosion Resistance

Considerable research has been done to differentiate and explain the mechanisms involved in the oxidation and hot-corrosion behavior of nickel-base alloys, and it will not be possible to treat these subjects exhaustively here. For in-depth review, the reader is referred to References 111 or 112, both prepared recently for MCIC and collectively representing over 220 references on the oxidation and hot corrosion of superalloys.

Stringer, et al.<sup>(113)</sup> observed that the presence of a fine dispersion of a stable oxide has a beneficial effect on the oxidation resistance of both nickel- and cobalt-base, heat-resisting alloys. In their study of the hot corrosion resistance of these alloys, they found that alloys forming  $\text{Cr}_2\text{O}_3$  scales appeared to be resistant to oxidation when coated with  $\text{Na}_2\text{SO}_4$  whereas an alloy normally forming an  $\text{Al}_2\text{O}_3$  scale suffered accelerated attack. During sulfidation, some of the alloys suffered an accelerated degradation, with sulfur penetrating rapidly along what appeared to be grain boundaries. The same effect was noted in sulfidation-oxidation experiments when the  $\text{Cr}_2\text{O}_3$ -forming alloys suffered accelerated oxidation, the effect of apparent removal of the dispersoid. An  $\text{Al}_2\text{O}_3$ -forming alloy resisted this form of attack well. Some of the conclusions reached by Stringer, et al. were:

- 1) Dispersoids greatly improve the adhesion of  $\text{Cr}_2\text{O}_3$  scales on Ni-Cr and Co-Cr alloys and of  $\text{Al}_2\text{O}_3$  scales on Co-Cr-Al alloys. The same beneficial effect has been observed on the adhesion of  $\text{Al}_2\text{O}_3$  scales to NiCrAl alloys.
- 2) Dispersoids promote the selective oxidation of chromium to form  $\text{Cr}_2\text{O}_3$  scales on Ni-Cr and Co-Cr alloys, but do not promote the selective oxidation of aluminum to form  $\text{Al}_2\text{O}_3$  scales on Co-Cr-Al alloys. More than 3.5 percent aluminum is required in CoCrAl alloys to allow the formation of  $\text{Al}_2\text{O}_3$  scales at 900 to 1200 C in 100 torr oxygen.
- 3) Oxide dispersoids lead to a change in the direction of growth of  $\text{Cr}_2\text{O}_3$  scales in Ni-Cr and Co-Cr alloys, but not of  $\text{Al}_2\text{O}_3$  scales on CoCrAl alloys; growth of  $\text{Al}_2\text{O}_3$  scales normally occurs at the metal/oxide interface.
- 4) The presence of an oxide dispersoid did not change the rate of evaporation of  $\text{Cr}_2\text{O}_3$  scales in high velocity gas environments; an  $\text{Al}_2\text{O}_3$ -CoCrAl alloy was more resistant than a similar  $\text{Cr}_2\text{O}_3$ -forming alloy in a burner rig test.
- 5) The effect of oxide dispersoids on the hot corrosion of Ni-Cr and Co-Cr base alloys is more difficult to define.

Wright, et al.<sup>(114)</sup> investigated the oxidation of Ni-20Cr alloys containing  $\text{Y}_2\text{O}_3$ ,  $\text{Al}_2\text{O}_3$ , and  $\text{ThO}_2$  in the temperature range 900-1200 C in slowly flowing oxygen at 100 torr. The results showed that, despite some anomalies, the oxidation behavior of these alloys was very similar. An  $\text{Al}_2\text{O}_3$  alloy with a relatively coarse dispersoid size behaved in a manner analogous to a dispersion-free Ni-20Cr alloy at 1100 C. The alloy with fine  $\text{Al}_2\text{O}_3$  particles behaved exactly like the  $\text{Y}_2\text{O}_3$ -containing

alloy at 1000 and 1100 C, but at 1200 C oxidized at a faster rate. It was noted that the adherent scales on the dispersion-strengthened alloys have a stabilized grain size whereas the non-adherent scales on dispersion-free alloys grow.

Tenney, et al.<sup>(115)</sup> reported on the oxidation behavior of TD-NiCr in a dynamic, high-temperature environment at 1100 and 1200 C. They point out that the oxidation resistance of this alloy in the 900 to 1200 C temperature range under static furnace atmosphere conditions had been reported in at least some 16 papers in the last 5 years (1969-1973). They suggested incorporating aluminum in the alloy on the basis that this would yield an external layer of  $Al_2O_3$ , which should offer better oxidation protection than NiO or  $Cr_2O_3$ . Also,  $Al_2O_3$  is not susceptible to rapid vaporization as is  $Cr_2O_3$ . The fact that the emissivity of  $Al_2O_3$  is lower than that of either NiO or  $Cr_2O_3$  would be a negative factor for an application such as metallic heat shield in a thermal protection system.

Centollanzi, et al.<sup>(116)</sup> arc-jet tested seven thoria-dispersion-strengthened nickel alloys to determine their degradation after 50 one-half-hour cycles at a nominal test temperature of 1366 K and a pressure of 0.01 atmosphere. The alloys investigated were TD-Ni-20Cr, DS-Ni-20Cr-15Fe, DS-Ni-20Cr, TD-Ni-16Cr-3.5Al-0.4Y, TD-Ni-16Cr-3.5Al, TD-Ni-20Cr-3.5Al, and TD-Ni. Several problems were encountered in trying to simultaneously evaluate these alloys.

Seltzer, et al.<sup>(117)</sup> doped the surface regions of DSNiCrAl alloy by a pack diffusion process with small amounts of manganese, iron, or cobalt to determine their effect on the total normal emissivity of the scales produced by subsequent high-temperature oxidation. While all three elements lead to a modest increase in emissivity (up to 23 percent greater than the undoped alloy), only the change caused by manganese was thermally stable. However, this increased emissivity is within 85 percent of that of TD-NiCr oxidized to form chromia scale. The manganese-doped alloy was some 50 percent weaker than undoped DSNiCrAl after the doping treatment and approximately 30 percent weaker after oxidation.

Schultz and Hulsizer<sup>(118)</sup> have described the approach used by the International Nickel Company to develop a corrosion resistant, mechanically alloyed, nickel-base alloy (Inconel MA755 A). Initial property targets were: 1038 C rupture strength, and both creep resistance and hot-corrosion resistance greater than that for Udimet 500 or IN-738. Secondary consideration was given to notch sensitivity, structural stability after 2000 hours at 816 C, and thermal fatigue resistance equal to that shown by IN-738. In addition to passing "crucible" tests for hot corrosion, the alloy also met the 100-hour INCO rig test at 927 C. A comparison of this alloy's oxidation and corrosion behavior with other nickel-base alloys is shown in Table 60.

Table 60. Hot Corrosion and Oxidation Resistance of Alloy MA 755E<sup>(118)</sup>

	Crucible Test <sup>(a)</sup> Max. Attack, $\mu m$	Rig Test <sup>(b)</sup> Max. Attack, $\mu m$	Cyclic Test <sup>(c)</sup> Metal Loss, $Mg/cm^2$
Alloy MA 755E	305	76	21
IN-738	254	102	80
Udimet 700	>7620	356	—
IN-100	>7620	3302	—
Alloy 713C	>7620	—	20

(a) 90 pct.  $Na_2SO_4$ —10 pct. NaCl, 300 hr, 927 C.

(b) 5 ppm sea water—0.3 pct. S JP5, 100 hr, 927 C.

(c) Air—5 pct.  $H_2O$ , 500 hr, 1100 C.

Following the reference list to this section is a bibliography of additional material on nickel-base alloys not referenced but of possible interest to the reader.

## REFERENCES

1. Baxter, J. R., and Roberts, A. L., "Development of Metal-Ceramics from Metal-Oxide Systems", Iron and Steel Institute Special Report 58, 315-324 (1954).
2. Grant, N. J., and Preston, O., "Dispersed Hard Particle Strengthening of Metals", Trans. AIME, 209, 349-357 (1957).
3. Anders, F. J., Alexander, G. B., and Wartel, W., "A Dispersion-Strengthened Nickel Alloy", Metal Progress, 88-91 (December 1962).
4. Portnoy, K. I., and Babich, B. N., "Dispersion Hardened Materials", Moscow Metallurgiya, 127-199 (1974). (ADB009 068).
5. Benjamin, J. S., "Dispersion Strengthened Superalloys by Mechanical Alloying", Met. Trans., 1, 2943-2951 (1970).
6. Morse, J. P., and Benjamin, J. S., "Mechanical Alloying", New Trends in Materials Processing, ASM Book (1976), pp 164-199.
7. Benjamin, J. S., and Cairns, R. L., "Elevated Temperature Mechanical Properties of a Dispersion Strengthened Superalloy", Modern Developments in Powder Metallurgy, 5, 47-71 (1971).
8. Bailey, P. G., "Oxide Dispersion Strengthened Alloys for Aircraft Turbine Engine Vanes", 6th National SAMPE Technical Conference, Dayton, Ohio (October 1974), pp 208-217.
9. Freche, J. C., and Ault, G. M., "Progress in Advanced High Temperature Materials Technology", NASA TM-X 71901, presented at Third International Symposium on Superalloys, Seven Springs (September 1976).
10. Rice, L. P., "Metallurgy and Properties of Thorium-Strengthened Nickel", DMIC Memorandum 210 (October 1965) Battelle Memorial Institute, Columbus, Ohio.
11. Ruscoe, M.J.H., Norris, L. F., Clegg, M. A., and Evans, D.J.I., "The Development of Thermomechanical Processes for Advanced Dispersion Strengthened Alloys", The Microstructure and Design of Alloys, proceedings of the Third International Conference on the Strength of Metals, 36, 96-100 (August 1973).
12. Quatintz, M., and Weeton, J. W., "Dispersion-Strengthened Nickel Produced from Ultrafine Comminuted Powders", NASA TN D-5421 (October 1969).
13. Marty, M., Walder, A., and Hivert, A., "Elaboration d'un alliage a phase dispersee Ni-ThO<sub>2</sub> a partir de composés organometalliques", High Temperatures-High Pressures, 3, 677-685.
14. Cheney, R. F., and Scheithauer, W., "The High-Temperature Strength of Oxide-Strengthened Nickel Alloys", Modern Developments in Powder Metallurgy, 5, Plenum Press, New York (1971), pp 137-148.
15. Arias, A., "Oxide Dispersion Strengthened Nickel Produced by Non-Reactive Milling", NASA TM-X 3331 (January 1976).
16. Norris, L. F., Fraser, R. W., and Evans, D.J.I., "Cold Rolling of Dispersion Strengthened Nickel", Powder Metallurgy for High-Performance Applications, J. J. Burke and V. Weiss, Editors, Syracuse University Press (1972), pp 257-280.
17. Babich, B. N., Lyukevich, V. I., Levinskaya, M. Kh., and Romashov, V. M., "Recrystallization of Nickel Hardened With ThO<sub>2</sub>", Metallovedenie i Termicheskaya Obrabotka Metallov, No. 3, 36-40 (1972).
18. Petrovic, J. J., and Ebert, L. J., "An Electron Microscopy Examination of Primary Recrystallization of TD-Ni", Metallurgical Trans. 3, 1123-1129 (1972).
19. Hotzler, R. K., Bahk, S., Misra, A. K., and Castleman, L. S., "Impurity Induced Recrystallization in Thoriated Nickel", Materials Science & Engineering, 12, 209-215 (1973).
20. Lasalmonie, A., and Strudel, J. L., "Internal Stress in TD-Ni During Creep", Phil. Mag., 31 (1), 115-134 (1975).
21. Footner, P. K., and Alcock, C. B., "Growth Kinetics of Dispersed ThO<sub>2</sub> in Ni and Ni-Cr Alloys", Metallurgical Trans., 3, 2633-2637 (1972).
22. Alcock, C. B., and Brown, P. B., "Physicochemical Factors in the Dissolution of ThO<sub>2</sub> in Solid Nickel", Metal Science JI., 3, 116-120 (1969).
23. Durber, G.L.R., and Davies, T. J., "Strain Hardening in Polycrystalline Nickel Containing a Dispersion of ThO<sub>2</sub>", Materials Science and Engineering, 5 (3), 142-148 (1970).
24. Ansell, G., "The Role of Process History, Phase Morphology and Interface Strength Upon the Mechanical Properties of Dispersion-Strengthened Alloys", Contract NAS 8-26007 (December 1972). (MCIC 87834)



# REFERENCES (Cont.)

25. Murr, L. E., Vydyanath, H. R., and Foltz, J. V., "Comparison of the Substructures and Properties of Nickel, TD-Ni, Chromel A, Inconel 600 and TD-NiCr Following Explosive-Shock Deformation", *Metallurgical Trans. I*, 3215-3223 (1970).
26. Murr, L. E., "Interfacial Energetics in the TD-Ni and TD-Nichrome Systems", *Jl. of Materials Science*, **9**, 1309-1319 (1974).
27. Thompson, A. W., "Hydrogen Compatibility of Dispersion Strengthened Alloys", *Metallurgical Trans.*, **5**, 1855 (1974).
28. Ikawa, H., Shin, S., and Habu, M., "Study on Weldability of Dispersion Hardening Alloy—Behavior of ThO<sub>2</sub> Under the Melting-Solidification of TD-Ni", *Jl. Japan Welding Soc.*, **43** (5), 21 (1974).
29. Dzenladze, Zh. I., Shchegoleva, R. P., Afonina, V. M., Lykova, V. F., and Golubeva, L. S., "Properties and Microstructure of Nickel and Nickel Alloy Wire Produced by Working Sintered Blanks", *Poroshkovaya Metallurgiya*, **151** (7), 83-92 (1975).
30. Severdenko, V. P., Lozhechnikov, E. B., Baek, M. A., and Stepanenko, A. V., "Rolling of Dispersion Strengthened Metals With the Application of Ultrasonic Vibrations", *Poroshkovaya Metallurgiya*, **134** (2), 14-16 (1974).
31. Buchta, R., and Schatt, W., "Untersuchungen zur Dispersionsverfestigung an galvanisch hergestellten Ni-Al<sub>2</sub>O<sub>3</sub> Legierungen", *Planseeberichte für Pulvermetallurgie*, **19**, 268 (1971).
32. Broszeit, E., Heinke, G., and Wiegand, H., "Über die Mechanischen Eigenschaften galvanisch hergestellter Nickel-dispersionsschichten mit Einlagerungen von Al<sub>2</sub>O<sub>3</sub> und SiC", *Metall*, **25** (5), 470-475 (1971).
33. Hancock, J. W., Dillamore, I. L., and Smallman, R. E., "Void Nucleation and Growth During the Low-Temperature Deformation of Ni-Co-Al<sub>2</sub>O<sub>3</sub> Alloys", *High-Temperature Materials*, 6th Plansee Seminar (1968), pp 467-479.
34. Kulikov, V. A., Sergenkova, V. M., Savitskii, A. P., Grigor'eva, V. V., and Savitskii, K. V., "Strength Loss During the Annealing of Deformed Ni-Al<sub>2</sub>O<sub>3</sub> Alloys", *Poroshkovaya Metallurgiya*, **51** (3), 56-63 (1967).
35. Sergenkova, V. M., and Berezutskii, V. V., "Influence of Titanium Addition on the Growth of Dispersed Al<sub>2</sub>O<sub>3</sub> Particles in a Nickel Matrix", Part 3, *Poroshkovaya Metallurgiya*, **57** (9), 28-31 (1967).
36. Sergenkova, V. M., "Growth Rate of Particles Dispersed in Nickel", *Communication I. Poroshkovaya Metallurgiya*, No. 7, 84-91 (1967).
37. Perry, B., and Smallman, R. E., "Comments on Coarsening of Al<sub>2</sub>O<sub>3</sub> Particles in Ni-Al<sub>2</sub>O<sub>3</sub>-Mg Alloys", *Scripta Metallurgica*, **6**, 149-154 (1972).
38. Faulkner, R., *Scripta Met.*, **5**, 717 (1971).
39. Sergenkova, V. M., Dubinin, V. P., and Osasyuk, V. V., "Effects of Oxide Particles on Properties of Sintered Nickel", *Poroshkovaya Metallurgiya*, No. 6 (78), 81-86 (1969).
40. Plechev, V. N., Shchegoleva, R. P., and Dzenladze, R. P., "Strengthening of a Ni-2w/o HfO<sub>2</sub> Alloy by Mechanico-thermal Treatment", *Soviet Powder Metallurgy and Metal Ceramics*, **14** (5), 373-375 (1975).
41. Timofeyeva, E. N., Beresten', N. E., and Levinskaya, M. Kh., "The Influence of Sintering Temperature on the Structure and Consolidation of Dispersion Strengthened Nickel", *Iszvest. Akad. Nauk, SSSR Metally*, (1), 130-132 (1975).
42. Timofeyeva, E. N., Kustov, Yu. A., and Beresten', N. E., "The Influence of Nickel Powder on the Structure and Properties of Deformed Dispersion Hardened Nickel", *Russian Metallurgy*, (2), 113-114 (1974).
43. Timofeyeva, E. N., and Beresten', N. E., "Behavior of HfO<sub>2</sub> Particles in DS-Ni During Isothermal Annealing", *Russian Metallurgy*, (3), 124-126 (1973).
44. Portnoi, K. I., Lyukevich, V. I., and Babich, B. N., "Properties of Nickel in Relation to Amount of Oxide Phase", *Metallovedenie i Termicheskaya Obrabotka Metallov*, (9), 55-57 (1974).
45. Babich, B. N., and Romanovich, I. V., "Effects of Compact Sintering Temperature Upon the Structure and Properties of DS-Ni", *Poroshkovaya Metallurgiya*, No. 4 (148), 29-33 (1975).
46. Yagubets, A. N., Timofeyeva, N. I., Buntushkin, V. P., Lyukevich, V. I., Bobanova, Zh. I., and Buzinova, V. P., "Production of Electrochemical Composites Based on Nickel With Disperse Particles of Metal Oxides", *Electronnaya Obrabot Met.*, (1), 62-67 (1972).
47. Sastry, D. H., and Vasu, K. I., "A Study of the Dispersion-Strengthening in Ni-ZrO<sub>2</sub> Composite Materials", *Trans. J.I.M.*, (12), 405-409 (1972).
48. Denisenko, E. T., and Olifirovich, Ya. V., "Effect of Thermomechanical Treatment on the Strength of Nickel Strengthened With ZrO<sub>2</sub>", *Soviet Powder Metallurgy and Metal Ceramics*, **13** (9), 757-760 (1975).
49. Gawrilow, G., "Die chemische Abscheidung von Dispersionsschichten", *Galvanotechnik*, **65**, 858-865 (1974).
50. Portnoy, K. I., *Izv. Vuzov Tsetnaya Metallurgiya*, No. 3, 101-105 (1971).
51. Schafer, R. J., Quatinetz, M., and Weeton, J. W., "Strength and High-Temperature Stability of Dispersion Strengthened Ni-MgO Alloys", *Trans. of the Metallurgical Soc. AIME*, **221**, 1099-1104 (1961).

# REFERENCES (Cont.)

52. Grewal, M. S., Sastri, S. A., and Grant, N. J., "Structure-Property Relationship in Thermomechanically Treated Beryllia Dispersed Nickel Alloys", *Metallurgical Trans.*, **6A**, 1393-1404 (1975).
53. Kaufmann, A. R., "Splat Cooled Nickel Slis Alloys", Contract NOw 66-0190-c (January 1967). (MCIC 69920)
54. Thibaudon, D., Roubin, M., and Paris, R. A., "Obtention de dispersions de carbures et de nitrures dans le Co et le Ni", *J. Less-Common Metals*, **29**, 171-182 (1972).
55. Rudio, B. L., Shorshorov, M. Kh., Matveev, G. M., Borok, B. A., and Shchegoleva, R. P., "Manufacture of Nickel Base Composites Materials With Dispersed Glass Particles by the Powder Metallurgy Method", Part I, *Poroshkovaya*, No. 3 (135), 65-69 (1974).
56. *Metal Progress*, **110** (3), 13 (1976).
57. Walsh, J. M., and Donachie, M. J., "Interdiffusion in the Ni-W and ThO<sub>2</sub> Dispersed Ni-W Systems", *Metal Science JI.*, **3**, 68-74 (1969).
58. Hancock, J., Dillamore, I. L., and Smallman, R. E., "The Creep of DS-Ni-Co Alloys", *Metal Science JI.*, **6**, 152-156 (1972).
59. Glasgow, T. K., "An Oxide Dispersion Strengthened Ni-W-Al Alloy With Superior High Temperature Strength", NASA TM-X 71888 (1976). (ADD 107 100)
60. Marty, M., Walder, A., Galmiche, P., and Hivert, A., "Elaboration d' alliages Ni-Cr-ThO<sub>2</sub> au moyen de diffusion de Cr par transporteur halogene dans un granule de Ni-ThO<sub>2</sub>", *High Temperatures-High Pressures*, **3**, 687-694 (1971).
61. Wilcox, B. A., and Clauer, A. H., "Creep of Dispersion-Strengthened Ni-Cr Alloys", *Metals Science JI.*, **3**, 26-33 (1969).
62. Arunachalam, V. S., and Lipsitt, H. A., "Stress Relaxation in Thoriated Nickel Alloys", *Metallurgical Trans.*, **4**, 1767-1769 (1973).
63. Lund, R. W., and Nix, W. D., "High Temperature Creep of Ni-20Cr-2ThO<sub>2</sub> Single Crystals", *Acta Metallurgica*, **24** (5), 469-481 (1976).
64. Klingler, L. J., Weinberger, W. R., Bailey, P. G., and Baranow, S., "Development of DS Ni-Cr-ThO<sub>2</sub> Sheet for Space Shuttle Vehicles", NASA 3-13490 (1972). (MCIC 84821)
65. Cook, R. C., and Norris, L. F., "Process Development for Ni-Cr-ThO<sub>2</sub> and Ni-Cr-Al-ThO<sub>2</sub> Sheet", NASA Cr-134484 (December 1973).
66. Johnson, R., and Killpatrick, D. H., "Phase I Summary Report of Evaluation of DS Ni-Base Alloy Shields for Space Shuttle Applications", NASA Cr-132360 (May 1973).
67. Klingler, L. J., Weinberger, W. R., Bailey, P. G., and Baranow, S., NASA Cr-120796 (1972) and NASA Cr-121164 (1973).
68. Davis, J. W., "Prediction and Verification of Creep Behavior in Metallic Materials and Components for the Space Shuttle Thermal Protection System", Contract No. NAS-1-11774 (1972).
69. Fritz, L. J., Koster, W. P., and Taylor, R. E., "Characterization of the Mechanical and Physical Properties of TD-NiCr Alloy Sheet", NASA Cr-121221 (1973).
70. Kane, R. D., Petrovic, J. J., and Ebert, L. J., "Metallographic Examination of TD-Ni Base Alloys", *Metallurgical Trans.*, **6A**, 1296-1299 (1975).
71. Wilson, D. J., and Ferrari, A., "Notch Sensitivity, Mechanical, and Microstructural Characteristics of TD-NiCr at Elevated Temperatures", *Trans. of the ASME series H., JI. of Engineering Materials and Technology*, **96** (2), 109-114 (1974).
72. Whittenberger, J. D., "Observations on the Relationship of Structure to the Mechanical Properties of Thin TD-NiCr Sheet", *Metallurgical Trans.*, **7A**, 611-619 (1976).
73. Raymond, L., and Neumann, I. P., "The High Temperature Stability of ThO<sub>2</sub> Strengthened Ni-Cr Alloys", *International Journal Powder Metallurgy*, **5** (2), 97-104 (1969).
74. Allen, R. E., "Directionally Recrystallized TD-NiCr", paper presented at 2nd International Cong. Superalloys Processing, *Superalloys Processing*, MCIC Report 72-10 (September 1972), pp X-1 to X-9.
75. Franklin, J. E., Judd, G., and Ansell, G. S., "The Particle-Matrix Interface Strength in TD-Nichrome", *The Microstructure and Design of Alloys*, Proceedings of 3rd International Conference on the Strength of Metals, England (1973), pp 345-349.
76. Pawar, A. V., and Tenney, D. R., "Interdiffusion in the Ni/TD-NiCr and Cr/TD-NiCr Systems", *Metallurgical Trans.*, **5**, 2139-2143 (1974).
77. Torgerson, R. T., "Development of Forming and Joining Technology for TD-NiCr Sheet", NASA Cr-121224.
78. Moore, T. J., "Solid-State and Fusion Resistance Spot Welding of TD-NiCr Sheet", NASA TN D-7256 (1973).
79. Holko, K. H., "An Improved Diffusion Welding Technique for TD-NiCr Sheet", NASA TN D-7153 (1973).

# REFERENCES (Cont.)

80. Holko, K. H., and Moore, T. J., "Enhanced Diffusion Welding of TD-NiCr Sheet", *Welding Research Supplement*, Welding JI., 51 (2), 81s-86s (1972).
81. Metcalfe, A. G., "Joining TDNiC by CSDB", Solar Research Report (February 1971). (MCIC 86981).
82. Kenyon, N., and Hrubec, R. J., "Brazing of a DS-Ni Base Alloy Made by Mechanical Alloying", *Welding JI.*, 53 (4), 145s (1974).
83. Filippi, A. M., "Td-NiCr Forging Studies", NASA Cr-134619 (1974).
84. Roach, T. A., and Wolf, W. L., "TD-NiCr Fastener Development", AFFDL-TR-72-150 (November 1972).
85. Barnett, W. J., and Bailey, P. G., "Manufacture of High Strength TD-Ni-Cr Tubing", AF33 (615)-69-C-1870 (April 1971). (AD 885 582)
86. Johnson, R., and Killpatrick, D. H., "Evaluation of DS Ni-Base Alloy Shields for Space Shuttle Applications", NASA Cr-2614 (1976). (ADD 102 820)
87. Antsiferov, V. N., and Sal'nikov, B. V., "Recrystallization of Sheet Nichrome Containing Dispersed Oxide Inclusions", *Permskiy Politekhicheskii Inst.*, (55), 97-100 (1969).
88. Antsiferov, V. N., and Yablonovskaya, R. R., "Growth of Dispersed Oxide Inclusions in 80Ni-20Cr Alloys During Annealing", *Poroshkovaya Metallurgiya*, No. 6 (102), 66-69.
89. Antsiferov, V. N., Karpova, G. P., Polyakov, V. A., and Tomilova, L. A., "Nichrome With Dispersed Oxide Inclusions", *Metallovedenie i Termicheskaya Obrabotka Metallov*, No. 6, 53-54 (1970).
90. Antsiferov, V. N., and Polyakov, V. A., "Strengthening of the 80Ni-20Cr Alloy with Dispersed Oxide Inclusions", *Poroshkovaya Metallurgiya*, No. 8, 63-65 (1969).
91. Bunshah, R. F., "New Techniques for the Synthesis of Metals and Alloys", UCLA-Eng. 7227 (April 1972). (MCIC 742821)
92. Meerson, G. A., Babich, B. N., and Kozyrev, A. S., "Pressing Behavior of Mixtures of DS-Nickel and Chromium Powders", *Poroshkovaya Metallurgiya*, No. 10 (130), 6-9 (1973).
93. Timbres, D. H., and Norris, L. F., "Improvement in the Mechanical Properties and Oxidation Resistance of DS-Ni-Cr Alloys", AFML-TR-74-8 (March 1974). (MCIC 89614)
94. Gangler, J. J., "New Materials in the Aerospace Industries", *The Microstructure & Design of Alloys*, Vol. 2, Paper No. 104, Inst. of Metals & Iron & Steel Inst., England (1975), pp 237-247.
95. Klarstrom, D. L., and Grierson, R., "Optimization of an Oxide DS-Ni-Cr-Al Alloy for Gas Turbine Engine Vanes", NASA 134901 (1975).
96. Personal communication with Stellite Division of Cabot Corporation (1976).
97. Trela, D. M., and Ebert, L. J., "Deformation and Annealing Study of NICRALY" (1975). (ADD 102 386)
98. Gyorgak, "Several Braze Filler Metals for Joining an ODS Ni-Cr-Al Alloy", NASA TN-D 8064 (September 1975). (ADD 102 831)
99. Benjamin, J. S., and Bomford, M. J., "Effect of  $Y_2O_3$  Volume Fraction and Particle Size on Elevated Temperature Strength of a DS-Superalloy", *Metallurgical Trans.*, 5, 615-621 (1974).
100. Cairns, R. L., "Effect of Annealing on Structure and Properties of a DS-Superalloy, IN-853", *Metallurgical Trans.*, 5, 1677-1684 (1974).
101. Cairns, R. L., and Benjamin, J. S., "Stress Rupture Behavior of a DS-Superalloy", *Trans. ASME*, 10-14 (January 1973).
102. Weber, J. H., and Bomford, M. J., "Comparison of Fatigue Deformation and Fracture in a DS and Conventional Ni-Base Superalloy", *Metallurgical Trans.*, 7A, 435-441 (1976).
103. Malu, M., and Tien, J. K., "The Elastic Modulus Correction Term in Creep Activation Energies Applied to ODS-Superalloy", *Scripta Metallurgica*, 9, 1117-1120 (1975).
104. Cairns, R. L., Curwick, L. R., and Benjamin, J. S., "Grain Growth in DS-Superalloys by Moving Zone Heat Treatments", *Metallurgical Trans.*, 6A, 179-188 (1975).
105. Kramer, K. H., "Pulvermetallurgische Herstellung hochwarmfester dispersionsgehärteter, aushartbarer Ni-basis-legierungen", *High Temperatures-High Pressures*, 6, 345-358 (1974).
106. Gessinger, G. H., "Mechanical Alloying of IN-738", *Metallurgical Trans.*, 7A, 1203-1209 (1976).
107. Glasgow, T. K., and Quatnetz, M., "Preliminary Study of ODS-B-1900 Prepared by Mechanical Alloying", NASA TM X-3303 (October 1975).
108. Morse, J. P., and Benjamin, J. S., "Mechanical Alloying", *New Trends in Materials Processing*, ASM (1976), pp 165-199.
109. Benjamin, J. S., "Superalloys by Powder Metallurgy Techniques", AIAA Aircraft Systems and Technology Meeting, Dallas, Texas, Paper 76-937 (September 27-29, 1976).



## REFERENCES (Cont.)

110. DeBoyd, J., "High Nickel Alloys for Gas Turbines", *Gas Turbine International*, 28-30 (September-October 1976).
111. Wright, I. G., "Oxidation of Iron-, Nickel-, and Cobalt-Base Alloys", MCIC Report 72-07 (June 1972).
112. Stringer, J., "Hot Corrosion in Gas Turbines", MCIC Report 72-08 (June 1972).
113. Stringer, J., El-Dahshan, M. E., and Wright, I. G., "Sulfidation and Sulfidation-Oxidation of Nickel- and Cobalt-Base Alloys Containing Dispersions of Stable Oxides", *Oxidation of Metals*, **8** (6), 361-377 (1974).
114. Wright, I. G., Wilcox, B. A., and Jaffee, R. I., "The High-Temperature Oxidation of Ni-20Cr Alloys Containing Various Oxide Dispersions", *Oxidation of Metals*, **9** (3), 275-305 (1975).
115. Tenney, D. R., Young, C. T., and Herring, H. W., "Oxidation Behavior of TD-NiCr in a Dynamic High-Temperature Environment", *Metallurgical Trans.*, **5**, 1001-1012 (1974).
116. Centolanzi, F. J., Probst, H. B., Lowell, C. E., and Zimmerman, N. B., *Arc Jet Tests of Metallic Thermal Protective System Materials*, NASA TM X62092 (1971).
117. Seltzer, M. S., Wright, I. G., and Wilcox, B. A., "Development of High-Emittance Scales on Thoriated Ni-Cr-Al Base Alloys", NASA-Cr 134514 (October 1973).
118. Schultz, J. W., and Hulsizer, W. R., "Corrosion-Resistant Nickel-Base Alloys for Gas Turbines", *Metals Engineering Quarterly*, 15-23 (August 1976).

## BIBLIOGRAPHY

- Anonymous, "New Thermal Fatigue Data for 26 Superalloys", *Materials Engineering*, **76** (5), 54 (1976).
- Curwick, L. R., "Dispersion Strengthened High Volume Fraction  $\gamma'$  Ni-Cr (10)-Al(10)-1Y<sub>2</sub>O<sub>3</sub> Alloys by Mechanical Alloying", *International Nickel Co.* (September 1975). (MCIC 94049)
- Nwoko, V. O., and Shreir, L. L., "Oxidation of Electrodeposited Ni-1.6w/o Al<sub>2</sub>O<sub>3</sub>", *Corrosion, NACE*, **31** (7), 252-254 (1975).
- Case, G. F., "Hot Corrosion Behavior of Newly Developed Gas Turbine Alloys and Protective Coatings", *MAT-75-50* (1975).
- Tenney, D. R., "Investigation of the Oxidation Behavior of Dispersion Stabilized Alloys When Exposed to a Dynamic High Temperature Environment", *Final Report NASA NGR 47-004-082* (1974).
- Eidinoff, H. L., and Rose, L., "Thermal-Structural Evaluation of TDNi-20Cr Thermal Protection System Panels", *NASA Cr-132487* (1974).
- England, M. N., "Dispersion-Strengthened Metal Fin Structural Test", *AFFDL-TR-74-36* (May 1974).
- Simmons, W. F., "Current and Future Materials Usage in Aircraft Gas Turbine Engines", MCIC 73-74 (June 1973).
- Davis, J. W., "Prediction and Verification of Creep Behavior in Metallic Materials and Components for the Space Shuttle Thermal Protection System", *Contract NAS 1-11774*.
- Timbres, D. H., Norris, L. F., and Clegg, M. A., "Improvement of the Oxidation Resistance of DS-Ni-Cr Alloys", *Contract F 33(615)-70-C-1199, Project 7351* (1972).
- Seltzer, M. S., Wilcox, B. A., and Jaffee, R. I., "Development of Oxidation Resistance in TD-Ni-Cr Base Alloys", *NAS 3-14326* (1972). (MCIC 82682)
- Sims, C. T., and Hagel, *The Superalloys*, Chapter 7, John Wiley & Sons (1972).
- Sikora, P. F., and Quatinetz, M., "Dispersion Strengthened Ni-Al<sub>2</sub>O<sub>3</sub> Alloy Produced From Comminuted Powders", *NASA TM-X-2548* (April 1972).
- Holko, K. H., Moore, T. J., and Gyorgak, C. A., "State-of-Technology for Joining TD-NiCr", MCIC-72-10, T-1 to T-33.
- Levinstein, M. A., "Enriched Aluminide Coatings for DS-Ni Materials", *Contract NAS 3-14314* (1971). (MCIC 87419)

#### BIBLIOGRAPHY (Cont.)

- Stott, F. H., Wood, G. C., and Hobby, M. G., "A Comparison of the Oxidation Behavior of Fe-Cr-Al, Ni-Cr-Al, and Co-Cr-Al Alloys", *Oxidation of Metals*, 3 (2), 103-113 (1971).
- Centolanzi, F. J., "Hypervelocity Oxidation Tests of TD-Ni-Cr Alloys", NASA TM X-62015 (1971).
- Sanders, W. A., and Barrett, C. A., "Oxidation Screening at 1204 C of Candidate Alloys for the Space Shuttle Thermal Protection System", NASA TM X-67864 (1971).
- Benjamin, J. S., and Cairns, R. L., "Elevated Temperature Mechanical Properties of a DS-Superalloy", *Modern Developments in Powder Metallurgy*, 5, 47-71 (1971).
- Ahmad, S. A., and Davies, T. J., "Mean Free Path and Particle Distribution Studies in Some Ni-ThO<sub>2</sub> Alloys", *Plansee Berichte für Pulvermetallurgie*, 19, 159 (1971).
- Benjamin, J. S., "Dispersion Strengthened Superalloys by Mechanical Alloying", *Metallurgical Trans.*, 1, 2943-2951 (1970).
- Kimmel, E. R., and Inman, M. C., "Recrystallization in ThO<sub>2</sub> Dispersed Sheet", *Trans. ASM*, 62 (2), 390-397 (1969).
- Wilcox, B. A., and Jaffee, R. I., "Direct and Indirect Strengthening Effect of ThO<sub>2</sub> Particles in Dispersion-Hardened Nickel", *Suppl. Trans. Japan Inst. of Metals*, 9, 575-579 (1968).
- Grierson, R., and Bonis, L. J., "An Electron Microscopy and X-ray study of the Recovery on Annealing of Cold-Worked DSM", *Preprint 34, 1965 Intern. Powder Met. Conf.*
- Wilcox, B. A., and Clauer, A. H., "Creep Fracture of TD-Ni", *Trans. Met. Soc. AIME*, 233, 253-255 (1965).

## LEAD

Lead is effectively hardened by lead oxide. This is due to the extremely low solubility of oxygen in solid lead, as demonstrated in 1962 by Roberts, et al.<sup>(1)</sup> They produced an oxidized grade of lead powder by atomization in air. The powders had oxide contents ranging from 0.5 to 9.5 percent and were consolidated by extrusion at room temperature using a reduction ratio of 40:1.

Table 61 shows some of the mechanical properties obtained for these alloys. One important result was the significant increase in the limit of proportionality at oxide contents above 3 percent which gives these alloys considerable springiness. Figure 67 compares the elevated-temperature tensile strengths for two of these Pb-PbO alloys with those for unalloyed lead and a commercial Pb-8Sb alloy. Stress-rupture data are given in Table 62. The corrosion rate of the Pb-PbO alloys was negligible in 10 and 50 percent solutions of H<sub>2</sub>SO<sub>4</sub>. Unfortunately, however, the corrosion resistance of the DS Pb-PbO alloys, in concentrated H<sub>2</sub>SO<sub>4</sub>, decreased with increasing oxide content (see Figure 68).

Table 61. Tensile Properties of Dispersion-Strengthened Pb-PbO Alloys<sup>(1)</sup>

Oxide Content, wt. %	1.8	2.9	3.2	3.6	4.4	5.4	6.1	6.7
Limit of Proportionality, psi (MPa)	1600 (11)	1600 (11)	1660 (11)	1520 (10)	1790 (12)	1660 (11)	1700-1900 (12-13)	1920 (13)
Modulus of Elasticity, lb/in <sup>2</sup> x 10 <sup>6</sup>	1.60-1.84	1.80-1.90	1.86	1.97-2.11	2.26-2.30	2.94-3.00	2.50-2.90	2.85
Proof Stress, lb/in <sup>2</sup>								
0.05%	2680-2800	3200-3250	3250-3320	3320-3380	3850	3400-4050	2800-3600	3830-3900
0.1%	3050-3250	3850-3950	3700-3900	4100-4150	4350-4400	4350-4730	3520-4300	4850-4900
0.2%	3500-3700	4460-4600	4300-4500	4850-4930	5000	5230-5600	4500-4850	5880-5950
Elongation in 1 in., %	15	13-11	11-10	12-10	11	10-8	9	7-5
UTS, psi (MPa)	5100-5300 (35-37)	5980-6200 (41-43)	6650-6970 (46-48)	7000-7370 (48-51)	7600-7700 (52-53)	8040-8300 (55-57)	7660-7800 (53-54)	9100-9500 (63-65)

Table 62. Stress-Rupture Properties of Lead and Dispersion-Strengthened Lead<sup>(1)</sup>

Material	Applied Stress		Time to Fracture, min	Elongation at Fracture in 1 in., %
	psi	MPa		
Lead	1300	9.0	200	20
(Cast and	1400	9.6	30	25
Wrought)	1500	10.3	8	29.5
No failures				
Dispersion-	2000	13.8	after 1000 hr	—
Strengthened	3000	20.7	10,080	—
Lead	3850	36.5	39	6.7
(1.5% oxide)	4000	27.6	34	7.9



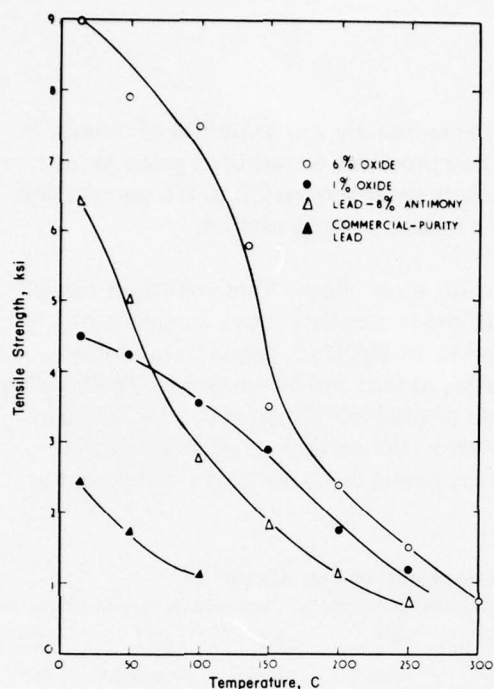


Figure 67. Elevated-Temperature Tensile-Strength Curves for Lead, Two Dispersion-Strengthened Lead Compositions, and a Lead-Antimony Alloy<sup>(1)</sup>

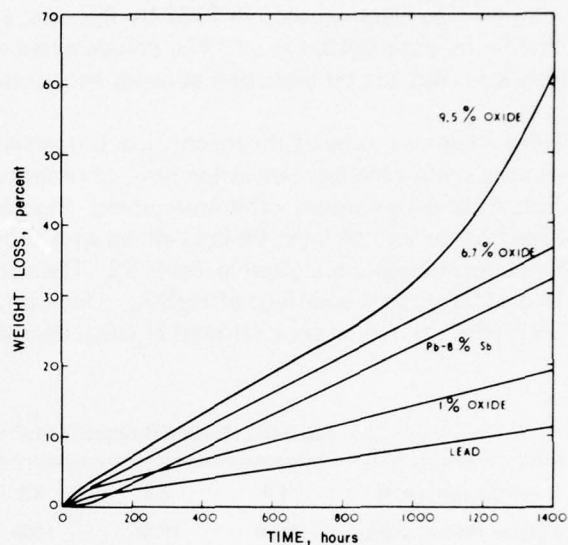


Figure 68. Corrosion Curves for Lead, Three Dispersion-Strengthened Lead Compositions, and a Lead-Antimony Alloy in Concentrated Sulphuric Acid<sup>(1)</sup>

Roberts and Ratcliff<sup>(2)</sup> later reviewed the properties of some DS-Pb-PbO alloys in relation to general application, but more particularly to battery grids. Table 63 summarizes the stress-rupture properties of these alloys and also shows the same data for a dispersion-strengthened Pb-0.2Sb alloy. As shown, the oxide additions were not nearly so effective in increasing the strength of the alloy as they were for unalloyed lead. Table 64 gives some fatigue properties for a Pb-1.5PbO alloy and two Pb-Sb compositions, and Table 65 shows some corrosion results in concentrated  $H_2SO_4$ .

Table 63. Stress-Rupture Results for Dispersion-Strengthened Lead and Dispersion-Strengthened Lead Alloy<sup>(2)</sup>

Material	Oxide Content, %	Test Temp., C	Stress		Rupture Time, hr	Elong. in 2 in., %
			psi	MPa		
Lead	—	80	300	2.1	470	35
Dispersion-Strengthened Lead	0.9	55	2000	13.8	75	10
	3.7	55	2000	13.8	310	3
	0.9	80	1500	10.3	288	10
	3.7	80	1500	10.3	344	4
Dispersion-Strengthened Lead Alloy	1.1	55	2250	15.5	49	3*
	4.0	55	4000	27.6	22.5	2
Lead Alloy (0.2% Sb)	1.1	80	2000	13.8	278	4*
	4.0	80	3500	24.1	38	1

\* Specimens fractured through gauge marks.

**Table 64. Fatigue Properties of Dispersion-Strengthened Lead and Some Lead Alloys<sup>(2)</sup>**

Test Specimen	Endurance Limit for 20 x 10 <sup>6</sup> cycles, lb/sq. in.*
Dispersion-Strengthened Lead (1.5% oxide)	±1950
Lead	± 400
Lead-1% antimony	±1100
Lead-6% antimony	±1700

\* Tested at 3000 reversals/min.

**Table 65. Corrosion Results in Concentrated Sulphuric Acid (20 C)<sup>(2)</sup>**

Material	Corrosion, % wt. loss of original weight		
	400 hr	800 hr	1400 hr
Lead	4.0	7.0	11.0
Dispersion-Strengthened Lead(1% PbO)	6.0	11.0	18.0
Dispersion-Strengthened Lead(7% PbO)	11.0	21.0	36.0
Lead-8% antimony	7.0	18.0	33.0

The fatigue properties of oxide-dispersion-strengthened lead were also studied by Snowden<sup>(3,4,5)</sup>, who showed these alloys to be quite sensitive to the presence of oxygen in the test atmosphere as illustrated in Figure 69. Metallography of the damage during and after fatigue fracture showed that the improved fatigue resistance of oxide-dispersion-strengthened lead over that of pure lead was due mainly to the mechanical strengthening effects of the dispersed oxide rather than an increase in the resistance to atmospheric corrosion fatigue. The ratio of the fatigue life of the DS lead in vacuum to that in air was ~8.5 at a strain of 0.45 percent. In specimens fatigued in air, failure occurred in grain boundaries. For those fatigued in vacuum, failure occurred by a mixture of intercrystalline and transcrystalline modes. In both environments, crack initiation was associated with grain growth, which occurred without a marked redistribution of oxide particles. The stability of the dispersoid and the grain structure appeared to be important factors in the high fatigue resistance of the dispersion-strengthened alloys.

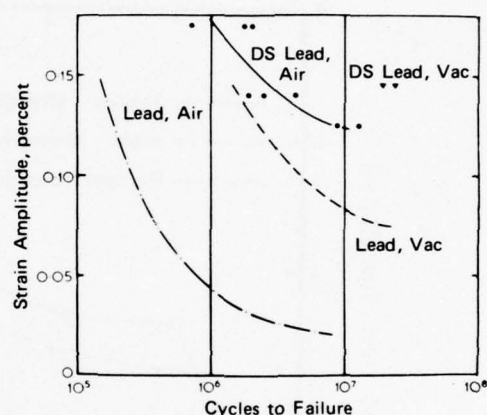


**Figure 69. Strain Amplitude Versus Fatigue Life for DS Lead and for Pure Lead (dashed curves)<sup>(3)</sup>**

Reynolds<sup>(6)</sup> studied the room-temperature creep of coarse-grained, recrystallized DS Pb-PbO alloys. Of particular interest were the stress dependence of the minimum creep rate and measurement of the internal stresses during steady state creep as functions of applied stress. Figure 70 shows the steady-state creep rates measured for the recrystallized alloys in the stress range of 1250 to 3250 psi (8.6 to 22.4 MPa). For comparison, Snowden's data<sup>(5)</sup> is included for an extruded P/M product having a grain size of approximately 0.06 mm and a PbO content of 2.5 weight percent. The creep rates for both alloys are several orders of magnitude lower than those observed for commercial purity lead (grain size 2 mm) in the same stress range. Uniform elongations prior to failure were 1.5-2.0 percent for the recrystallized material as opposed to 4-16 percent for the as-extruded material.<sup>(5)</sup> No further recrystallization,

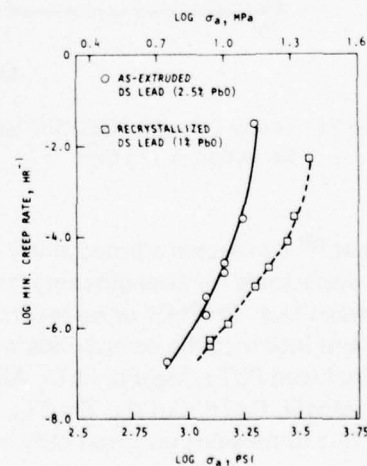


**Figure 70. Creep Data for Two DS Pb-PbO Alloys<sup>(6)</sup>**

i.e., reversion to a fine grain size pinned by the dispersoid, occurred during creep tests in the recrystallized material.

Research into the dispersion strengthening of lead by the coprecipitation method has also been conducted at the Bureau of Mines.<sup>(8)</sup> Lead produced by precipitation of  $\text{PbCO}_3$  from an aqueous solution of  $\text{Pb}(\text{NO}_3)_2$ , followed by roasting and  $\text{H}_2$  reduction, showed a considerable increase in tensile strength and corresponding decrease in ductility compared to chemical Pb. The coprecipitation of  $\text{Al}_2(\text{OH})_3$  with  $\text{PbCO}_3$  from an aqueous solution of lead and aluminum nitrates with subsequent roasting and  $\text{H}_2$  reduction resulted in additional increases in tensile strength. The powders were isostatically pressed into billets, which were extruded into rods and rolled into strip. Alloys containing 0.5, 1, 2, and 3 vol. % of  $\text{Al}_2\text{O}_3$  were tested in short-time tensile tests with the results shown in Figure 71. Table 66 compares the creep rates determined for these alloys with those for pure lead and several other lead alloys.

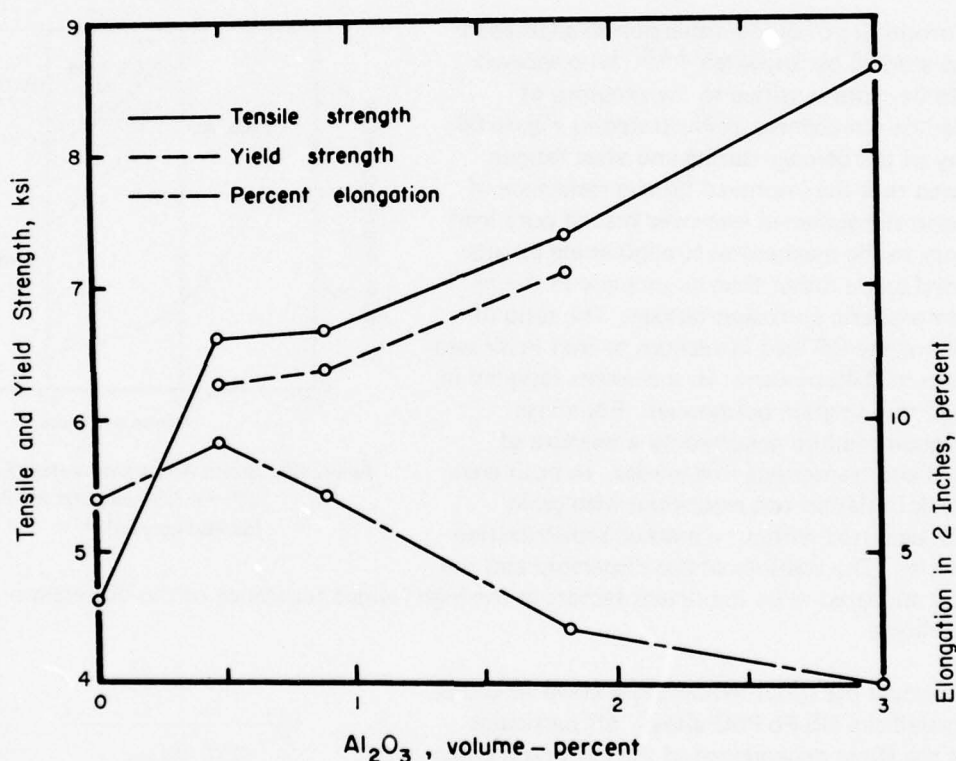


Figure 71. Tensile Strength, Yield Strength, and Percent Elongation of  $\text{Pb-Al}_2\text{O}_3$  Alloys Rolled to 75-Percent Reduction at  $125^\circ\text{C}$ <sup>(7)</sup>

Lund, et al.<sup>(8)</sup> conducted a broad study of many oxides and insoluble metals and intermetallics as possible dispersoids for strengthening lead. The oxides were prepared either by consolidating oxidized lead powders (e.g.,  $\text{Pb-PbO}$ ) or by incorporating other powdered oxides (e.g.,  $\text{Al}_2\text{O}_3$ ) in lead powder. Metallic and intermetallic compounds were obtained in lead by freezing suitable alloys. These compounds included  $\text{PbTe}$ ,  $\text{Mg}_2\text{Pb}$ ,  $\text{PbLi}$ ,  $\text{AlP}$ ,  $\text{AlSb}$ ,  $\text{ZnTe}$ ,  $\text{Mg}_2\text{Ca}$ ,  $\text{MgZn}_2$ ,  $\text{Mg}_3\text{Bi}_2$ ,  $\text{Mg}_2\text{Cu}$ ,  $\text{MgCu}_2$ ,  $\text{Mg}_5\text{Al}_8$ ,  $\text{Mg}_2\text{Si}$ ,  $\text{CuZn}$ ,  $\text{CuCd}_3$ ,  $\text{Zn}_x\text{Ti}_y$ , and  $\text{SbSn}$ . For most of the metallic second phases studied, suitably fine dispersions occurred only where fine powders were used because very high solidification rates were necessary. Some systems involving a metallic phase or intermetallic compounds were identified which permitted fine dispersions to be obtained in relatively coarse-grained lead. In a few cases,



Table 66. Creep Rates of Pb Alloys<sup>(7)</sup>

Composition	Stress		Test Temp., F	Condition	Test Duration, days	Total Elong., %	Creep Rate, % in 10,000 hr
	psi	MPa					
Pb (prepared by precipitation)	2000	13.8	90±3	Rolled 75% at 125 C	17-fractured	0.7	7.79
PB-3Sb	2000	13.8	90±3	Rolled at room temp.	<18 hours fractured	62	6.7 x 10 <sup>4</sup>
Pb-0.5Al <sub>2</sub> O <sub>3</sub> <sup>1</sup>	2000	13.8	90±3	Rolled 75% at 125 C	364-fractured	0.9	.516
Pb-1Al <sub>2</sub> O <sub>3</sub> <sup>1</sup>	3000	20.7	90±3	do	520-terminated	0.8	.322
Pb-2Al <sub>2</sub> O <sub>3</sub> <sup>1</sup>	3000	20.7	90±3	do	820-continuing	0.2	.011
Pb-2Al <sub>2</sub> O <sub>3</sub> <sup>1</sup>	4000	27.6	90±3	do	234-fractured	0.5	.700
Pb-8Sb <sup>2</sup>	425	2.9	86	Cold Rolled	Unknown	Unknown	1.0
Pb-0.15As-0.10Sn-0.10Bi <sup>2</sup>	425	2.9	110	Unknown	do	Unknown	1.03
Dispersion-strengthened lead, <sup>4</sup>	2000	13.8	Room	do	do	Unknown	0.13

1) Nominal volume percent.

2) Data from Metals Handbook, v. 1, 1961, pp 1063-1065; composition in weight percent.

3) Percent per year (1 year = 8,760 hours).

4) St. Joe Minerals Corp.

the intermetallics were found to be sufficiently soluble in lead that dispersions were unstable at 21 C, i.e., coarsening of the intermetallic particles occurred with time. Stable metallic dispersions (e.g., in Pb-Ge) and stable intermetallics in the systems Pb-Cu-Zn and Pb-Cu-Cd, however, gave encouraging degrees of strengthening in extrusions fabricated from coarse powders. In terms of strength and creep resistance, the best intermetallic systems (e.g., Pb-Cu-Zn) offered tensile and creep properties intermediate between those of the strongest conventional Pb alloys (cast, or cast and wrought) and those of the strongest Pb-PbO alloys from extruded fine powders. Table 67 describes the preparation and mechanical properties of a Pb-1Zn-1Cu alloy which was one of the most outstanding materials revealed in this study.

**Table 67. Processing and Properties of Pb-1Zn-1Cu Alloy 186<sup>(8)</sup>**

Preparation: Melted at 1600 F (871 C), (single melt).						
Atomized with 40 psi air, into H <sub>2</sub> O.						
Dried in 300 F (149 C) air for 20 minutes.						
Screen analysis: 3% plus 10 mesh; 6% 10 x 14 mesh; 29% 14 x 35 mesh;						
31% 35 x 70 mesh; 8% 70 x 100 mesh; 23% minus 100 mesh.						
Extrusion (186a) made from 35 x 70 mesh fraction.						
Strain Rate	Test Temp., F	Tensile Properties		U.T.S.		Elong., %
		0.2% Yield				
		psi	MPa	psi	MPa	
0.003	70	3420	23.5	3680	25.3	1.5
0.03	70	3820	26.3	4120	28.4	1.5
0.03	70	4360	30.0	4640	32.0	2
0.03	-40	5270	36.3	5850	40.3	2.5
0.3	-148	6100	42.0	7120	49.0	2.0
0.3	-220	7200	49.6	8000	55.1	2.6
0.3	-320	7260	50.0	9450	65.1	4

Williams, et al.<sup>(9)</sup> used similar techniques to explore the properties of Pd-Cd-Ni alloys, using nickel powder as the dispersoid. The culmination of this work was the development of a Pb-1.5Cd-0.2Ni composition, which was characterized by good bend-fatigue resistance (resistance to corrosion fatigue), good creep resistance over a range of stresses, high tensile strength, and good fabricability (see Table 68). As shown in Table 69, the corrosion resistance of the alloy in H<sub>2</sub>SO<sub>4</sub> is approximately the same as copperized lead.

Previously, Williams and others<sup>(10)</sup> had prepared a series of lead alloys containing very large quantities (up to 30 volume percent) of metallic powders as a dispersed phase. These alloys were called "lead cemented alloys" and were made by stirring the powders into molten lead, then casting and extruding the ingots. Representative tensile strength properties for some of the more outstanding alloys from this study are listed in Table 70 along with some corrosion test data.

At about the same time, Lenel<sup>(11)</sup> reported property data for several Pb-Al and Pb-Cu alloys prepared by atomizing from a temperature at which the aluminum or copper was dissolved in liquid lead. The powders were then compacted and extruded into wires. At room temperature, the alloys had a combination of strength and ductility superior to most lead alloys, including those strengthened by the dispersion of PbO. The creep rate of the alloys was investigated at room temperature and at

Table 68. Properties of Commercial Lead-1.5 Cadmium-0.2 Nickel\*(9)

	Expected Properties Based on Laboratory Extruded Strip	Commercial 0.104-in. Sheet	
		As-received	Annealed**
Tensile strength, psi	4,000	3,120	4,670
Bend resistance, cycles to failure at 75 F	40,000	31,700	22,400
Tensile creep resistance, % plastic strain in			
3000 hr at 300 psi	0.15	0.20 (in 1000 hr)	0.12 (in 1000 hr)
500 hr at 500 psi	0.05	1.45	0.48
50 hr at 1000 psi	>0.05	3.00	0.12

\* 1.4% Cd-0.2% Ni by analysis.

\*\* Annealed 1 hr at 400 F and air cooled.

Table 69. Resistance of Lead-Base Alloys to Sulphuric Acid Solutions at 140 F(9)

Composition	Metal Loss, mils per year* in sulfuric acid concentrations of					
	10%	20%	40%	60%	80%	95%
Pb-0.05Cu	1.73	1.40	1.44	2.56	6.00	35.40
Pb-1Cd-0.2Ni	1.00	0.48	1.15	2.05	4.56	58.40
Pb-2Cd-0.2Ni	0.46	1.82	2.87	3.86	5.27	64.20

\* Based on 144-hr test.

Table 70. Tensile and Corrosion Properties of Lead Cemented Alloys(10)

Alloy Content, vol. %	Tensile Properties			Weight Loss in H <sub>2</sub> SO <sub>4</sub> at 140 F After 96 hr, g/in <sup>2</sup>		
	Ultimate Strength	Elong. %	Red. of Area, %	40%	95%	
	psi					MPa
Unalloyed Pb	1940	13.4	65	98	0.092	4.887
18Co	4820	33.2	12	26	0.112	1.820
15Ni	2480	17.1	10	15	—	—
30Ni	5150	35.5	12	22	—	—
30Cu	4050	27.9	6	9	0.156	14.510
30W	4450	30.7	14	26	0.170	4.960

temperatures up to 100 C. A Pb-0.55Al alloy was one of the more important compositions evaluated. This material had steady-state creep rates of 1 percent per year at stresses up to 2500 psi (17 MPa) at 25 C and up to 1200 psi (8 MPa) at 100 C. The creep resistance of the Pb-Cu alloys was somewhat lower.

As with other dispersion-strengthened metals, one of the basic problems inhibiting the more widespread application of DS lead is that of joining the material satisfactorily. Roberts, et al.<sup>(1)</sup> touched on this problem briefly and suggested low-melting (150-200 C), lead-alloy solders along with suitable joint design. Adhesive joining was also recommended. Bagshaw and Evans<sup>(12)</sup> provided a more comprehensive review of these joining problems and also demonstrated the feasibility of using a low-pressure,



cold-welding process for dispersion-strengthened lead. These authors cautioned, however, that further work will be necessary to apply this practice successfully in cable sheathing, storage batteries, and acid plants.

The reader's attention is also called to an extensive review on dispersion-strengthened lead which was prepared by Torralba and Ruiz<sup>(13)</sup> in 1971, based on 45 references.

#### REFERENCES

1. Roberts, D. H., Ratcliff, N. A., and Hughes, J. E., "Dispersion Strengthened Lead and its Applications", Powder Metallurgy, (10), 132-157 (1962).
2. Roberts, D. H., and Ratcliff, N. A., "Dispersion Strengthened Lead in Batteries", Metallurgia, 70, 223-227 (1964).
3. Snowden, K. U., "The Fatigue Behavior of Dispersed-Oxide-Strengthened Lead in Air and Vacuum", JI. Materials Science, 6, 1178-1181 (1971).
4. Snowden, K. U., Acta Metallurgica, 11, 675 (1963).
5. Snowden, K. U., JI. Materials Science, 2, 324 (1967).
6. Reynolds, G. H., "Room Temperature Creep of Recrystallized Dispersion Strengthened Lead", Scripta Metallurgica, 8, 781-784 (1974).
7. Tilman, M. M., Crosby, R. L., and Desy, D. H., "Dispersion Strengthening of Lead by Coprecipitation", Rep. Inv. 7570, U. S. Bureau of Mines (1971).
8. Lund, J. A., Tromans, D., and Walker, B. N., "Lead Powder Metallurgy", Project LM-8, Dept. of Metallurgy, The University of British Columbia, Canada (January 1968). (MCIC 95903)
9. Williams, D. N., Grube, K. R., and Jaffee, R. I., "Wrought Pb-Cd-Ni Alloys", Trans. ASM Quarterly, 54, 96-105 (1961).
10. Williams, D. N., Houck, J. A., and Jaffee, R. I., "A New Class of Pb-Base Alloys", Metal Progress (February 1960).
11. Lenel, F. V., "Preparation and Selected Properties of Certain Dispersion-Strengthened Lead Base Alloys", Powder Metallurgy, (10), 119-132 (1962).
12. Bagshaw, N. E., and Evans, J. A., "Cold Welding and Dispersion Strengthened Lead", Metallurgia, 76, 229-232 (1967).
13. Torralba, M., and Ruiz, J. L., "El Pb Reforzado por Dispercion", Rev. Met., 7, 41-59 (1971).

## PLATINUM

Platinum is the only metallic structural element capable of operating for long periods of time at high temperatures. It is not surprising that an effort has been made to improve these high-temperature properties by dispersion strengthening.

Of historical interest is the fact that DS Pt-ThO<sub>2</sub> was introduced as early as 1942<sup>(1)</sup> as a logical extrapolation of techniques well established for tungsten filaments for the lamp industry. Figure 72 shows the improvement of DS Pt-ThO<sub>2</sub> over the alloys of the time.

In later work<sup>(3)</sup>, a Pt-12.5ThO<sub>2</sub> alloy was prepared that had much higher stress-rupture strength at high temperatures than Pt-Rh alloys (see Figure 73). However, engineers at Engelhard Industries<sup>(4)</sup> selected 0.6 percent ThO<sub>2</sub> as an optimum amount to provide desired strength in platinum with good working and manufacturing characteristics. As shown in Figure 74, the high temperature stress-rupture strength of this alloy at 1450 C exceeds those of the standard commercial Pt-Rh alloys. The electrical resistivity of DS Pt-0.6ThO<sub>2</sub> is within 2 percent of that of pure platinum.

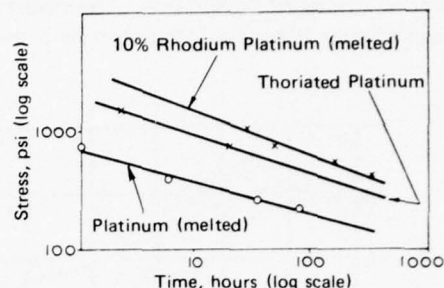


Figure 72. Stress-Rupture Data on Thoriated Platinum Wires Compared With Those of Pure Platinum and Rhodium-Platinum Wires Produced by Conventional Methods<sup>(2)</sup>

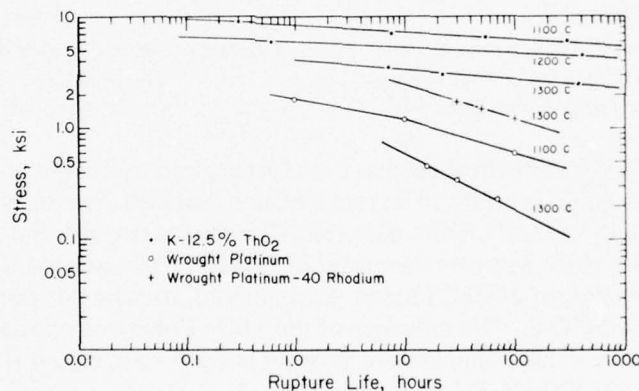


Figure 73. Log Stress-Log Rupture Life Properties of Platinum-12.5 Vol. % Thorium Oxide and Wrought Platinum and Platinum-40 Rhodium<sup>(3)</sup>

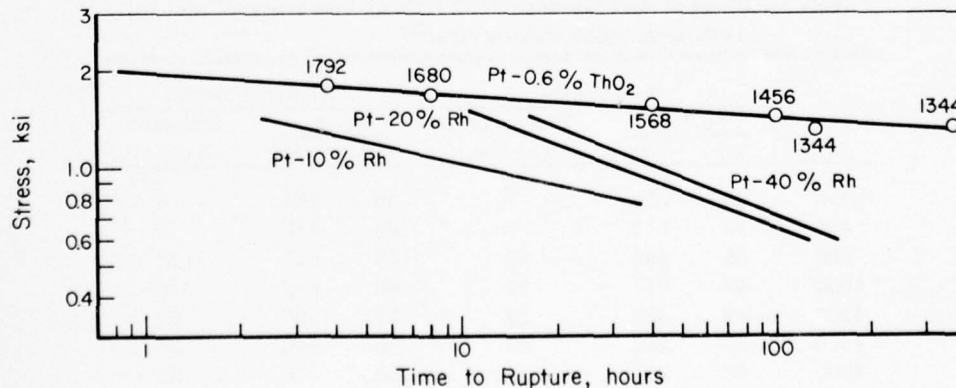


Figure 74. Stress Versus Time-to-Rupture for Platinum-0.6% Thoria and Platinum-Rhodium Alloys at 1450 C in Air<sup>(4)</sup>

Recently, Fuschillo and Gimpl<sup>(5)</sup> have measured electrical and tensile properties of Pt-ThO<sub>2</sub>, where the dispersoid particles were less than 0.05 micron in average diameter and the ThO<sub>2</sub> contents were 1.8 and 2.2 percent by volume. The results are summarized in Figures 75 and 76. The electrical resistivity was greater than that predicted by a simple volume effect due to the dispersoid.

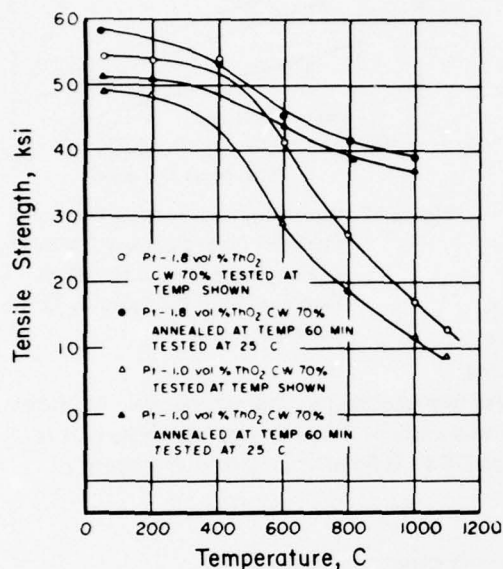


Figure 75. Tensile Strength of Pt-ThO<sub>2</sub> Alloys at Various Temperatures and at 25 C After Annealing for 60 Min. at Temperatures Shown<sup>(5)</sup>

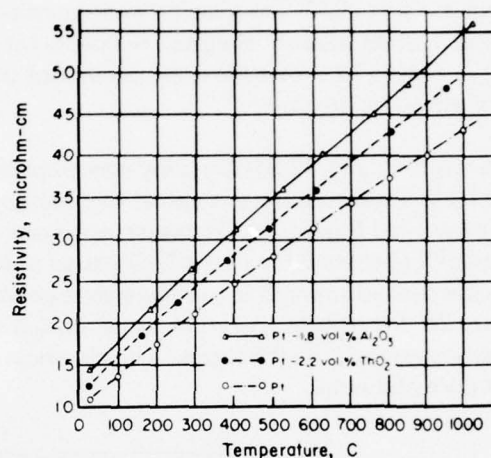


Figure 76. Resistivity Versus Temperature for Pt-2.2 Vol. % ThO<sub>2</sub>, Pt-1.8 Vol. % Al<sub>2</sub>O<sub>3</sub> Alloys and Pt (Wrought)<sup>(5)</sup>

Additions of 0.5 vol. % ThO<sub>2</sub> to Pt-Rh alloys has been investigated by Knight and Taylor<sup>(6)</sup>. The low dispersoid content allowed high ductility to be retained, and repeated drawing with intermediate anneals was used to produce wire of 1.5-mm diameter. The tensile strength and the elongation of thoriated and non-thoriated Pt-10Rh wires are compared in Table 71. Whereas the ductility of the Pt-Rh alloy was reduced on annealing at 1400 C (due to grain growth), this did not occur in the Pt-Rh-ThO<sub>2</sub> alloy even on annealing to 1600 C. The influence of the ThO<sub>2</sub> dispersoid on room-temperature strength is not great, but the increase in high-temperature strength is significant, e.g., it is equivalent to increasing the working temperature by 300-400 C (see Figure 77).

Table 71. Effect of Heat Treatment for 1 Hour on Cold-Worked Platinum, 10 Percent Rhodium Alloy Wires<sup>(6)</sup>

Temp., C	Melted Alloy			Thoriated Alloy		
	U.T.S.		Elongation, % on 2 in.	U.T.S.		Elongation, % on 2 in.
	ksi	MPa		ksi	MPa	
Room	90	620	4	96	661	4
400	74	510	5	83	572	5
800	65	448	13	75	517	10
1000	46	317	32	68	469	16
1200	44	303	32	52	358	30
1400	43	296	32	50	345	34
1500	42	289	20	50	345	34
1600	40	276	18	50	345	34



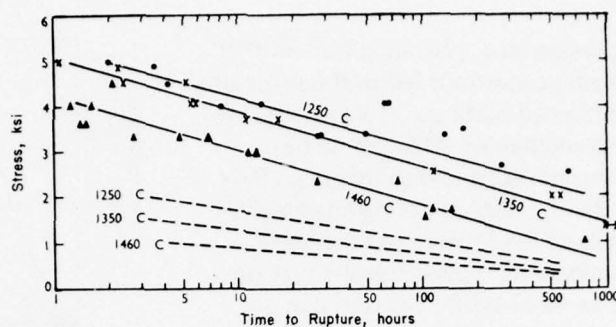


Figure 77. Thoriated Platinum-10 Percent Rhodium Alloy; Stress/Time-to-Rupture Relationship, Determined on Wires 0.062 in. in Diameter (Broken lines show interpolated data for Pt-10Rh alloy produced by melting)<sup>(6)</sup>

Portnoy<sup>(7)</sup> comments that screen catalysts of Pt-Rh-ThO<sub>2</sub> have a catalytic activity equal to screens made of cast alloys, and also have greater durability and retain their shape as, for example, when used in the production of HNO<sub>3</sub>.

Many other oxide dispersants for the strengthening of platinum have been proposed; chiefly Al<sub>2</sub>O<sub>3</sub>, MgO, and ZrO<sub>2</sub>. All of these provide effective strengthening of platinum and they are stable under strongly oxidizing conditions. However, if the atmosphere is not strongly oxidizing, all of the oxides, including ThO<sub>2</sub>, have the shortcoming of partial dissociation. For example, if the oxidizing potential of the surrounding atmosphere is reduced below a certain level, these oxides dissociate and allow platinum to extract metal from the refractory to form dilute alloys and low-melting-point phases.

Work at the Johnson Matthey research laboratories<sup>(8)</sup> indicated that of the above oxides, ZrO<sub>2</sub> was the most reactive, while MgO was the least. The character and intensity of reactions of platinum with ThO<sub>2</sub> were between the above extremes and were similar to those which occurred with Al<sub>2</sub>O<sub>3</sub>. ZrO<sub>2</sub> was tested because the oxide was considered to be more stable than Al<sub>2</sub>O<sub>3</sub>. However, platinum has a very high affinity for zirconium and when these metals are heated together at temperatures as low as 1100 C, they form Pt<sub>3</sub>Zr with a vigorous reaction. On the other hand, there were few signs of reactions between platinum and MgO even under conditions of very low oxidizing potential. MgO was the only refractory examined that resisted decomposition under a neutral atmosphere that occurred with the other refractories at temperatures as low as 1200 C.

Fuschillo, et al.<sup>(5)</sup> investigated the tensile properties (see Table 72) and the electrical properties (see Figure 76) of DS-Pt-Al<sub>2</sub>O<sub>3</sub>. The platinum was precipitated on Al<sub>2</sub>O<sub>3</sub> particles of 0.05 micron average diameter. The resulting powder was dried, degassed, pressed, extruded, heat treated, and worked by normal powder-metallurgy techniques to form rods or wire. At 1000 C, the Al<sub>2</sub>O<sub>3</sub> particles showed rapid growth. The Al<sub>2</sub>O<sub>3</sub> dispersion produced a greater increase in resistivity for a given volume than the ThO<sub>2</sub> particles.

Table 72. Tensile Properties of Dispersion-Strengthened Platinum Alloys<sup>(5)</sup>

Alloy	Test Temp., C	Ultimate Tensile Strength		0.2% Yield Strength		Elong., %
		ksi	MPa	ksi	MPa	
Pt-1.8Al <sub>2</sub> O <sub>3</sub> , cold-rolled 50%	25	48	330	47.9	330	1.2
	260	37	255	36.5	251	1.5
	537	34.9	240	33.9	234	2.5
Cold-rolled + annealed at 1000 C	25	26.5	183	18.4	127	12.0
As extruded	25	36	248	32	220	11.0

The desire to produce dispersion-strengthened platinum that was stable under low oxidizing conditions led to the surprising finding that carbides strengthened platinum more effectively than oxides and that this strengthening effect could be achieved with concentrations of dispersoid so low (e.g., 0.04 to 0.08 percent TiC) that the ductility, working characteristics, and electrical properties of the Pt were not seriously impaired.<sup>(2)</sup> Figure 78 shows some typical creep curves obtained on 1/8-in.-diameter wires of DS Pt-TiC tested in air at 1400 C. Cold working (especially biaxial deformation) was found to markedly increase the high-temperature creep strength of this material. While rolling of sheet improved the high-temperature creep strength, processes such as swaging and wire drawing, which deformed the metal in two directions, were particularly effective in inducing working textures with high creep strength. These effects are illustrated by the stress-rupture properties of DS Pt-TiC sheet and wire versus pure platinum given in Table 73. Table 73 also contains data that show that the TiC dispersions were equally effective in increasing the stress-rupture life of Pt-10Rh wire. Selected physical properties of these alloys are given in Table 74.

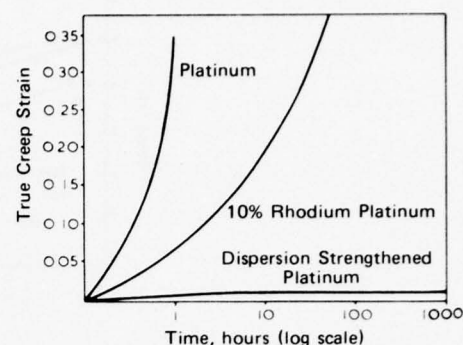


Figure 78. Creep Curve of Dispersion-Strengthened Platinum Stabilized with a Refractory Carbide Compared with Those of Pure Platinum and 10% Rhodium-Platinum Produced by Conventional Methods (Temp. 1400 C, stress 750 lb/in<sup>2</sup>)<sup>(2)</sup>

Table 73. Stress-Rupture Properties of TiC-Dispersion-Strengthened Platinum and Pt-10Rh Alloy<sup>(2)</sup>

Material	Minimum Life, hours, at 1400 C, under stress level indicated		
	700 psi	1400 psi	2800 psi
Pure Pt wire	0.5-1	—	—
Pt-TiC wire <sup>(a)</sup>	1000	800	30
Pt-10Rh wire	50	10	1
Pt-10Rh-TiC wire <sup>(a)</sup>	1000	1000	100
Pt sheet	0.5	—	—
Pt-TiC sheet <sup>(a)</sup>	150	30	—

(a) TiC content from 0.04 to 0.08 weight percent.

Table 74. Physical Properties of TiC-Dispersion-Strengthened Platinum and a Rhodium-Platinum Alloy<sup>(2)</sup>

Alloy	Specific Gravity, gms/cc	Specific Resistance at 20 C, $\mu$ ohm cm	Temperature Coefficient, 0-100 C	U.T.S. (annealed)		Elongation (annealed), %	Modulus of Elasticity (annealed)	
				ksi	MPa		psi	MPa
Melted Pt	21.4	10.6	.00392/C	22.4	154	40	$22 \times 10^6$	$.152 \times 10^6$
Dispersion-Strengthened Pt	21.288	12.0	.0036/C	30.9	213	35	$23 \times 10^6$	$.158 \times 10^6$
Melted 10% Rh-Pt	20	18.4	.0017/C	47.0	324	35	$27 \times 10^6$	$.186 \times 10^6$
Dispersion-Strengthened 10% Rh-Pt	19.862	21.22	.0016/C	51.5	355	30	$28 \times 10^6$	$.193 \times 10^6$

However, in spite of the attractive properties achieved with the carbide-dispersion-strengthening of platinum, problems associated with obtaining consistent and reproducible properties on a large scale have not been satisfactorily solved. The blending together of platinum with very small amounts of inert powder, either directly or via intermediate compounds, have apparently presented serious manufacturing problems.

These seem to have been solved, however, by the engineers of Johnson Matthey since the introduction of their ZGS platinum, which is a  $\text{ZrO}_2$  dispersion-strengthened grade. Their process involves selective oxidation of zirconium in a platinum alloy containing only 600 ppm of zirconium metal in solid solution. One patent<sup>(9)</sup> describes the process as spraying a molten metal and a reactive constituent on a target. The reactive constituent is passed through an atmosphere that converts it into a material that forms a dispersion phase within the host material when the latter is deposited on the target. Some room-temperature properties of the ZGS alloy are compared with those of platinum and the Pt-10Rh alloy in Table 75. The stress-rupture properties of ZGS at 1400 C are compared with those for platinum and some Pt-Rh alloys in Figure 79. The steady-state creep rates of these same materials in sheet form are shown as a function of applied stress at 1400 C in Figure 80. Similarly, the ultimate tensile strength of these materials at room temperature and elevated temperatures are listed in Table 76.

**Table 75. Room-Temperature Properties of ZGS Platinum, Pure Platinum, and 10% Rhodium-Platinum<sup>(10)</sup>**

	ZGS Pt	Melted Pt	Melted 10% Rh-Pt
Specific gravity at 20 C, g/cm <sup>3</sup>	21.38	21.45	20.00
Specific resistance at 20 C, $\mu$ ohm cm	11.12	10.6	18.4
Temperature coefficient of resistance per C, Mean 0-100 C	0.0031	0.0039	0.0017
U.T.S., kg/mm <sup>2</sup> (MPa) (annealed)	18.6 (182)	12.7 (124)	33.7 (330)
Elongation, % (annealed)	42	40	35
Hardness, H <sub>v</sub> (annealed)	60	40.42	75

**Table 76. Ultimate Tensile Strength of ZGS Platinum, Melted Platinum, and Several Rhodium-Platinum Alloys at Room and Elevated Temperature<sup>(10)</sup>**

Test Temperature	Tensile Strength									
	Pure Pt		10% Rh-Pt		20% Rh-Pt		40% Rh-Pt		ZGS Pt	
	kg/mm <sup>2</sup>	MPa	kg/mm <sup>2</sup>	MPa	kg/mm <sup>2</sup>	MPa	kg/mm <sup>2</sup>	MPa	kg/mm <sup>2</sup>	MPa
20 C annealed	12.7	124	33.75	331	48.8	478	57.5	564	18.6	182
1200 C	—	—	4.8	47	10.1	99	—	—	3.8	37
1400 C	< 0.40	3.9	3.6	35	5.5	54	7.87	77	2.9	28
1500 C	—	—	—	—	—	—	—	—	2.4	24

The ZGS platinum, as is true with most other dispersion-strengthened alloys, displays its most superior properties at very high temperatures. At room temperature, the alloy is only moderately stronger than pure platinum and is considerably weaker than the solid-solution strengthened Pt-Rh alloys.

The properties of ZGS-Pt wire are equal to or slightly higher than those of sheet material. The mechanical working of wire shapes (as described previously) imparts added improvement in properties by including a highly aligned, recrystallized texture. A most significant factor related to ZGS wire is that for all practical purposes its electrical characteristics are similar to those of pure platinum, which allows direct substitution of the alloy for pure platinum in electrical equipment.



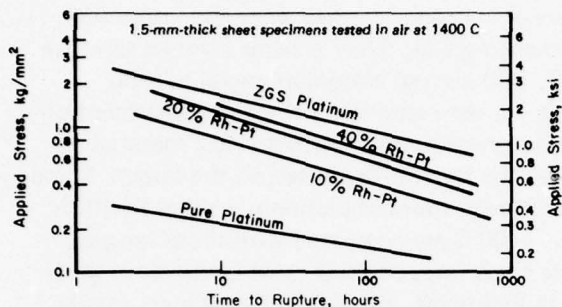


Figure 79. Stress-Rupture Properties of ZGS Platinum Compared to Those of Pure Platinum and Some Commercially Important Rhodium-Platinum Alloys<sup>(10)</sup>

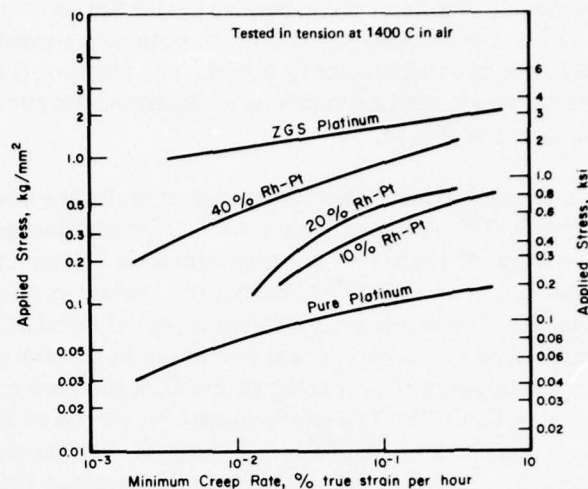


Figure 80. Minimum Creep Rate Curves for Platinum, 10% Rhodium-Platinum and ZGS Platinum Sheet<sup>(10)</sup>

The ZGS alloy is also commercially available as rod, plate, strip, and foil. It is suggested for handling molten glass, for use in spinnerets for glass-fiber manufacture, optical glass stirrers, glass holding bowls, electrical contacts, elements for high-temperature furnaces, laboratory equipment, crucibles, and dishes.

Hughes<sup>(11)</sup> recently discussed the characteristics of ZGS platinum as a production material. He points out the need for care in design. The joining of dispersion-strengthened metals is normally difficult, but, because platinum is free from surface oxidation, it can be readily joined by non-fusion techniques such as diffusion bonding or pressure deformation bonding. In many cases, because of the excellent formability of the ZGS alloy, welds can be eliminated or removed to regions of lower temperature or stress.

## REFERENCES

1. British Patent No. 578,956.
2. Darling, A. S., Selman, G. L., and Bourne, A. A., "Dispersion-Strengthened Platinum—Improved High-Temperature Creep Properties", *Platinum Metals Review*, **12**, 7-13 (January 1968).
3. Bufferd, A. S., Zivlisky, K. M., Blucher, J. T., and Grant, N. J., "Oxide Dispersion Strengthened Platinum", *Inter. J. of Powder Metallurgy*, **3** (1), 17-26 (1967).
4. Albert, H. J., and Hill, J. S., "Development of a Pt-ThO<sub>2</sub> Alloy for Resistojet Thruster Use", NASA Cr-111959 (July 1971). (MCIC 81944)
5. Fuschillo, N., and Gimpl, M. L., "Electrical and Tensile Properties of Cu-ThO<sub>2</sub>, Au-ThO<sub>2</sub>, Pt-ThO<sub>2</sub>, Au-Al<sub>2</sub>O<sub>3</sub>, and Pt-Al<sub>2</sub>O<sub>3</sub> Alloys", *J. of Materials Sciences*, 1078-1086 (1970).
6. Knight, J. R., and Taylor, B., "Production and Properties of Grain-Stabilized Platinum and Platinum Alloys", *Powder Metallurgy*, (10), 108-118 (1962).
7. Portnoy, K. I., and Babich, B. N., "Dispersion Hardened Metals", Moscow, Metallurgiya (1974).
8. Darling, A. S., Selman, G. L., and Rushforth, R., "Platinum and the Refractory Oxides—Compatibility and Decomposition Processes at High Temperatures", *Platinum Metal Review*, **14** (2), 54-60 (1970).
9. U. S. Patent No. 3,696,502 (October 10, 1972).
10. Selman, G. L., Day, J. G., and Bourne, A. A., "Dispersion Strengthened Platinum—Properties and Characteristics of a New High-Temperature Material", *Platinum Metals Review*, **18** (2), 46-57 (1974).
11. Hughes, J. E., "Dispersion Strengthening of Platinum", *Planseeberichte f. Pulvermetallurgie*, **22**, 292-296 (1974).

## TIN

For tin, room temperature represents 60 percent of the temperature scale from absolute zero to its melting point, e.g.,  $0.6 T_m$ . Thus, any room-temperature hardening of tin can be regarded as increasing its "heat resistance".

Tin-oxide, dispersion-strengthened tin has been prepared from tin powders by extrusion.<sup>(1)</sup> This material showed a higher tensile strength than cast and extruded tin, and, under creep conditions at 150 C ( $0.84 T_m$ ), was superior to any of the usual tin-base alloys. Further work by Eastwood and Robins<sup>(2)</sup> explored the effect of the degree of  $\text{SnO}_2$  dispersion on the properties of DS tin. Separate fractions of tin powder in the range 35 to <8 microns were formed into rod by extrusion. The room-temperature strength increased with decreasing powder particle size and was accompanied by a marked reduction in ductility (see Table 77).

**Table 77. Oxide Content and Room-Temperature Properties of Sn-SnO Alloys<sup>(2)</sup>**

Powder	Particle Size, $\mu\text{m}$	Oxide Content, wt. % $\text{SnO}$ in g	Tensile Strength		Elongation, %	Hardness, HV
			ksi	MPa		
Cast and extruded tin	—	—	3.36	23	80	8
Original powder	-53	0.94	8.28	57	16	16
Original powder after oxidation	-53	1.7	8.74	60	16	16
Coarse fraction	-52 +30	0.65	7.39	51	30	15
Medium fraction	-20 +15	0.78	7.84	54	20	16
Fine fraction	- 8	1.1	9.18	63	6	19

Stress-to-rupture testing at 100 C showed that the finest powder gave the best elevated-temperature properties. It was concluded that the degree of oxide dispersion, rather than the total amount of oxide, was the important factor. However, the retardation of grain growth at elevated temperatures appeared to be dependent on the total amount of oxide present rather than its degree of dispersions. DS tin has no great advantage over pure tin and its alloys on the basis of short-term strength, but does show a significant superiority in long-term strength. Figure 81 compares the time-to-rupture for these materials as function of initial stress at 150 C, while Figure 82 shows stress-to-rupture tests at 100 C for DS tin containing dispersoids of various grain size. These figures show that, for a 100-hour life, the rupture stress for the DS tin alloys is 4 to 6 times greater than that of the cast alloys or pure tin.

Sartor, et al.<sup>(4)</sup> have developed a technique using ultrasound to disperse  $\text{Al}_2\text{O}_3$  in molten tin. Figure 83 shows the temperature dependence of the tensile strength of pure tin and Sn-SnO alloys of increasing oxide content. Figure 84 is a similar plot for another series of Sn-SnO alloys made with an oxide of smaller particle size. These alloys also contain 0.25 or 0.75 percent titanium since this alloying element favors the dispersion of the oxide within the matrix. For both alloy series, the tensile strength of the dispersion-strengthened alloys remains almost double that for pure tin, even up to  $0.90 T_m$ .

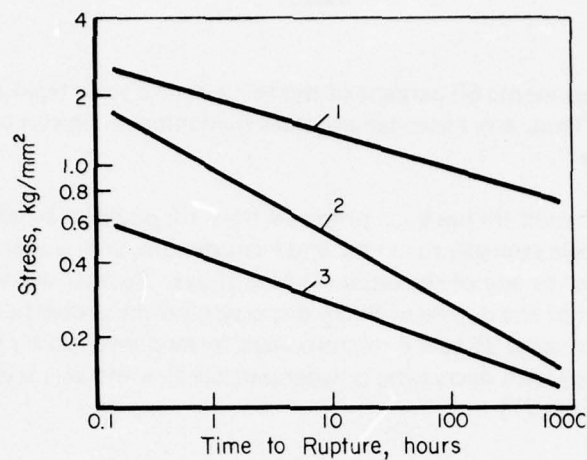


Figure 81. Time-to-Rupture as a Function of Initial Stress at 150 C: 1-Sn+25% SnO<sub>2</sub>; 2-Sn+6% Sb; 3-Pure Tin<sup>(3)</sup>

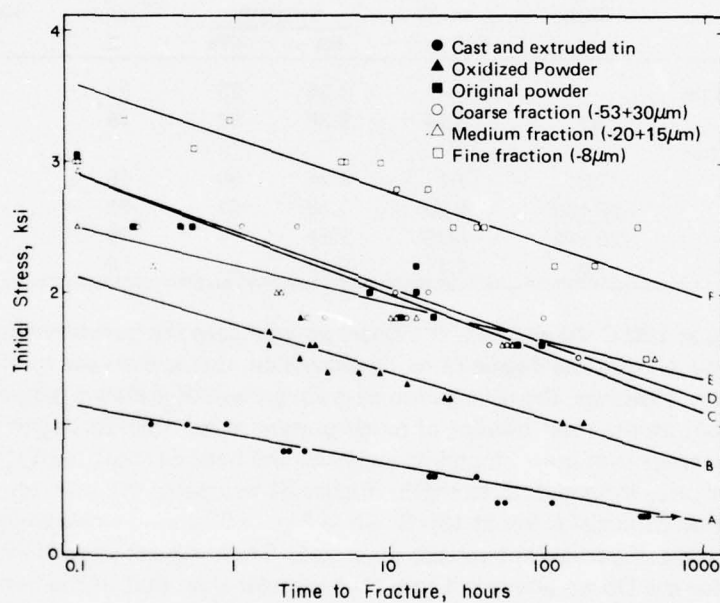


Figure 82. Stress-to-Rupture Tests at 100 C<sup>(2)</sup>



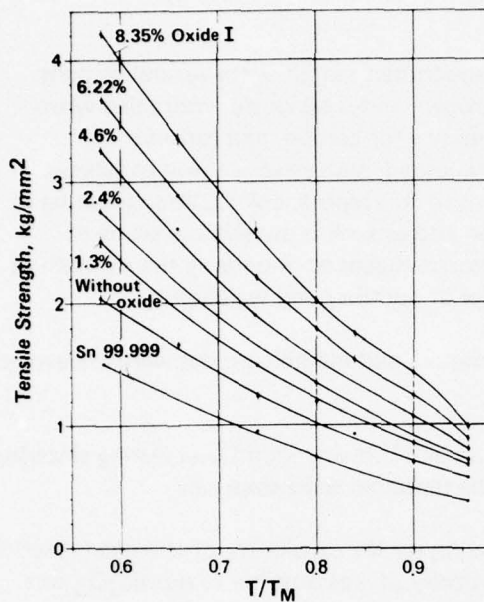


Figure 83. Temperature Dependence of Tensile Strength of Sn-0.25Ti Samples with Different Contents of Tin Oxide, Oxide Particle Size of 1.85 Microns<sup>(4)</sup>

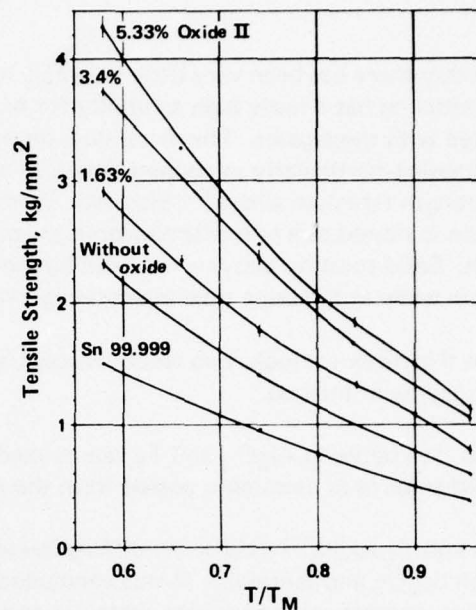


Figure 84. Temperature Dependence of Tensile Strength of Sn-0.75Ti Samples with Different Contents of Tin Oxide, Oxide Particle Size of 1.15 Microns<sup>(4)</sup>

#### REFERENCES

1. Eastwood, B. J., and Robins, D. A., Powder Metallurgy, 7 (14), 99 (1964).
2. Eastwood, B. J., and Robins, D. A., "The Effect of Particle Size and Oxide Dispersion on the Properties of Tin Extruded from Powder", Powder Metallurgy, 9 (18), 175-184 (1966).
3. Portnoy, K. I., and Babich, B. N., "Dispersion Hardened Materials", Moscow, Metallurgiya, 127-199 (1974).
4. Sartor, B., Staats, H., and Seemann, H. J., "Untersuchungen über Ultraschalldispersion von  $Al_2O_3$  in Zinnschmelzen", Metall, 28 (8), 771-777 (1974).

## TANTALUM

Apparently there has been very little incentive to dispersion strengthen tantalum for several reasons. First, tantalum has a fairly high solubility for oxygen and nitrogen, and is seriously embrittled when saturated with these gases. The metal does have a greater tolerance for carbon, and carbide-strengthening—particularly in conjunction with solid-solution alloying—is an effective way to achieve high-strength tantalum alloys.<sup>(1)</sup> However, from the viewpoint of this report, carbide strengthening in tantalum is viewed as a precipitation-strengthening mechanism and as such is outside the scope of interest. Solid-solution alloying has been by far the most effective means of improving the strength of tantalum while at the same time maintaining a reasonable level of ductility and weldability.

Despite this bleak outlook, two recent Russian articles on tantalum and metallic oxides were uncovered which may be of interest.

The reaction between  $\text{Al}_2\text{O}_3$  and Ta was studied by Elyutin, et al.<sup>(2)</sup> It was found that during sintering a certain amount of aluminum passed from the  $\text{Al}_2\text{O}_3$  into the tantalum solid solution.

Dubok and Tyutkalo<sup>(3)</sup> used X-ray diffraction analysis to investigate the possibility of chemical reactions between  $\text{Sc}_2\text{O}_3$  and tantalum. It was concluded that, theoretically, it was possible to use  $\text{Sc}_2\text{O}_3$  as a dispersion-strengthening phase for tantalum and to coat tantalum "artifacts" with  $\text{Sc}_2\text{O}_3$ .

## REFERENCES

1. Chang, W., "Effect of Carbide Dispersion in Tantalum-Base Alloys", Refractory Metals and Alloys IV, Research and Development, Volume 1, Metallurgical Society Conferences, French Lick, Indiana, 41 (1965), pp 405-422.
2. Elyutin, V. P., Mozhukhin, E. I., and Varenkov, A. N., "Reaction Between  $\text{Al}_2\text{O}_3$  Inclusions and Ta Metal", *Izvestiya Akad. Nauk, SSSR, Metalliy*, 47 (1969).
3. Dubok, V. A., and Tyutkalo, L. I., "High-Temperature Compatibility of Refractory Metals With  $\text{Sc}_2\text{O}_3$ ", *Poroshkovaya Metallurgiya*, No. 1, 83-87 (1968).

## TITANIUM

Since titanium has a relatively high melting point, 1668 C, it is expected that the metal should retain significant strength at  $0.5 T_m$ . However, prior research has shown that the allotropic transformation temperature 882 C is more indicative of the high-temperature strength capability of titanium than the melting temperature. The practical-use temperature limit for existing titanium alloys has been approximately 535 C (1000 F). There has been continued interest in developing titanium alloys that can be used at higher temperatures than those now commercially available.

Dispersion strengthening offers at least a theoretical possibility of achieving strength at higher temperatures in titanium-base materials. Much research was conducted in this area from 1950-1960. Many of these early results are summarized in Reference 1. These include experiences with the following types of dispersoids:

- Intermetallics— $Ti_5Si_3$ , TiC, TiAl,  $TiB_2$ , TiB,  $Ti_2Cu$ , TiS, TiP, and  $B_4C$
- Oxides— $Al_2O_3$ ,  $ThO_2$ ,  $ZrO_2$ ,  $Y_2O_3$ ,  $Ge_2O_3$ ,  $La_2O_3$ ,  $CeO_2$ , and  $Ce_2O_3$ .

Holladay<sup>(1)</sup> concluded on reviewing the researches of the decade that dispersion strengthening of titanium with insoluble particles was probably useful for both short-time and long-time improvement at high temperatures. However, the optimum compounds and processing conditions had not yet been discovered. Dispersion hardening with mechanically dispersed metallic particles offered little promise. If sufficiently fine particles were used to obtain strengthening, the solution rate of the particles in the titanium matrix became excessive. On the other hand, intermetallic compounds, such as  $Ti_5Si_3$ ,  $Ti_2Cu$ , and TiC, and oxides, such as  $CeO_2$  or other rare-earth type oxides, showed promise.

Dispersion strengthening by silicon additions to titanium alloys via melt-casting, fabrication, and heat treatment, to form  $Ti_5Si_3$  and possibly other silicides as dispersants, was practiced as an integral part of alloy development techniques in both Great Britain and the Soviet Union in the late 1950's and into the 1960's. A typical British alloy, Imperial Metals Industries designation IMI-679, Ti-11Sn-5Zr-2.25Al-1Mo-0.25Si, was evaluated in the early 1960's on both sides of the Atlantic. Typical Soviet alloys were: VT3-1, Ti-5.5Al-2Mo-2Cr-1Fe-0.2Si, and alloys of the AT series, e.g., AT4, Ti-4Al-0.8Cr-0.6Fe-0.4Si-0.01B. By the mid 1960's, IMI developed a complex alloy containing both silicon and tungsten, IMI-684, Ti-6Al-5Zr-1W-0.2Si, which had quite good elevated-temperature properties and metallurgical stability as indicated by the data in Table 78 and 79. A whole series of silicon-strengthened British alloys were developed which included the following:

IMI-679	Ti-2.25Al-11Sn-5Zr-1Mo-0.2Si
IMI-680	Ti-2.25Al-11Sn-4.2Mo-0.25Si
IMI-684	Ti-6Al-5Zr-1W-0.2Si
IMI-700	Ti-6Al-5Zr-4Mo-1Cu-0.2Si-0.07C
Hylite-55	Ti-3Al-6Sn-5Zr-0.5Si
Hylite-60	Ti-3Al-6Sn-5Zr-2Mo-0.5Si
Hylite-65	Ti-3Al-5.5Sn-5.5Zr-0.5Mo-0.5Si.

At about this time various, U.S. researchers showed a renewed interest in dispersion-strengthened titanium alloys. Anthony<sup>(3)</sup> investigated the high-temperature strength and stability characteristics of complex alpha-titanium alloys, (e.g., Ti-6Al-3Sn-3Zr) that contained dispersions of silicide, carbide, and boride particles. Boride dispersions were coarse and generally ineffective with respect to strength. Carbide dispersions increased high-temperature strength but simultaneously reduced low-temperature toughness and ductility to dangerously low levels after creep exposure. Silicide dispersions ( $Ti_5Si_3$  and  $Zr_5Si_3$ ) increased the high-temperature tensile strength of the matrix in the alpha-worked condition, but alpha-beta and/or beta heat treatments were required to increase high-temperature creep strength.



**Table 78. Typical Tensile Properties for Alloy IMI-684 Solution Heat Treated at 1913 F (1045 C), Oil Quenched, and Aged for 24 Hours at 932 F (500 C)<sup>(2)</sup>**

Test Temp., F	0.1% Offset Yield Strength		Ultimate Tensile Strength		Elong., % in 4 diam.	Reduction in Area, %
	ksi	MPa	ksi	MPa		
70(RT)	132	909	150	1034	17	22
212	111	765	130	896	15	26
392	95	655	115	792	14	29
572	86	593	105	723	14	31
752	78	537	98	675	16	31
932	73	503	94	648	18	31
1022	70	482	90	620	19	31

**Table 79. Thermal Exposure Stability Test Data Obtained for Alloy IMI-684 Samples From 0.5-Inch-Diameter Rod<sup>(2)</sup>**

Exposure Time at 977 F, hours	0.1% Offset Yield Strength		Ultimate Tensile Strength		Elong., % in 4 diam.	Reduction in Area, %
	ksi	MPa	ksi	MPa		
None	137	944	153	1054	16	23
100	140	965	157	1082	14	21
300	142	978	160	1102	9	19
1000	142	978	159	1096	9	12

(a) Solution heat treated for 3/4 hour at 1913 F (1045 C), oil quenched and aged for 24 hours at 932 F (500 C).

The research has been continued intermittently through the years. For example, in 1970, two alloy development programs were completed which illustrate the success possible in achieving high strengths with this type of alloy, but at the same time illustrate the problems involved in selecting a balanced composition. At General Electric Aircraft Engine Division<sup>(4)</sup> and at Reactive Metals<sup>(5)</sup>, objectives were Air Force-established goals which included the following combinations of characteristics:

	As Heat Treated	
	RT	900 F
Ultimate Tensile Strength, ksi	140-143	104-105
Yield Strength, ksi	130	90
Tensile Strength Ratio	1.5(a)	—
10,000 Cycle Fatigue Strength, ksi	90(b)	—
Creep Strength to Limit Creep to 0.2%		
in 10,000 hours exposure, ksi	—	55-58
in 100 hours exposure ksi	—	(65 at 1000 F)

After Simulated 900 F/10,000 Hour Exposure (0.1% Creep)		
Ultimate Tensile Strength, ksi	0.9(140-143)	—
Yield Strength, ksi	0.9(130)	—
Tensile Elongation, percent	5	—
Tensile Reduction in Area, percent	10-15	—
Tensile Strength, Ratio	1.4(a)	—
5,000 Cycle Fatigue Strength, ksi	—	90(b)

(a) Notched ( $K_t=4$ ) to unnotched ratio.

(b)  $K_t=1.0$ .

The basis for composition selection involved maximizing the alpha stabilizer content (aluminum, tin, zirconium, gallium, and oxygen) to improve strength, modifying with beta stabilizers (molybdenum, vanadium, columbium, tungsten, manganese, iron, and chromium) in combination with a dispersoid phase-forming element (silicon) to further increase strength (particularly creep strength), and, at the same time, maintaining a metallurgically stable alloy. As an example of metallurgical limitations, alpha-stabilizer content must be maintained below an equivalent aluminum content of about 8 weight percent because above this level, titanium alloys become embrittled by an ordering reaction (forming  $Ti_3Al$ ). Alpha-alloy bases that were selected included combinations of titanium-aluminum with zirconium, zirconium-tin, or zirconium-tin-gallium, as a means for minimizing the  $Ti_3Al$ -type embrittling reaction while at the same time alloying to promote the maximum strengthening effect. To such a base, beta-stabilizer and compound-forming additions are made in as large amounts as tolerable in order to strengthen the material further without causing embrittlement.

Interestingly, at the conclusion of composition screening, each research group arrived at similar alloy selections for meeting target goals. The General Electric alloy selections were Ti-6.5Al-4Zr-1.5Mo-0.7Si and Ti-4.5Al-2Sn-3Zr-3Ga-1Mo-0.5Si.<sup>(4)</sup> Reactive Metals alloy choices were Ti-5Al-5Sn-2Zr-0.8Mo-0.5Si and Ti-5Al-5Sn-2Zr-0.8Mo-0.7Si.<sup>(5)</sup> The degree to which these materials meet the target goals is illustrated in Table 80 and Figure 85. Both companies recognized that optimization was incomplete, but concurred that further slight alloy modification of these materials combined with additional thermomechanical research could lead to a full satisfaction of the original goals.

More recently, Dixon and Skelly<sup>(6)</sup> added  $ThO_2$  and  $Ce_2O_3$ -2ZrO<sub>2</sub> to titanium and several titanium alloys during arc melting. The refractory compounds apparently dissolved during melting but precipitated as dispersed phases on cooling. Although the tensile strengths of the base materials at room temperature and 540 C were improved the tensile ductilities were reduced by these oxide additions. It was also noted that the refractory particle size and interparticle spacing were larger than recommended for maximum dispersion strengthening. Heat treating further increased the size of the refractory particles. Attempts to incorporate  $Y_2O_3$  by this technique were not successful. However, other studies<sup>(7)</sup> of the reaction of the molten titanium with certain rare oxides indicated  $Y_2O_3$  to be most stable. For example, it was concluded that at temperatures less than  $0.6 T_m$ ,  $Y_2O_3$  is not reduced by solid titanium and coexists with an oxygen level of less than 1500 ppm.

Waugh<sup>(8)</sup> has also evaluated 16 oxides primarily for their elevated-temperature compatibility with titanium. Lutecium-oxide ( $Lu_2O_3$ ), neodymium-oxide ( $Nd_2O_3$ ), and dysprosium-oxide ( $Dy_2O_3$ ) dispersoids showed no detectable reaction with the titanium after vacuum sintering for 4 hours at 1065 C.  $Pr_6O_{11}$  and  $Tb_2O_5$ , with titanium, reacted at 560 and 520 C, respectively.

**Table 80. Mechanical Properties of Candidate Alloys for 900 F (482 C) Jet Engine Service<sup>(4,5)</sup>**  
(Solution heat treatments and aging conditions vary from alloy to alloy)<sup>(a)</sup>

Property	Goals	Composition, percent				
		Ti-5Al-5Sn- 2Zr-0.8Mo- 0.5Si	Ti-5Al-5Sn- 2Zr-0.8Mo- 0.7Si	Ti-4.5Al-2Sn- 3Ga-3Zr-1Mo- 0.5Si	Ti-6.5Al-4Zr- 1.5Mo-0.7Si	
<u>As Heat Treated</u>						
Ultimate Tensile Strength (RT), ksi (MPa)	140 (965)	156 (1075)	163 (1123)	160 (1102)	162-166 <sup>(b)</sup> (1116-1144)	
Yield Strength (RT), ksi (MPa)	130 (896)	137 (944)	144 (992)	146 (1006)	147-150 <sup>(b)</sup> (1013-1034)	
Ultimate Tensile Strength (900 F), ksi (MPa)	105 (723)	112 (772)	116 (799)	111 (765)	123 <sup>(b)</sup>	
Yield Strength (900 F), ksi (MPa)	90 (620)	87 (599)	88 (606)	92 (634)	94-101 <sup>(b)</sup> (648-696)	
100,000 Cycle Fatigue (RT), ksi (MPa)	—	—	—	~80 (551)	—	
10,000 Cycle Fatigue (RT), ksi (MPa)	90 (620)	—	—	>90 (620)	—	
<u>Creep Strength (0.2%)</u>						
100 hr (1000 F), ksi (MPa)	65 (448)	65 (448)	50 (345)	55-60 (379-413)	>55 <sup>(c)</sup> (379)	
10,000 hr (900 F), ksi (MPa)	55-58 (379-400)	57-58 (393-400)	<50 (345)	58 (400)	53-60 <sup>(b)</sup> (365-413)	
<u>Post Creep Exposure<sup>(d)</sup></u>						
Ultimate Tensile Strength (RT), ksi (MPa)	0.9(140) (965)	162 (1116)	167 (1151)	155 (1068)	165 (1137)	
Yield Strength (RT), ksi (MPa)	0.9(130) (896)	147 (1013)	152 (1047)	147 (1013)	151 (1040)	
Elongation (RT), percent	5	9	14	4	9.5	
Reduction in Area (RT), percent	10-15	14	24	6	18	

(a) Typical solution temperatures, 1870-1900 F (1021-1037 C). Typical aging condition, 2 hours at 1100 F (593 C).

(b) Two heat treatments are represented.

(c) This value represents the strongest condition tested.

(d) 200 hours at 1000 F (538 C) and 55 ksi (379 MPa) exposure. These properties represent the most stable conditions tested.

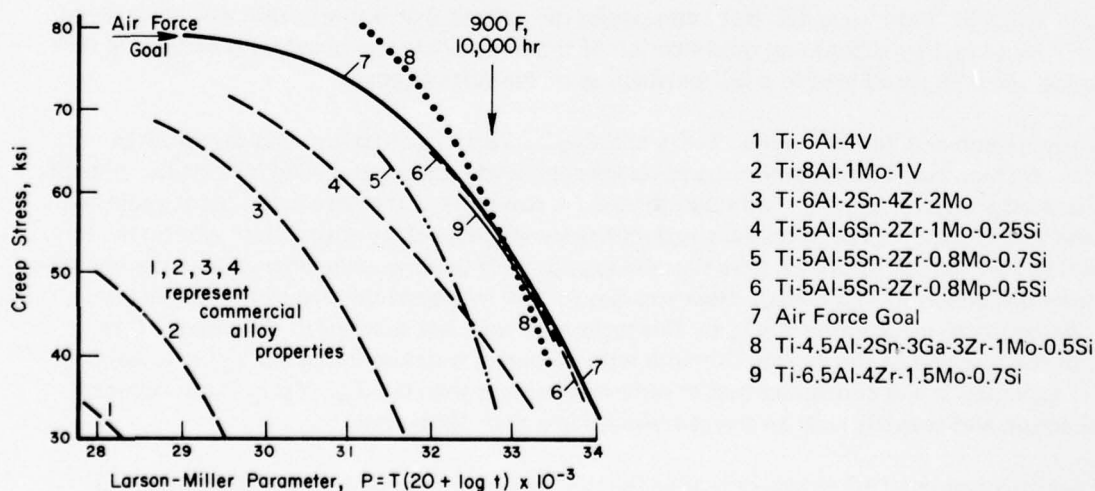


**Figure 85. Comparison of 0.2% Creep Data Obtained for Commercial and Experimental Titanium-Based Alloys<sup>(4,5)</sup>**



Wright and Wilcox<sup>(9)</sup> attempted to prepare dispersion-strengthened Ti-6Al-4V-Y<sub>2</sub>O<sub>3</sub> by attritor milling, in view of the success this technique had with DS-nickel alloys. Because of the pyrophoric nature of titanium, a Szegvare 1-SB attritor was modified to operate under vacuum or under slowly flowing purified helium. Loading and unloading operations were carried out in a helium atmosphere by first evacuating the relevant vessels and then backfilling with helium. After attriting, the alloy powder was transferred in a helium-filled, sealed glass bottle to an argon-filled glove box where it was screened, weighed, sampled, and then tamped into mild-steel extrusion cans. The extrusion cans were sealed by electron-beam welding and vacuum outgassed at 300 C through a nose tube and then extruded at 915 C. In a typical batch of Ti alloy, the following contamination occurred as a result of the above processing: iron increased by 0.07 wt. %, carbon by 0.027 wt. %, nitrogen by 0.105 wt. %, hydrogen by 0.011 wt. %, and oxygen by 0.112 wt. %. Because of concern with impurity pick-up, the alloy structure and distribution of the dispersoid was not evaluated.

Recently, Antsiferov<sup>(10)</sup> reported on the effect of adding ZrO<sub>2</sub> particles of less than 1 micron to titanium. Calcium-hydride titanium and electrolytic titanium were used. In addition, ZrO<sub>2</sub> was also dispersed in several alloys with the chemical compositions listed in Table 81. The mechanical properties of the alloys at 20 C and 550 C are given in Table 82. The addition of ZrO<sub>2</sub> increased the elevated-temperature strength of the titanium alloys, but decreased their ductility.

Earlier, Antsiferov<sup>(11)</sup> had studied the influence of dispersed MgO and ZrO<sub>2</sub> on the resistance of titanium to plastic deformation. He concluded that the increased resistance was not related to the strengthening influence of the dispersoids. The possibility of changes in the state of dispersant solid solution must be taken into account in every specific case.

Portnoy<sup>(12)</sup> reports that Ognev and Anokhin had shown that the hardening effect produced by the addition of oxides to titanium is not great. For example, at room temperature, specimens sintered at 1150-1200 C had a maximum strength of 90 kg/mm<sup>2</sup> (882 MPa) with a content of 0.5 percent Al<sub>2</sub>O<sub>3</sub>, 0.8 percent ZrO<sub>2</sub>, or 0.6 percent TiO<sub>2</sub>, and the oxides introduced could not be detected as independent phases. When oxides were introduced to titanium alloyed with molybdenum, some additional hardening was observed. However, Portnoy also concluded that even if dispersion-strengthened titanium alloys were produced, they could not compete as to strength and heat resistance with the existing commercial titanium alloys, which have short-term strength of up to 90 kg/mm<sup>2</sup> (882 MPa) at 500 C and a 100-hour, long-term strength of up to 70 kg/mm<sup>2</sup> (686 MPa) at this same temperature.

Table 81. Chemical Compositions of Titanium Alloys<sup>(10)</sup>

Alloy No.	Material Designation	Chemical Composition, wt. %						
		Mo	Al	Nb	Cr	V	Sn	Zr
1	T <sub>c</sub> M3B2Kh1	3	—	2	1	—	—	—
2	T <sub>e</sub> M3B2Kh1	3	—	2	1	—	—	—
3	T <sub>e</sub> Yu4M3F3	3	4	—	—	3	—	—
4	T <sub>e</sub> Yu4M2Ts401	2	4	—	—	—	1	4
5	T <sub>e</sub> Yu4M2Ts402.5	2	4	—	—	—	2.5	4
6	T <sub>c</sub> M30	30	—	—	—	—	—	—

Note: T<sub>e</sub> is electrolytic titanium and T<sub>c</sub> is calcium hydride grade titanium. A study was made also of alloys Nos. 1, 2, 3, and 6 containing zirconium dioxide additions.

Table 82. Properties of Titanium Alloys<sup>(10)</sup>

Alloy No.	Alloy Designation	Test Temperature						
		20 C				550 C		
		U.T.S., MPa	Elong., %	Reduction in Area, %	Impact Strength, kg-m/cm <sup>2</sup>	U.T.S., MPa	Elong., %	Reduction in Area, %
1	T <sub>c</sub>	892-911	1-1.5	1-2	2.5-3.5	235	42	38
2	T <sub>e</sub>	343-353	10-14	18-22	16	108	29	36
3	T <sub>c</sub> M3B2Kh1	1137	4-9	0.0	1-2	265	22	44
4	T <sub>c</sub> M3B2Kh1-ZrO <sub>2</sub>	1176-1225	0.5-1.5	0.0	0.5-0.7	372	14	42
5	T <sub>e</sub> M3B2Kh1	784-823	8.5-9	9-17	9	274	7	20
6	T <sub>e</sub> M3B2Kh1-ZrO <sub>2</sub>	872-921	5-8	10-17		304	10	17
7	T <sub>e</sub> Yu4M3F3	970-1009	5-7	6-13	7	402	7-8	18
8	T <sub>e</sub> Yu4M3F3-ZrO <sub>2</sub>	637-725	0.2	0.5	0.5-1	627	4	7
9	T <sub>e</sub> Yu4M2Ts401	1117-1137	0.0	1-3	0.8-1.0	470	8	16
10	T <sub>e</sub> Yu4M2Ts402.5	833	0.0	0.0	1.2-1.5	608	4	14-17
11	T <sub>c</sub> M30	1078	0.5-1.0	7-10	7	—	—	—
12	T <sub>c</sub> M30-ZrO <sub>2</sub>	343-402	0.0	0.0	—	—	—	—

## REFERENCES

- Holladay, J. W., "Titanium Alloys for High-Temperature Use Strengthened by Fibers or Dispersed Particles", OTS PB 151073, DMIC Report 117 (August 1959).
- Wood, R. A., "Review of Recent Developments, Titanium and Titanium Alloys", DMIC, Battelle's Columbus Laboratories (July 20, 1966).
- Antony, K. C., and Clark, J. W., "Dispersion Strengthened Alpha Titanium Alloys", AFML TR 66-105 (May 1966). (MCIC 64984)
- Redden, T. K., and Shamblen, C. E., "900 F Titanium Alloy Development", Final Report AFML-TR-70-168, General Electric Company, Contract F33(615)-69-C-1423 (September 1970).
- Russo, P. A., Seagle, S. R., and Bomberger, H. B., "Development of a 900 F Titanium Alloy", Final Report AFML-TR-70-125, Reactive Metals, Inc., Contract F33(615)-69-C-1405 (July 1970).
- Dixon, C. F., and Skelly, H. M., "Dispersion Strengthening Titanium With Refractory Oxides", Canadian Metallurgical Quarterly, **11** (3), 491-495 (1972).
- Lyon, S. R., Inouye, S., Alexander, C. A., and Niesz, D. E., "The Interaction of Titanium With Refractory Oxides", Titanium Science & Technology, Plenum Press, New York-London (1973), pp 271-284.
- Waugh, R. C., "Suitable Oxides for Dispersion Strengthening Titanium Alloys", Intern. J. of Powder Metallurgy and Powder Technology, **12** (2), 85-89 (1976).
- Wright, I. G., and Wilcox, B. A., "Synthesis of Dispersion Strengthened Titanium Alloys by Attritor Milling", AFML-TR-72-238 (June 1972). (MCIC 87256)
- Antsiferov, V. N., Belykh, Y. A., Shubin, V. N., Khuden'kikh, N. N., Lobanova, L. F., and Denisov, A. M., "Effects of Alloying and the Addition of Dispersed ZrO<sub>2</sub> Phase on the Mechanical Properties of Sintered Titanium", Poroshkovaya Metallurgiya, No. 8 (152), 26-31.
- Antsiferov, V. N., Khuden'kikh, N. N., and Shubin, V. N., "The Influence of a Disperse Phase on the Resistance of Titanium to Plastic Deformation", Ziz. Metal. Metalloved, **32** (4), 831-835.
- Portnoy, K. I., and Babich, B. N., "Dispersion Hardened Materials", Moscow Metallurgiya, 127-199 (1974).

## URANIUM

In 1961, Arbiter, et al.<sup>(1)</sup> pointed out the desirability of a uranium-rich metallic fuel material having good elevated temperature strength and capable of high burn. They investigated the possibilities of dispersion strengthening uranium by hot pressing and extruding uranium powder that was covered with a surface oxide film. These materials contained 6 to 18 volume percent  $\text{UO}_2$  and were called "SUP" for sintered uranium product. One alloy containing 18.6 volume percent  $\text{UO}_2$  had a Meyer hardness of 5650 psi (38.9 MPa) at 1500 F (815 C) on holding 15 minutes. The authors expected that this material would have essentially the same creep resistance at 815 C as a U-10Mo alloy which had a Meyer hardness of 5880 psi (40.5 MPa). The relation between hardness and oxide content of the SUP alloys is shown in Figure 86.

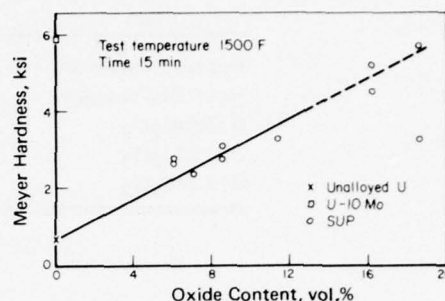


Figure 86. Meyer Hardness Vs. Oxide Content of SUP Samples<sup>(1)</sup>

These workers also studied the effects of cyclical heat treatments, across uranium's alpha-to-beta transformation temperature, on these materials. Each cycle consisted of heating to 730 C and cooling to 610 C over 20 minutes. After 120 cycles, an alloy containing 18 volume percent of  $\text{UO}_2$  retained a smooth surface and practically unchanged geometric dimensions. Specimens of pure uranium under these same conditions had swollen significantly and displayed a very coarse surface texture.

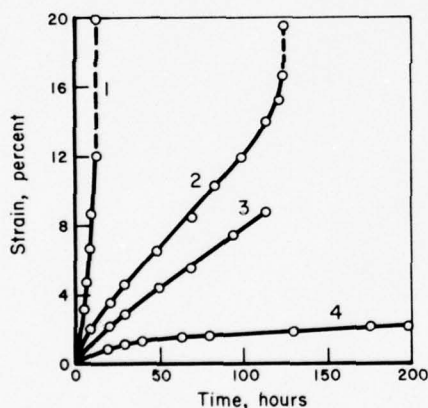


Figure 87. Creep of Dispersion-Hardened Uranium at 600 C and Load of 4 kg/mm<sup>2</sup>: 1) U+18UC; 2) U+18UO<sub>2</sub>; 3) U+9UBe<sub>13</sub>; 4) U+18UBe<sub>13</sub><sup>(2)</sup>

Other Soviet investigators, as reported by Meerson<sup>(2)</sup>, found that additions of dispersed  $\text{UO}_2$ , UC, and  $\text{UBe}_{13}$  in amounts up to 18 volume percent raised the strength of pure uranium at 20 C by 40, 32, and 24 percent, respectively, and at 600 C by 44, 69, and 69 percent respectively. The creep behavior of these materials is illustrated in Figure 87.  $\text{UBe}_{13}$  was the most effective addition. Tests were also carried out in which specimens were subjected to cyclic heat treatments within the alpha-phase limits (600 C and water cool) or with transition through the alpha-beta boundary (620-700 C). The highest resistance to thermal cycling was shown by a DS-U-18UO<sub>2</sub> alloy. After 400 cycles in the alpha region, the length of rods of these materials increased by 0.5-0.6 percent. With thermal cycling across the alpha-beta boundary, after 300 cycles, the U-18UBe<sub>13</sub> rods increased in length by 8 percent and the U-18UO<sub>2</sub> rods by 2.5 percent.

Portnoy, et al.<sup>(3)</sup> prepared U-Al<sub>2</sub>O<sub>3</sub> alloys containing up to 7.5 percent Al<sub>2</sub>O<sub>3</sub>. The creep properties of these alloys at 500 C and 600 C are given in Table 83.



**Table 83. High-Temperature Creep of Hot-Rolled and Dispersion-Hardened Uranium<sup>(3)</sup>**

Alloy	Temp., C	Stress, MPa, With Stable Creep Rate, %/hr		
		10 <sup>-1</sup>	10 <sup>-2</sup>	10 <sup>-3</sup>
Hot-rolled uranium	500	55	41	28
Hot-rolled uranium	600	27	15	8
U+3.5Al <sub>2</sub> O <sub>3</sub>	500	137	96	79
U+7.5Al <sub>2</sub> O <sub>3</sub>	500	158	137	117
U+7.5Al <sub>2</sub> O <sub>3</sub>	600	117	96	82

#### REFERENCES

1. Arbiter, W., and Stern, G., "Some Aspects of Dispersion Hardening in the Uranium-Uranium Oxide System", *Planseeberichte für Pulvermetallurgie*, **9**, 113-121 (1961).
2. Meerson, G. A., "Sintered Materials for Atomic Engineering", *Soviet Powder Metallurgy and Metal Ceramics*, No. 11, 893-904 (1967).
3. Portnoy, K. I., and Babich, B. N., "Dispersion Hardened Materials", Moscow, *Metallurgiya* (1974).

## TUNGSTEN

Tungsten has two outstanding properties which have dominated its application as a structural material for the past 70 years. These are its high melting point (3410 C) and its relative inertness to most chemicals. These may be contrasted with two of its most disadvantageous properties (from the viewpoint of structural materials), which are its high ductile-to-brittle transition temperature (DBTT) and its high density.

Much research has been done in recent years on the dispersion strengthening of tungsten in an effort to further improve its potential as a structural material at elevated temperatures. This work is summarized in this section for three types of DS tungsten alloys.

### W-ThO<sub>2</sub> Alloys

Historically, the use of thoria in tungsten lamp wire in the early 1900's probably represents the first practical demonstration of oxide-dispersion strengthening of a metal. Here, thoria additions of 0.75 to 1 percent were found to markedly inhibit grain growth in the tungsten filaments at their high operating temperatures and, as a result, greatly improved their resistance to "sagging" and, hence, to creep deformation.

It is well known that many processing variables affect the properties of dispersion-strengthened tungsten in general and W-ThO<sub>2</sub> alloys in particular. A good historical accounting of these developments up through 1952 is given in the treatise by Smithells.<sup>(1)</sup>

More recently, Tardiff<sup>(2)</sup> studied the sintering behavior of the W-ThO<sub>2</sub> blends where the tungsten had an average particle size of 0.05 micron and the ThO<sub>2</sub> 0.011 micron. He found a severe coarsening of the ThO<sub>2</sub> on sintering at 1100 C in a moist hydrogen atmosphere. Sell, et al.<sup>(3)</sup> avoided coarsening by using a unique, low-temperature blending process which caused most of the ThO<sub>2</sub> to be trapped within the tungsten powder particle by adding the ThO<sub>2</sub> dispersoid to tungstic oxide prior to the reduction process.

Dunham<sup>(4)</sup> investigated the distribution and deformation characteristics of ThO<sub>2</sub> particles during processing from powder to wire in W-1 wt. % ThO<sub>2</sub> alloy. The larger particles (greater than 1 micron) deformed concomitantly with the dispersant (or matrix) to cigar-shaped particles and then fractured into segments as deformation of the matrix proceeded. Smaller particles remained relatively spherical and undeformed. The deformation of the ThO<sub>2</sub> particles results from (a) the large particles having a lower effective yield strength due to the presence of dislocations and (b) the stresses developed during plastic deformation, which are greatest in the vicinity of the large particles.

Dunham<sup>(4)</sup> points out the two ramifications of large particle deformation. First, since the morphology a particle assumes is a function of the state of stress at the particle, different processing modes can produce drastically different dispersoid morphologies in a given material. This implies that W-ThO<sub>2</sub> materials having the same nominal composition and size should not be compared unless the materials have been processed to that size in an identical fashion. Second, based on Ashby's model for work hardening of dispersion-strengthened materials, W-ThO<sub>2</sub> alloys will work harden at a much lower rate when the larger ThO<sub>2</sub> particles are deforming.

Moon and Stickler<sup>(5)</sup> studied the creep behavior of pure, doped, and thoriated tungsten wires to be used for fiber reinforcement in high-temperature composites, for coils in incandescent lamps, for

heater wires in electronic tubes, and for wire-mesh heaters in heat-treating furnaces. The investigation included an AKS grade of wire which was produced from metal obtained by reducing tungstic oxide that had been doped with small amounts of potassium and aluminum alkali silicates. This wire had a significantly higher creep strength than the UDW wire (pure W) or the W-ThO<sub>2</sub> wire in the temperature range investigated, 2450 to 3000 C. Dispersed bubbles present in the AKS grade effectively pinned dislocations and accounted for its superior creep strength (see Figure 88).

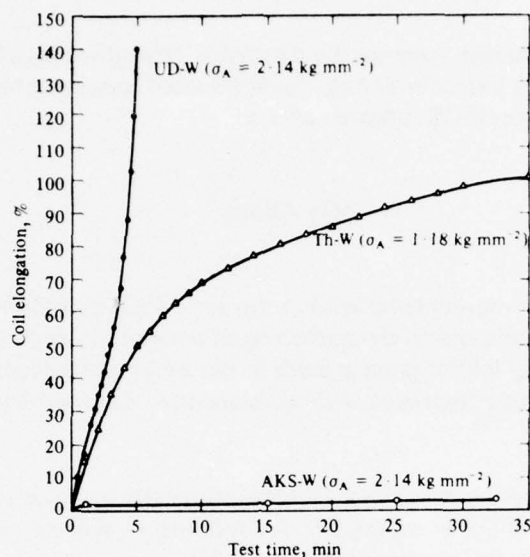


Figure 88. Creep Curves for UD-W, Th-W, and AKS-W wires at 2500 C<sup>(5)</sup>

Dunham and Heheman<sup>(6)</sup> investigated the effect of thermal treatments on crack volume change in W-ThO<sub>2</sub> materials by means of density measurements. It was found that the density of a W-1 wt. % ThO<sub>2</sub> material decreases monotonically with increasing wire drawing strain to 0.762 mm as a result of the continued deformation and fracture of large ThO<sub>2</sub> particles. Further deformation resulted in a slight increase in density due to a reduced degree of ThO<sub>2</sub> fracture and to a partial mechanical healing of the cracks between particle segments. The density decrease for a given amount of deformation was directly related to the volume fraction of ThO<sub>2</sub> contained within the material. Cracks in W-ThO<sub>2</sub> wire can heal prior to extensive grain-boundary migration at annealing temperatures less than or equal to 2000 C. Rapid heating to 2575 C results in a large, elongated grain structure and a partial healing of some of the cracks. Additional annealing at 2000 C of material heated to 2575 C does not result in further crack healing, indicating that a majority of the cracks are trapped within the large grains.

McCoy<sup>(7)</sup> recently reported the creep and stress-rupture properties for a W-2ThO<sub>2</sub> alloy at 1650 C and 2200 C (see Figures 89 and 90). The mean ThO<sub>2</sub> particle size was about 750 angstroms with an interparticle spacing of about 0.3 micron. The microstructure of this material did not change detectably, even after testing at 2200 C, while a standard material completely recrystallized after testing at 2000 C. The excellent stability and creep properties at 2200 C of the improved alloy is believed to be due to the fine dispersion of the ThO<sub>2</sub> particles.

King<sup>(8)</sup> investigated the yield strength of a W-3.8 vol. % ThO<sub>2</sub> alloy and compared it with that of recrystallized pure tungsten over the temperature range 325 to 2400 C (see Figure 91). The specimens were annealed at 2400 C. From this investigation it was concluded that the fine ThO<sub>2</sub> dispersion imparted a direct strengthening effect due to dislocation-particle interaction. The magnitude of this effect is in good agreement with that predicted by the Orowan mechanism. A further strengthening



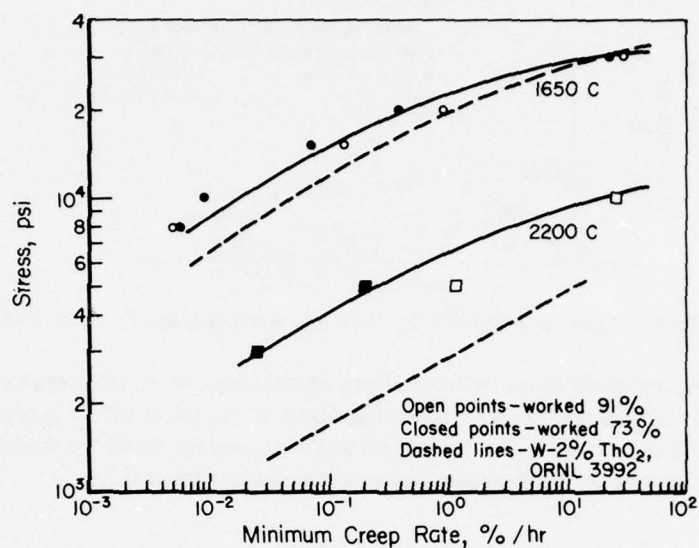


Figure 89. Creep Properties of W-2ThO<sub>2</sub> at 1650 and 2200 C in Vacuum<sup>(7)</sup>

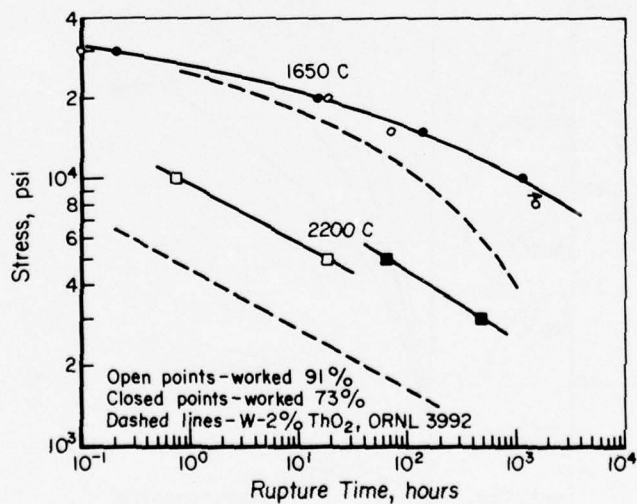


Figure 90. Stress-Rupture Properties of W-2ThO<sub>2</sub> at 1650 and 2200 C in Vacuum<sup>(7)</sup>

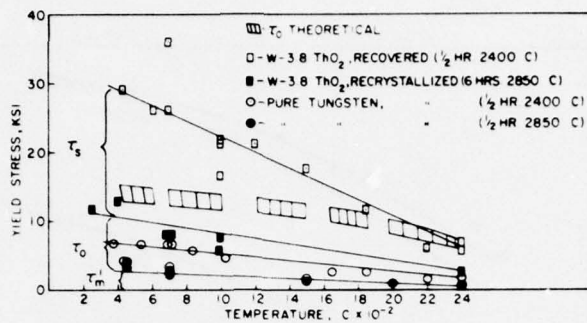


Figure 91. Yield Stress of Pure Tungsten and W-3.8ThO<sub>2</sub>, Various Annealed, as a Function of Test Temperature<sup>(8)</sup>

effect occurs in the recovered alloy as an indirect effect of the dispersion, and results from the stabilization of substructure at high temperatures. The magnitude of the latter effect is greater than that resulting directly from the dispersoid. The true stress-strain curves for both the W-3.8ThO<sub>2</sub> alloy and pure tungsten as a function of test temperature are reproduced in Figure 92.

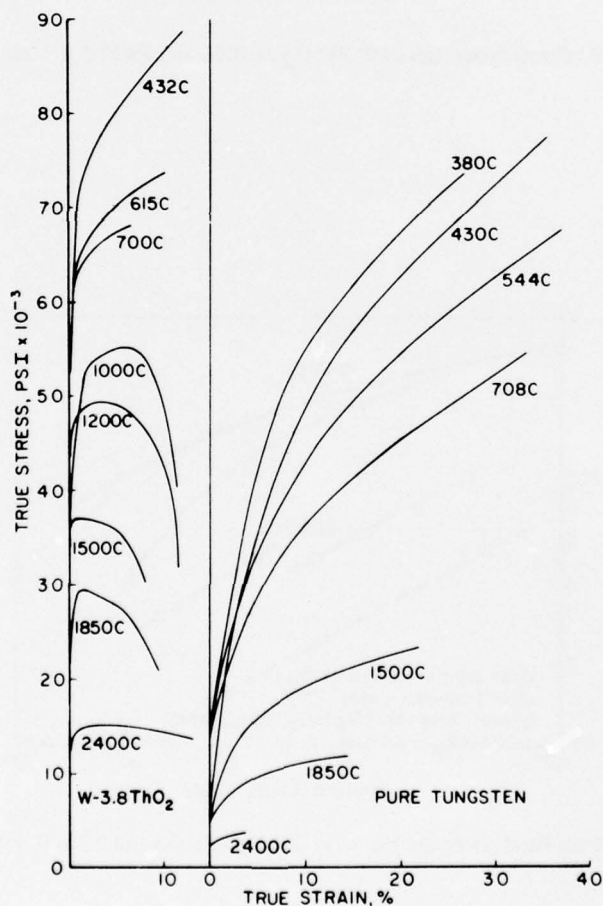


Figure 92. True Stress-Strain Curves of Pure Tungsten and W-3.8ThO<sub>2</sub> at Various Temperatures<sup>(8)</sup>

Another interesting development in the past 12 years was the finding by Ratliff, et al.<sup>(9)</sup> on the effectiveness of certain dispersoids on lowering the DBTT of tungsten. As shown in Figure 93, increasing amounts of ThO<sub>2</sub> (and ZrO<sub>2</sub>) in amounts up through 8 volume percent were found to be increasingly effective in decreasing the bend-transition temperature of tungsten, in both the stress-relief-annealed (1 hour at 1000 C and 1200 C) and recrystallized (1 hour at 1800 C) conditions.

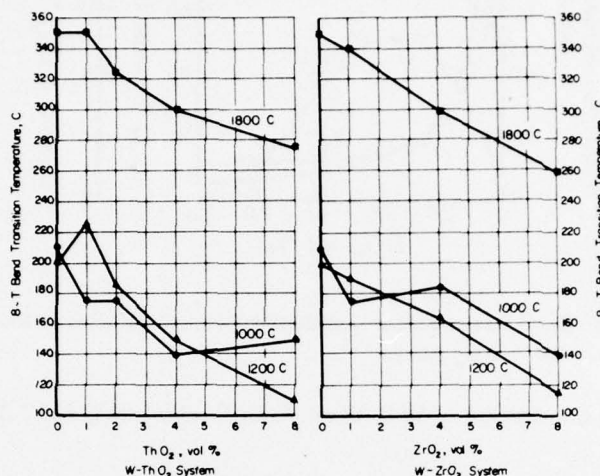


Figure 93. Effect of Increasing Dispersoid Content on the Ductile-to-Brittle Transition Temperature of W-ThO<sub>2</sub> and W-ZrO<sub>2</sub> Alloys Annealed for 1 Hour at the Indicated Temperature<sup>(9)</sup>

#### Other Dispersoids in Unalloyed Tungsten

Zirconia has received almost as much attention as a dispersion strengthener for tungsten as has thoria. As noted in the preceding paragraph, fine dispersions of ZrO<sub>2</sub> and ThO<sub>2</sub> as binary additions, were found by Ratliff, et al.<sup>(9)</sup> to have an equivalent effect, on a volume percent basis, on the DBTT of tungsten. This was also true for their beneficial effects on recrystallization behavior. However, in ternary combinations with rhenium, thoria showed superior stability to zirconia.<sup>(10)</sup>

Movchan<sup>(11)</sup> conducted a study of the properties of binary W-ZrO<sub>2</sub> alloys containing up to 2.5 vol. % ZrO<sub>2</sub>. These alloys were prepared by electron-beam evaporation and subsequent condensation on a substrate preheated to 1600 C. The dispersed ZrO<sub>2</sub> was nearly spherical and distributed at random. The tensile properties of these materials were determined at 3000 C with the results shown in Figure 94. According to X-ray diffraction analysis, no interaction occurred between the ZrO<sub>2</sub> and the tungsten matrix.

Blickensderfer, et al.<sup>(12)</sup> explored the elevated-temperature strength properties of W-ZrO<sub>2</sub> alloys prepared by the internal oxidation of W<sub>2</sub>Zr or ZrN particles, which were incorporated in a tungsten matrix. Tensile properties were determined on these alloys after sintering, extrusion, and stress-relief annealing for 15 minutes at 1350 C. Both the W<sub>2</sub>Zr and ZrN particles were converted into ZrO<sub>2</sub> particles of sub-micron size (0.02 to 0.5 micron) which had a strengthening effect on the matrix. At 1650 C, the alloys prepared using ZrN particles (designated as WZN alloys) had slightly higher ultimate tensile strengths than those made with W<sub>2</sub>Zr (designated as ZOW alloys), e.g., 70 to 80 ksi (482 to 551 MPa) versus 59 to 70 ksi (406 to 482 MPa), but at 1920 C, the tensile strengths for both alloy types were similar and in the range of 21 to 25 ksi. Figure 95 plots the tensile strengths of a series of ZOW alloys at 1650 C as a function of their zirconium and oxygen content. A maximum strength of



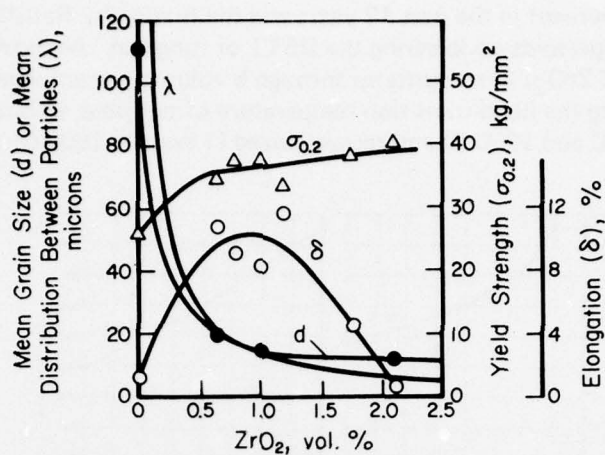


Figure 94. Relationship of Mean Grain Size and Mean Distribution Between Particles on the 3000 C Yield Strength and Tensile Elongation of W-ZrO<sub>2</sub> Alloys<sup>(11)</sup>

around 70 ksi occurred at a composition of W-0.42 wt. % Zr-0.09 wt. % O or W-0.85Zr-0.90 (atomic percent).

Blickensderfer<sup>(13)</sup> later determined the creep and stress-rupture properties for a W-0.4Zr-0.10 (weight percent) alloy prepared from W<sub>2</sub>Zr powder. The rupture data obtained are shown in Figure 96. He also compared the stress-rupture life of this alloy at a 10-ksi stress level with that for a number of other alloys from other investigations. These data are given in Figure 97.

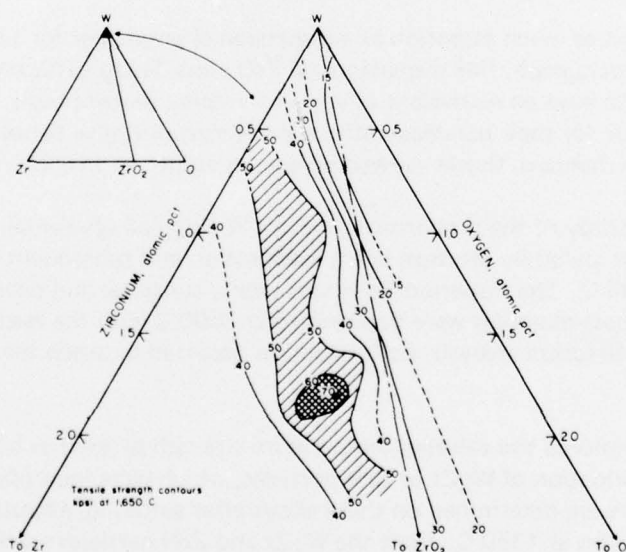


Figure 95. Ultimate Tensile Strength Contours of W-Zr-O Alloys at 1650 C<sup>(12)</sup>

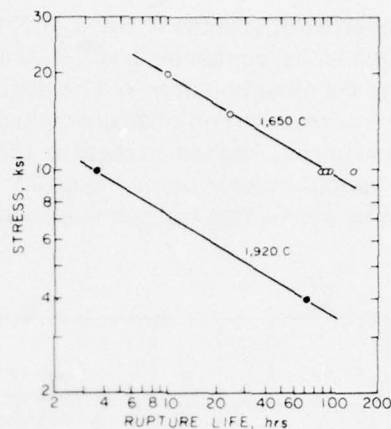


Figure 96. Stress-Rupture Life of Alloys Containing W-0.4Zr-0.1O<sup>(12)</sup>

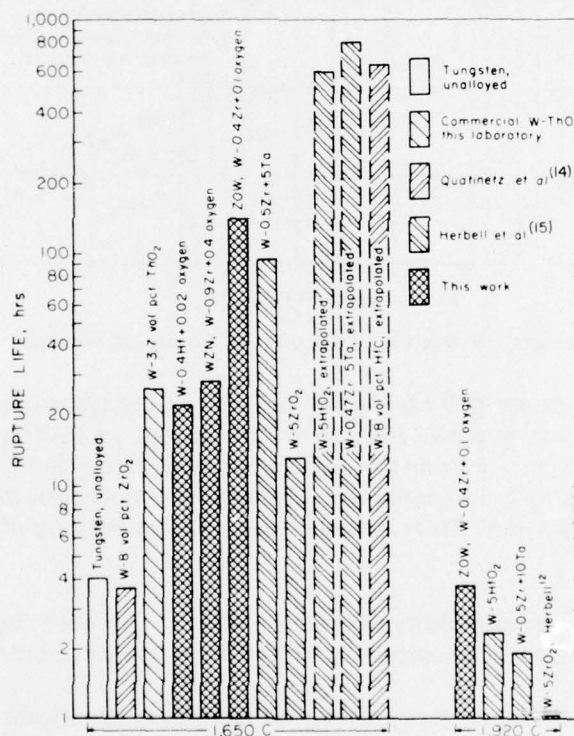


Figure 97. Comparative Stress-Rupture Life of Tungsten Alloys at 10,000 psi<sup>(12)</sup>

Antsiferov and Shafit<sup>(16)</sup> studied the thermal stability and spark erosion resistance of W-ZrO<sub>2</sub> alloys at temperatures up to 3300 C. To raise the thermal conductivity and ablatational power, additions of 3, 5, and 7 percent Cu were added to a W-10ZrO<sub>2</sub> alloy containing 0.4 percent Ni. The authors believe there is an increase in the spark erosion resistance of these alloys by the addition of ZrO<sub>2</sub>, and that this is connected with the absorption of heat during the decomposition of ZrO<sub>2</sub> and the sublimation of its constituents. Previously,<sup>(17)</sup> the apparent density of W-0.4Ni alloys with O-40ZrO<sub>2</sub>, and W-0.4Ni-10ZrO<sub>2</sub> with 0 to 15 percent Cu had been investigated.

Herbell, et al.<sup>(15)</sup> investigated the properties of selected W-HfO<sub>2</sub>, W-ZrO<sub>2</sub>, and W-ThO<sub>2</sub> alloys prepared by two different techniques. One series (containing 5 vol. % of either HfO<sub>2</sub>, ZrO<sub>2</sub>, or ThO<sub>2</sub> and 0.5 wt. % zirconium) was made by the reduction of mixed oxides derived from chemical salts. The other, W-0.5 wt. % Zr, was made by comminution of an arc-melted ingot. All materials were either cold or hot pressed and extruded to rod. Highest strength at 1650 C was achieved in the W-5HfO<sub>2</sub> alloy, which is compared with various other alloys in Figure 97. The W-ZrO<sub>2</sub> alloy composites produced either by coprecipitation or by arc-melting and comminution showed similar strength properties at 1650 C.

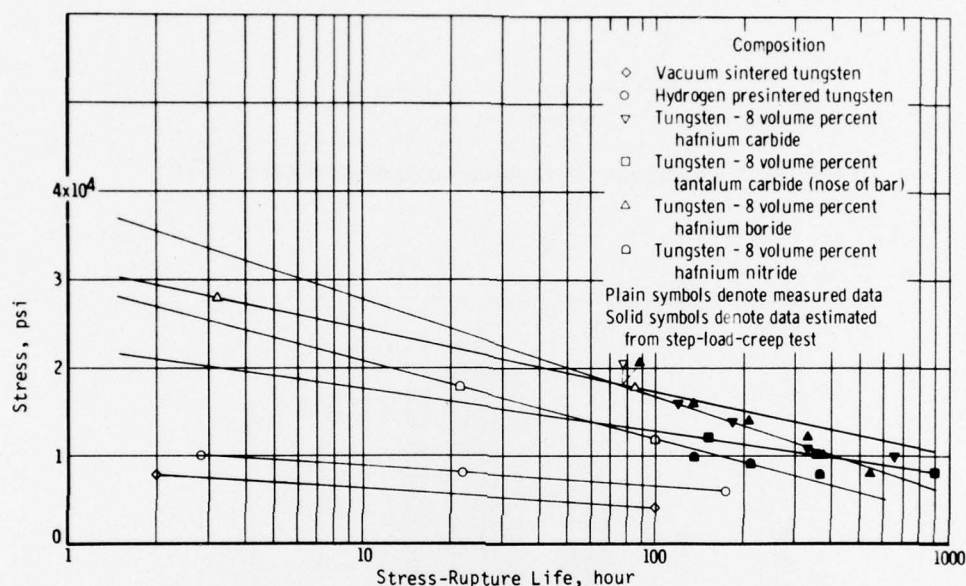


Figure 98. Stress-Rupture Life of Tungsten, Refractory-Compound Composites, at Temperature of 3000 F (1650 C)<sup>(14)</sup>

Kuznetsov and Suvorov<sup>(18)</sup> investigated W-Lu<sub>2</sub>O<sub>3</sub> and W-Sm<sub>2</sub>O<sub>3</sub> alloy systems as possible substitutes for the W-1ThO<sub>2</sub> alloy, which is an effective electron emitter but has the disadvantage of being naturally radioactive. Up to 1800 C, the emission of tungsten with the Lu<sub>2</sub>O<sub>3</sub> and SmO<sub>3</sub> differed little from that of W-ThO<sub>2</sub>. The W-Lu<sub>2</sub>O<sub>3</sub> was easier to activate and W-Sm<sub>2</sub>O<sub>3</sub> was more difficult. W-Lu<sub>2</sub>O<sub>3</sub> can apparently compete with W-ThO<sub>2</sub>, although the emission capacity of the latter is higher in the low-temperature range.

Dubok and Tyukalo<sup>(19)</sup> studied the possibility of chemical reactions between Sc<sub>2</sub>O<sub>3</sub> with tungsten and found none after heating these materials together to 2100 C for 4 hours in a protective atmosphere.

Strashinskaya and Stashevskaya<sup>(20)</sup> used X-ray diffraction analysis to investigate the stability of tungsten with five intermetallic compounds after heating alloy mixtures at temperatures from 1700 C to 2200 C. The heating environment used was not disclosed. The dispersoid phases used and results obtained are summarized as follows:

**W-HfC.** At 1700 C and above, additions of HfC up to 10 weight percent appeared to be dissolving in the tungsten matrix whose lattice parameter had been expanded from 3.16 to 3.17 angstroms after the 2200 C reaction (reaction times not specified).

**W-TaC.** At 1700 C, additions of TaC up to 10 weight percent had expanded the tungsten lattice parameter to 3.17 angstroms.



W-ZrC. At 1800 C and higher, a 10 weight percent ZrC addition had expanded the tungsten lattice parameter to 3.17 angstroms.

W-ZrN. No reactions with ZrN additions up through 10 weight percent were indicated at temperatures from 1800 C to 2200 C.

W-ZrO<sub>2</sub>. No reactions with ZrO<sub>2</sub> additions up through 10 weight percent were indicated at temperatures to 2200 C.

These results were generally consistent with the findings of Jaffee, et al.<sup>(21)</sup> who attempted to prepare tungsten alloys containing 2 volume percent additions of HfC, TaC, Ta<sub>2</sub>C, TiN, ZrN, HfN, and TaN by vacuum sintering for 2 hours at 2600 C to 2800 C. Under these conditions, none of these intermetallics were stable. Thus, the nitrogen and carbon were evaporated leaving the residual metallics in the tungsten matrix.

Morcom and Cerulli<sup>(22)</sup> also reported that oxide, nitride, and probably carbide mixtures of hafnium and zirconium tended to form solid solutions with tungsten on heating in vacuum at temperatures to 1750 C.

Landingham and Casey<sup>(23)</sup> dispersed small particles (less than 10 angstroms) of HfN in tungsten by the hydrogen reduction of halide mixtures of WCl<sub>6</sub> and HfCl<sub>4</sub> in a gas stream that also contained NH<sub>3</sub>. The dispersoid was formed during deposition by the reaction of hafnium with the NH<sub>3</sub>. Because of oxygen contamination from the halides, a complex dispersoid of Hf-O-N was obtained rather than the intended HfN. The microstructure of the deposits could be altered from fine, columnar grains perpendicular to the surface, to fine layers parallel to the surface. Slight changes in the dispersoid composition and dispersion produced pronounced effects on the hot microhardness of the covapor deposited material.

Quatinetz, et al.<sup>(14)</sup> determined stress-rupture and hardness data on tungsten alloys containing 8 to 10 volume percent of ZrO<sub>2</sub>, Y<sub>2</sub>O<sub>3</sub>, HfO, HfB, HfN, HfC, and TaC. Stress-rupture data on some of the higher strength alloys are included in Figure 98. Data for the W-8HfC alloy are also shown in Figure 97.

### W-Re Alloys

In 1955, Geach and Hughes<sup>(24)</sup> first reported the unique and remarkable effects of rhenium additions, in amounts up through 30 weight percent, in decreasing the DBTT of tungsten. Since then, numerous studies have been made to determine how the properties of tungsten-rhenium alloys are affected by dispersoid additions.

Ratliff, et al.<sup>(9)</sup> were among the first to show that the beneficial effects of binary additions of rhenium, iridium, osmium, and thoria on the DBTT of tungsten were indeed additive (see Figure 99).

A continuation of their work indicated that an optimum combination of good fabrication characteristics and low-temperature ductility occurred in a W-5 wt. % Re-2.2 wt. % ThO<sub>2</sub> alloy. Through the use of an alkali-silicate-doped tungsten powder base, isostatic hot pressing, and hot rolling an extremely fine-grained sheet product could be obtained.<sup>(25)</sup> As stress relief annealed, this material showed good tensile ductility at temperatures as low as 0 C and a recrystallization temperature of 2000 C. The alloy also maintained good tensile ductility at low temperatures in the recrystallized condition. The stress to cause rupture at 1915 C (3500 F) was measured on two recrystallized samples with the following results:

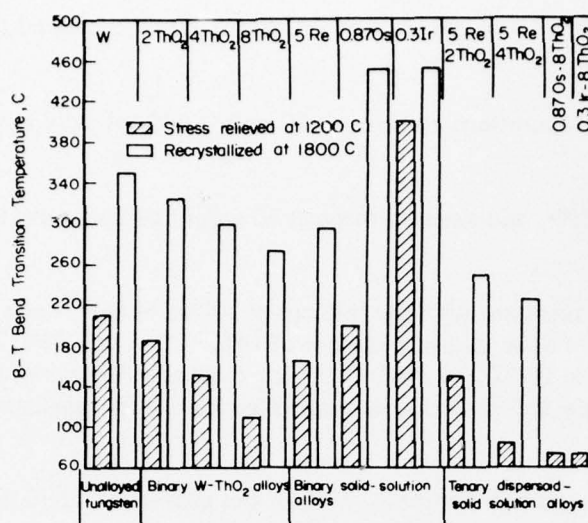


Figure 99. Effects of Binary and Ternary Combinations of Selected Alloying Additions on the Ductile-to-Brittle Transition Temperature of Tungsten<sup>(9)</sup>

Stress, ksi (MPa)	Rupture Time, hr
5 (34)	1.1
3 (21)	13.0

In another investigation<sup>(26)</sup>, weldability studies were made on W-5Re-2.2ThO<sub>2</sub> sheet using electron-beam as well as gas-tungsten-arc welding techniques. All the welds showed defects in the form of porosity and/or undercutting and poor ductility.

Sell, et al.<sup>(27,28)</sup> explored four different processing techniques in an effort to prepare alloys containing 5 to 10 weight percent rhenium plus 1 to 2 wt. % thoria. These included 3 combinations of the co-reduction of tungstic oxide with various additives plus mechanical mixing of metal powders with thoria. A fine thoria distribution could only be achieved by the co-reduction processes, but none of these alloys could be hot worked. However, ingots of a W-5Re-2ThO<sub>2</sub> sintered from the blended metal powders and thoria were successfully swaged to rods. The resulting alloys contained coarse thoria particles, which were not effective in causing dispersion strengthening.

Earlier, these same workers had shown that solid-solution strengthening and dispersed-particle strengthening were additive in a W-25Re-1ThO<sub>2</sub> alloy.<sup>(29)</sup>

Wirth<sup>(30)</sup> developed stress-rupture and creep data for a W-3Re-2ThO<sub>2</sub> alloy in sheet and rod shapes between 1800 and 2200 C in vacuum. The stress-rupture data is summarized in Figure 100. At 2200 C, the elongated ThO<sub>2</sub> particles began to spheroidize. This process was accelerated by creep deformation. The effect of rhenium and ThO<sub>2</sub> on the secondary creep rate of tungsten produced by powder metallurgy processes is reproduced in Figure 101.

Majdic and Wirth<sup>(31)</sup> investigated the recrystallization behavior of W-3Re-2ThO<sub>2</sub> alloy and compared it with undoped tungsten. They concluded that the threshold for primary recrystallization in the alloy is shifted to higher temperatures (100 to 400 C, depending on the degree of cold working) compared to unalloyed tungsten. The secondary recrystallization observed in tungsten does not occur in the alloy at the same temperatures. Primary recrystallization in tungsten seems to occur by grain-boundary

migration for small degrees of cold working. However, in the case of larger deformation, it is initiated by a nucleation process. Recrystallized grains in the alloy are extended in the rolling direction parallel to the strings of the particles. Loss of shape stability of the  $\text{ThO}_2$  particles occurred after annealing for 1 hour at 2400 C, and at 2200 C after longer annealing times. Nevertheless, the effect of these particles on the recrystallization behavior was observed in all cases.

The possibility of hardening tungsten and tungsten-base alloys by nitriding was investigated by Iden and Himmel.<sup>(32)</sup> They found a significant hardening effect on internal nitriding W-3Hf, W-25Re-Hf, and W-25Re-30Mo-Hf alloys. The HfN particles formed as a result of the nitriding precipitate as plates, and this shape is retained up to at least 2400 C.

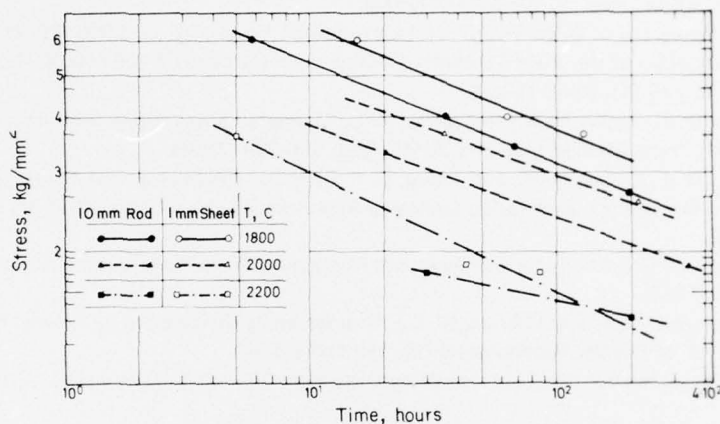


Figure 100. Stress-Rupture Strength of W-3Re-2ThO<sub>2</sub> Sheet and Rod at Various Temperatures<sup>(30)</sup>

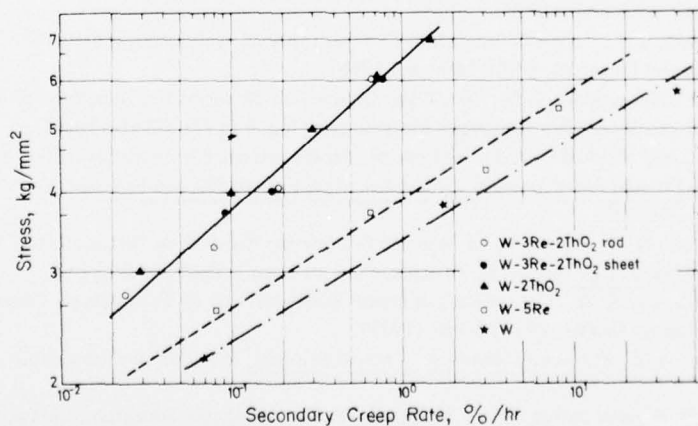


Figure 101. Influence of Rhenium and Thoria on the Secondary Creep Rate at 1800 C of Tungsten Produced by Powder Metallurgy Processes<sup>(30)</sup>



## REFERENCES

1. Smithells, C. J., Tungsten, A Treatise on its Metallurgy, Properties, and Applications, 3rd Edition, Chapman and Hall, Ltd., London (1952), p 131.
2. Tardiff, G. E., "On the Sintering Behavior of Submicron W-ThO<sub>2</sub> Blends", Intern. JI. of Powder Metallurgy, **5** (4), 29-39 (1969).
3. Sell, H. G., Morcom, W. R., and King, G. W., "Development of Dispersion Strengthened Tungsten Base Alloys", Westinghouse Electric Company Technical Report AFML-TR-65-407, Part I (November 1965); Part II (November 1966).
4. Dunham, T. E., "Effect of Deformation on ThO<sub>2</sub> Particle Morphology in W-1 Wt. % ThO<sub>2</sub> Materials", Metallurgical Trans., **2**, 2797-2804 (1971).
5. Moon, D. M., and Stickler, R., "Creep Behavior of Fine Wires of Powder-Metallurgical, Pure, Doped, and Thoriated Tungsten", High Temperature-High Pressures, **3** (5), 503-516 (1971).
6. Dunham, T. E., and Hehemann, R. F., "Density Changes Accompanying the Annealing of Wrought Thoriated Tungsten Wire", Metallurgical Trans., **5**, 2365-2373 (1974).
7. McCoy, H. E., "Creep Properties of W-2% ThO<sub>2</sub>", Jl. Less Common Metals, **37**, 303-306 (1974).
8. King, G. W., "An Investigation of the Yield Strength of a Dispersion-Hardened W-3.8 Vol. % ThO<sub>2</sub> Alloy", Trans. Metallurgical Soc. AIME, **245** (1), 83-89 (1969).
9. Ratliff, J. L., Maykuth, D. J., Ogden, H. R., and Jaffee, R. I., "Tungsten Sheet Alloys with Improved Low-Temperature Ductility", Trans. Metallurgical Soc. AIME, **230**, 490-500 (1964).
10. Ratliff, J. L., Maykuth, D. J., Ogden, H. R., and Jaffee, R. I., "Further Development of a Ductile Tungsten-Base Sheet Alloy", Battelle's Columbus Laboratories, Summary Report on Bureau of Naval Weapons Contract N600(19)-59738 (April 30, 1964).
11. Movchan, B. A., "Structural Conditions for the Maximum Plasticity of Two-Phase Metallic Materials", Sov. Phys. Dokl., **20** (7), 515-516 (1975).
12. Blickensderfer, R., Copeland, M. I., and O'Brian, W. L., "Strengthening of Tungsten by Powder Metallurgical Internal Oxidation", Intern. JI. of Powder Metallurgy, **8** (3), 145-155 (1972).
13. Blickensderfer, R., "Creep Behavior of a Tungsten Alloy Dispersion Strengthened by ZrO<sub>2</sub>", Metallurgical Trans., **5**, 2347-2350 (1974).
14. Quatinetz, M., Weeton, J. W., and Herbell, T. P., "Studies of Tungsten Composites Containing Fibered or Reacted Additives", NASA TN D-2757 (April 1965).
15. Herbell, T. P., Weeton, J. W., and Quatinetz, M., "Structure and Properties of Tungsten-Base Powder Metallurgy Composites", NASA TN D-3610 (September 1966).
16. Antsiferov, V. N., and Shafit, I. A., "Erosion Tests on Tungsten Containing Dispersed ZrO<sub>2</sub> Inclusions", Fiziko-Khimicheskaya Mekhanika Materialov, **8** (6), 104-105 (1972).
17. Antsiferov, V. N., and Shafit, I. A., "Technological Characteristics of W-Ni-Cu Alloys Containing Dispersed ZrO<sub>2</sub> Inclusions", Poroshkovaya Metallurgiya, No. 11 (47), 43-45 (1966).
18. Kuznetsov, V. A., and Suvorov, A. L., "Auto-Electron Microscopy of Tungsten With Additions of Lu<sub>2</sub>O<sub>3</sub> and Sm<sub>2</sub>O<sub>3</sub>", Russ. Metall, (5), 172-173 (1973).
19. Dubok, V. A., and Tyukalo, L. I., "High-Temperature Compatibility of Refractory Metals With Sc<sub>2</sub>O<sub>3</sub>", Soviet Powder Metallurgy and Metal Ceramics, 64-66 (January 1968).
20. Strashinskaya, L. B., and Stashevskaya, I. A., "An X-ray Diffraction Study of the Reactions of Molybdenum and Tungsten With Disperse Inclusions", Poroshkovaya Metallurgiya, No. 5 (137), 93-95 (1974).
21. Jaffee, R. I., Allen, B. C., and Maykuth, D. J., "Effects of Dispersions on the Recrystallization and Ductile-Brittle Transition of Tungsten", Powder Metallurgy in the Nuclear Age, Fourth Plansee Seminar, Metallwerk Plansee AG, Reutte/Tyrol (1962), pp 770-798.
22. Morcom, W. R., and Cerulli, N. F., "Stability of Selected Submicron Refractory Dispersoids in Tungsten", Modern Developments in Powder Metallurgy, Ed. H. H. Hausner, Plenum Press (1966), pp 203-214.
23. Landingham, R. L., and Casey, A. W., "Ultrafine Dispersion Strengthening of Tungsten by Chemical Covapor Deposition", Jl. Less Common Metals, **26**, 173-198 (1972).
24. Geach, G. A., and Hughes, J. E., Plansee Proceedings, Second Seminar, Metallwerk Plansee AG, Reutte/Tyrol (1955), p 245.
25. Maykuth, D. J., Ogden, H. R., and Jaffee, R. I., "W-5Re-2.2ThO<sub>2</sub>, A Ductile Tungsten Sheet Alloy", Refractory Metals & Alloys, Res. & Dev., Volume 1, Metallurgical Society Conference, **41**, French Lick, Indiana (October 1965), pp 597-620.

# REFERENCES (Cont.)

26. Maykuth, D. J., Grube, K. R., Hauser, D., and Bartlett, E. S., "Property Characterization of a Ductile, Tungsten-Base Sheet Alloy", Battelle's Columbus Laboratories, Final Report on Bureau of Naval Weapons Contract N0w 66-0319 c (November 1966). (MCIC 66833)
27. Sell, H. G., Morcom, W. R., and King, G. W., "Development of Dispersion-Strengthened Tungsten-Base Alloys", Westinghouse Electric Company Technical Report AFML-TR-65-407, Part II (November 1966).
28. Sell, H. G., and Stickler, R., "The Effect of Rhenium on the Mechanical Properties of W-2ThO<sub>2</sub>", Planseeber. Pulvermet, 17, 71-101 (1969).
29. King, G. W., Morcom, W. R., and Sell, H. G., "The High Temperature Tensile Properties of Tungsten and Tungsten-Rhenium Alloys Containing a Dispersed Second Phase", Metallurgical Society Conferences, 41, 621-636 (1965).
30. Wirth, G., "Hochtemperatur-kriechverhalten einer W-3% Re Legierung mit ThO<sub>2</sub> - Dispersionshartung Verschiedener Teilchenform", JI. Less Common Metals, 29, 41-63 (1972).
31. Majdic, M., and Wirth, G., "Über das Recrystallisations verhalten einer mit ThO<sub>2</sub> Dispersionsgeharteten Wolfram-Rhenium - Legierung im Vergleich zu reinem Wolfram", JI. Less Common Metals, 24, 341-367 (1971).
32. Iden, D. J., and Himmel, L., Acta Met., 17, 1483-1499 (1969).

## ZINC

The strengthening of zinc is desirable since, at 21 C, it is operating at 42 percent of its melting point and recovery processes occur rapidly when the metal is deformed. As with most metals, air-atomized zinc and zinc alloy powders are covered with a layer of oxide. On rolling or extrusion of these powders, a dispersion-strengthened material should result. This was indeed found to be the case by Lund, et al.<sup>(1)</sup> One characteristic feature of this material, noted by Lund, was the strong influence of second-phase-particle morphology on its properties. Deformation, leading to fragmentation and spheroidization of second-phase particles, or the use of spherical particles in the process of producing these alloys, significantly changed the alloy's behavior. Alloys with spherical inclusions had a lower ultimate tensile strength than pure zinc, but very high ductility. For example, whereas the tensile reduction of area of pure zinc is generally below 20 percent, in the presence of spherical second-phase particles, the reduction may reach 93 percent.

An increase in mechanical strength is achieved if the hardening phase, usually ZnO, is present either as a continuous grid or fine flakes. Creep resistance of the particulate alloys was found to be greatly superior to a conventionally wrought zinc alloy when hard intermetallic particles are formed.<sup>(3)</sup> Melt-fragmentation of some eutectic alloys, or near eutectic alloys, was found a useful technique of making such composites. A series of binary alloys containing 0.8 percent titanium, and ternary alloys containing titanium (0.2-0.8 percent), and copper (1 percent), nickel (0.6 percent) or chromium (0.05-0.07 percent) were investigated. Atomized alloy powders were converted to wrought materials by a batch compaction- and extrusion process. The strongest of the alloys was actually prepared from 35 x 100 mesh powder. Table 84 compares data from some of the best alloys with those for comparable commercial alloy sheet. In general, the powder metallurgy alloys showed the possibilities of a wide variety of property improvements over the commercial alloy.

Table 84. Tensile and 25 C Creep Properties of Zn Alloys<sup>(3)</sup>

Composition	Tensile Data					Creep Data, 25 C			
	U.T.S.		Y.S.		Elong. in 1 in., %	Stress		Min. Creep Rate, %/yr	Test Time, hours
	ksi	MPa	ksi	MPa		ksi	MPa		
.23Ti-.05Cr	69.2	477	64.3	443	12.5	20	138	0.41	3550
.21Ti-.07Cr	67.0	462	63	434	9.5	20	138	0.21	3390
.21Ti-.07Cr	70.4	485	67.2	463	8.0	20	138	0.09	2550
.81Ti-1Cu	57.6	397	49.5	341	37.4	20	138	0.29	2520
Commercial alloy: .14Ti-0.7Cu	31.8	219	27.4	189	35.3	13	90	44	1040*

\* Fractured on test.

McCarthy, et al.<sup>(2)</sup> investigated the high-temperature, compression creep characteristics of dispersion-strengthened zinc. Room-temperature tensile tests results were unexpected in that the dispersed particles (ZnO,  $\alpha$ -Al<sub>2</sub>O<sub>3</sub>, carbon black, and tungsten) reduced the strength and increased the ductility of zinc. However, materials containing ZnO in platelet rather than spherical form behaved in a more conventional manner.<sup>(4)</sup> The effect of oxide content and of type of dispersion is shown in Figure 102. The dispersion softening probably relates to the phenomenon of "superplasticity".

In the case of zinc-based composites containing spherical dispersoids, slip is very fine and duplex slip may be observed. The composites that would show the greatest thermal stresses upon cooling from the annealing temperature are also the most ductile. The same authors found also that zinc containing a ZnO network possessed mechanical strength at above the melting point of zinc.<sup>(5)</sup>



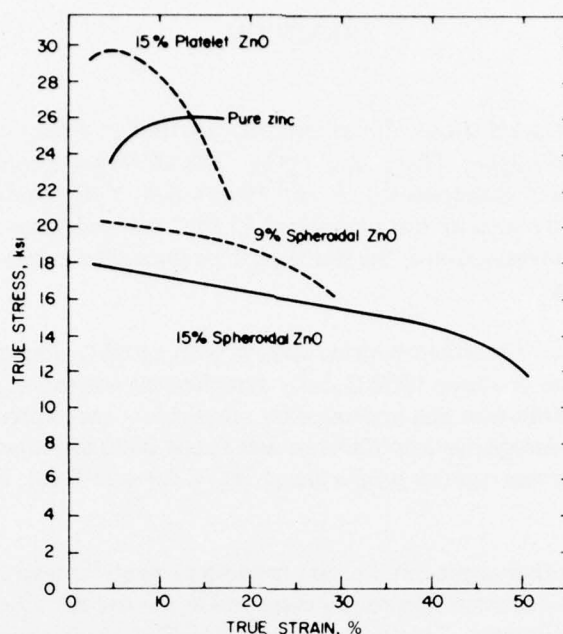


Figure 102. Effect of Oxide Content and Morphology on the Tensile Properties (True Stress-True Strain Curves) of Zinc-Zinc Oxide Alloys (Strain Rate Approximately 3 Percent Per Minute)<sup>(4)</sup>

At the same University<sup>(6)</sup> yield points and strain-aging effects were found to appear above 0.5 to 0.6  $T_m$  and to persist at temperatures up to the melting temperature. The strain-aging yield point is associated with the dispersed particles. The strain-aging yield point behavior has been observed in Zn-15Al<sub>2</sub>O<sub>3</sub> and Zn-25W alloys. These strain-aging yield points in the Zn-Al<sub>2</sub>O<sub>3</sub> system were believed to be caused by more than a single mechanism. The results seem consistent with the author's model based on generation of vacancies or dislocations at dispersed particles.

#### REFERENCES

1. Lund, J. A., et al., "Fundamental Investigation of Zinc Powder Metallurgy", Dept. of Metallurgy, University of British Columbia, Vancouver, B.C., Canada (June 1965).
2. McCarthy, W. H., Shyne, J. C., and Sherby, O. D., "Dispersion-Softened Zinc Alloys", *Nature*, **208** (5010), 579-580 (1965).
3. Lund, J. A., Tromans, D., and Radtke, S. F., "The Particulate Metallurgy of Zinc Alloys", *International J. of Powder Metallurgy*, **4** (1), 41-48 (1968).
4. McCarthy, W. H., Shyne, J. C., and Sherby, O. D., "Some Novel Consolidation Techniques for Dispersing Hard Second Phases in Metals and the Effects of Dispersoid Morphology Upon Mechanical Properties of Zinc", *Trans. of the ASM*, **62**, 117-129 (1969).
5. McCarthy, W. H., Shyne, J. C., and Sherby, O. D., "Compression Strength of Zinc/Zinc Oxide Composites at Temperatures Above the Melting Point of Zinc", *Metal Science J.*, **4**, 74-77 (1970).
6. Huseby, I. C., Hsu, S. E., McNelly, T. R., Edwards, G. R., Francois, D., Shyne, J. C., and Sherby, O. D., "Yield Points and Strain Aging in Hexagonal-Based Particulate Composites", *Metallurgical Trans., A*, **6A**, 2005-2008 (1975).

## ZIRCONIUM

Weinstein and Holtz<sup>(1)</sup> investigated alloys of mechanically attritioned zirconium powder containing 7-volume-percent additions of  $\text{La}_2\text{O}_3$ ,  $\text{ThO}_2$ , and  $\text{Y}_2\text{O}_3$ . The alloys were cold pressed and hot extruded. Anthony and Klepfer<sup>(2)</sup> dispersed 0.1, 1, and 10 vol. % of  $\text{Y}_2\text{O}_3$  in Zircaloy-2 hydride mill scrap and produced material by vacuum hot pressing at 1125 C with subsequent beta quenching and extrusion at 815 C. In both investigations, the oxide-particle parameters were not suitable for significant dispersion strengthening.

Rezek, et al.<sup>(3)</sup> re-milled milled-zirconium-hydride sponge with suitably prepared  $\text{Y}_2\text{O}_3$  powder. The cold compact was sintered at above 1000 C, fully densified by hot rolling, and clad in mild steel. It was noted that particle distribution was improved by rehydriding and reprocessing. At a sintering temperature of 1000 C, the average particle diameter was about 2000 angstroms. No tensile measurements were reported but stress-rupture properties at 500 C for a Zr-5 vol. %  $\text{Y}_2\text{O}_3$  alloy showed a tenfold improvement.

Skelly and Dixon<sup>(4)</sup> tried another approach, i.e., arc melting of zirconium with  $\text{ThO}_2$ ,  $\text{Y}_2\text{O}_3$ ,  $\text{La}_2\text{O}_3$ , and cerium zirconate. The refractories apparently dissolved in the molten zirconium and precipitated as a dispersed phase on solidification. Tensile strengths at 650 C of up to twice that for Zircaloy-2 were observed for arc-melted specimens. The size and distribution of  $\text{ThO}_2$  and cerium-zirconate particles were found to vary depending on the heat treatment, but ideal interparticle spacing was not achieved.

Parsons and Adolph<sup>(5)</sup> tried to develop and optimize the properties of dispersion-strengthened Zircaloy-2, yttria alloys and determine their mechanical properties. The properties are compared with those of currently used alloys, Zircaloy-2, and Zr-2.5 wt. % Nb in Table 85. Special precautions were taken to avoid the pick up of gaseous impurities, which degrade the properties of zirconium alloys. No noticeable grain growth was observed in the alloys investigated after aging at 700 C for 1000 hours. It was found that the  $\text{Y}_2\text{O}_3$  particles were reasonably stable during fabrication at temperatures less than 800 C. At reactor-operating temperatures, the particles should be very stable. An investigation was also made on the effect of irradiation for a period of 2790 hours with a neutron dose of  $9.2 \times 10^{20} \text{ n/cm}^2$  thermal and  $23 \times 10^{20} \text{ n/cm}^2$  fast, E 1 MeV. Irradiation included six cycles which cooled the specimens at 25 C/min. After exposure, tensile tests were performed in argon at 250 and 350 C at a strain rate of  $7.6 \times 10^{-5} \text{ sec}^{-1}$  up to 0.6-1 percent plastic strain and thereafter at  $7.6 \times 10^{-3} \text{ sec}^{-1}$  up to fracture. The tensile properties of these alloys followed the generally observed trend for irradiated Zircaloy-2, i.e., the proportional limit, the 0.2 percent proof stress, and the ultimate tensile strength were all increased and the elongation was reduced.

Over the plastic-strain range it was noted that the unirradiated alloys all continued to work harden. In the case of the irradiated alloys, there was a difference in behavior between alloys with and without  $\text{Y}_2\text{O}_3$ . The alloys without  $\text{Y}_2\text{O}_3$  ceased to work harden and the stress dropped after very low plastic strains of about 0.25 percent. The alloys containing  $\text{Y}_2\text{O}_3$  continued to work harden up to at least 0.6-1.0 percent plastic strain.

The creep properties obtained are summarized in Table 86. The lower creep rates, longer rupture lives, and good creep-rupture ductilities obtained for the dispersion-strengthened Zircaloy-2- $\text{Y}_2\text{O}_3$  alloys shows them to have a clear advantage over cold-worked Zircaloy-2. At about 350 C, the stress-rupture life of the 10 vol. %  $\text{Y}_2\text{O}_3$  alloy would compare to the properties of Zr-2.5 wt. % Nb alloy, but the  $\text{Y}_2\text{O}_3$ -containing alloys were shown to have better rupture lives at higher temperatures. The behavior of Zircaloy-2- $\text{Y}_2\text{O}_3$  when irradiated at 280 C showed a continuation in work hardening to

greater plastic strains than alloys without  $Y_2O_3$ . This would be a beneficial property in fuel-cladding applications.

Corrosion tests in steam of the Zircaloy-2- $Y_2O_3$  alloys have shown widely scattered results. However, Parsons and Adolph<sup>(5)</sup> feel that it should be possible to produce corrosion-resistant zirconium alloys containing dispersed particles of  $Y_2O_3$ . Thermodynamic considerations of the stability of  $Y_2O_3$  in zirconium indicate that approximately 3000-4000 ppm  $O_2$  is required in solution at 700 C for yttria to remain completely stable.

Table 75. Tensile Properties of Zircaloy-2 Alloys<sup>(5)</sup>

Alloy	Temp., C	0.2% Proof Stress		U.T.S.		Elong., %
		ksi	MPa	ksi	MPa	
Zircaloy-2	RT	46.0	317	79.0	544	18.7
Extruded	350	28.0	193	41.0	282	27.8
Commercial	500	22.6	155	34.0	234	30.0
Metal rod	600	13.3	92	18.0	124	—
Zircaloy-2-0	RT	60.0	413	88.8	612	19.7
vol. % yttria	350	28.0	193	45.3	312	28.3
	500	22.6	156	34.1	235	36.4
	600	13.3	92	19.9	137	68.3
Zircaloy-2-5	RT	96.0	661	117.6	810	6.1
vol. % yttria	350	47.5	327	69.0	475	20.0
	500	33.4	230	45.0	310	23.1
	600	20.0	138	27.1	187	37.0
Zircaloy-2-10	RT	130.0	896	138.9	957	1.3
vol. % yttria	350	70.0	482	82.6	569	9.8
	500	44.6	307	57.3	395	15.4
	600	26.6	183	31.0	214	27.9

Table 86. Creep-Rupture Properties of Zirconium Alloys<sup>(5)</sup>

Alloy	Temp., C	Stress		Time to Rupture, hours	Min. Creep Rate, %/hr	Elong., %
		ksi	MPa			
Zircaloy-2-0	500	21.0	145	4.1	4.31	47.7
vol. % $Y_2O_3$	500	15.6	107	40.9	0.30	49.4
	500	10.0	69	1176.0	$2.00 \times 10^{-2}$	59.7
Zircaloy-2-5	500	25.0	172	21.6	$7.10 \times 10^{-1}$	49.7
vol. % $Y_2O_3$	500	19.9	137	155.8	$4.80 \times 10^{-2}$	42.8
	500	15.6	107	991.3	$1.80 \times 10^{-2}$	62.2
	400	43.4	299	30.8	$4.2 \times 10^{-1}$	26.0
	400	37.7	260	207.7	$6.4 \times 10^{-2}$	26.9
	350	59.8	412	18.1	$6.2 \times 10^{-1}$	22.3
	350	51.2	353	257.3	$3.7 \times 10^{-2}$	15.8
Zircaloy-2-10	500	30.6	211	20.6	$4.7 \times 10^{-1}$	28.8
vol. % $Y_2O_3$	500	24.9	172	246.1	$2.5 \times 10^{-2}$	31.9
	400	62.5	431	3.0	2.4	10
	400	54.8	376	39.2	$2.7 \times 10^{-1}$	17.8
	400	51.2	353	169.1	$5.2 \times 10^{-2}$	17.4



## REFERENCES

1. Weinstein, D., and Holtz, F. C., "On Dispersion Strengthening of Zirconium", Trans. Metallurgical Society of AIME, 227 (5), 1463-1465 (1963).
2. Anthony, K. C., and Klepfer, H. H., "Dispersion Strengthened Zirconium Alloys", JI. Less Common Metals, 8, 36-46 (1965).
3. Rezek, J., and Childs, R. G., "Structure and Properties of Yttria-Zirconium Dispersions", JI. of Nuclear Materials, 26, 285-299 (1968).
4. Skelly, H. M., and Dixon, C. F., "Zirconium-Refractory Alloys", JI. Less Common Metals, 23, 415-425 (1971).
5. Parsons, P. D., and Adolph, E., "Zirconium Alloys Dispersion Strengthened with Yttria", Canadian Metallurgical Quarterly, 11, 223-235 (1972).